SEE FOLLOWING NOTE

VOIR NOTE CI-APRÈS

PARTS OF THE ORIGINAL DOCUMENT ARE OF POOR REPRODUCTIVE QUALITY.

MICROMEDIA LIMITED HAS ATTEMPTED TO PRODUCE THE BEST POSSIBLE COPY.

CERTAINES PARTIES DU DOCUMENT ORIGINAL SONT DE PIÈTRE QUALITÈ DE REPRODUCTION.

MICROMEDIA LTEE A ESSAYEE DE PROCURER LE MEILLEUR EXEMPLAIRE POSSIBLE.

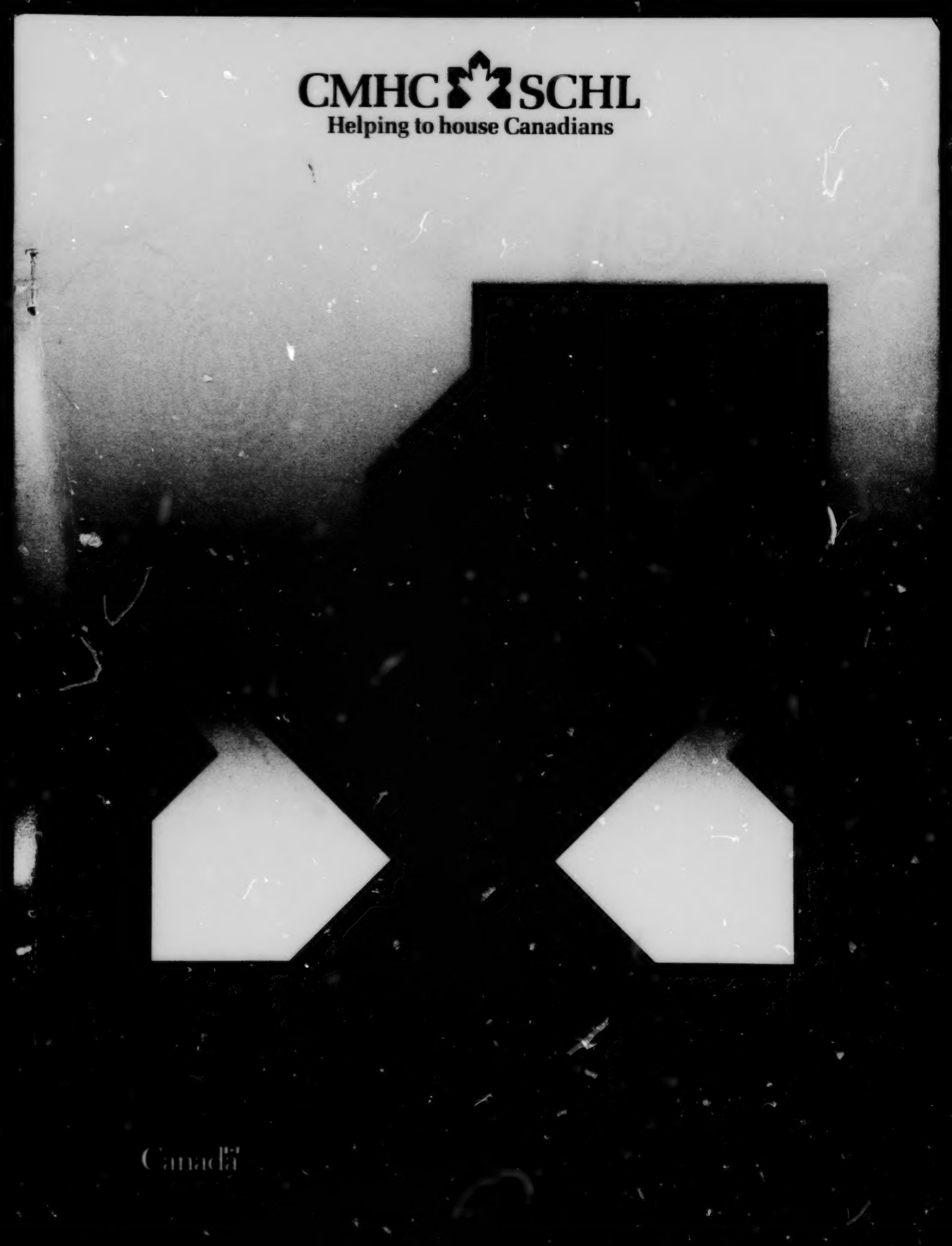
CMHC SCHL
Helping to house Canadians
Canada

91-04482/

REPORT FOR CANADA MORTGAGE AND HOUSING CORPORATION

Comparison of WALLDRY Predictions with Atlantic Canada Moisture Test Hut Data

FILE: 9293/92930755

Prepared by:

G.K. YUILL AND ASSOCIATES LIMITED

1441 Pembina Highway
WINNIPEG, Manitoba
R3T 2C4

JANUARY 12, 1990

COMPARISON OF WALLDRY PREDICTIONS WITH ATLANTIC CANADA MOISTURE TEST HUT DATA

TABLE OF CONTENTS

INTRODUCTION 1

PHASE I - ANALYSIS OF THE ATLANTIC CANADA MOISTURE TEST HUT DATA

SUMMARY - PHASE I 3

1.0 INTRODUCTION 4

2.0 ATLANTIC CANADA MOISTURE TEST HUT DATA 5

2.1 The Need for Repeating the Analysis "The Drying of Walls - Atlantic Canada" [Ref. 1] 5
2.2 data Conversion and Extraction 5

3.0 Analysis 6

3.1 Introduction 6
3.2 Selection of Noon-Hour Data 7
3.3 Analysis of Phase 1 Data 7
3.4 Analysis of Phase 2 Data 8

4.0 DISCUSSION 10

5. CONCLUSIONS 14

PHASE II - VALIDATION OF WALLDRY COMPUTER PROGRAM

1.0 INTRODUCTION 20

1.1 What is the WALLDRY Program? 20
1.2 Validation of WALLDRY 21

2.0 WEATHER DATA CONVERSION 22

2.1 Solar Model 23
2.2 Binary Conversion of Weather Data 26

3.0 WALLDRY VALIDATION 26

3.1 Preliminary WALLDRY Computer Runs 26
3.2 Validation of the Solar Model 27
3.3 Checking the Moisture Model 29
3.4 Overall Validation Criteria 30
3.5 WALLDRY Simulations of the Atlantic Canada Test Hut Panels 31
3.6 Validation of WALLDRY Using Alp Keresteciogiu's Model (FEMALP 2.1) 32

4.0 DISCUSSION OF RESULTS 35

INTRODUCTION

This is the final report to CMHC on the "Comparison of WALLDRY Predictions with Atlantic Canada Moisture Test Hut Data". The project was carried out in two phases.

During Phase I of the project, a detailed analysis of the corrected Atlantic Canada Moisture Test Hut Data was carried out in order to establish a correlation between the time a panel takes to dry to 19% and the configuration of the various panels. The moisture data from the Atlantic Canada Test Huts was collected by Oboe Engineering Ltd. They had also analysed the data in its original form. However, the moisture data has since been altered by applying a correction algorithm to it. The moisture data in its present form was analysed during Phase I of this project. It was discovered that the conclusions that emerged from the analysis of the corrected data were slightly different than those from Oboe's analysis.

Phase II of the project involved the comparison of the WALLDRY predictions with the corrected moisture data analysed in Phase I. WALLDRY was used to simulate the drying/wetting of the Atlantic Canada Test Hut walls by using hourly airport weather data. The simulation results were compared with the Test Hut measured data to assess the validity of the WALLDRY computer program. In more than half the simulated wall configurations, WALLDRY adequately predicted the drying/wetting phenomena. However, a number of weaknesses in the model were recognized. Several modifications to WALLDRY have been suggested, which might improve its performance.

PHASE I - ANALYSIS OF THE ATLANTIC CANADA MOISTURE TEST HUT DATA

SUMMARY - PHASE I

Phase I of this report describes an analysis of the corrected Atlantic Canada Test Hut data which had been obtained by Oboe Engineering Limited. The purpose of this analysis was to establish key trends in the data and to reach conclusions about the effects on drying of the construction materials and the details used in the test panels.

Several different approaches to the presentation of the data were tried, in an attempt to find the one that would best display the significant trends. It was finally decided that an inspection of the variation in noon-hour stud moisture content was most useful. A large number of graphs of this type were prepared, for most of the wall panels, and for many pairs of wall panels whose comparison was expected to be interesting.

The main conclusions drawn about the drying of studs were as follows:

1. The permeability of the sheathing had a substantial effect on the drying rate.

2. The use of furring strips appreciably increased the drying rates of the walls with very permeable sheathing, but not of the walls with less permeable sheathing.

In spite of the large amount of data reviewed, and the several different perspectives taken, no other conclusions could be reached which were unambiguous and which would have significance to the house building industry in selecting wall components. One reason for this occurrence could be the errors in data collection associated with the incorrect installation of the wood moisture pins.

It was concluded that the best way of obtaining more general conclusions from this data would be to use it in the validation of the WALLDRY program. WALLDRY might then be used to extend the results to other wall configurations and other climates. WALLDRY can also be used to investigate the detailed moisture movement mechanisms which are difficult to observe in the field but which may

provide insight into how to build walls which will be less subject to moisture damage.

1.0 INTRODUCTION

This chapter describes Phase I of the project "Comparison of WALLDRY Predictions with Atlantic Canada Moisture Test Hut Data", carried out for CMHC. The object of this part of the study was to establish a correlation between the configurations of the various panels and their drying time . A panel or a wall is said to have dried when the moisture content of the framing lumber within the wall has reached below 19%. A great deal of effort has already been made by Oboe Engineering Ltd. in collecting and analyzing the Atlantic Canada Test Hut Moisture Data. [Ref. 1]. However, the moisture data has been corrected since that analysis. The object of Phase I of this project was to redo and extend the analysis using the corrected moisture data.

The monitoring and collection of the moisture data by Oboe Engineering Ltd. was carried out in two phases. During the first phase, from March 1986 to August 1987, the moisture data was collected at sites in Fredericton, New Brunswick; Halifax, Nova Scotia; and St. John's, Newfoundland. Data collection during the second phase was carried out only in Halifax and St. John's. The panel configurations of the test huts for the first phase are described in Figures 1 and 2, and for the second phase in Figures 3 and 4 for Halifax and in Table 1 for St. John's. The monitoring periods for the three houses in Phase 1 and two houses in Phase 2 are listed in Table 2. For more information on the collection and compilation of data, refer to the "Manual for Atlantic Canada Hut Project" prepared for CMHC by Oboe Engineering Ltd. on March 6, 1989, [Ref. 2].

A preliminary analysis of the corrected moisture data revealed that the diurnal fluctuations were only significant during the first month of data collection. Therefore, an analysis based on noon hour values was used. Since the magnitude of the Atlantic Canada Moisture data is so great, the data had to be simplified before any statistical or graphical analysis could be carried out. The moisture data (in binary form) from the Atlantic Canada Hut Project supplied by the CMHC was first converted to ASCII format. The data was then simplified by

extracting the noon hour values for the purpose of the analysis. The simplified data files, being much smaller in size, were easily graphable. This approach obscured the short-term (hourly) wetting and drying processes, but analyzing these short-term processes provides little information about the long-term drying rates which are influenced by wall configurations and materials.

2.0 ATLANTIC CANADA MOISTURE TEST HUT DATA

The Atlantic Canada moisture Test Hut Data was made available for the analysis by CMHC. The moisture data had been monitored and collected by Oboe Engineering Ltd. from the test huts built in the three cities in Atlantic Canada, [Ref. 1]. After the completion of data collection, Oboe Engineering Ltd. had analysed the moisture data and reached certain conclusions. After the completion of their analysis of the moisture data and before the start of the present project, the data was adjusted by applying a temperature correction to the moisture content elements of the data. It should be mentioned here that during the collection of moisture data from Atlantic Canada Test Huts, the wood moisture pins were incorrectly installed across the isotherms.

2.1 The Need for Repeating the Analysis "The Drying of Walls - Atlantic Canada" [Ref. 1]

Since the present moisture data differs from the moisture data Oboe Engineering Ltd. used during their analysis, it was found necessary to repeat some of Oboe's work. Redoing the analysis determined the effect of the temperature correction on the moisture data, and led to conclusions which differed in some cases from those of Oboe's.

2.2 Data Conversion and Extraction

The Atlantic Canada Hut Project moisture data was supplied by CMHC in binary format. A utility program also provided by CMHC was used to convert the data from the binary format to ASCII. When the converted ASCII files were examined, it was discovered that the conversion program had converted the data incorrectly. The converted data in ASCII files is stored in a tabular form. A visual inspection of

this data revealed that there was a shift in the table values when the number of hours in the hour column exceeded 999. The apparent bug in the conversion program was reported to CMHC for correction. Once recognized, the error was corrected by importing the data into LOTUS and shifting the blocks of data to their appropriate coordinates. However, the last column in all the data sets lost during the conversion process could not be recovered. The analysis done so far does not require the use of the data in the last column, though it might be needed in future analysis and therefore the corrected conversion program should be made available. The lost data in each file was the last element of the data format shown in Table 4. This included the relative humidity of the indoor air or the ambient windspeed.

A computer program was written to simplify the data files by extracting the noon-hour data sets, thereby eliminating the handling of the remaining 23 hours of the data each day. This step saved analysis time without sacrificing useful information. The simplified files were 1/24th the size of the original data files and thus were much easier to import into LOTUS.

3.0 ANALYSIS

3.1 Introduction

After the Atlantic Canada Moisture Data was converted, extracted, and imported into LOTUS, several graphs were plotted in order to establish a correlation between the drying rates of wall panels and air-tightness, permeability, outdoor relative humidity, orientation of the wall sections, wall panel configuration, and thermal resistance, etc.. The plots for the moisture contents of the studs in Phase 1 and the moisture contents of the wood siding in Phase 2 vs the drying time for the various panels of the test huts are shown in Figures 13 through 70. The graphs may be identified by the data file abbreviation HxPn for Phase 1, and 2HxPn for Phase 2, where, x is the house number and n is the panel number. The houses in Fredericton, Halifax, and St. John's are numbered 1, 2, and 3 respectively. The panels 1 to 8 are south panels and panels 9 to 16 are north panels.

3.2 Selection of Noon-Hour Data

Hourly lower and upper stud moisture content profiles were plotted for the studs in south panel 1 (waferboard sheathing, no strapping) in St. John's. These plots are shown in Figures 5 to 12. The diurnal fluctuations in the stud moisture contents are substantial for the initial period of about 15 to 30 days. After this period the curves start smoothing off and soon the fluctuations disappear. Therefore, the use of only the noon hour values in the analysis is expected to produce satisfactory results.

3.3 Analysis of Phase 1 Data

The drying times for the three houses in the first phase are summarized in Table 3. On the average, the furred panels 2,4, and 6 dried slightly faster than the non-furred panels 1,3, and 5 respectively. The difference in the drying times between the furred and non-furred panels was minor in most cases. However, the panels with high permeability showed a considerable difference in the drying times of the furred and non-furred panels. Panel 3 dried in 19 weeks and its furred version, panel 4 dried in 7 weeks. The effect of furring strips on the drying time of lower permeability panels was negligible. It appears that for the lower permeability panels the drying rates are controlled predominantly by the permeability and the air-tightness of these wall panels, and not by the furring strips. It is important to note that the vinyl siding was installed in such a way that the bottom end of the furred cavity was completely blocked.

The air-tightness and permeability data from Table 3 was used to produce Figures 71 and 72, which demonstrate the effect of these two parameters on the average drying times (of the three huts) of the various panel configurations. The average drying time for each panel was calculated based only on the panels in the south walls. For example, the average drying time for panel 1 in the south wall of all the three huts is 42 weeks (Table 3, column 5). Since both these relationships would be expected to be inverse ones, hyperbolas were fitted to the data. As would be expected, Figure 71 showed that the higher the air-tightness of the panel (that is, the lower the ELA) the longer it takes it to dry. Figure 72 showed that the higher the permeability (or lower the diffusion resistance) the shorter the drying time. When the average drying times were plotted against permeability,

the panels with approximately the same ELA (panels 2, 3, 4, 5 and 6) were used; and when the average drying times were plotted against ELA, the panels with approximately the same permeability (panels 1, 2, 5, & 6) were used. In physical terms, this means that, provided the moisture migration potential exists in that direction, the migration of moisture from the wall cavity outwards is highly dependent on the permeability and the air-tightness of the wall sections. Panels 3 and 4 have the highest permeability and thus have the lowest drying times (19 and 7 weeks respectively), whereas panels 5 and 6 with the lowest permeability result in the highest average drying times of 52 and 47 weeks respectively.

The analysis of the Atlantic Canada Moisture data was made difficult by the fact that the starting conditions for all the panels monitored in a house (or Test Hut) were significantly different. It appears from the graphs that the orientation of the panels also affects their drying rates. This effect is not obvious from an inspection of the shapes of the drying curves, but it is evident from the times to dry to 19% shown in Figures 17, 18, 19 for House 1, Figures 27, 28, 29 for House 2, and Figures 36, 37, 38 for House 3. The measured noon-hour ambient data from the test hut in Fredericton was plotted (Figures 73 to 76) to evaluate the temperature and pressure differences across the north wall and across the south wall. The temperature and pressure differentials across a wall were not measured separately for each panel. There was only one common measurement for all the panels in one wall. Figures 73 and 74 showed that the noon hour pressure differential profiles for the north wall and the south wall were nearly the same. However, Figures 75 and 76 showed that the noon hour temperature differential profiles for the north wall and the south wall were substantially different. The north wall showed larger temperature differentials across it than the south wall. The analysis of the pressure and temperature differentials across the north and south wall suggest that the difference in drying rates of the north and the south walls is due mainly to the solar effect and not the wind (pressure) effect.

3.4 Analysis of Phase 2 Data

During Phase 2, moisture data was collected only in House 2 (Halifax) and House 3 (St. John's). The panel configurations for Halifax (Panel 3 and 4, north and south) and St. John's (all panels) were modified. In St. John's, the upper and lower sensors were moved to the siding. The moisture contents of the studs in

St. John's house was not monitored, during phase 2. There were two main types of wall panels in St. John's house during phase 2; coupled and decoupled. The difference between the two was that decoupled wall panels contained 12 mil polyethylene on exterior of sheathing.

The analysis of the data plotted in Figures 39 to 54 for House 2 (Halifax) revealed that there was no significant change in the stud moisture content of most panels. The stud moisture content of most of the panels, except panels 3, 4, 7, 11, 12, and 15 was the same at the start of the second phase as at the end of the first phase. The replacement of sheathing in panels 3, 4, 11, and 12 introduced moisture into the panels and resulted in an increase of stud moisture content as shown in Figures 41, 42, 49 and 52. The only conclusion that can be drawn from the Phase 2 Halifax house is that all the panels had either dried or were very close to drying at the end of the monitoring. Panel 7, with wet sprayed cellulose fibre insulation, was the slowest drying panel and the only one with a high moisture content through most of Phase 2.

The moisture content of the studs within the panels was not monitored in St. John's hut during phase 2. Therefore, nothing could be concluded about the effects of furring and decoupling on the drying of the building materials within the cavity. These effects were studied only for the wood siding as only its moisture content data was available.

The effect of decoupling in the panels on the south wall was not evident, however, for the decoupled panels in the north wall, the moisture content of the wood siding actually increased considerably from the start of the monitoring till the middle of January. This effect was even greater for the case of furred decoupled panels in the north wall. The above mentioned decoupling effect on the moisture content of siding can be seen in Figures 59, 60, 61, and 62 for the south wall panels and Figures 67, 68, 69 and 70 for the north wall panels.

4.0 DISCUSSION

The Atlantic Canada Test Hut Project produced a very large amount of data about wall conditions. However, it has been difficult to extract from it useful generalizations about how wall construction influences drying of studs and siding.

This difficulty is due to several factors. One is the lack of uniform starting conditions. Because of the variability of the moisture contents of the installed studs and the difficulty of ensuring equal drying up to the start of monitoring, some of the comparisons were obscured. A second factor is the variability of real weather conditions, which also obscures the comparisons. A third factor is the large number of variables which influence drying. These include both controlled general variables such as wall geometry and choice of materials, and uncontrollable variables such as airtightness of subcomponents, variations in material properties, etc. A fourth factor could be the incorrect installation of wood moisture pins across the isotherms that may have produced false data.

The CMHC/CHBA Task Force on Moisture Problems in Atlantic Canada has already reviewed the data being examined here. They concluded that "furring strips ... had no significant effect on the moisture content to which the framing lumber... ... dried during the monitoring period." They also concluded that "...sheathing materials with a very low permeability to water vapor in combination with wet framing lumber or insulation materials having a high moisture content, puts wall to a high degree of risk of moisture problems."

In the present work, the time to dry to 19% moisture content was examined instead of the moisture content at the end of the test. From this perspective, it was clear that the furring strips did have a noticeable effect on the drying time of the studs covered with a highly permeable sheathing material (fiberglass board), and did not have a significant effect when the sheathing was less permeable (waferboard or polystyrene).

This result is not surprising. There are two main resistances to moisture flow from the surface of the studs to the atmosphere. One is the sheathing; the other is the siding. If the sheathing is impermeable, its resistance predominates, and enhancing the removal of moisture from the outside of the sheathing by the use of

furring strips has a negligible effect. If, on the other hand, the permeability of the sheathing is high, then the resistance of the siding to moisture transport becomes the predominant effect. In this case, the use of furring strips decreases this critical resistance, and the wall dries significantly faster. This suggests that a combination of furring strips and permeable sheathing should be used wherever wet framing lumber is likely to be used and it is necessary to ensure that it can dry quickly.

This suggestion can only be tentative at present. In the Atlantic Canada Test Hut study, a particular vinyl siding was used, with a particular panel airtightness and a particular arrangement of vents to the atmosphere. It is not certain that the results would be the same with a different siding system. It might be that a better ventilated siding system would enhance the effect of the furring strips by allowing the flow of air behind the siding to increase. On the other hand, it could be that a better ventilated siding would offer so little resistance to moisture transport to the atmosphere that the addition of the furring strips would make no significant difference.

It should be noted that Oboe Engineering Ltd., in their "Final Report on the Drying of Walls - Atlantic Canada", dated November 26, 1987 [Ref. 1], concluded that "The presence or absence of furring made very little difference to the drying rate of the studs of the high permeance panels, 3 and 4 with fiber glass board sheathing." This disagrees with the present conclusion, discussed above. This disagreement is probably due to a difference in the importance attributed to particular parts of the drying curve. It points out strongly the difficulty of drawing absolute conclusions from data of this type.

The second conclusion made by the CMHC/CHBA Task Force and Oboe Engineering Ltd. [Ref. 1 & 3] concerned the effect of impermeable sheathing material. This is entirely borne out by the present analysis. Figure 71 (using Table 3 data) shows the drying time versus the permeability of the sheathing for five south panels (2, 3, 4, 5 and 6) which were selected because they all have approximately the same ELA. The higher permeability panels showed lower average drying times. The curve shown is the best fit to the data with the form:

$$(D - D_O)\, P = C$$

where D = the drying time.
D_O = the drying time for an infinitely permeable sheathing.
P = the sheathing permeability.
C = a constant.

This hyperbolic equation has the form that would be expected for the relationship between drying time and sheathing permeability.

A similar hyperbolic equation was fitted to the data for average drying time as a function of wall ELA. In this case, four panels with similar permeabilities were selected (Panels 1, 2, 5 and 6). The results are plotted in Figure 72 (using Table 3 data), which suggests an inverse relationship between ELA and drying time. The panels with higher ELA showed lower average drying times. This disagrees with the results of Forintek's statistical analysis, which indicated little effect of ELA on drying time in the presence of a permeability variable. One reason for the disagreement could be that Forintek's analysis was based on monthly averages.

The comparison of non-furred and furred panels with waferboard sheathing (1 and 9 and panels 2 and 10) shows that, in general, the studs dry faster in the south walls than in the north walls. However, this effect was not consistent in all locations, nor was it consistent with time of year. Figure 17 shows that in Fredericton the north panel dried faster until June, then the south panel suddenly caught up. Figure 18 shows that the behavior of the equivalent panels with furring strips was not at all similar. Figures 26 and 27 show that, in Halifax the south panels were always drier than the north panels, but in the case with the furring strips, this is caused by a difference in starting conditions, not drying rates. No conclusion can be drawn from Figure 36 for the non-furred panels in St. John's, because of different starting conditions. Figure 37 shows an effect for the furred panels in St. John similar to that for the non-furred panels in Fredericton.

The effect of wind and solar radiation incident on the north and south walls in Fredericton was studied by plotting Figures 73-76. It is evident from Figures 73 and 74 that the pressure differentials across north and south walls are similar.

Therefore, when comparing the drying of north and south walls, the wind pressure variable can be ignored. The difference in the temperature differentials across the north and south walls is the only parameter that affects the difference in drying rates of north and south walls. Figures 75 and 76 show that there is a significant difference in the temperature differential profiles across the north and south walls. The higher average temperature differential across the south wall is due to the higher solar radiation incident on the south wall. The temperature gradients across the wall and the moisture gradients are the two main parameters that influence the moisture transfer phenomenon. At this stage of the data analysis, it can't be positively concluded whether or not higher siding temperatures help drive the moisture out of these walls.

The above discussion is based on a visual inspection of the drying curves. If, instead, only the time to dry to 19% moisture content is considered, then the effect of the sun is more apparent, The south facing panels reach this value more quickly than those on the north.

This review of the data on the effect of facing direction on the drying of the studs for one kind of sheathing is typical of most of the other reviews of potential controlling variables which have been carried out. The results are ambiguous and sometimes apparently contradictory. There is no obvious trend which permits a firm conclusion to be drawn.

Even in those cases (such as the effect of sheathing permeability) where conclusions could be drawn, there is no certainty that they will apply to wall types other than those tested. For example, a tight siding might negate entirely the effect of a permeable sheathing material.

These difficulties of interpretation of measured data are not surprising. They occur frequently in field experiments involving complex processes in complex systems. This does not mean that such experiments are without value. Rather, it points up the need for a particular approach to the analysis of the field data. This is the use of a theoretically based computer model. The field data is then useful to validate the model. The model is useful to extend the experimental results to other systems and other conditions.

These attempts to extract information from the Atlantic Canada Test Hut data were made without using the model available in the WALLDRY program. This approach was taken so that the data could be looked at from a fresh perspective, without specific expectations or prejudices. However, in the next phase of this project, the data was used to validate WALLDRY, which yields more insight into the moisture movement processes which are taking place in the walls.

5. CONCLUSIONS

The effect of the furring strips on the drying of wall panels with low permeabilities was not significant when vinyl siding is used. However, panels with high permeability showed a decrease in the drying time when furring strips were used behind vinyl siding.

The permeability of the sheathing was a decisive factor in determining the drying rates of the panels. The panels with higher permeability dried quicker than the panels with lower permeability.
The rank of the panels, in terms of drying rate was:

4 - fiberglass sheathing, furred siding
3 - fiberglass sheathing, no furring
8 - polystyrene insulation, sheathing paper, no furring
2 - waferboard sheathing, furred siding
1 - waferboard sheathing, no furring
5 - polystyrene sheathing, no furring
6 - polystyrene sheathing, furred siding
7 - wet sprayed cellulose insulation

The study of the effect of panel orientation on the drying rate revealed that the south panels dried more quicker than the north panels. Solar radiation was the determining parameter, not wind direction. However, the results were ambiguous.

The decoupling of non-furred wall panels on the north wall raised the moisture content of the wood siding well above 19%. This effect was even greater for the decoupled furred panels.

To make full use of the data collected in the Atlantic Canada Test Hut study, it will be necessary to use a computer program based on a detailed moisture movement model to examine it and to extend it.

TABLE 1: ST. JOHN'S PHASE 2 TEST WALL CONFIGURATION

Coupled Wall Panels (Interactive with the Inner Wall)

PANEL 1

12.7 mm drywall, 4 mil poly, 38 x 140 mm stud @ 400 mm O.C., RSI 3.52 batt insulation, 9.5mm waferboard sheathing, Tyvek* building paper, wood siding.

PANEL 2

Same as Panel 1, with 19 x 64 mm vented furring strips.

PANEL 5

12.7 mm drywall, 4 mil poly, 38 x 89 mm stud @ 400 mm O.C., RSI 2.11 batt insulation, extruded polystyrene, Tyvek* building paper, wood siding.

PANEL 3

Same as Panel 5, with 19 x 64 mm vented furring strips.

Decoupled Wall Panels (Isolated from the Inner Wall)

PANEL 7

Same as Panel 1, with 12 mil polyethylene on exterior of sheathing.

PANEL 6

Same as Panel 7, with 19 x 64 mm vented furring strips over the 12 mil polyethylene.

PANEL 4

Same as Panel 5, with 12 mil polyethylene on exterior of sheathing.

PANEL 8

Same as Panel 4, with 19 x 64 mm vented furring strips, over the 12 mm polyethylene.

*Registered Trade Marks

TABLE 2

Phase 1: Monitoring Period

FIRST HOUR:

- Fredericton: 0118 MAR 05 1986.
- Halifax: 0118 MAR 07 1986.
- St. John's: 0115 MAR 10 1986.

LAST HOUR:

- Fredericton: 1008 APR 05 1987.
- Halifax: 0606 AUG 23 1987.
- St. John's: 0605 AUG 25 1987.

Phase 2: Monitoring Period

FIRST HOUR:

- Halifax: 0103 AUG 28 1987.
- St. John's: 0112 AUG 27 1987.

LAST HOUR:

- Halifax: 1214 APR 01 1988
- St. John's: 1101 APR 01 1988

TABLE 3: Drying Times, ELA and Permeability For South Panels

SOUTH PANELS

Panel No.	Drying Time (Weeks) House 1 (H1)	House 2 (H2)	House 3 (H3)	Average Drying Time (H1+H2+H3)/3 (Weeks)	ELA cm^2	Permeability of the Sheathing Assemblies $ng/Pa.s.m^2$
1	36	49	42	42	1.50	43
2	17	64	42	41	0.9	43
3	11	36	11	19	0.96	5366
4	11	08	02	07	1.10	5366
5	42	68	45	52	0.65	35
6	**	60	34	47*	0.85	35
7	**	**	**	**	0.88	43

*AVERAGE BASED ON LESS THAN THREE HOUSES.

**THE PANEL NEVER DRIED

TABLE 4

DATA FORMAT

PHASE 1

This format is similar for all sites. The format for St. John's, is shown below:

FILE H3P1:

DATA:	1	-2.4	-7.3	1.3	1.4	1.4	39.2	26.3	43.9	34.8	33.2	33.6
FORM:	HR	T1	T2	T3	P1	P2	E1	E2	E3	C1	C2	C3

FILE H3P2:

DATA:	1	-.8	-2.6	.6	-10.0	1.0	1.7	-.3	40.9	16.9	38.2	47.6	1.1	13.7	6.1
FORM:	HR	T1	T2	T3	T4	P1	P2	P3	E1	E2	E3	C1	C2	C3	RH1

FILE H3P3:

DATA:	1	1.3	.3	3.8	1.4	1.0	101.4	67.7	23.1	26.7	21.2	
FORM:	HR	T1	T2	T3	P1	P2	E1	E2	C1	C2	C3	

FILE H3P4:

DATA:	1	.9	-.5	4.1	-10.2	1.7	2.4	-.3	87.9	29.6	5.1	17.8	45.9	6.4
FORM:	HR	T1	T2	T3	T4	P1	P2	P3	E1	E2	C1	C2	C3	RH1

FILE H3P5:

DATA:	1	.9	-.3	4.1	1.4	1.4	83.2	34.9	26.3	18.6	21.9
FORM:	HR	T1	T2	T3	P1	P2	E1	E2	C1	C2	C3

FILE H3P6:

DATA:	1	1.7	2.7	7.3	-9.7	1.7	2.4	.0	37.7	24.4	18.0	25.8	21.6	5.7
FORM:	HR	T1	T2	T3	T4	P1	P2	P3	E1	E2	C1	C2	C3	RH1

FILE H3P7:

DATA:	1	11.9	11.3	15.7	.0	.3	13.5	2.4	10.3	35.0	31.9	30.0
FORM:	HR	T1	T2	T3	P1	P2	E1	E2	E3	C1	C2	C3

FILE H3P8:

DATA: 1 7.3 6.6 .0 .0 3.9 -999.0 18.4 30.7
FORM: HR T1 T2 P1 P2 E1 E2 C1 C2

FILE H3P9 TO H3P16 SIMILAR TO H3P1 TO H3P8 RESPECTIVELY.

FILE H3A1:

DATA: 1 -10.8 .0 .0 .0 .0 .0 -999.0 .0
FORM: HR TA PANL PANH PASL PASH RHA WD WS

FILE H3A2:

DATA: 1 -10.7 -14.5 11.6 1.0 6.0
FORM: HR SST NST TIN PIN RHIN

DATA FORMAT PHASE 2

The format is similar to that in Phase I, (Appendix C) except that the pressures (P1, P2 and P3) are no longer in the format.

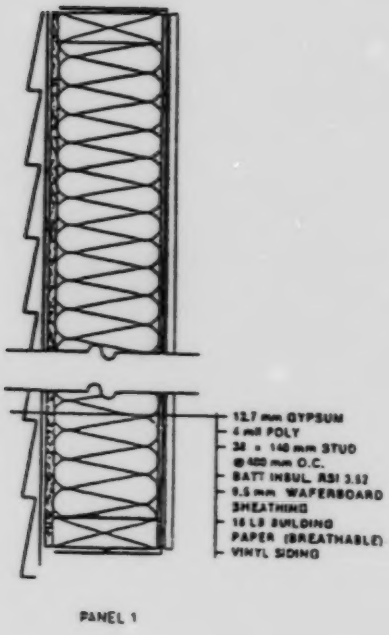

PANEL 1

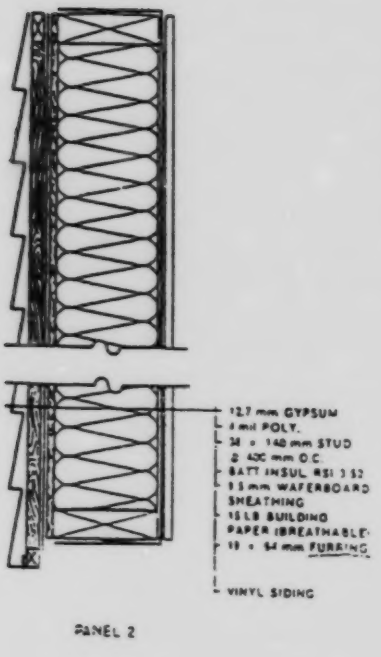

PANEL 2

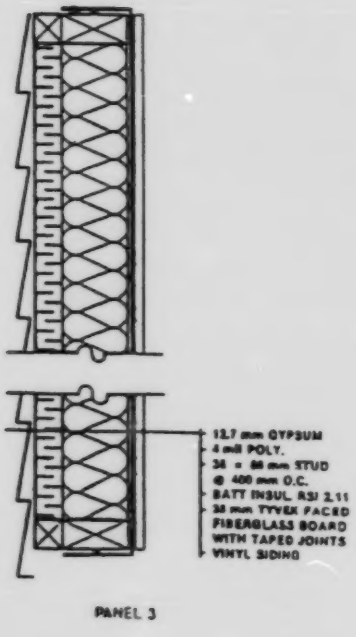

PANEL 3

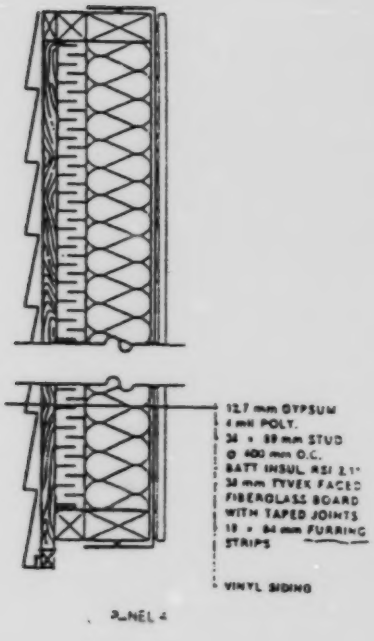

PANEL 4

Figure 1 Wall Configurations, Test Panels 1 to 4 in the south and 9 to 12 in the north wall, Phase 1, All Houses.

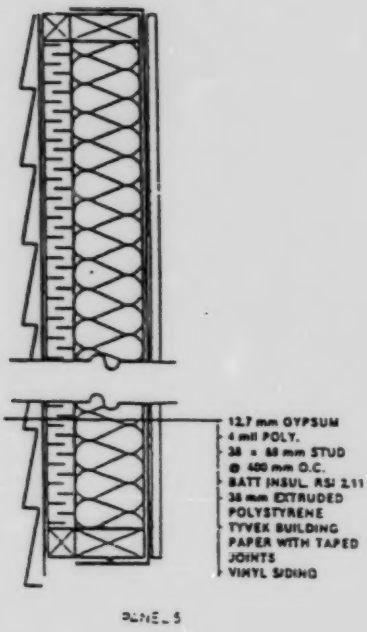

PANEL 5

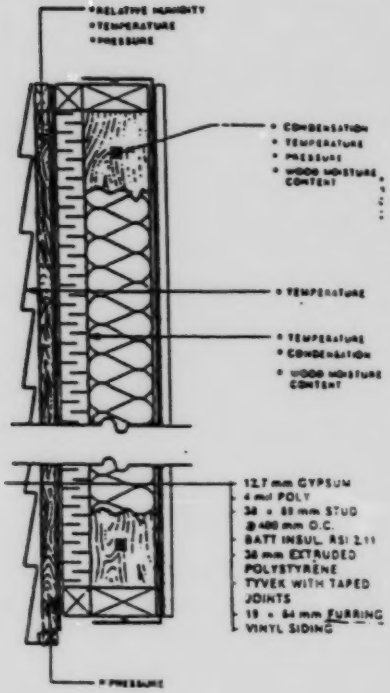

PANEL 6

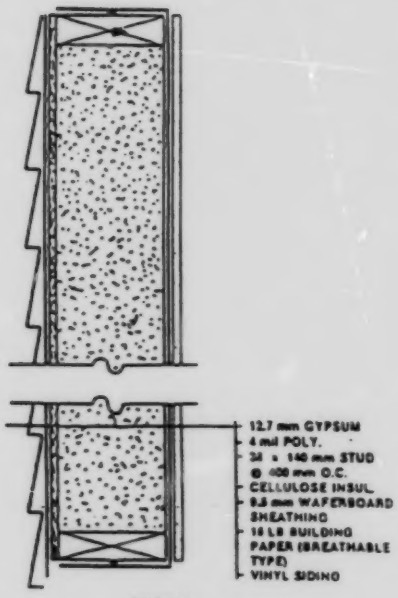

PANEL 7

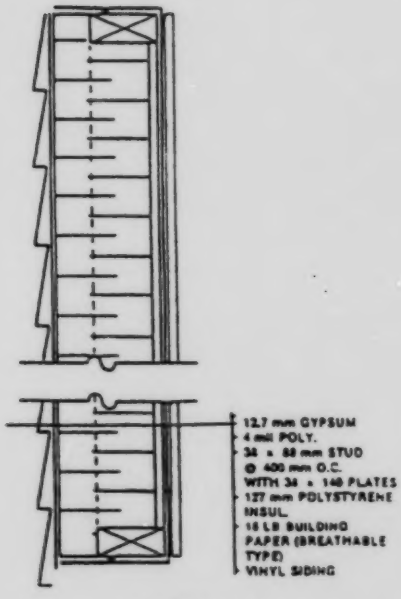

PANEL 8

Figure 2 Wall Configurations, Test Panels 5 to 8 in the south and 13 to 16 in the north wall, Phase 1, All Houses.

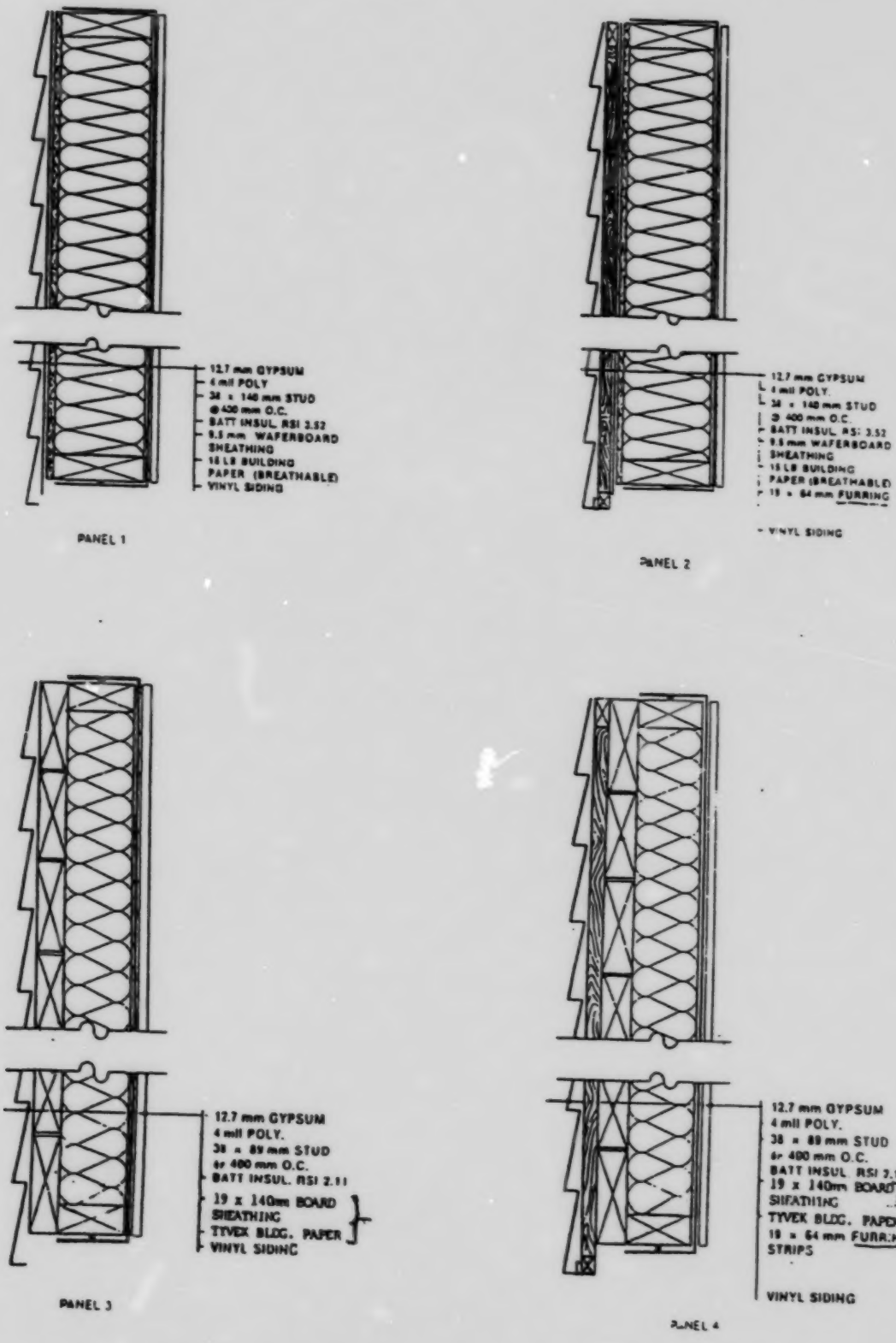

Figure 3 Wall Configurations, Test Panels 1 to 4 in the south and 9 to 12 in the north wall, Phase 2, Halifax Hous.

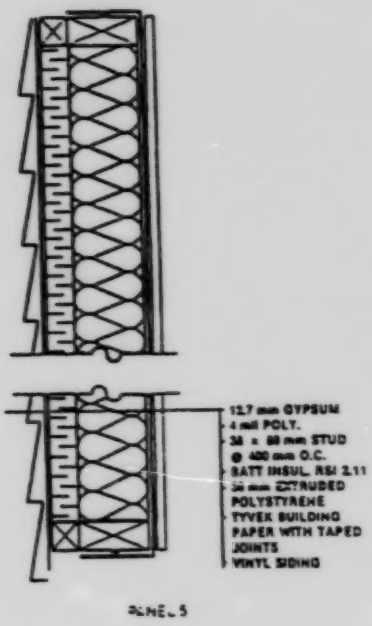

PANEL 5

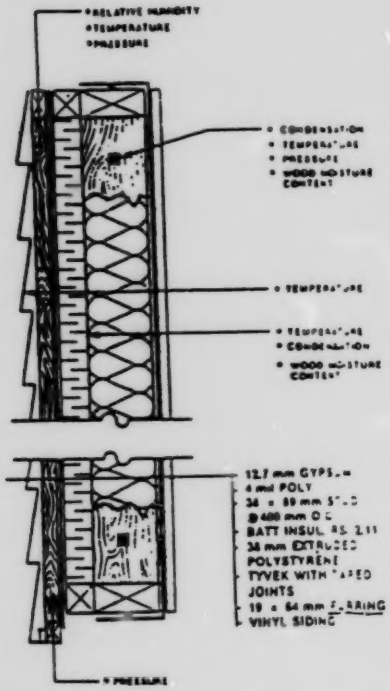

PANEL 6

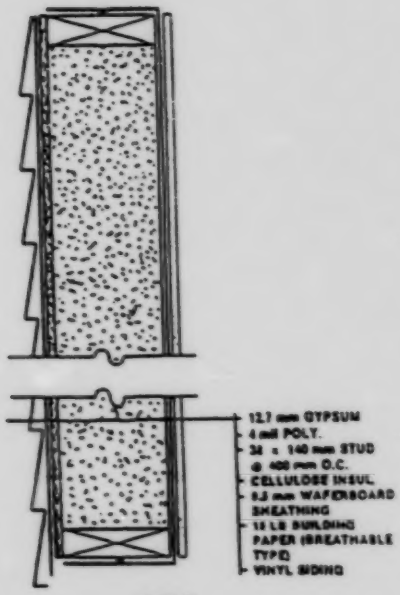

PANEL 7

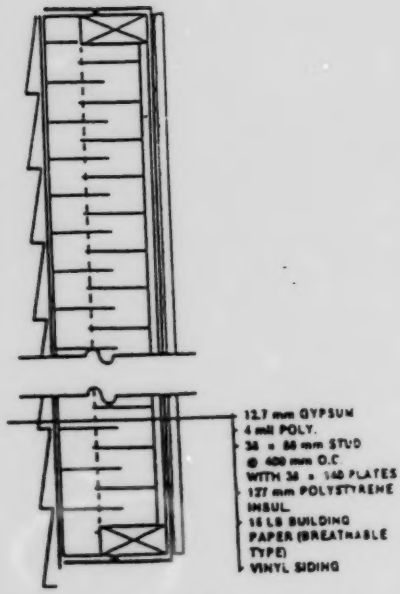

PANEL 9

Figure 4 Wall Configurations, Test Panels 5 to 8 in the south and 13 to 16 in the north wall, Phase 2, Halifax House.

HOURLY M/C PROFILES USING ATLANTIC HUT DATA

ST. JOHNS, SOUTH PANEL 1

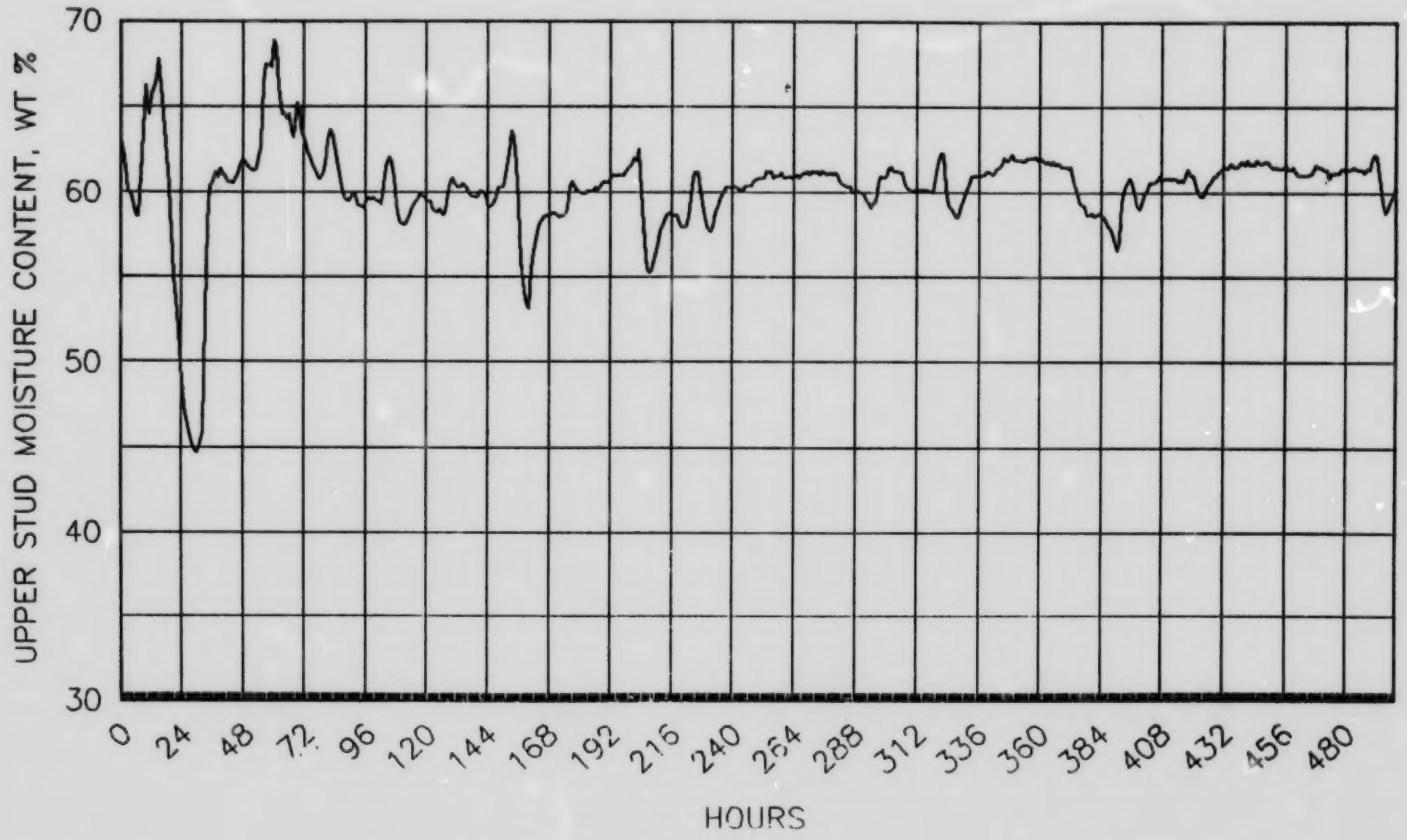

HRLYP1(ALL3)

Figure 5a

HOURLY M/C PROFILES USING ATLANTIC HUT DATA
ST. JOHNS, SOUTH PANEL 1

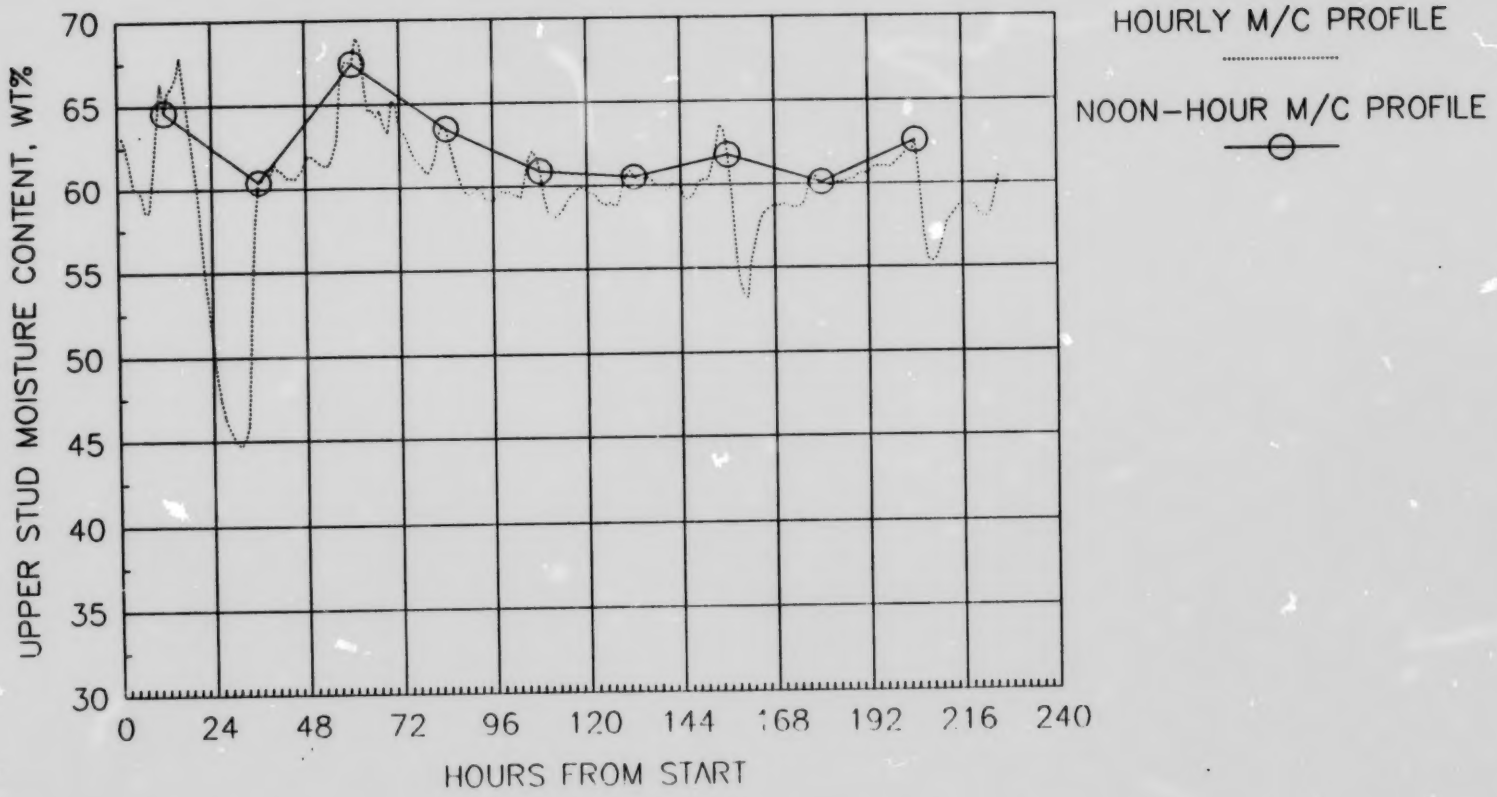

MONITORING STARTING TIME: 0115 MAR 10 1986

HRLYP1(ALL3)

Figure 5b

HOURLY M/C PROFILES USING ATLANTIC HUT DATA

ST. JOHNS, SOUTH PANEL 1

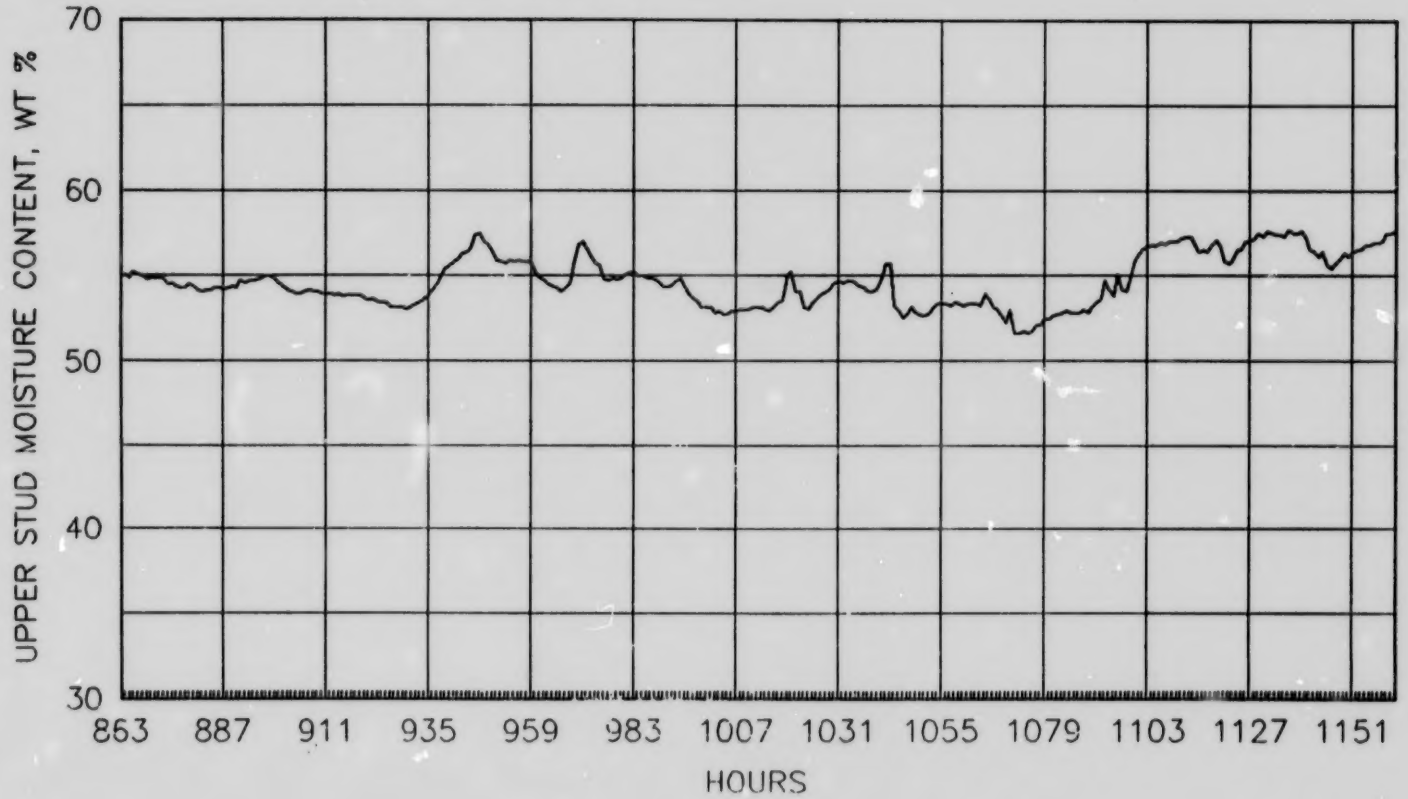

Figure 6

p1dset2(p1dset2c)

HOURLY M/C PROFILES USING ATLANTIC HUT DATA

ST. JOHNS, SOUTH PANEL 1

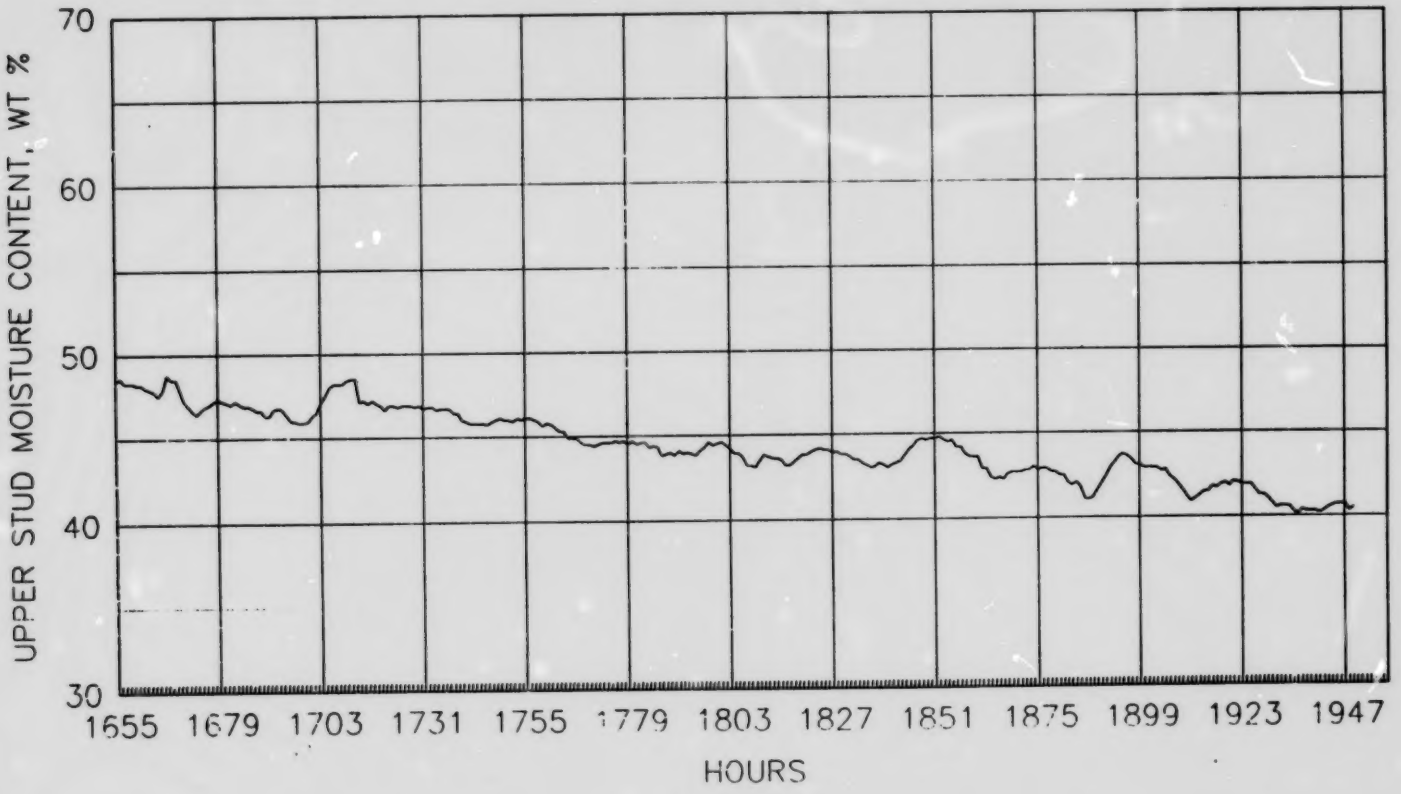

p1dset2(p1dset2b)

Figure 7

HOURLY M/C PROFILES USING ATLANTIC HUT DATA

ST. JOHNS, SOUTH PANEL 1

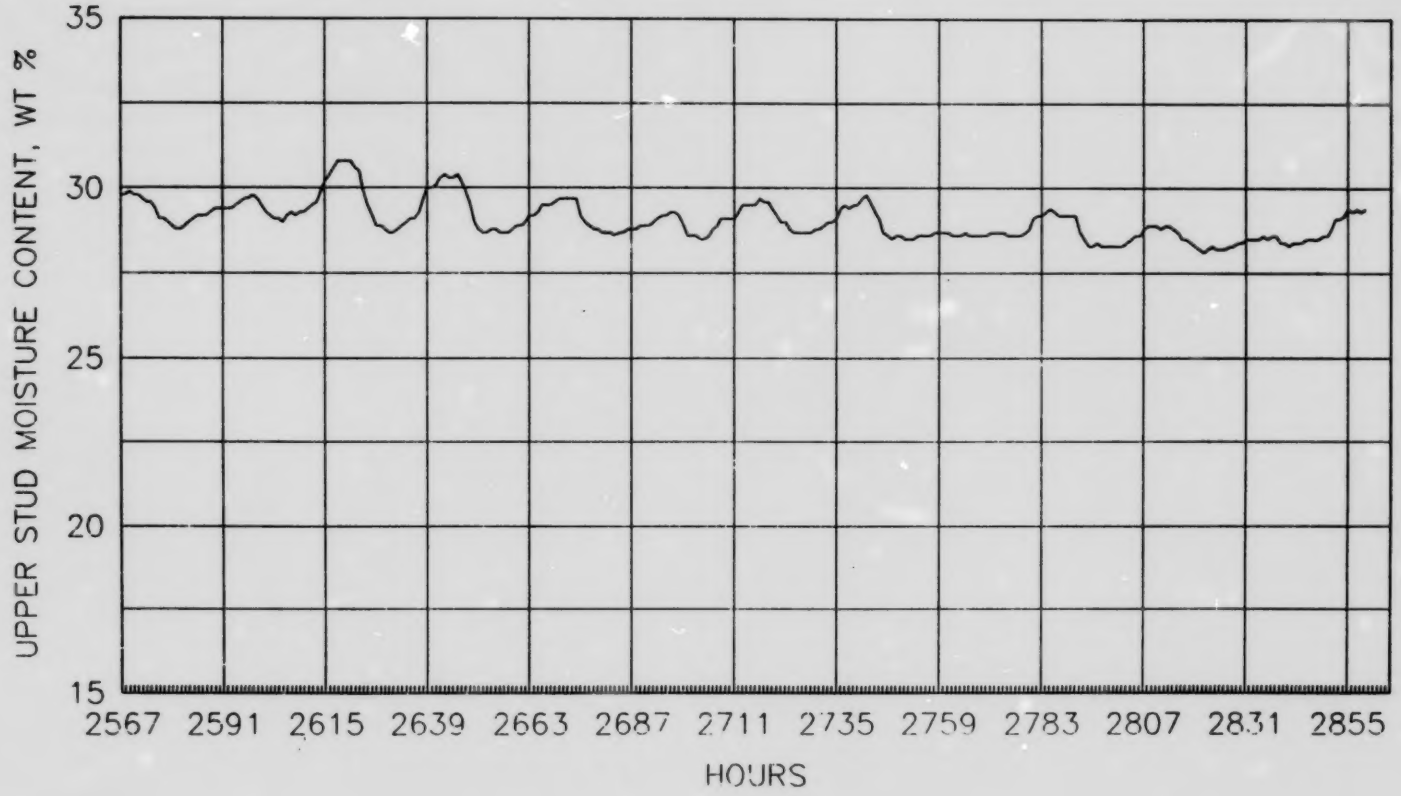

p1dset3(p1dset3)

Figure 8

HOURLY M/C PROFILES USING ATLANTIC HUT DATA

ST. JOHNS, SOUTH PANEL 1

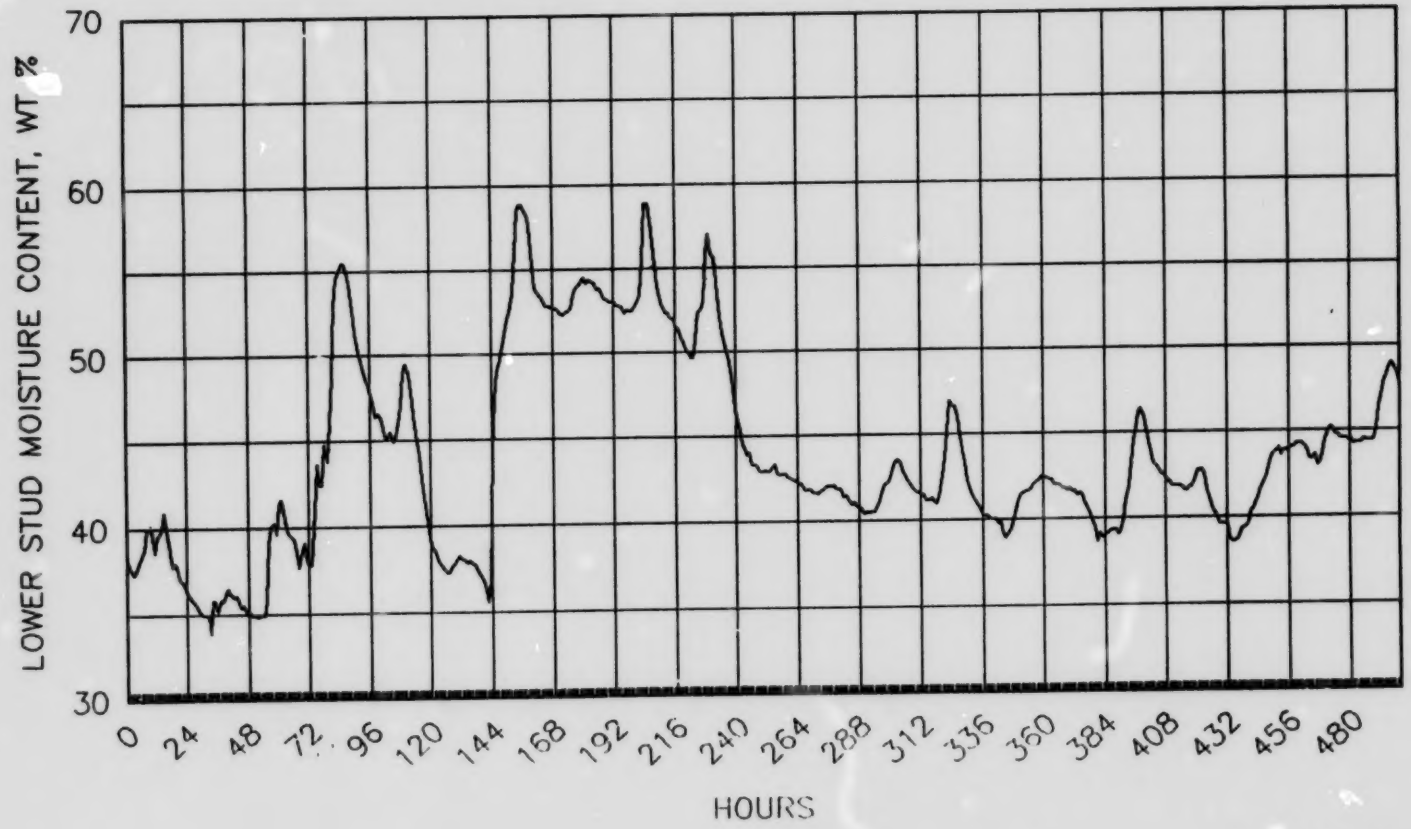

hrlyp1(p1e1-1)

Figure 9a

HOURLY M/C PROFILES USING ATLANTIC HUT DATA
ST. JOHNS, SOUTH PANEL 1

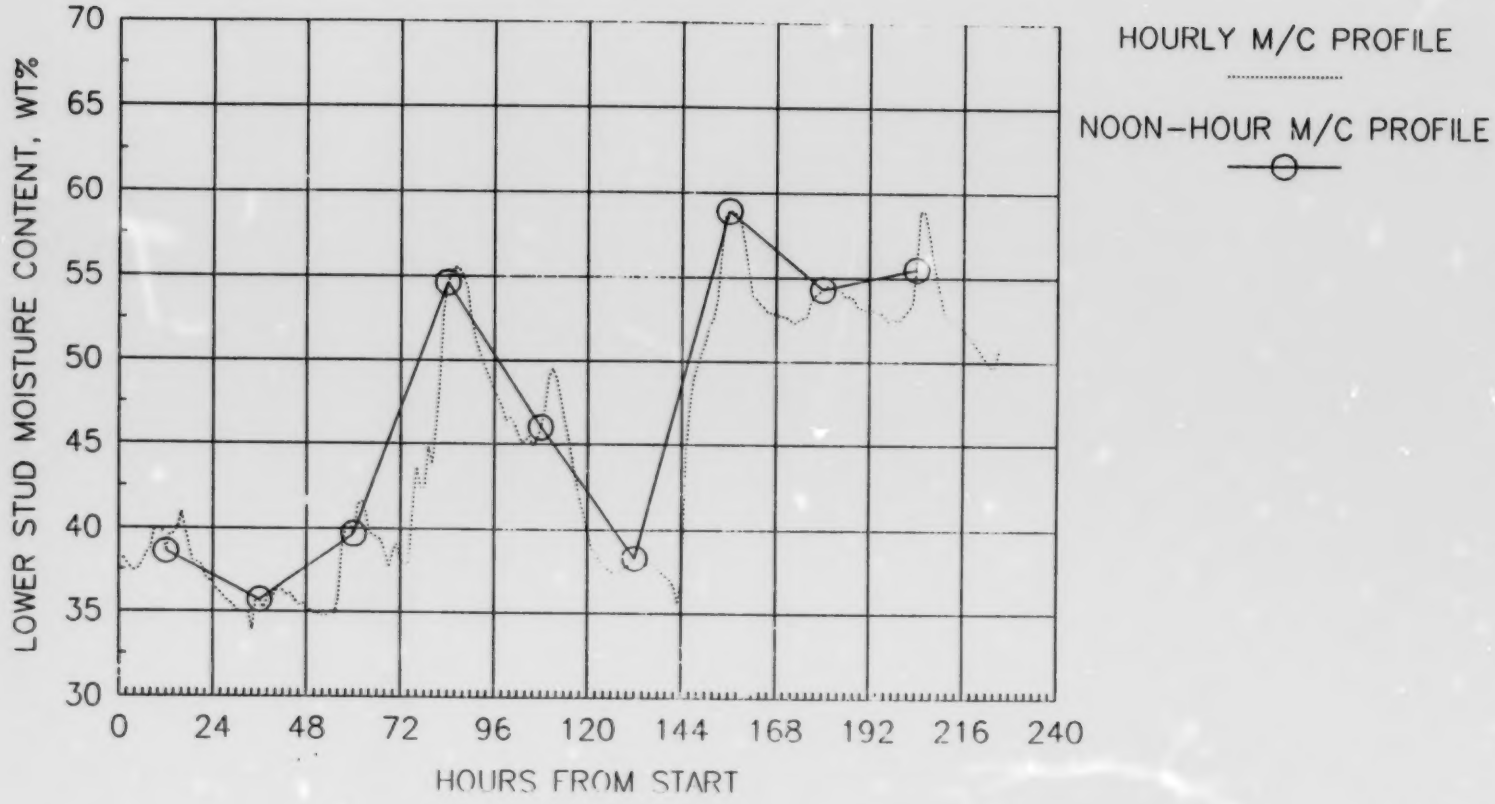

MONITORING STARTING TIME : 01 15 MAY 10 1 . .

HRLYP1(ALL1)

Figure 9b

HOURLY M/C PROFILES USING ATLANTIC HUT DATA

ST. JOHNS, SOUTH PANEL 1

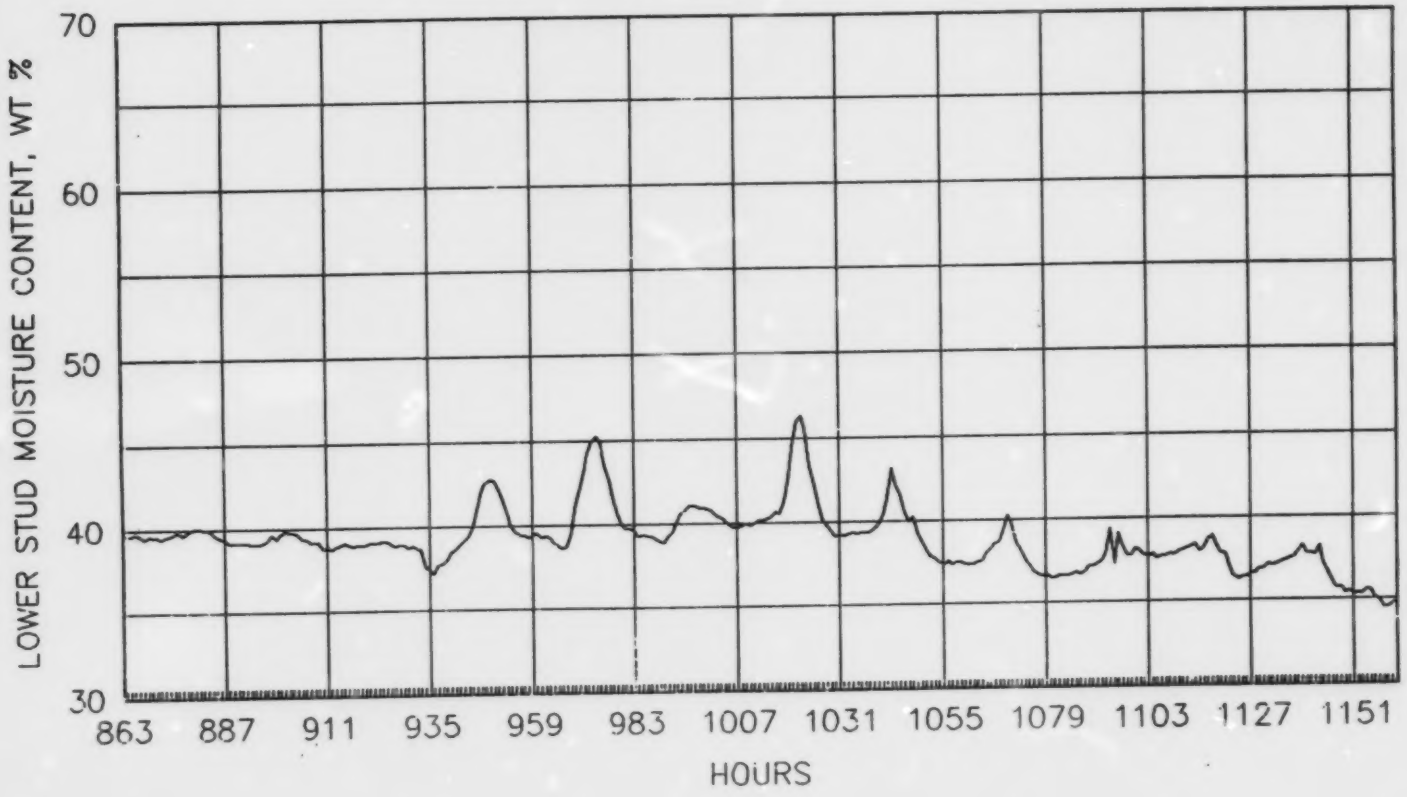

Figure 10

p1dset2(p1e1-2a)

HOURLY M/C PROFILES USING ATLANTIC HUT DATA

ST. JOHNS, SOUTH PANEL 1

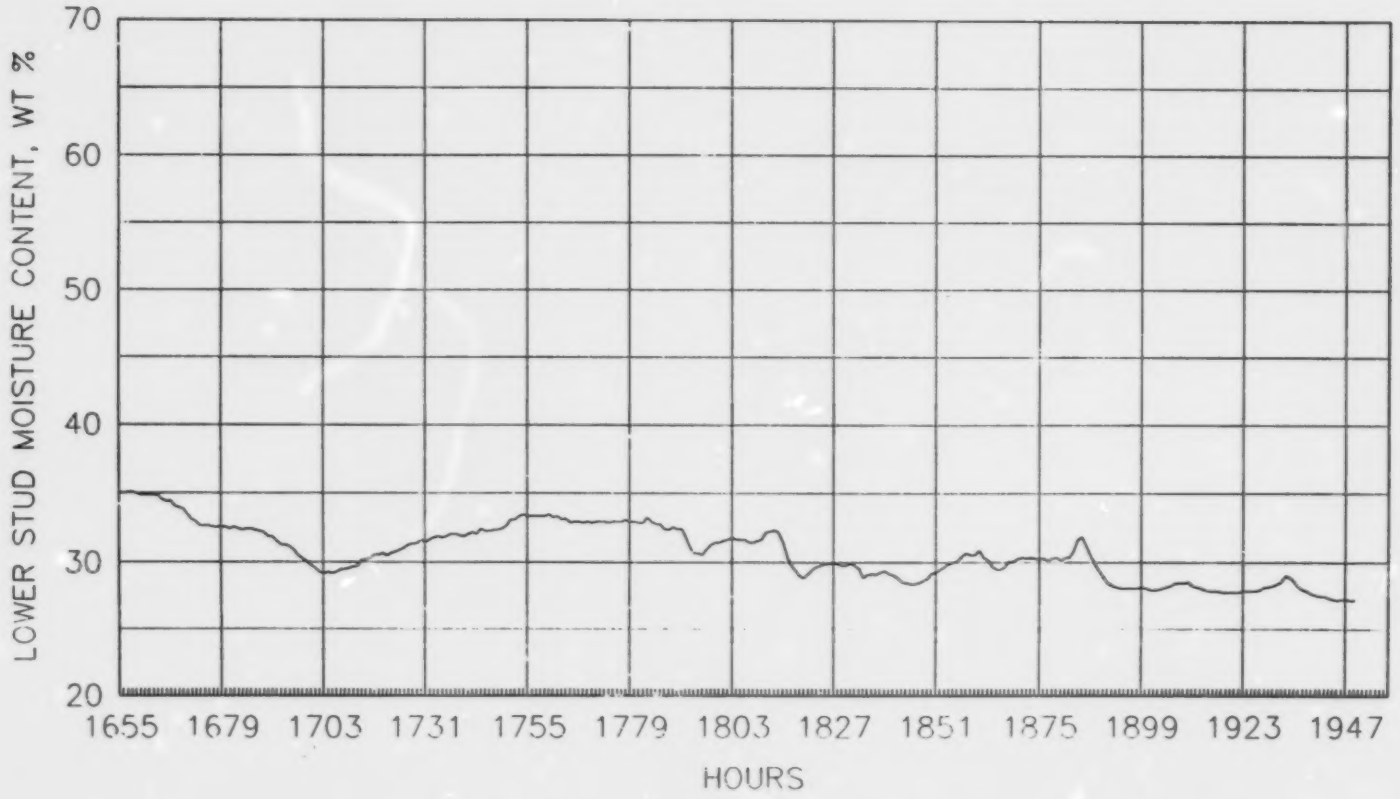

p1dset2(p1e1-2b)

Figure 11

HOURLY M/C PROFILES USING ATLANTIC HUT DATA

ST. JOHNS, SOUTH PANEL 1

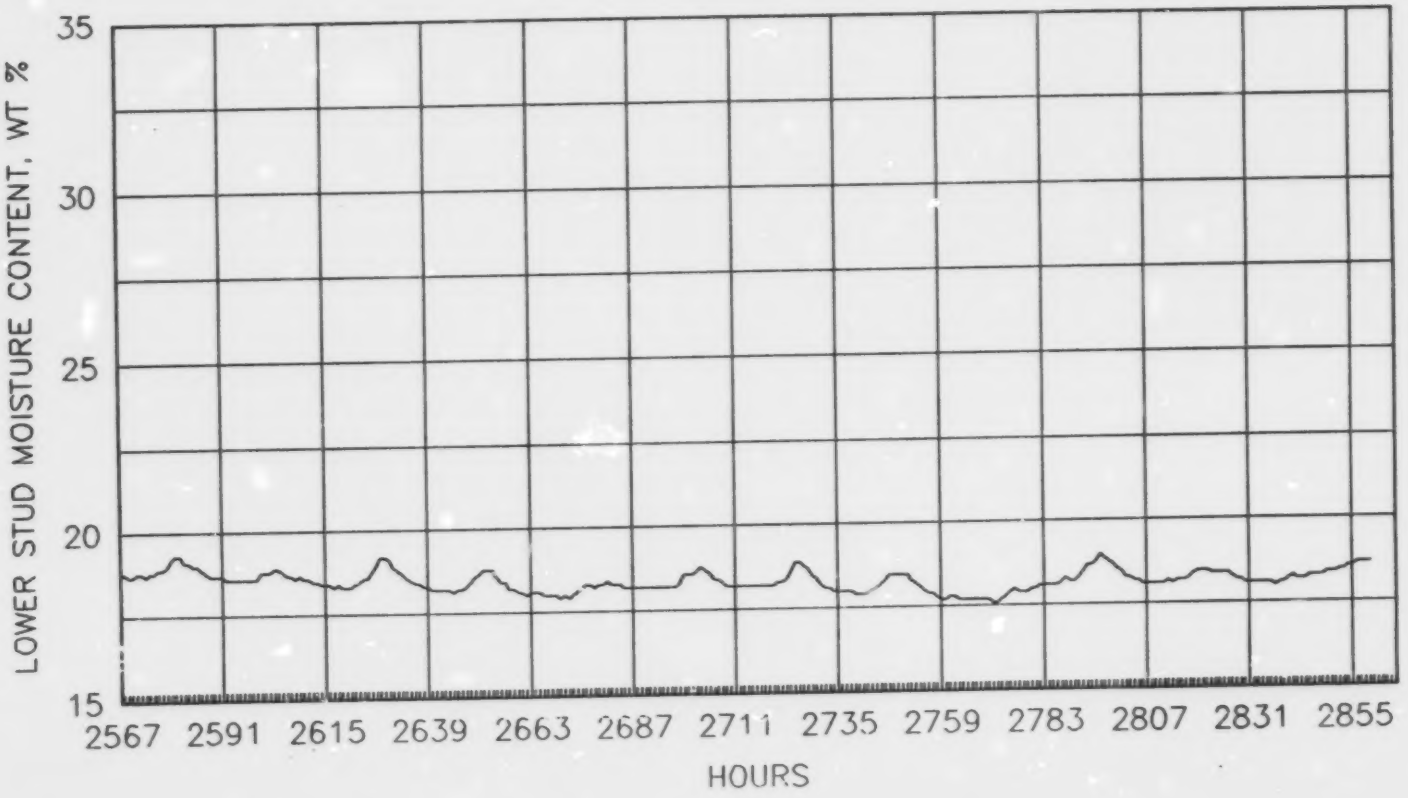

Figure 12

p1dset3(p1e1-3)

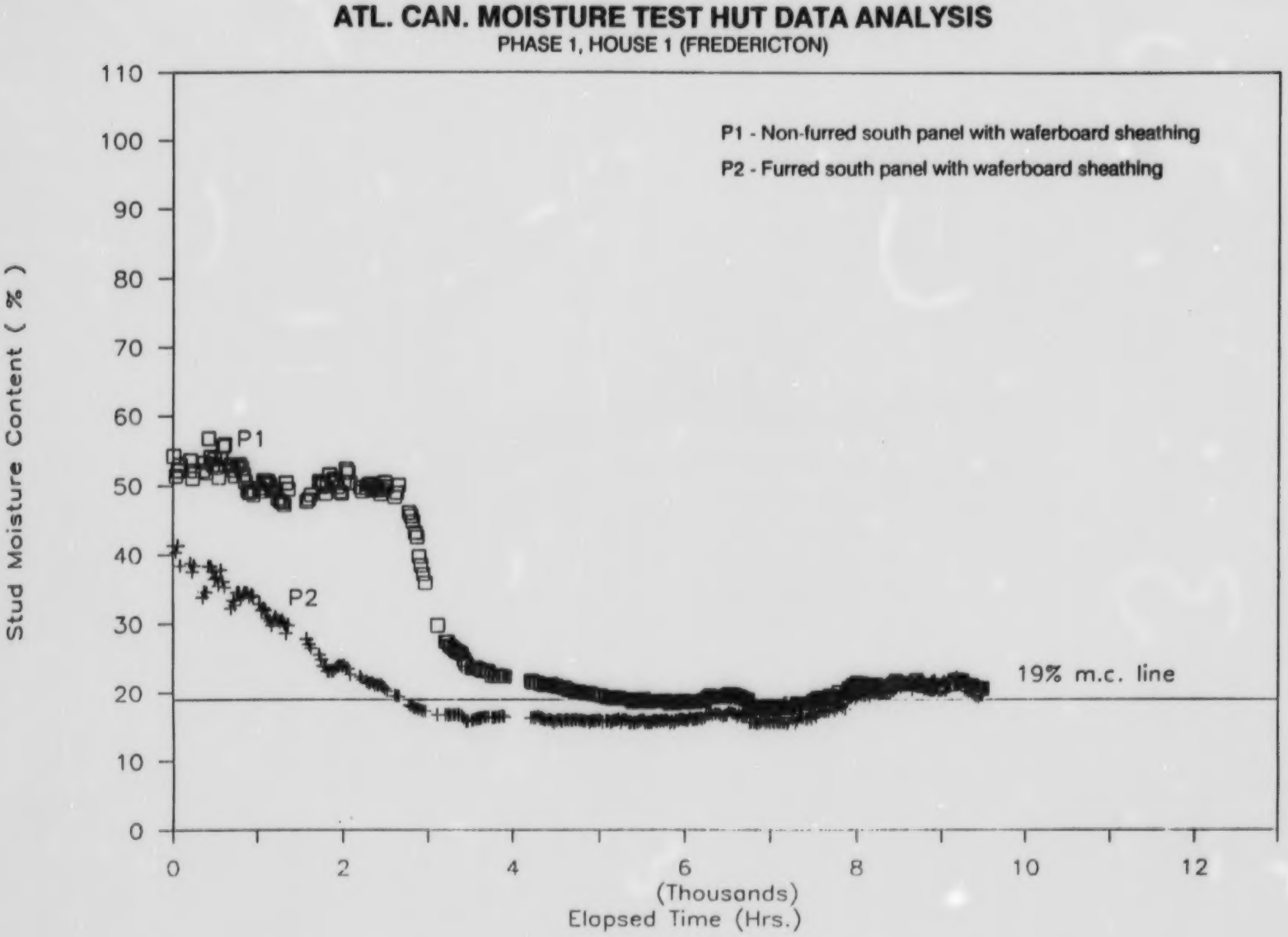
ATL. CAN. MOISTURE TEST HUT DATA ANALYSIS
PHASE 1, HOUSE 1 (FREDERICTON)
P1 - Non-furred south panel with waferboard sheathing
P2 - Furred south panel with waferboard sheathing
Stud Moisture Content (%)
110
100
90
80
70
60
50
40
30
20
10
0
P1
P2
19% m.c. line
0
2
4
6
8
10
12
(Thousands)
Elapsed Time (Hrs.)

Figure 13

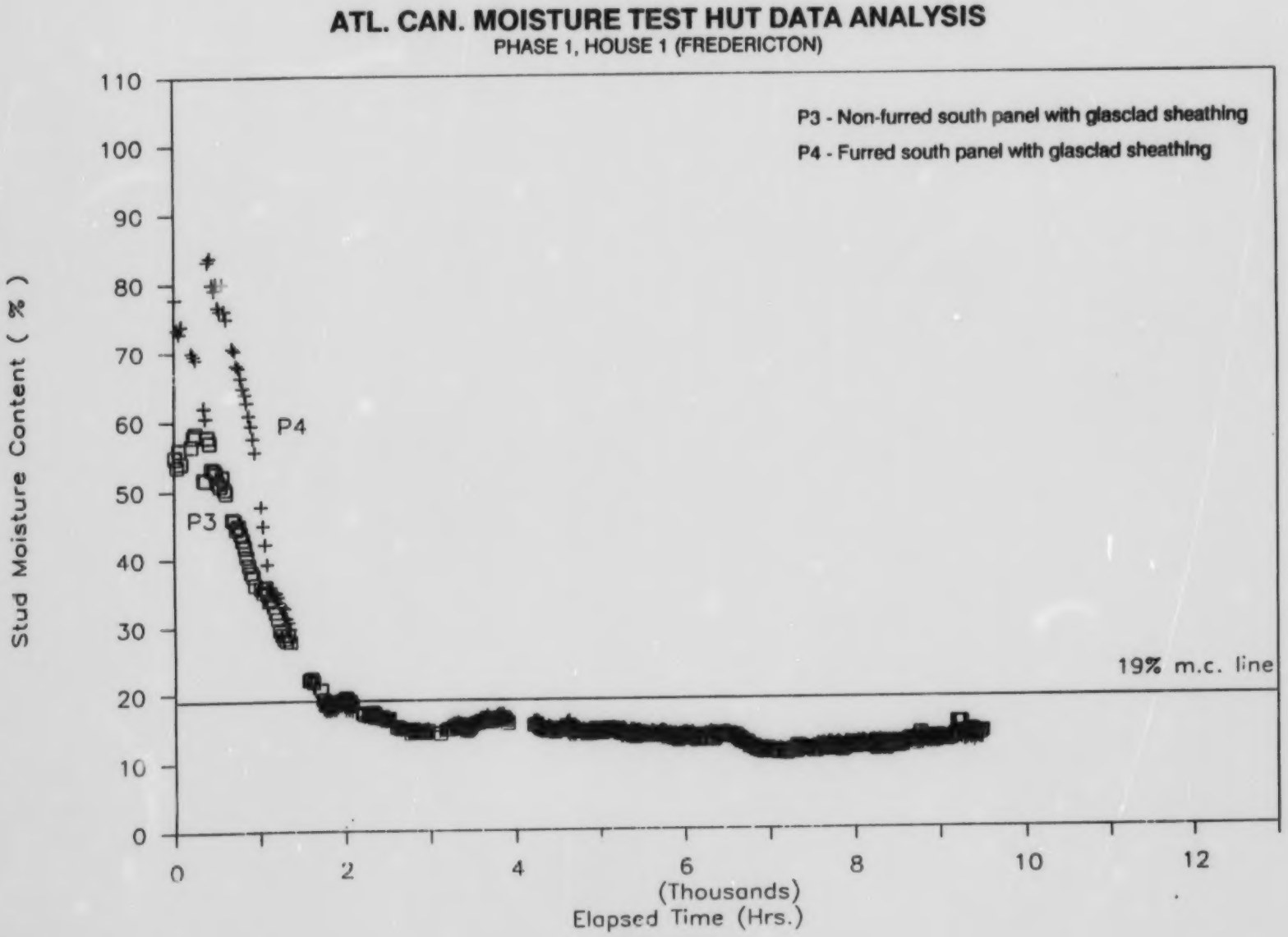
ATL. CAN. MOISTURE TEST HUT DATA ANALYSIS
PHASE 1, HOUSE 1 (FREDERICTON)
P3 - Non-furred south panel with glasclad sheathing
P4 - Furred south panel with glasclad sheathing
Stud Moisture Content (%)
110
100
90
80
70
60
50
40
30
20
10
0
P4
P3
19% m.c. line
0
2
4
6
8
10
12
(Thousands)
Elapsed Time (Hrs.)

Figure 14

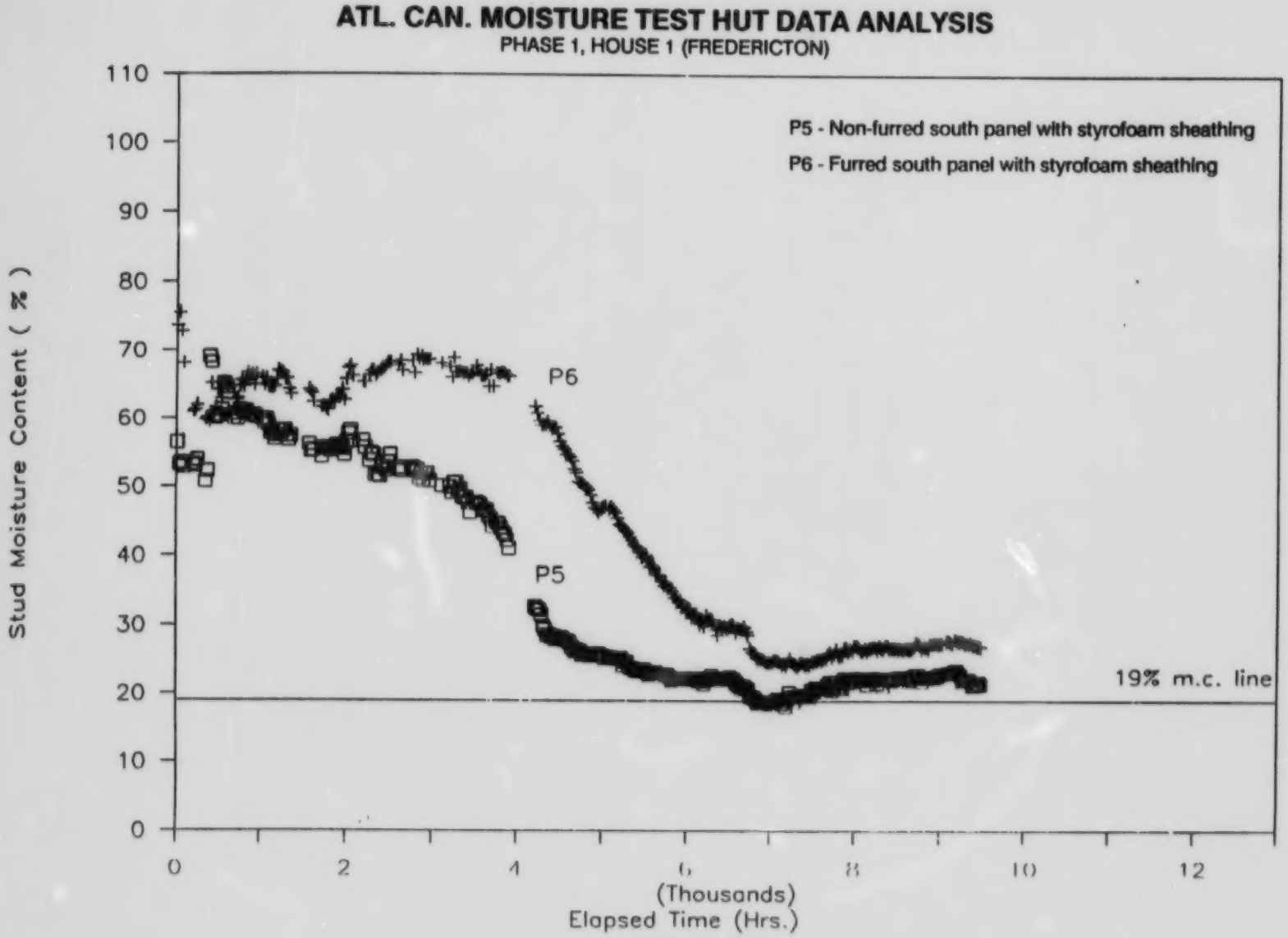
ATL. CAN. MOISTURE TEST HUT DATA ANALYSIS
PHASE 1, HOUSE 1 (FREDERICTON)
P5 - Non-furred south panel with styrofoam sheathing
P6 - Furred south panel with styrofoam sheathing
P6
P5
19% m.c. line
Stud Moisture Content (%)
110
100
90
80
70
60
50
40
30
20
10
0
0
2
4
6
8
10
12
(Thousands)
Elapsed Time (Hrs.)

Figure 15

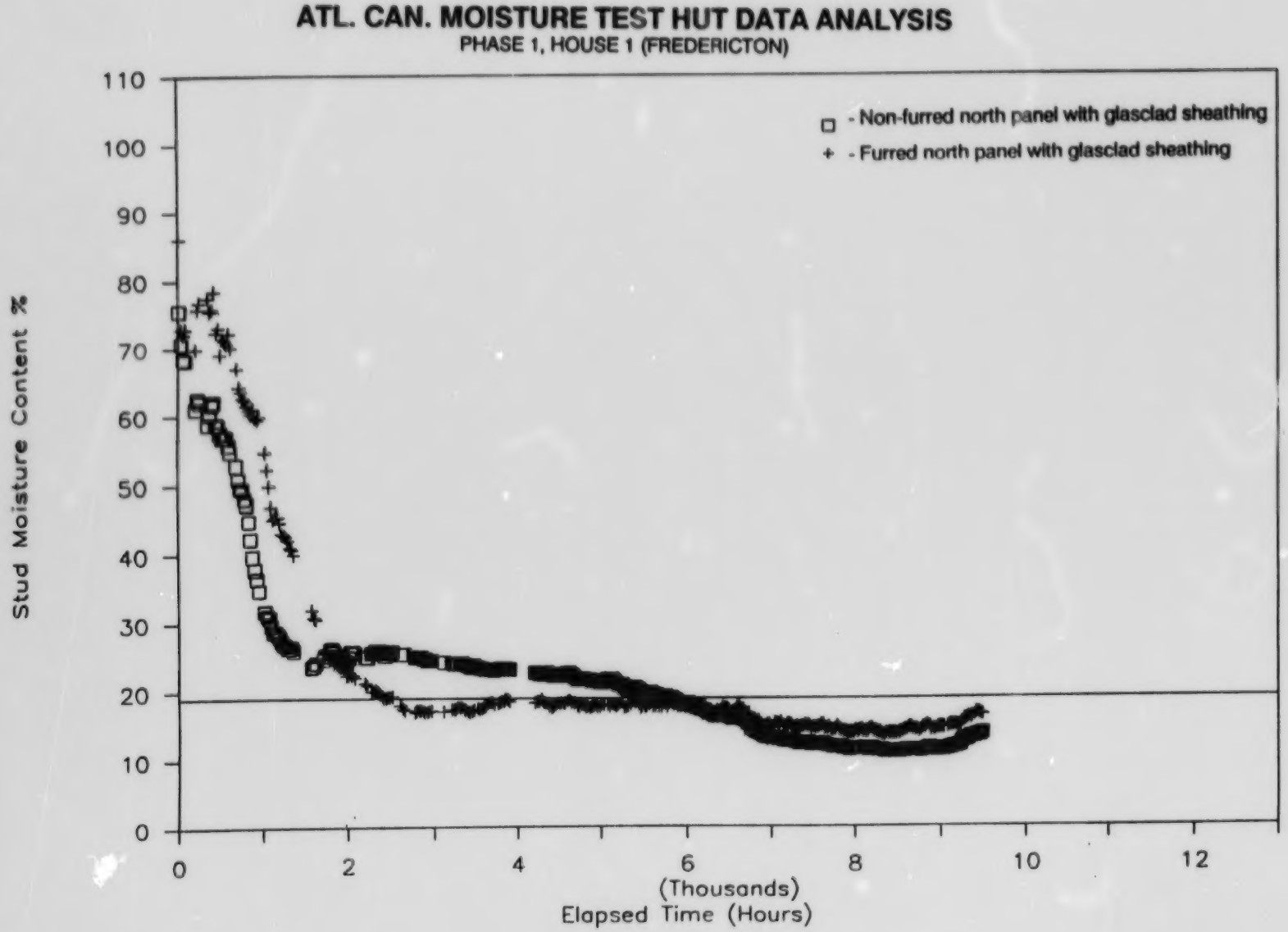
ATL. CAN. MOISTURE TEST HUT DATA ANALYSIS
PHASE 1, HOUSE 1 (FREDERICTON)
□ - Non-furred north panel with glasclad sheathing
+ - Furred north panel with glasclad sheathing
Stud Moisture Content %
110
100
90
80
70
60
50
40
30
20
10
0
0
2
4
6
8
10
12
(Thousands)
Elapsed Time (Hours)

Figure 16

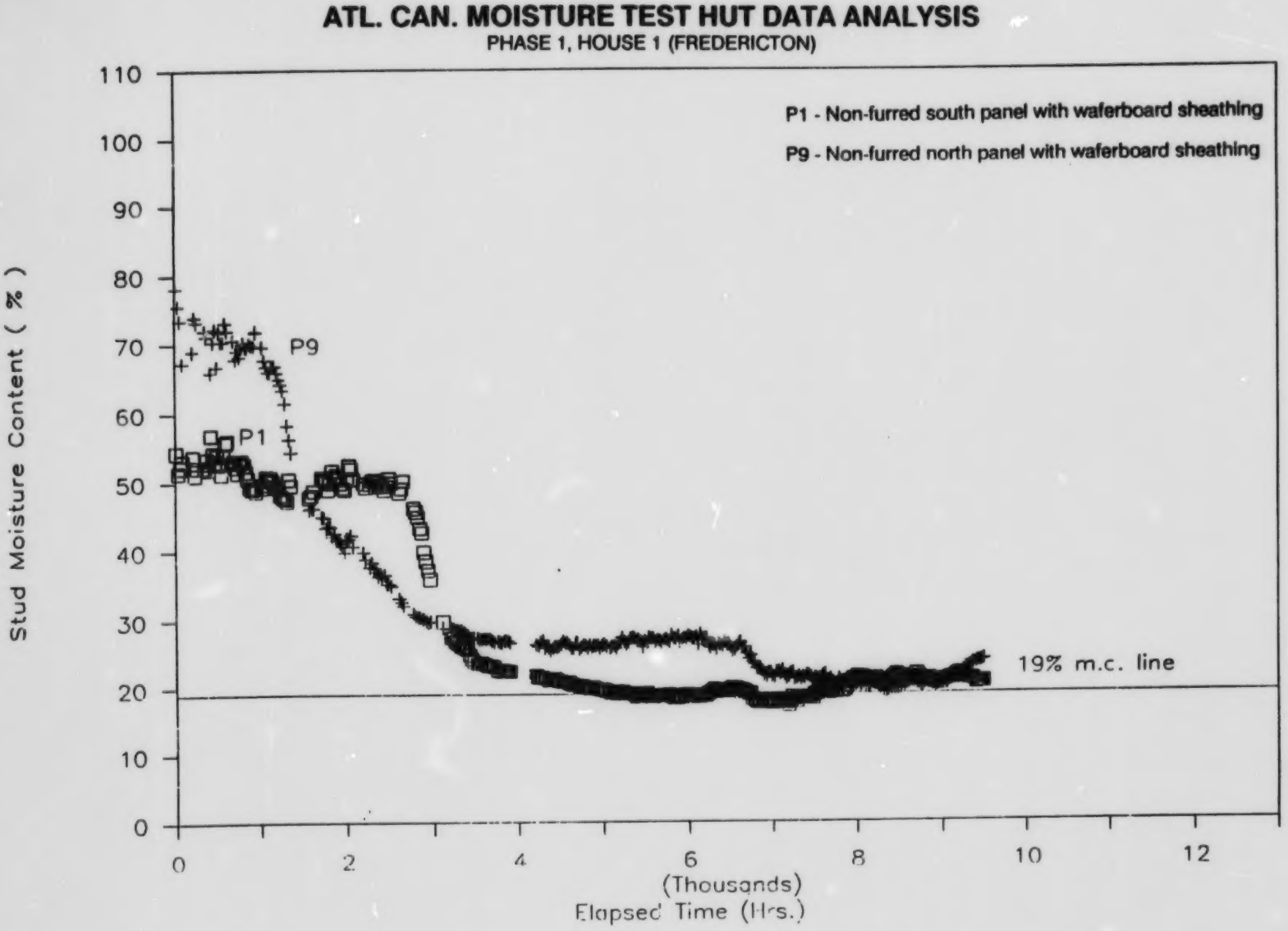
ATL. CAN. MOISTURE TEST HUT DATA ANALYSIS
PHASE 1, HOUSE 1 (FREDERICTON)
P1 - Non-furred south panel with waferboard sheathing
P9 - Non-furred north panel with waferboard sheathing
Stud Moisture Content (%)
110
100
90
80
70
60
50
40
30
20
10
0
P9
P1
19% m.c. line
0
2
4
6
8
10
12
(Thousands)
Elapsed Time (Hrs.)

Figure 17

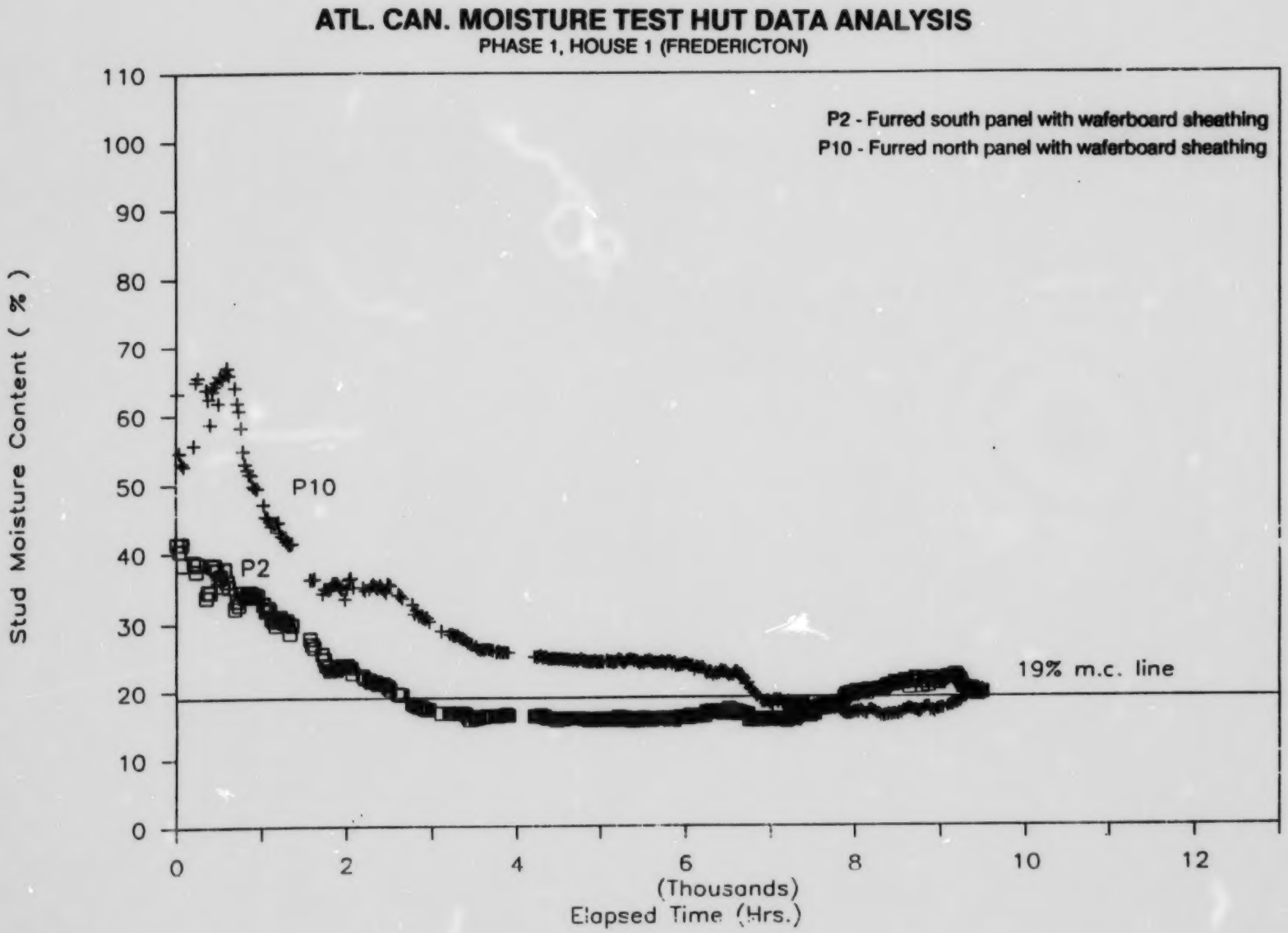
ATL. CAN. MOISTURE TEST HUT DATA ANALYSIS
PHASE 1, HOUSE 1 (FREDERICTON)
P2 - Furred south panel with waferboard sheathing
P10 - Furred north panel with waferboard sheathing
Stud Moisture Content (%)
110
100
90
80
70
60
50
40
30
20
10
0
P10
P2
19% m.c. line
0
2
4
6
8
10
12
(Thousands)
Elapsed Time (Hrs.)

Figure 18

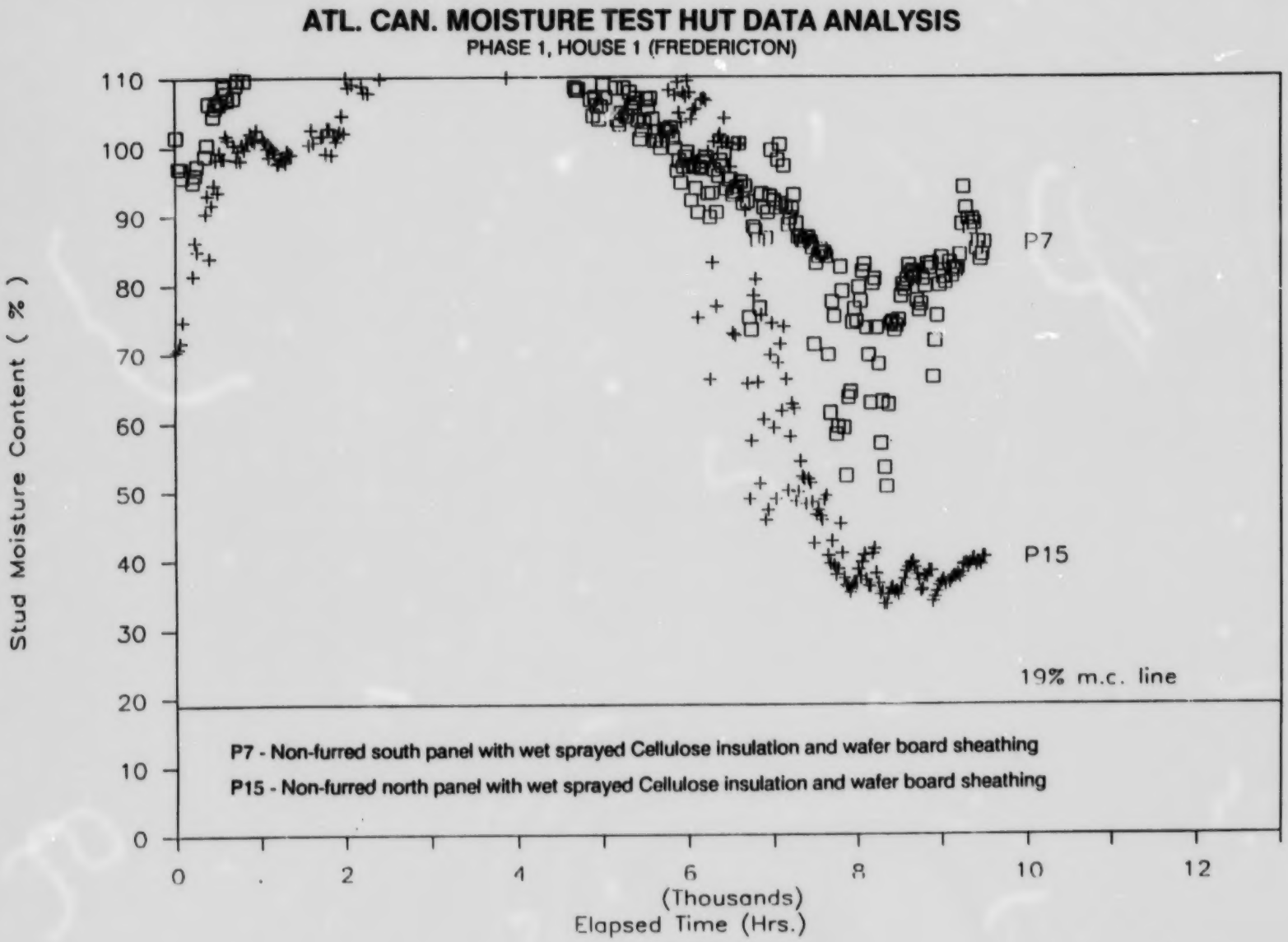
ATL. CAN. MOISTURE TEST HUT DATA ANALYSIS
PHASE 1, HOUSE 1 (FREDERICTON)
Stud Moisture Content (%)
110
100
90
80
70
60
50
40
30
20
10
0
P7
P15
19% m.c. line
P7 - Non-furred south panel with wet sprayed Cellulose insulation and wafer board sheathing
P15 - Non-furred north panel with wet sprayed Cellulose insulation and wafer board sheathing
0
2
4
6
8
10
12
(Thousands)
Elapsed Time (Hrs.)

Figure 19

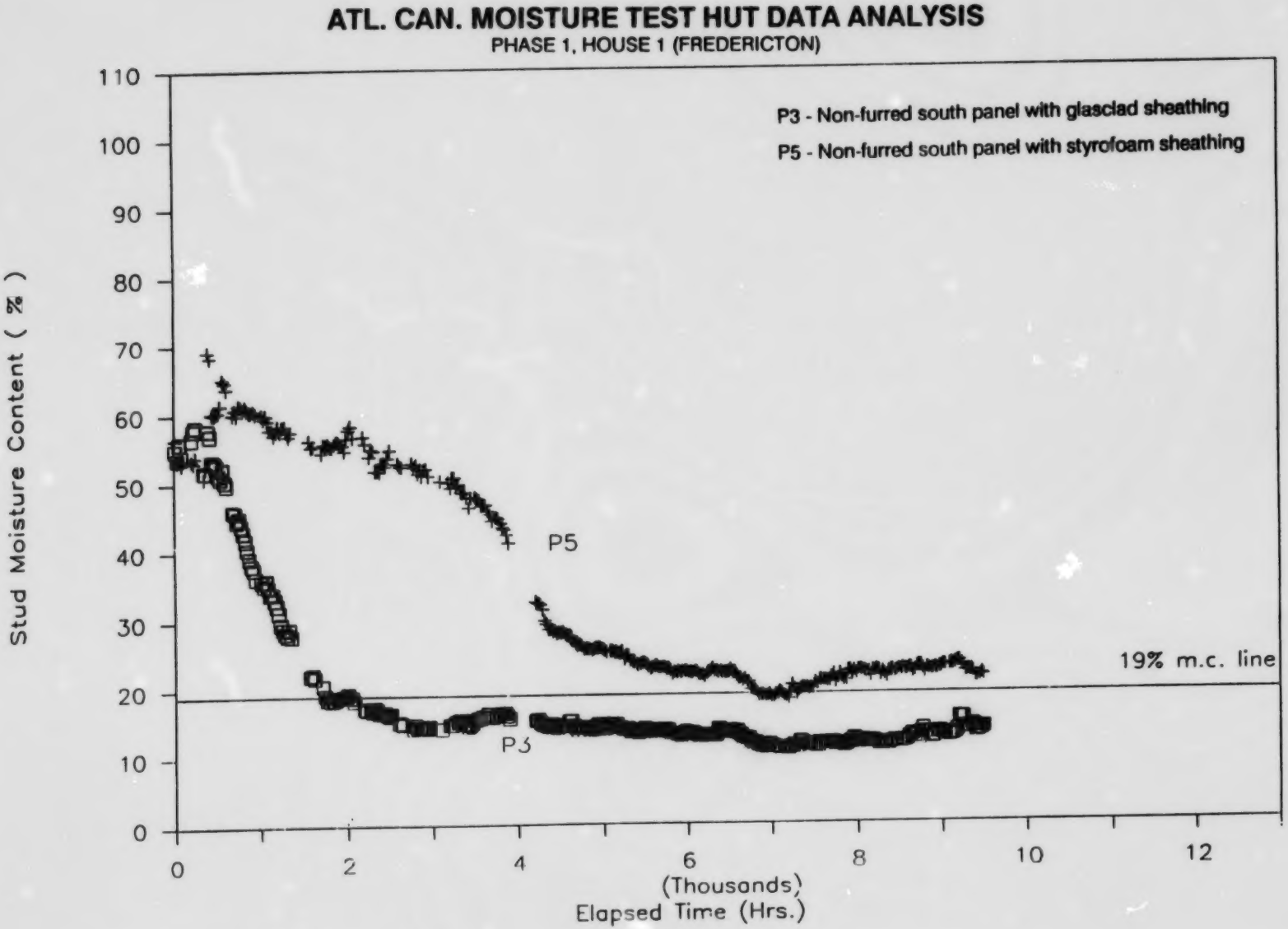
ATL. CAN. MOISTURE TEST HUT DATA ANALYSIS
PHASE 1, HOUSE 1 (FREDERICTON)
P3 - Non-furred south panel with glasclad sheathing
P5 - Non-furred south panel with styrofoam sheathing
Stud Moisture Content (%)
110
100
90
80
70
60
50
40
30
20
10
0
P5
P3
19% m.c. line
0
2
4
6
8
10
12
(Thousands)
Elapsed Time (Hrs.)

Figure 20

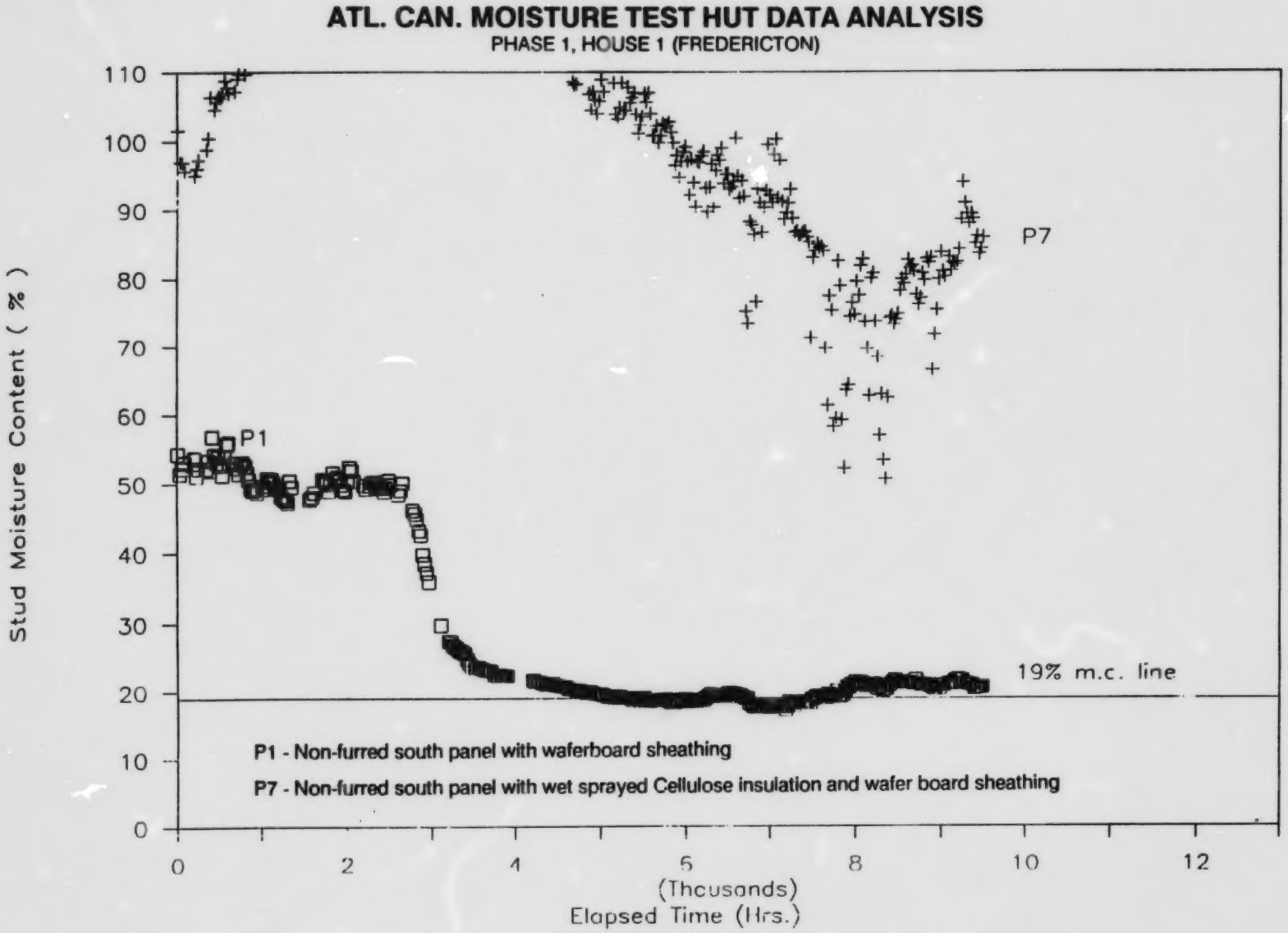
ATL. CAN. MOISTURE TEST HUT DATA ANALYSIS
PHASE 1, HOUSE 1 (FREDERICTON)
Stud Moisture Content (%)
110
100
90
80
70
60
50
40
30
20
10
0
P1
P7
19% m.c. line
P1 - Non-furred south panel with waferboard sheathing
P7 - Non-furred south panel with wet sprayed Cellulose insulation and wafer board sheathing
0
2
4
6
8
10
12
(Thousands)
Elapsed Time (Hrs.)

Figure 21

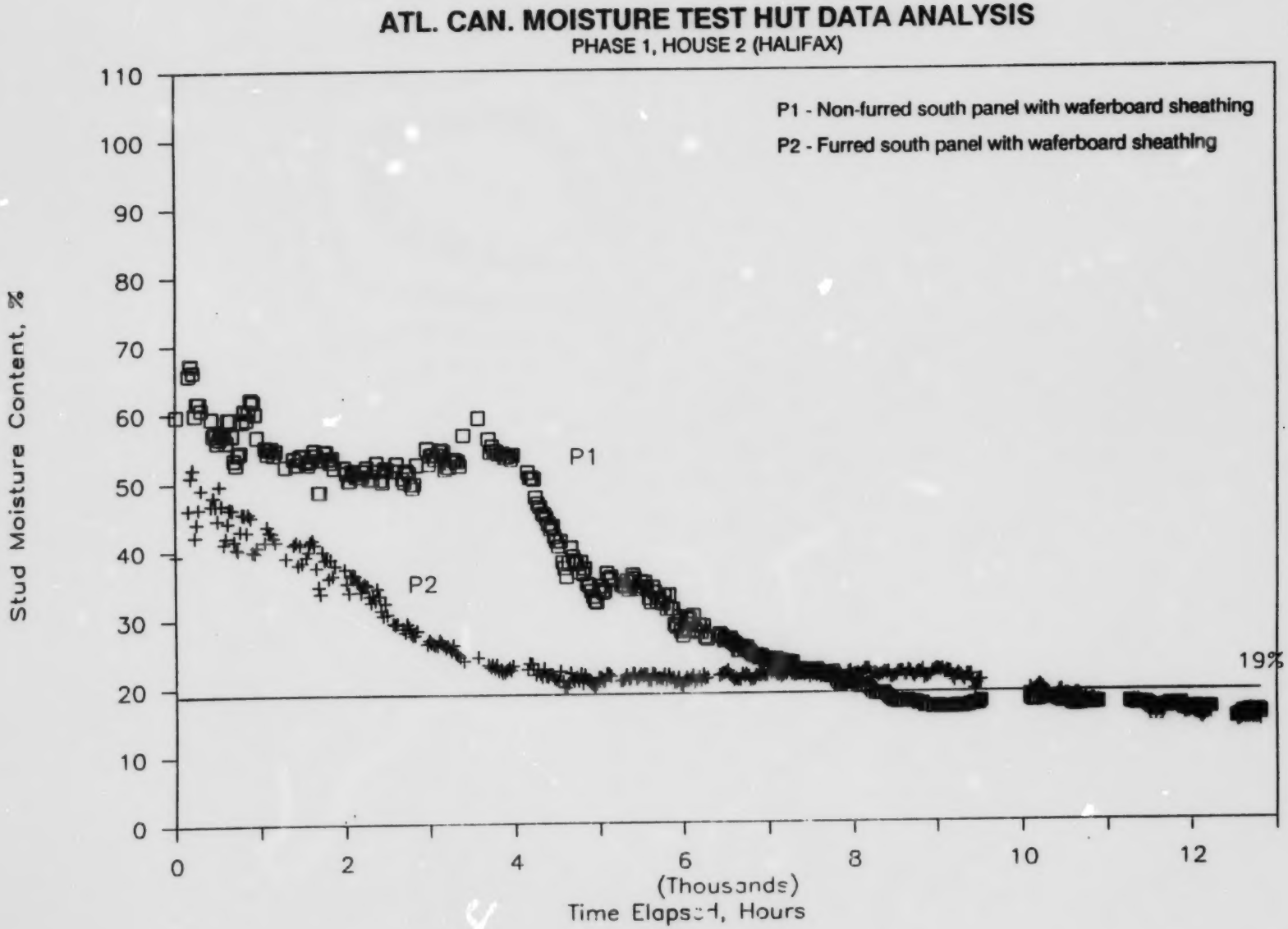
ATL. CAN. MOISTURE TEST HUT DATA ANALYSIS
PHASE 1, HOUSE 2 (HALIFAX)
P1 - Non-furred south panel with waferboard sheathing
P2 - Furred south panel with waferboard sheathing
Stud Moisture Content, %
110
100
90
80
70
60
50
40
30
20
10
0
P1
P2
19%
0
2
4
6
8
10
12
(Thousands)
Time Elapsed, Hours

Figure 22

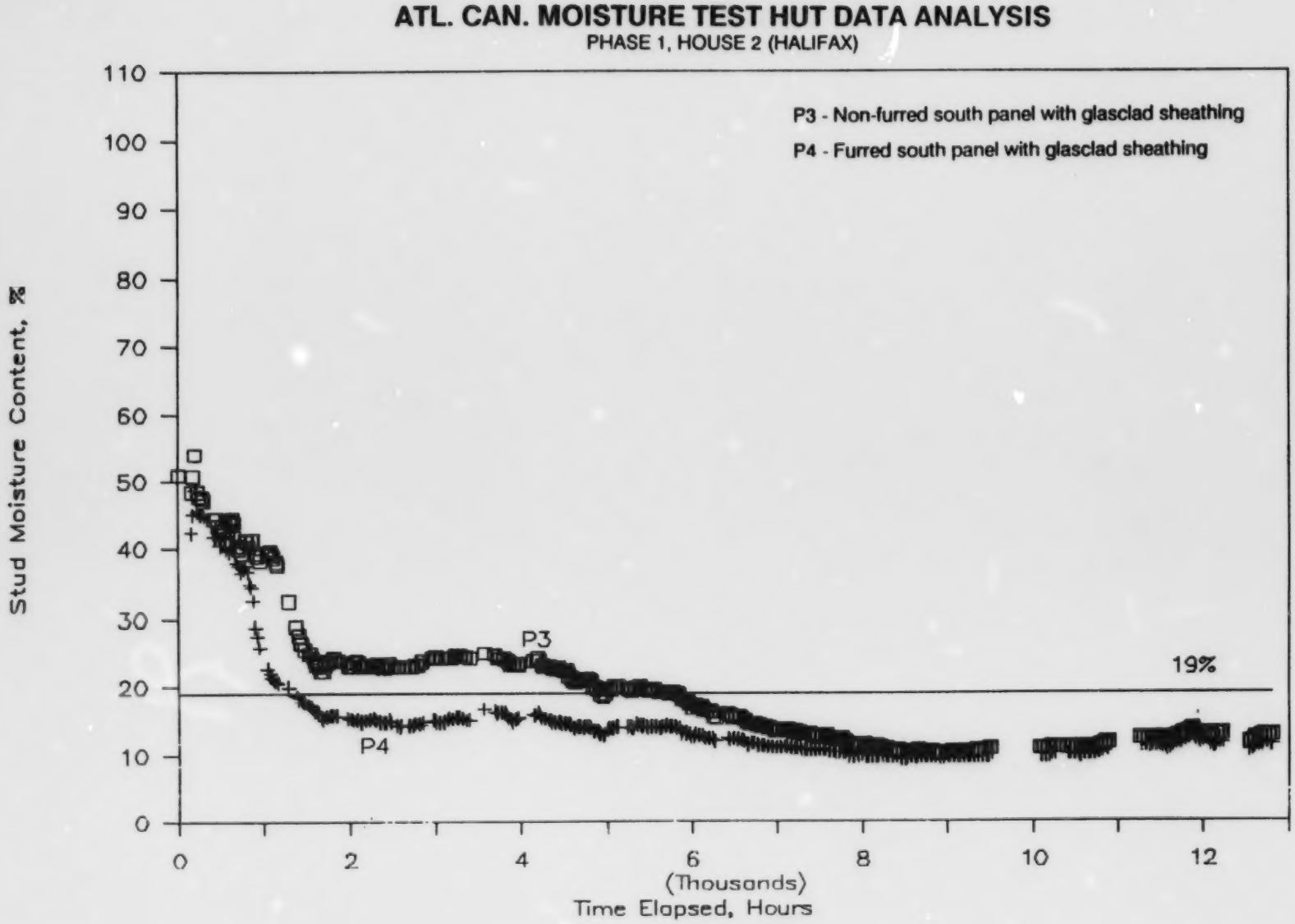
ATL. CAN. MOISTURE TEST HUT DATA ANALYSIS
PHASE 1, HOUSE 2 (HALIFAX)
P3 - Non-furred south panel with glasclad sheathing
P4 - Furred south panel with glasclad sheathing
Stud Moisture Content, %
110
100
90
80
70
60
50
40
30
20
10
0
P3
P4
19%
0
2
4
6
8
10
12
(Thousands)
Time Elapsed, Hours

Figure 23

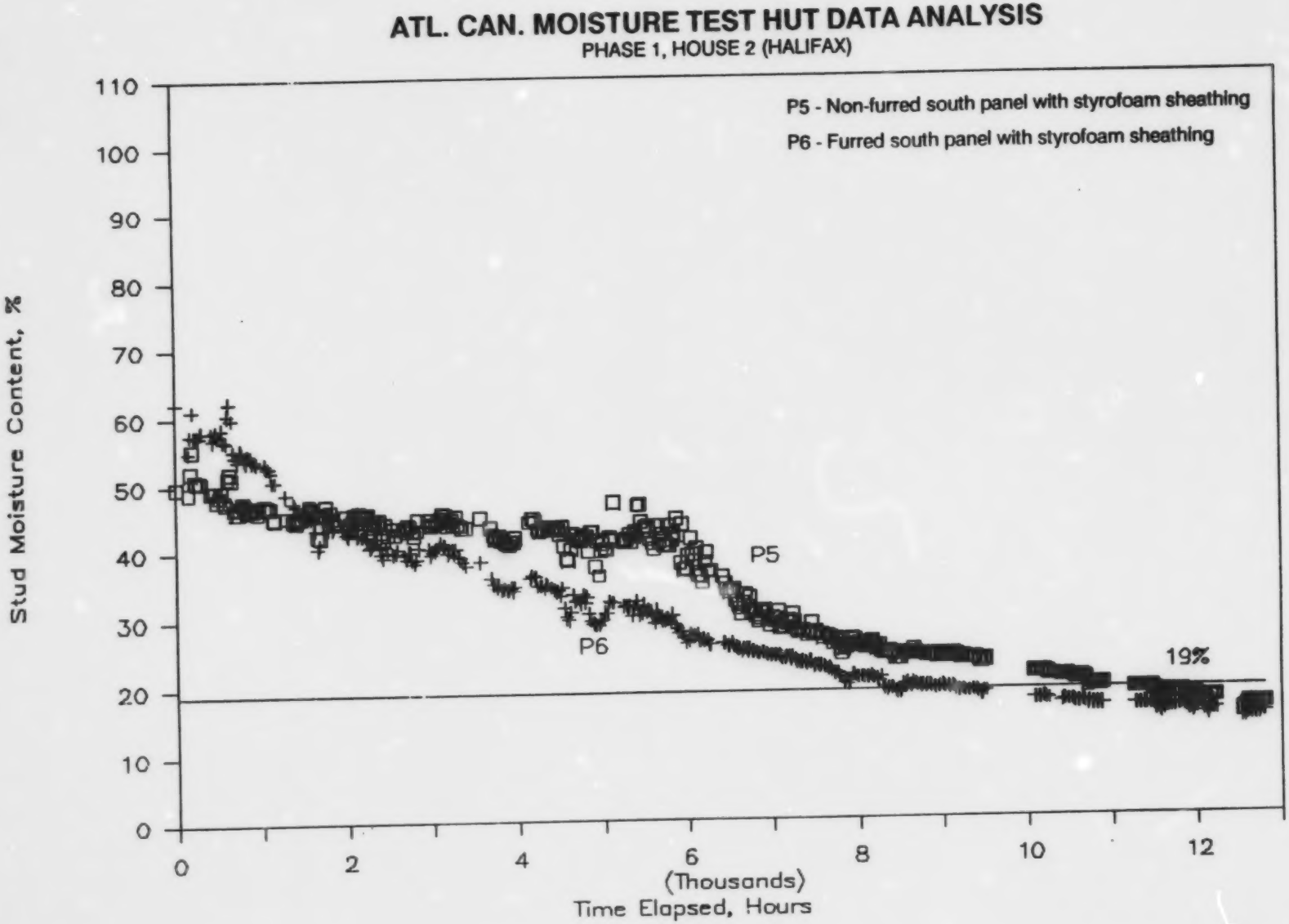
ATL. CAN. MOISTURE TEST HUT DATA ANALYSIS
PHASE 1, HOUSE 2 (HALIFAX)
P5 - Non-furred south panel with styrofoam sheathing
P6 - Furred south panel with styrofoam sheathing
Stud Moisture Content, %
110
100
90
80
70
60
50
40
30
20
10
0
P5
P6
19%
0
2
4
6
8
10
12
(Thousands)
Time Elapsed, Hours

Figure 24

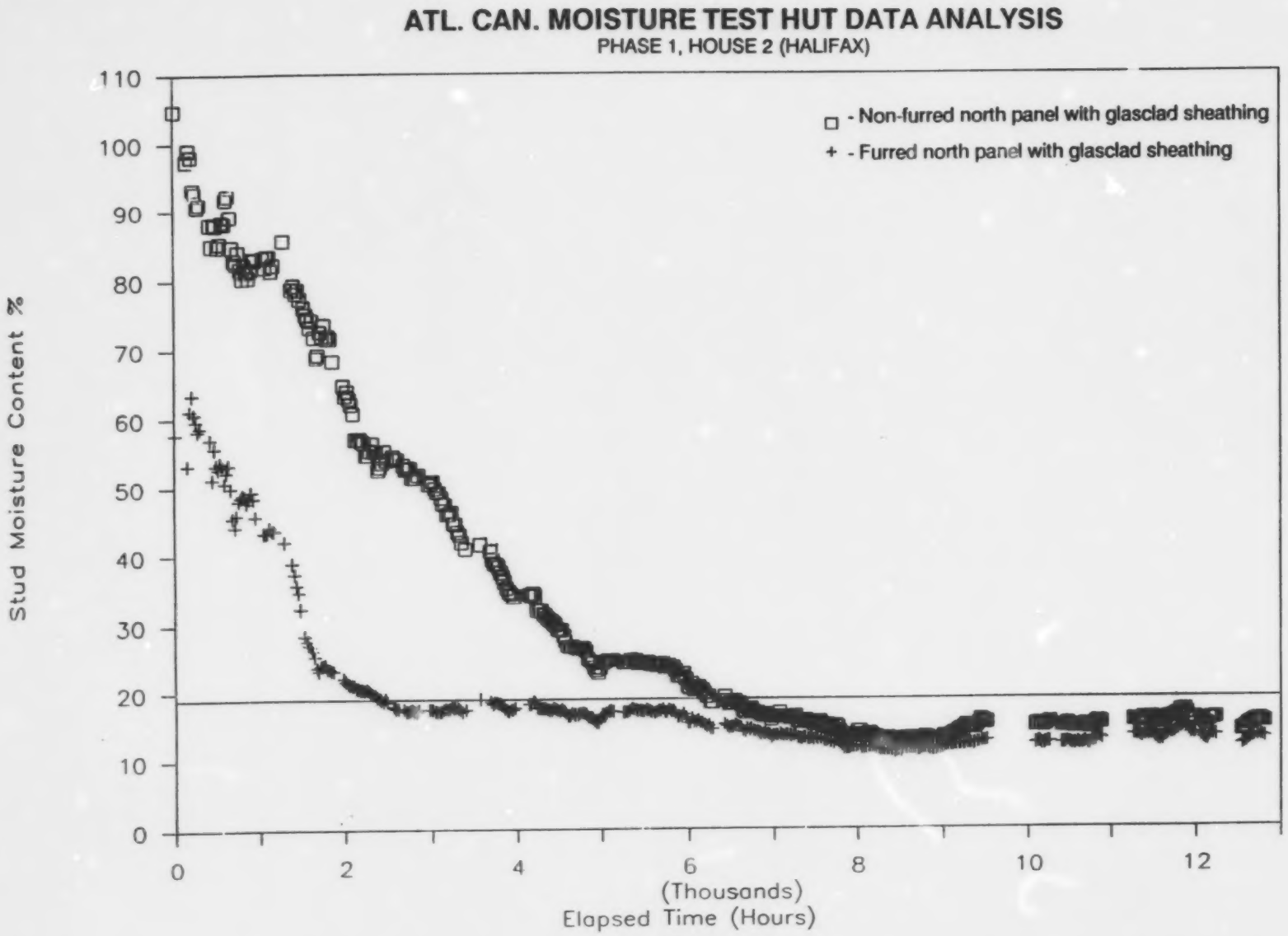
ATL. CAN. MOISTURE TEST HUT DATA ANALYSIS
PHASE 1, HOUSE 2 (HALIFAX)
□ - Non-furred north panel with glasclad sheathing
+ - Furred north panel with glasclad sheathing
Stud Moisture Content %
110
100
90
80
70
60
50
40
30
20
10
0
0
2
4
6
8
10
12
(Thousands)
Elapsed Time (Hours)

Figure 25

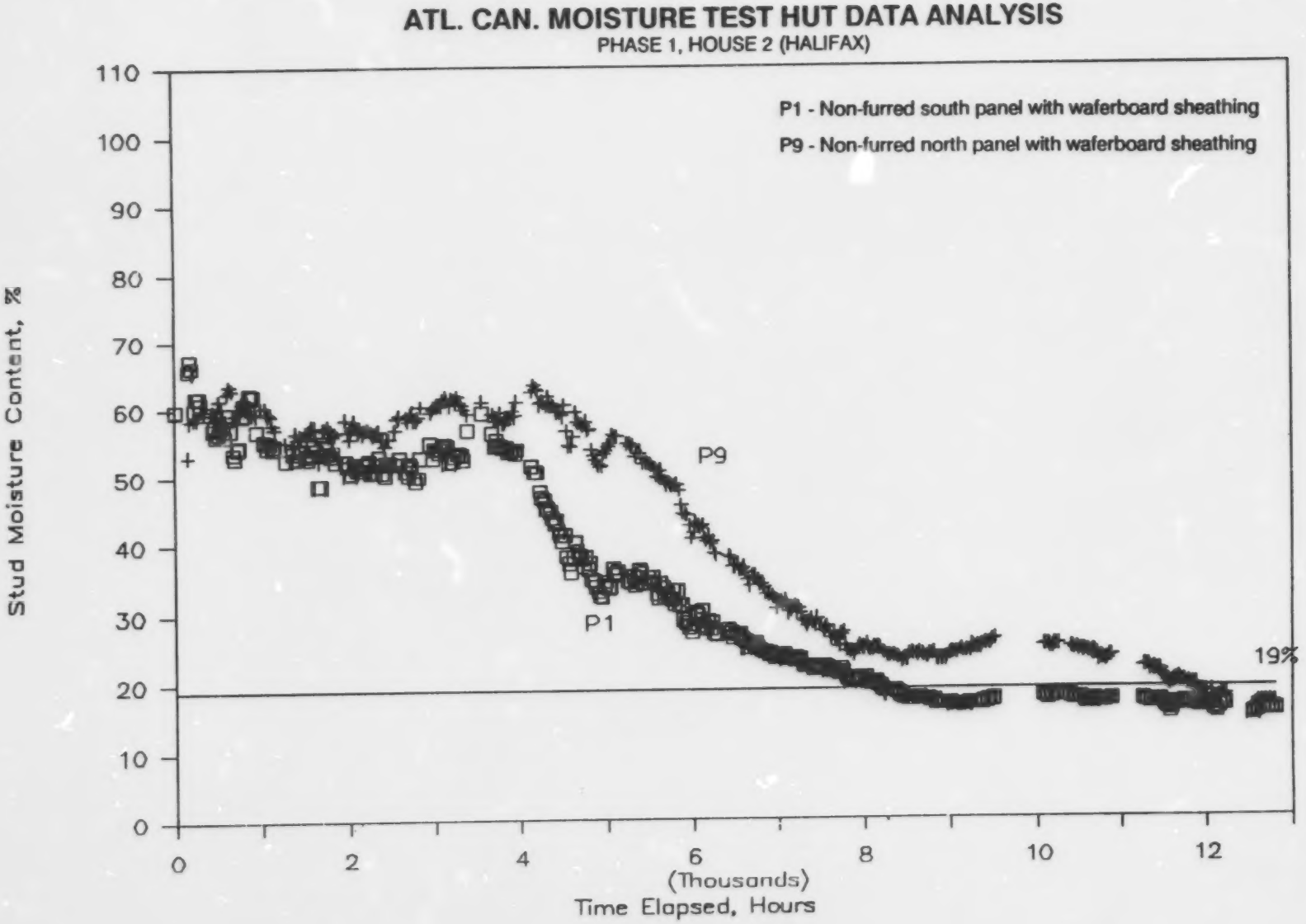
ATL. CAN. MOISTURE TEST HUT DATA ANALYSIS
PHASE 1, HOUSE 2 (HALIFAX)
P1 - Non-furred south panel with waferboard sheathing
P9 - Non-furred north panel with waferboard sheathing
Stud Moisture Content, %
110
100
90
80
70
60
50
40
30
20
10
0
P9
P1
19%
0
2
4
6
8
10
12
(Thousands)
Time Elapsed, Hours

Figure 26

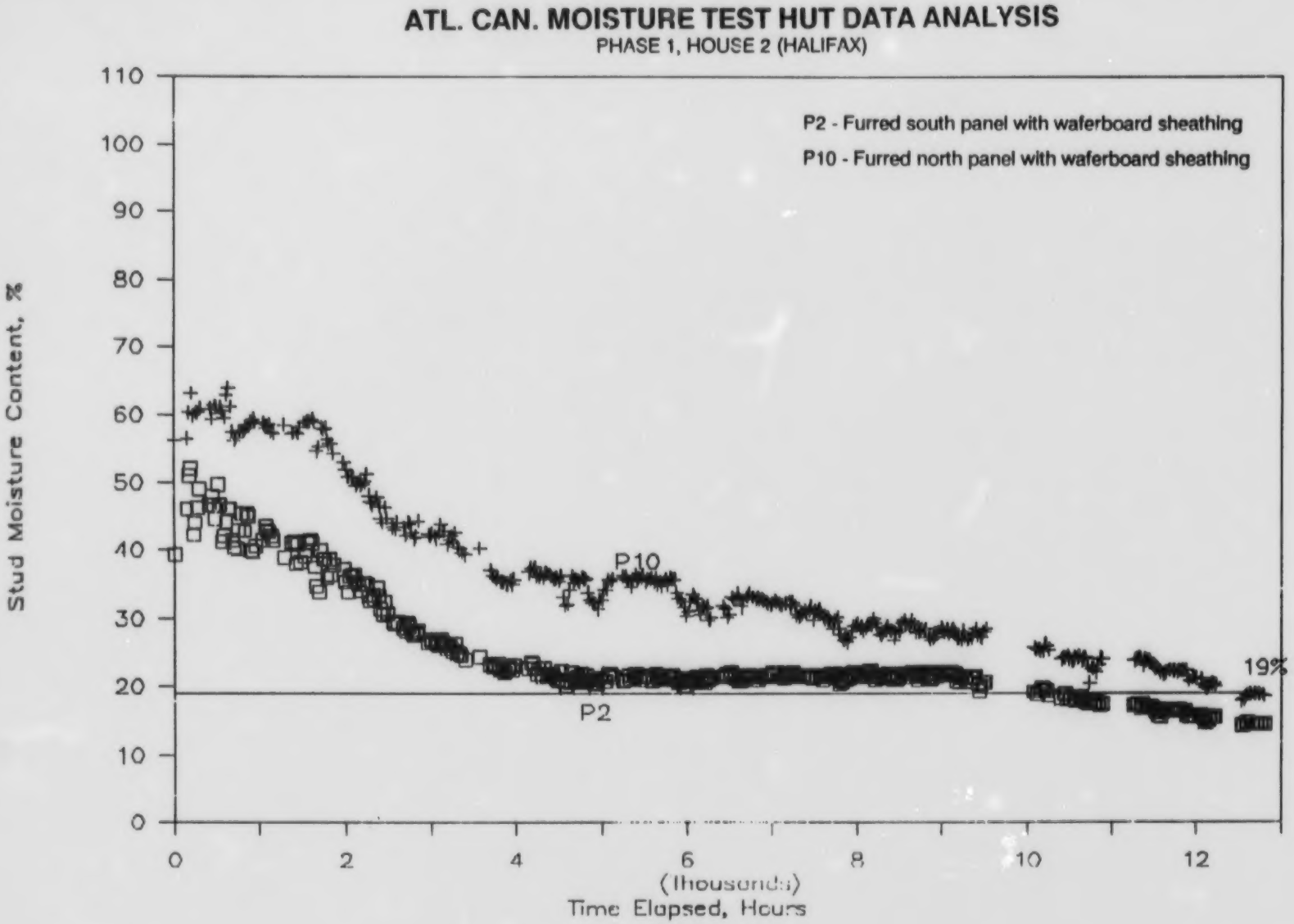
ATL. CAN. MOISTURE TEST HUT DATA ANALYSIS
PHASE 1, HOUSE 2 (HALIFAX)
P2 - Furred south panel with waferboard sheathing
P10 - Furred north panel with waferboard sheathing
Stud Moisture Content, %
110
100
90
80
70
60
50
40
30
20
10
0
P10
P2
19%
0
2
4
6
8
10
12
(Thousands)
Time Elapsed, Hours

Figure 27

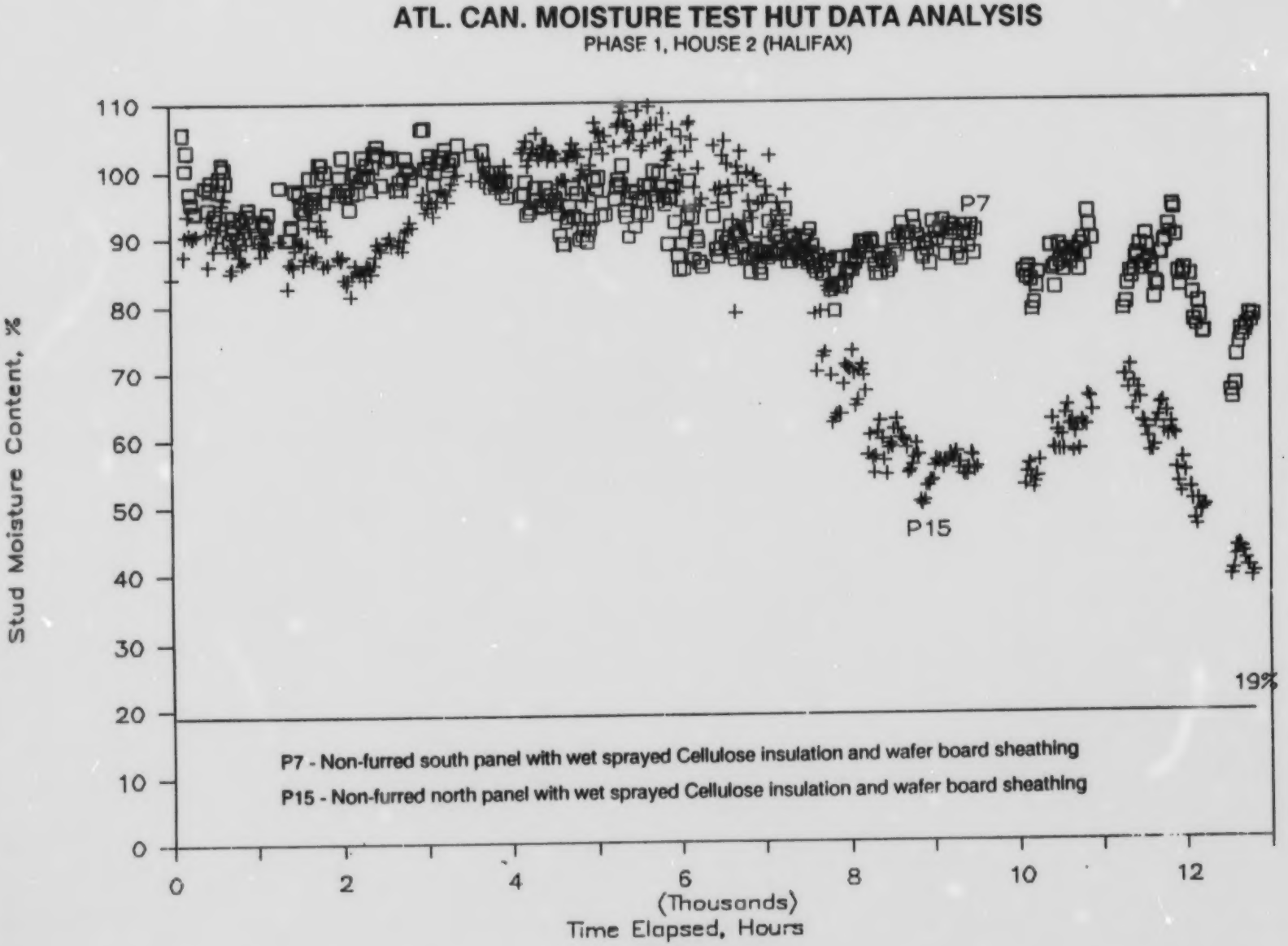
ATL. CAN. MOISTURE TEST HUT DATA ANALYSIS
PHASE 1, HOUSE 2 (HALIFAX)
Stud Moisture Content, %
110
100
90
80
70
60
50
40
30
20
10
0
P7
P15
19%
P7 - Non-furred south panel with wet sprayed Cellulose insulation and wafer board sheathing
P15 - Non-furred north panel with wet sprayed Cellulose insulation and wafer board sheathing
0
2
4
6
8
10
12
(Thousands)
Time Elapsed, Hours

Figure 28

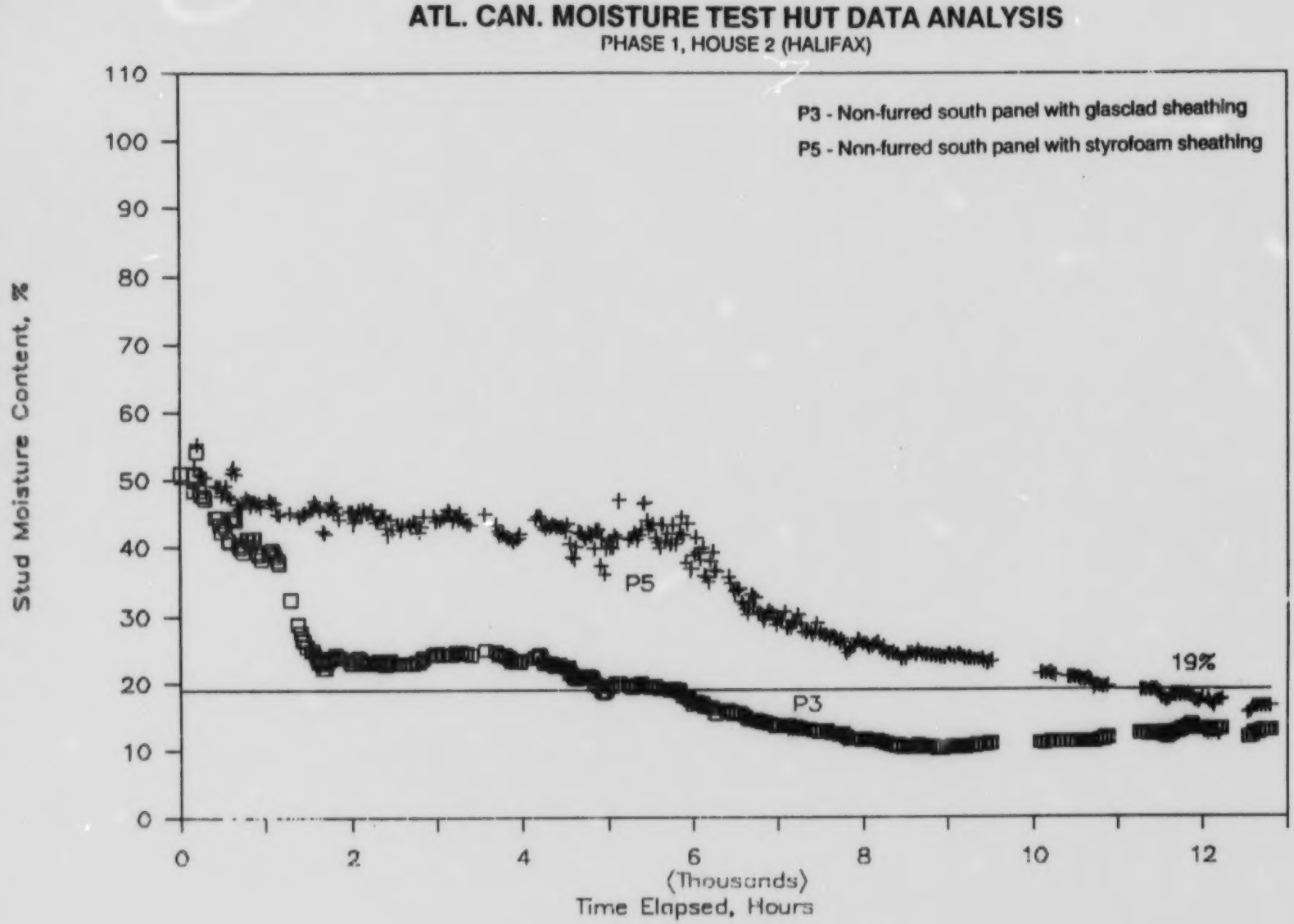
ATL. CAN. MOISTURE TEST HUT DATA ANALYSIS
PHASE 1, HOUSE 2 (HALIFAX)
P3 - Non-furred south panel with glasclad sheathing
P5 - Non-furred south panel with styrofoam sheathing
Stud Moisture Content, %
110
100
90
80
70
60
50
40
30
20
10
0
P5
P3
19%
0
2
4
6
8
10
12
(Thousands)
Time Elapsed, Hours

Figure 29

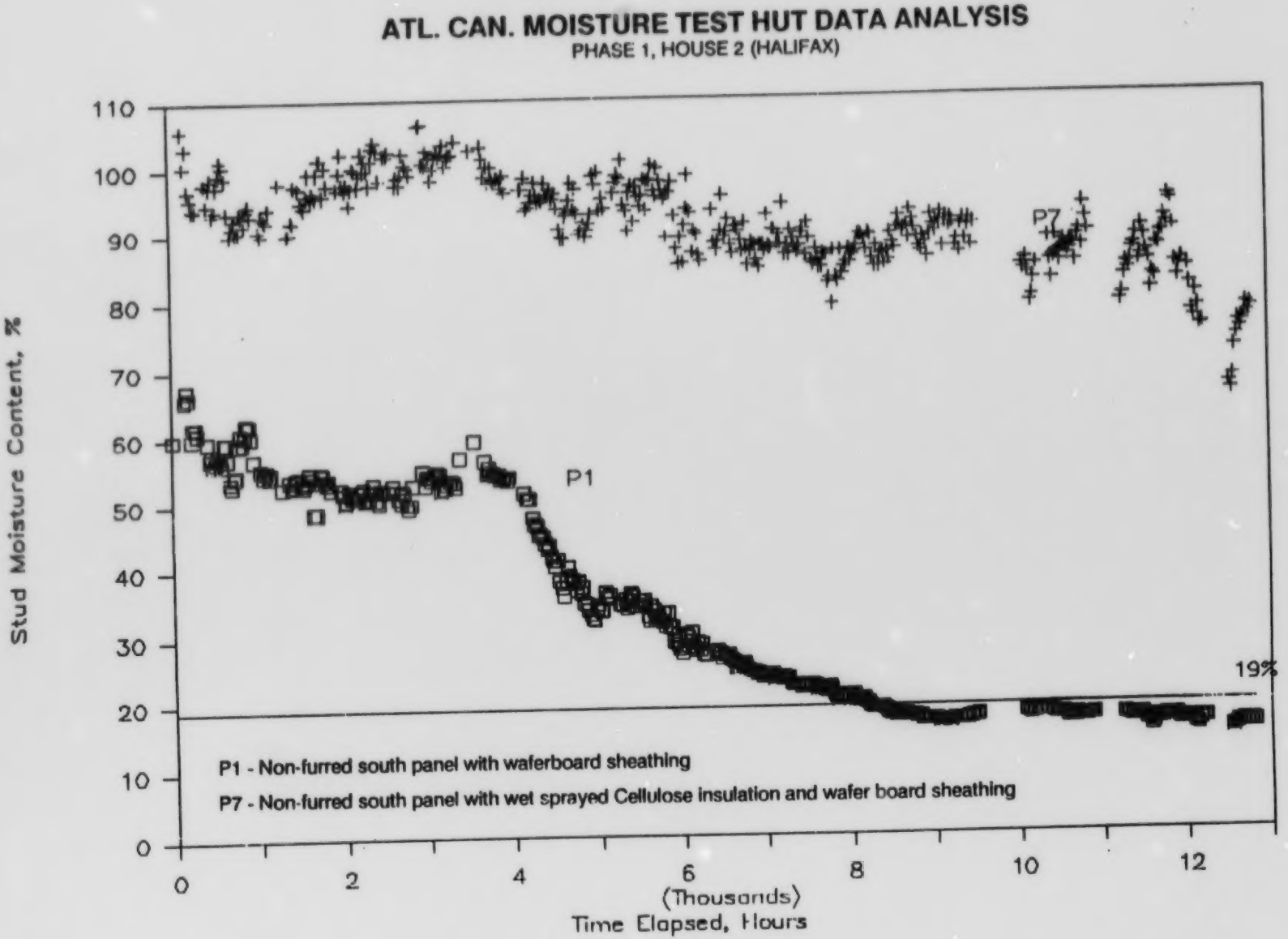
ATL. CAN. MOISTURE TEST HUT DATA ANALYSIS
PHASE 1, HOUSE 2 (HALIFAX)
Stud Moisture Content, %
110
100
90
80
70
60
50
40
30
20
10
0
P7
P1
19%
P1 - Non-furred south panel with waferboard sheathing
P7 - Non-furred south panel with wet sprayed Cellulose insulation and wafer board sheathing
0
2
4
6
8
10
12
(Thousands)
Time Elapsed, Hours

Figure 30

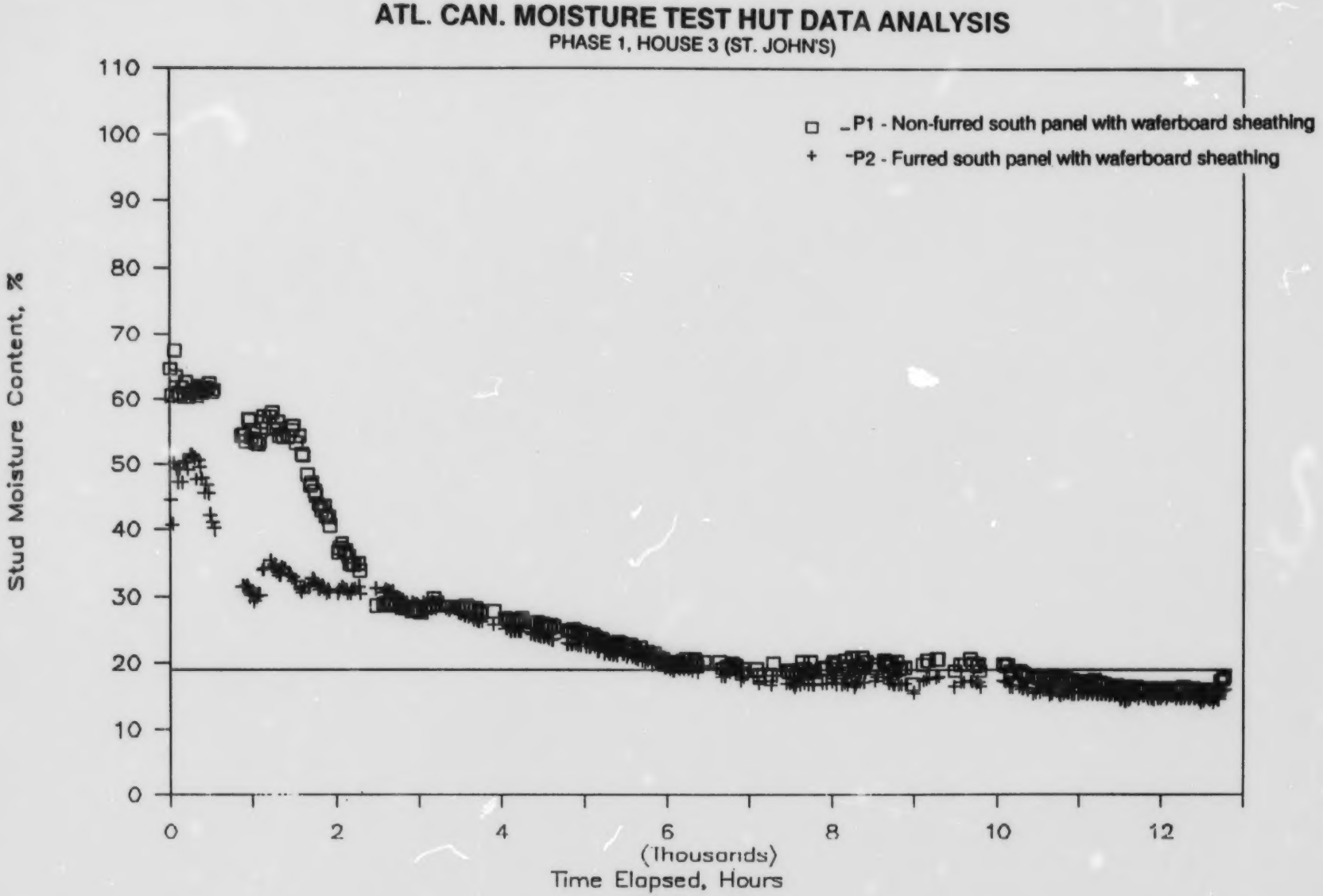
ATL. CAN. MOISTURE TEST HUT DATA ANALYSIS
PHASE 1, HOUSE 3 (ST. JOHN'S)
P1 - Non-furred south panel with waferboard sheathing
P2 - Furred south panel with waferboard sheathing
Stud Moisture Content, %
110
100
90
80
70
60
50
40
30
20
10
0
0
2
4
6
8
10
12
(Thousands)
Time Elapsed, Hours

Figure 31

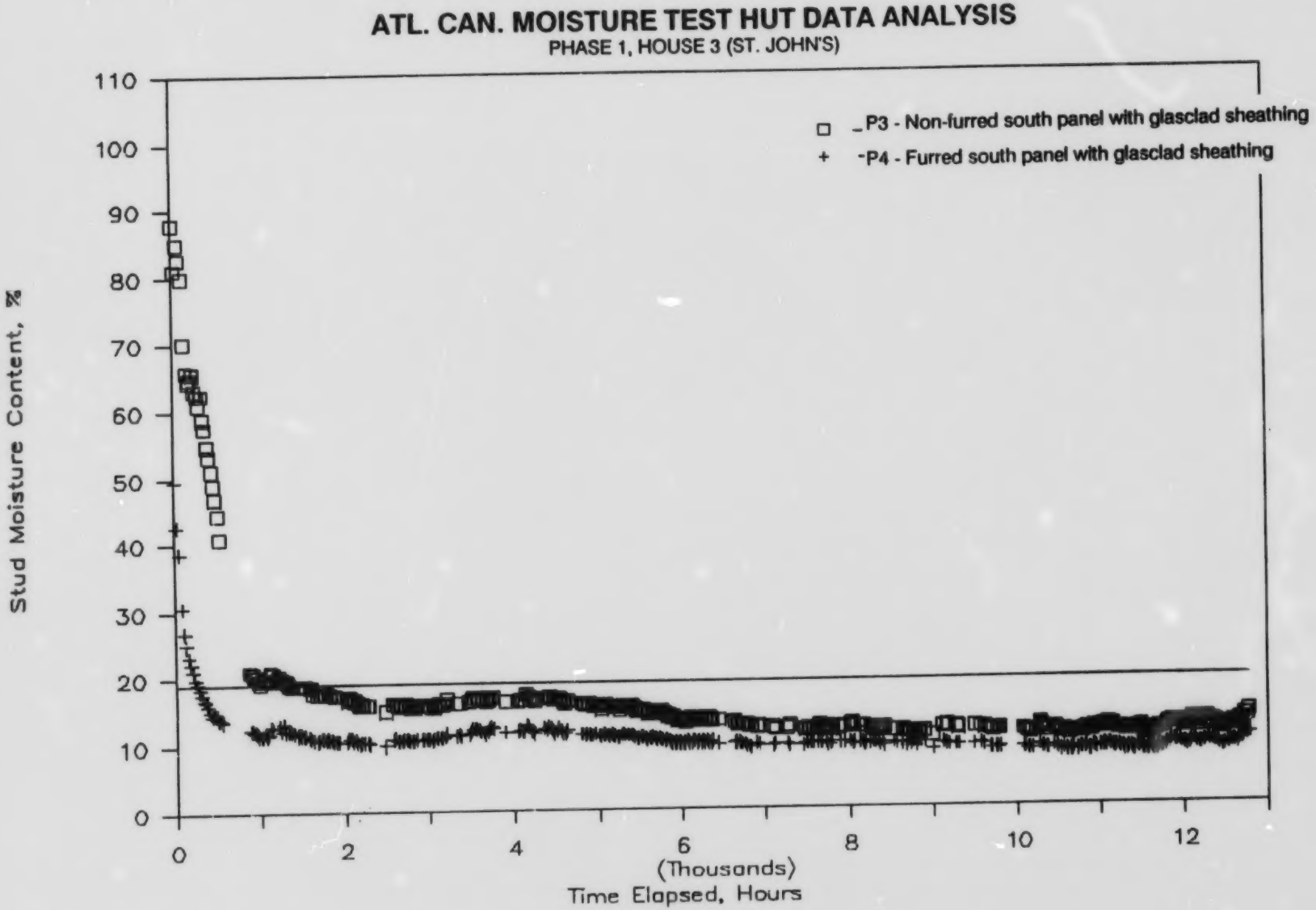
ATL. CAN. MOISTURE TEST HUT DATA ANALYSIS
PHASE 1, HOUSE 3 (ST. JOHN'S)
P3 - Non-furred south panel with glasclad sheathing
P4 - Furred south panel with glasclad sheathing
Stud Moisture Content, %
110
100
90
80
70
60
50
40
30
20
10
0
0
2
4
6
8
10
12
(Thousands)
Time Elapsed, Hours

Figure 32

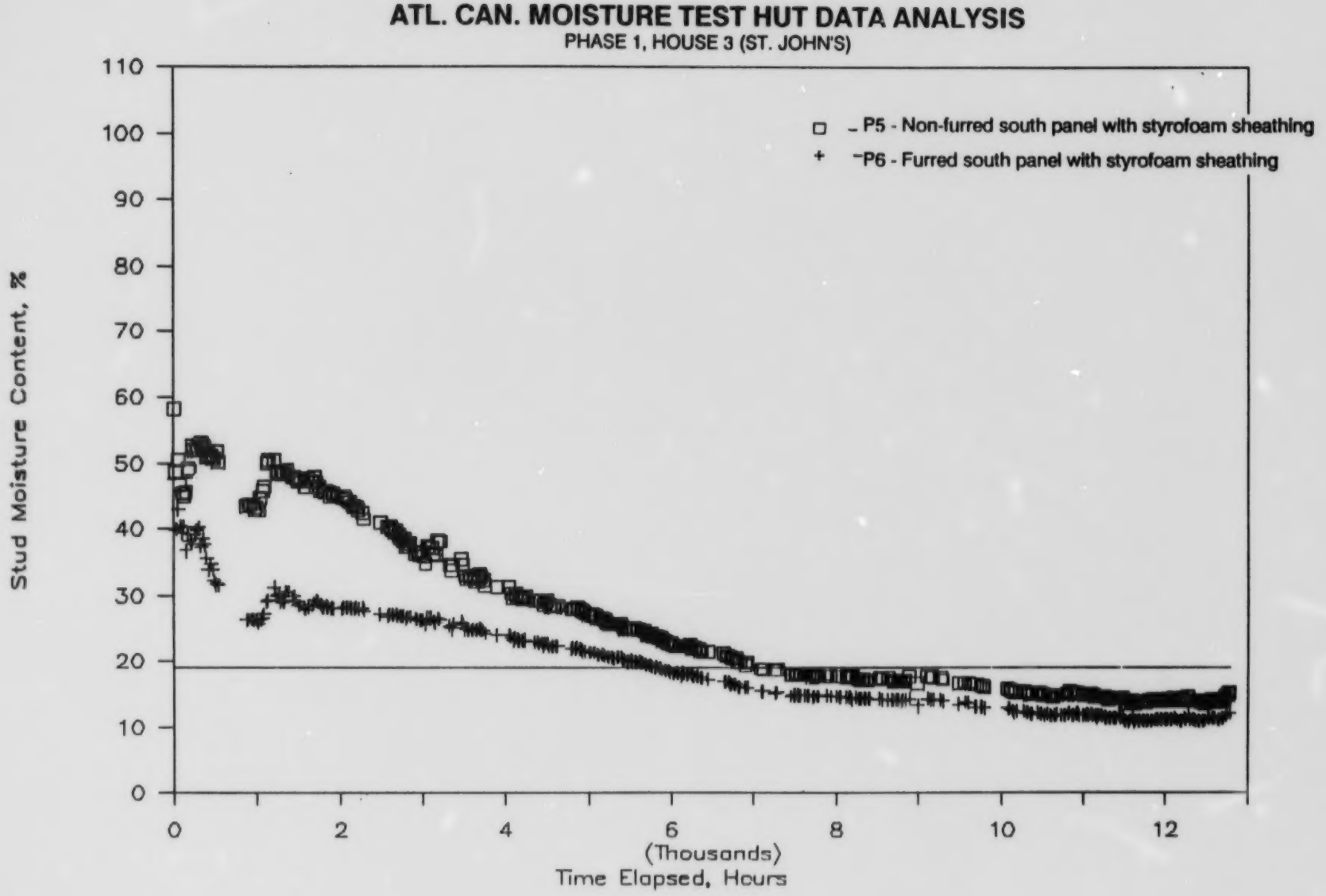
ATL. CAN. MOISTURE TEST HUT DATA ANALYSIS
PHASE 1, HOUSE 3 (ST. JOHN'S)
P5 - Non-furred south panel with styrofoam sheathing
P6 - Furred south panel with styrofoam sheathing
Stud Moisture Content, %
110
100
90
80
70
60
50
40
30
20
10
0
0
2
4
6
8
10
12
(Thousands)
Time Elapsed, Hours

Figure 33

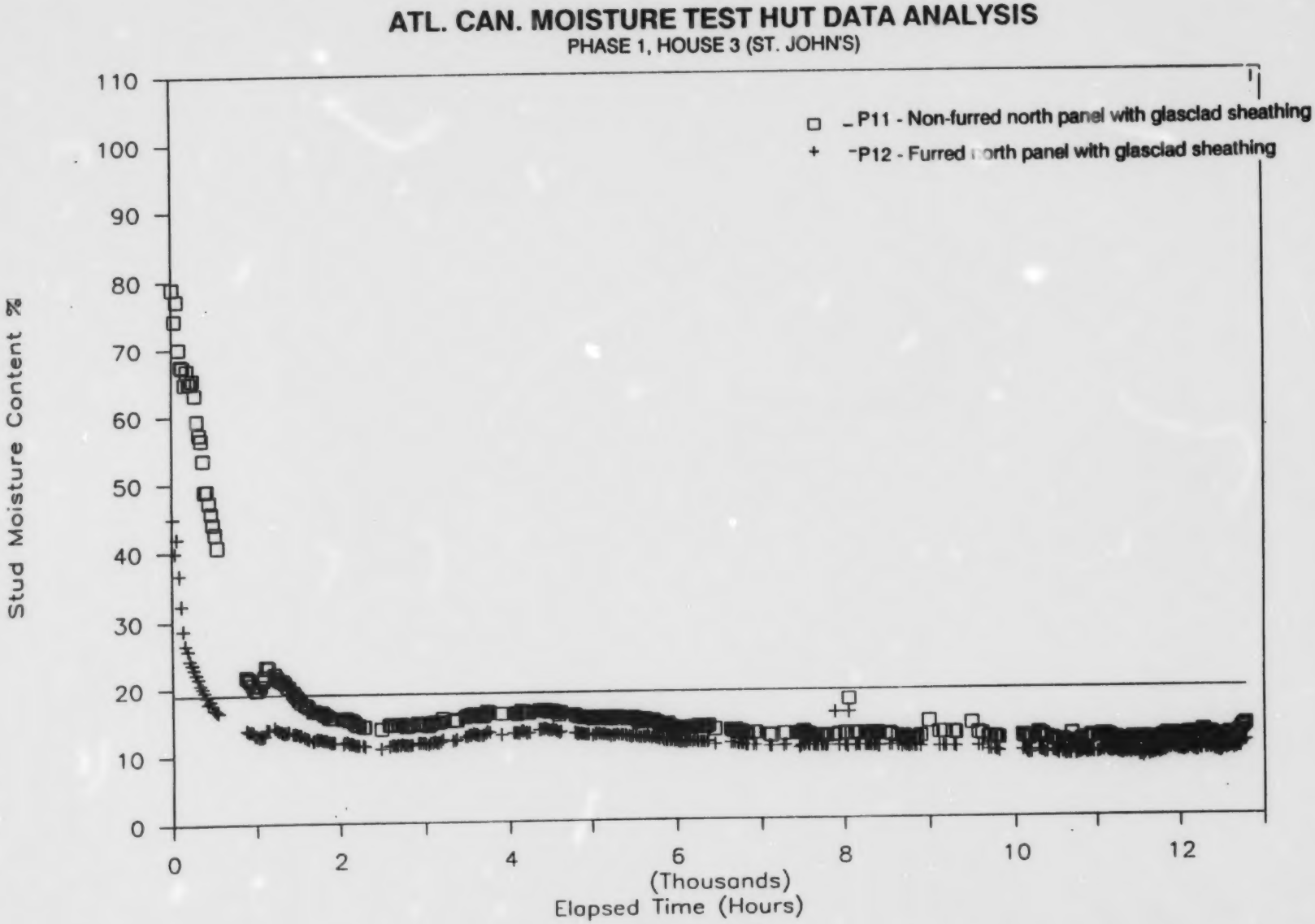
ATL. CAN. MOISTURE TEST HUT DATA ANALYSIS
PHASE 1, HOUSE 3 (ST. JOHN'S)
P11 - Non-furred north panel with glasclad sheathing
P12 - Furred north panel with glasclad sheathing
Stud Moisture Content %
110
100
90
80
70
60
50
40
30
20
10
0
0
2
4
6
8
10
12
(Thousands)
Elapsed Time (Hours)

Figure 34

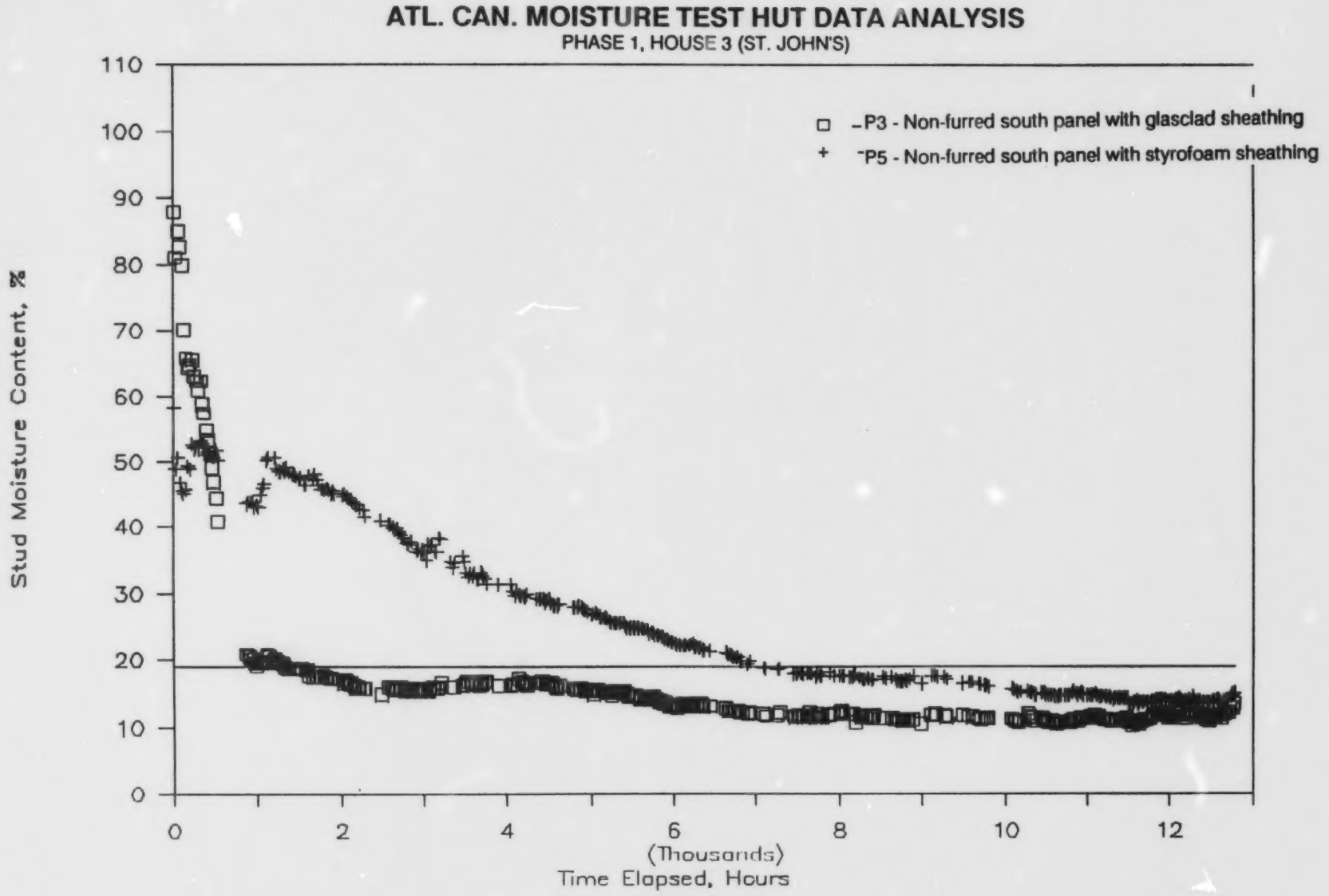
ATL. CAN. MOISTURE TEST HUT DATA ANALYSIS
PHASE 1, HOUSE 3 (ST. JOHN'S)
P3 - Non-furred south panel with glasclad sheathing
P5 - Non-furred south panel with styrofoam sheathing
Stud Moisture Content, %
110
100
90
80
70
60
50
40
30
20
10
0
0
2
4
6
8
10
12
(Thousands)
Time Elapsed, Hours

Figure 35

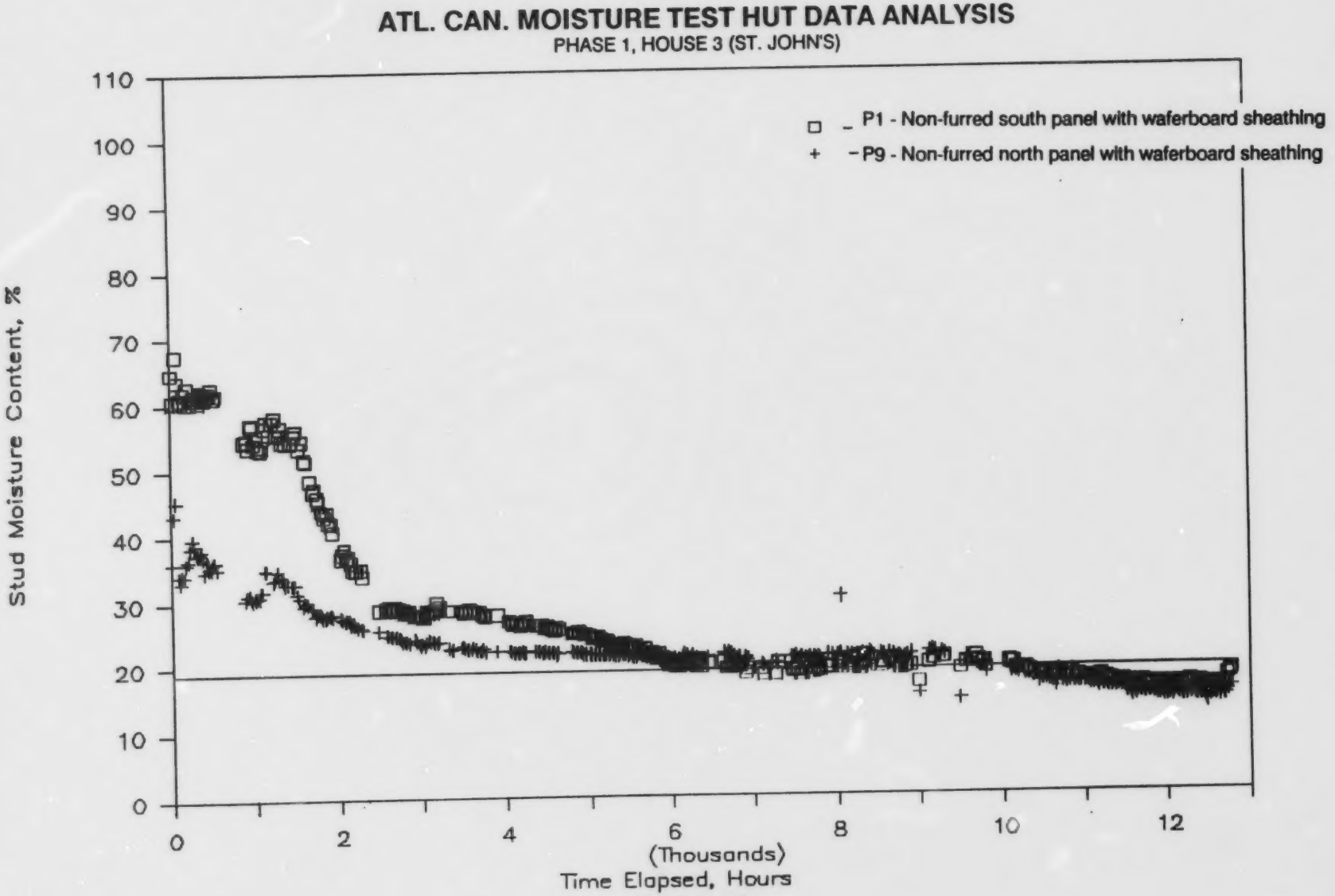
ATL. CAN. MOISTURE TEST HUT DATA ANALYSIS
PHASE 1, HOUSE 3 (ST. JOHN'S)
P1 - Non-furred south panel with waferboard sheathing
P9 - Non-furred north panel with waferboard sheathing
Stud Moisture Content, %
110
100
90
80
70
60
50
40
30
20
10
0
0
2
4
6
8
10
12
(Thousands)
Time Elapsed, Hours

Figure 36

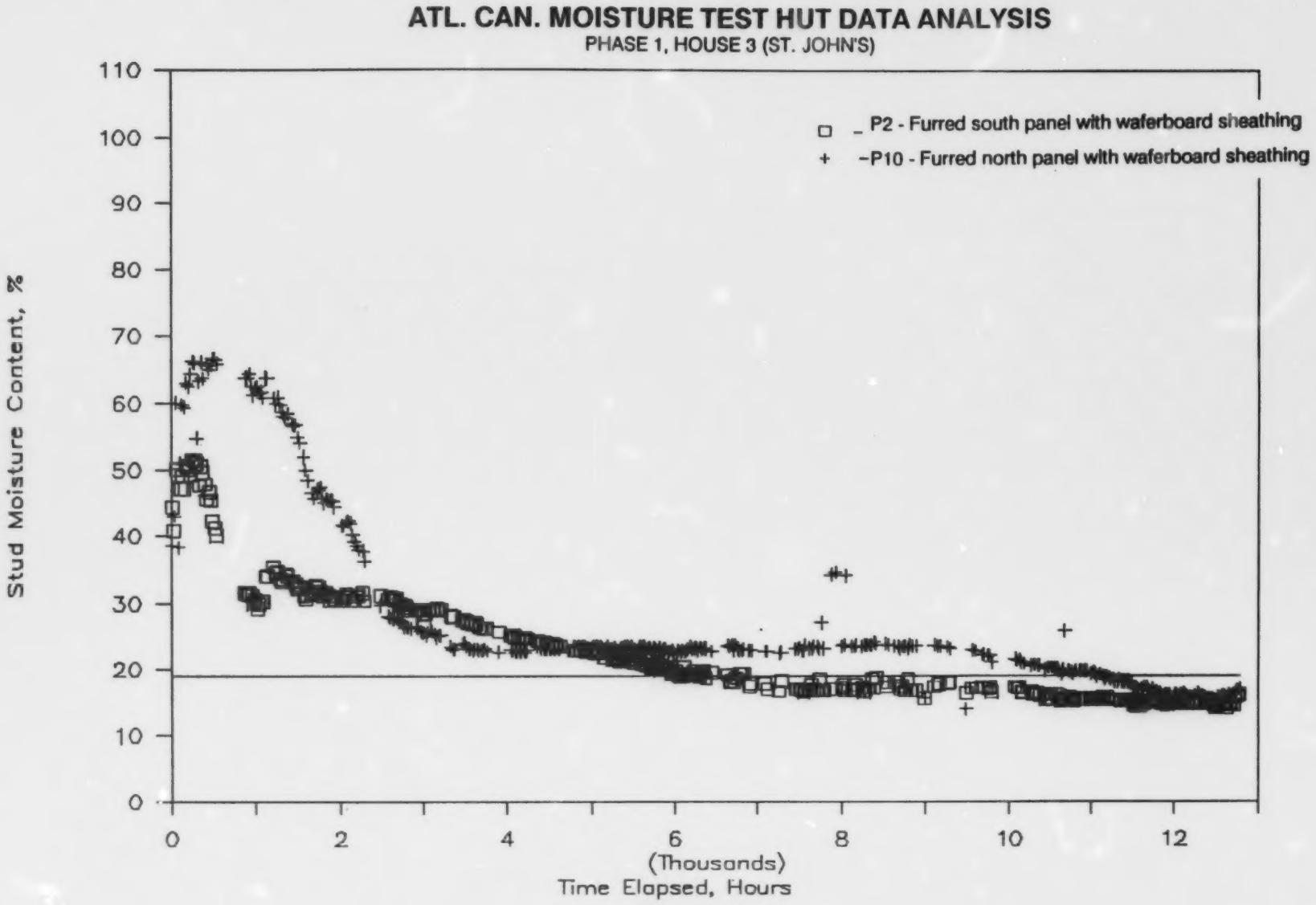
ATL. CAN. MOISTURE TEST HUT DATA ANALYSIS
PHASE 1, HOUSE 3 (ST. JOHN'S)
P2 - Furred south panel with waferboard sheathing
P10 - Furred north panel with waferboard sheathing
Stud Moisture Content, %
110
100
90
80
70
60
50
40
30
20
10
0
0
2
4
6
8
10
12
(Thousands)
Time Elapsed, Hours

Figure 37

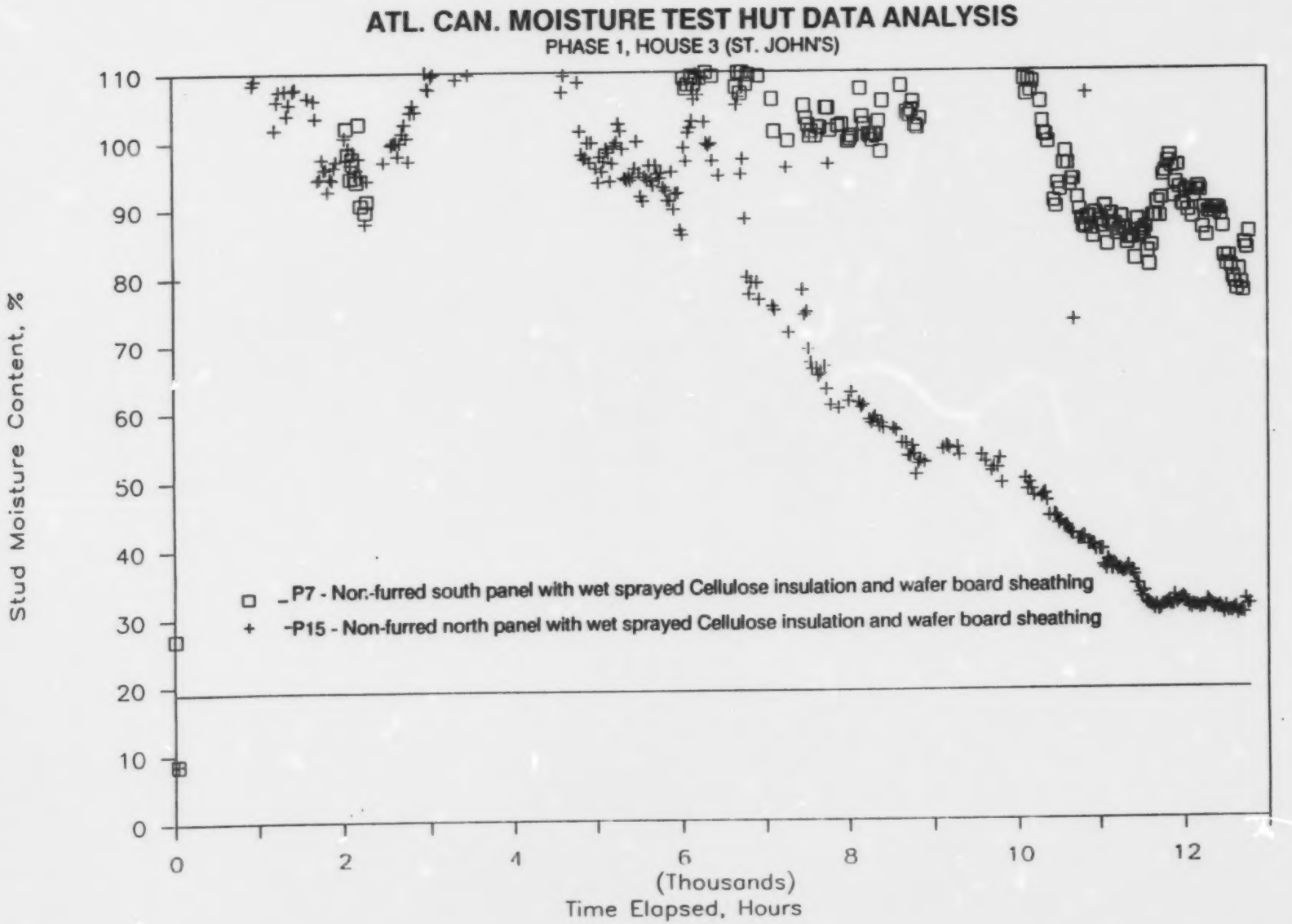
ATL. CAN. MOISTURE TEST HUT DATA ANALYSIS
PHASE 1, HOUSE 3 (ST. JOHN'S)
Stud Moisture Content, %
110
100
90
80
70
60
50
40
30
20
10
0
0
2
4
6
8
10
12
(Thousands)
Time Elapsed, Hours
P7 - Nor:-furred south panel with wet sprayed Cellulose insulation and wafer board sheathing
P15 - Non-furred north panel with wet sprayed Cellulose insulation and wafer board sheathing

Figure 38

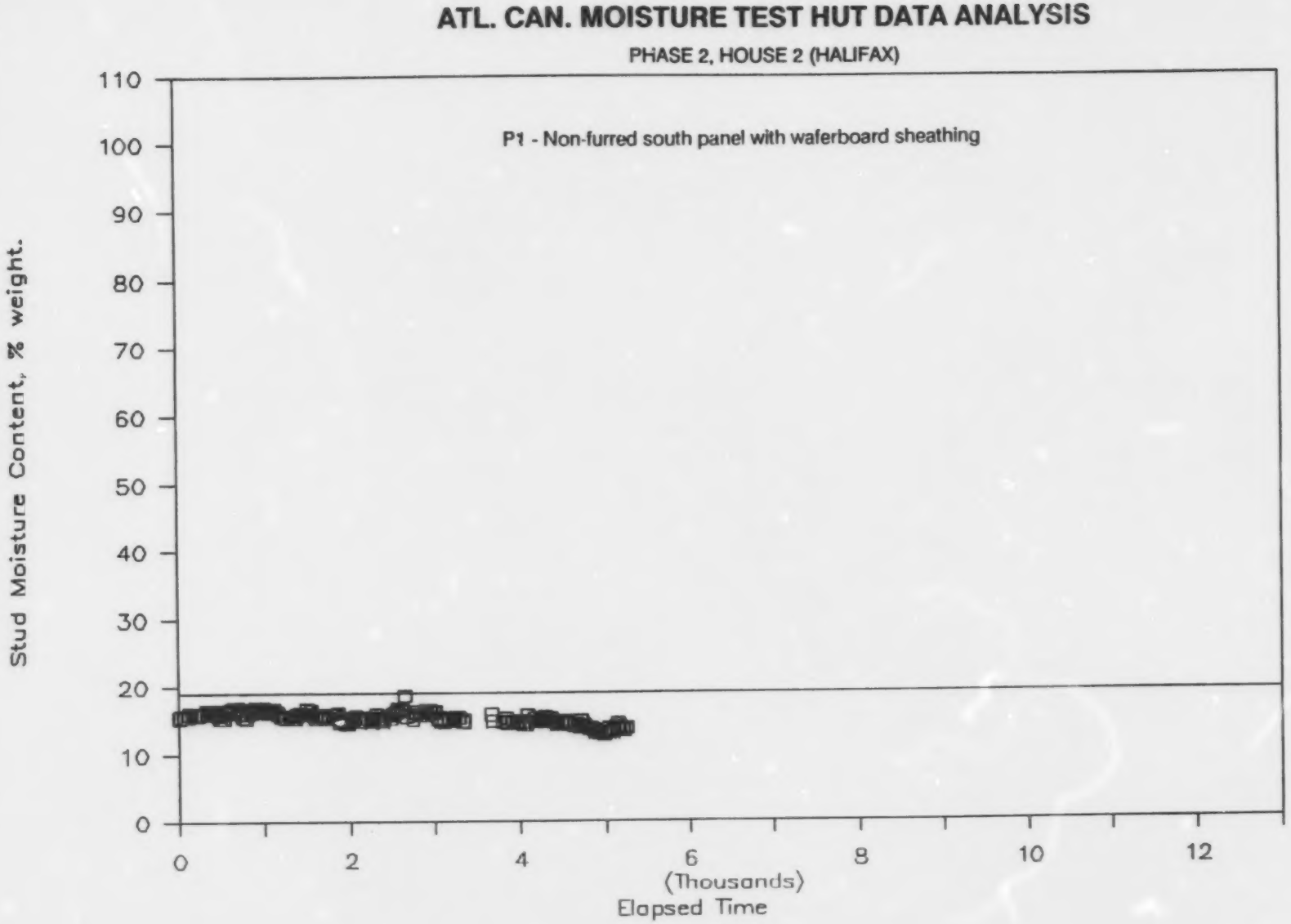
ATL. CAN. MOISTURE TEST HUT DATA ANALYSIS
PHASE 2, HOUSE 2 (HALIFAX)
P1 - Non-furred south panel with waferboard sheathing
Stud Moisture Content, % weight.
110
100
90
80
70
60
50
40
30
20
10
0
0
2
4
6
8
10
12
(Thousands)
Elapsed Time

Figure 39

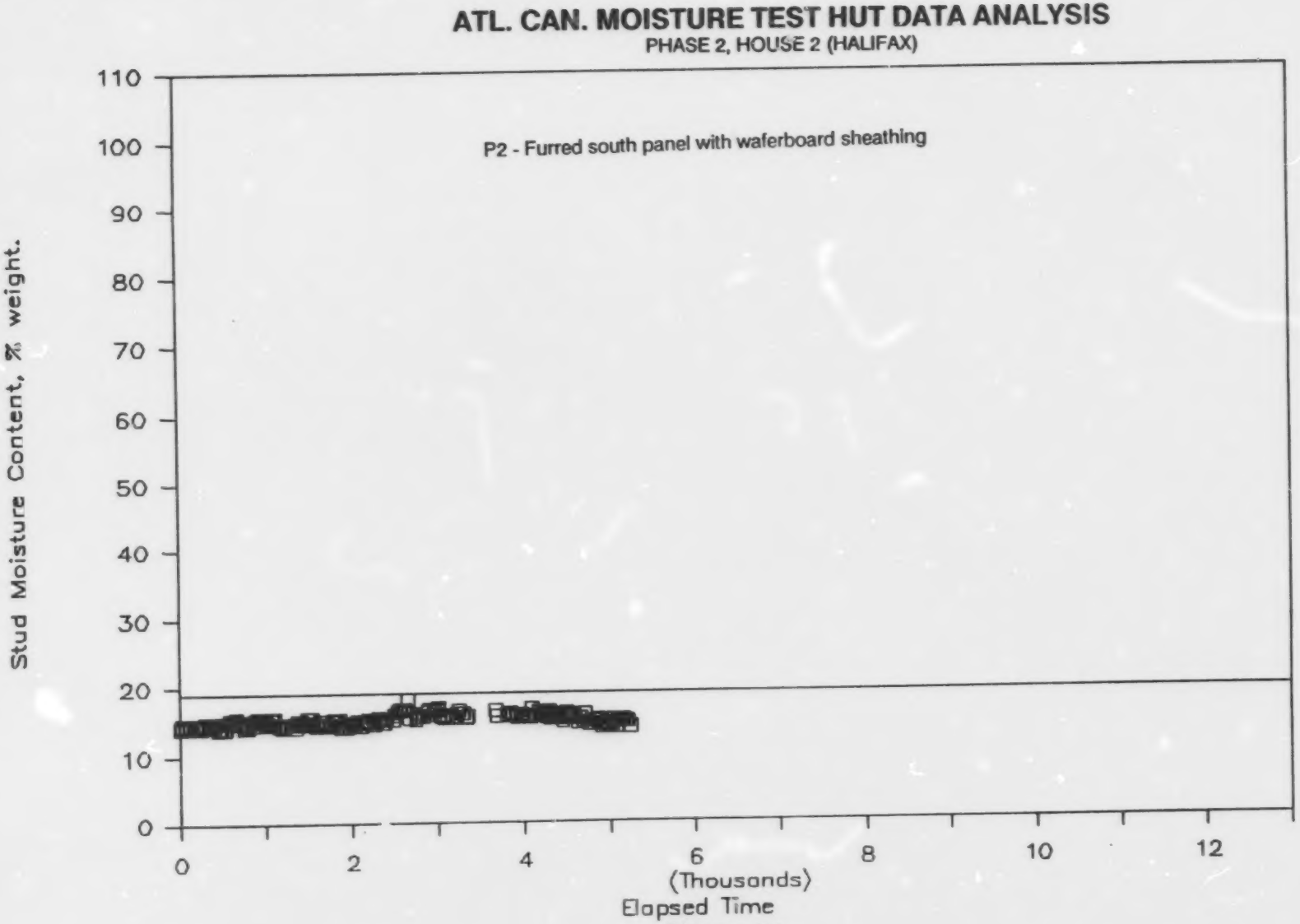
ATL. CAN. MOISTURE TEST HUT DATA ANALYSIS
PHASE 2, HOUSE 2 (HALIFAX)
P2 - Furred south panel with waferboard sheathing
Stud Moisture Content, % weight.
110
100
90
80
70
60
50
40
30
20
10
0
0
2
4
6
8
10
12
(Thousands)
Elapsed Time

Figure 40

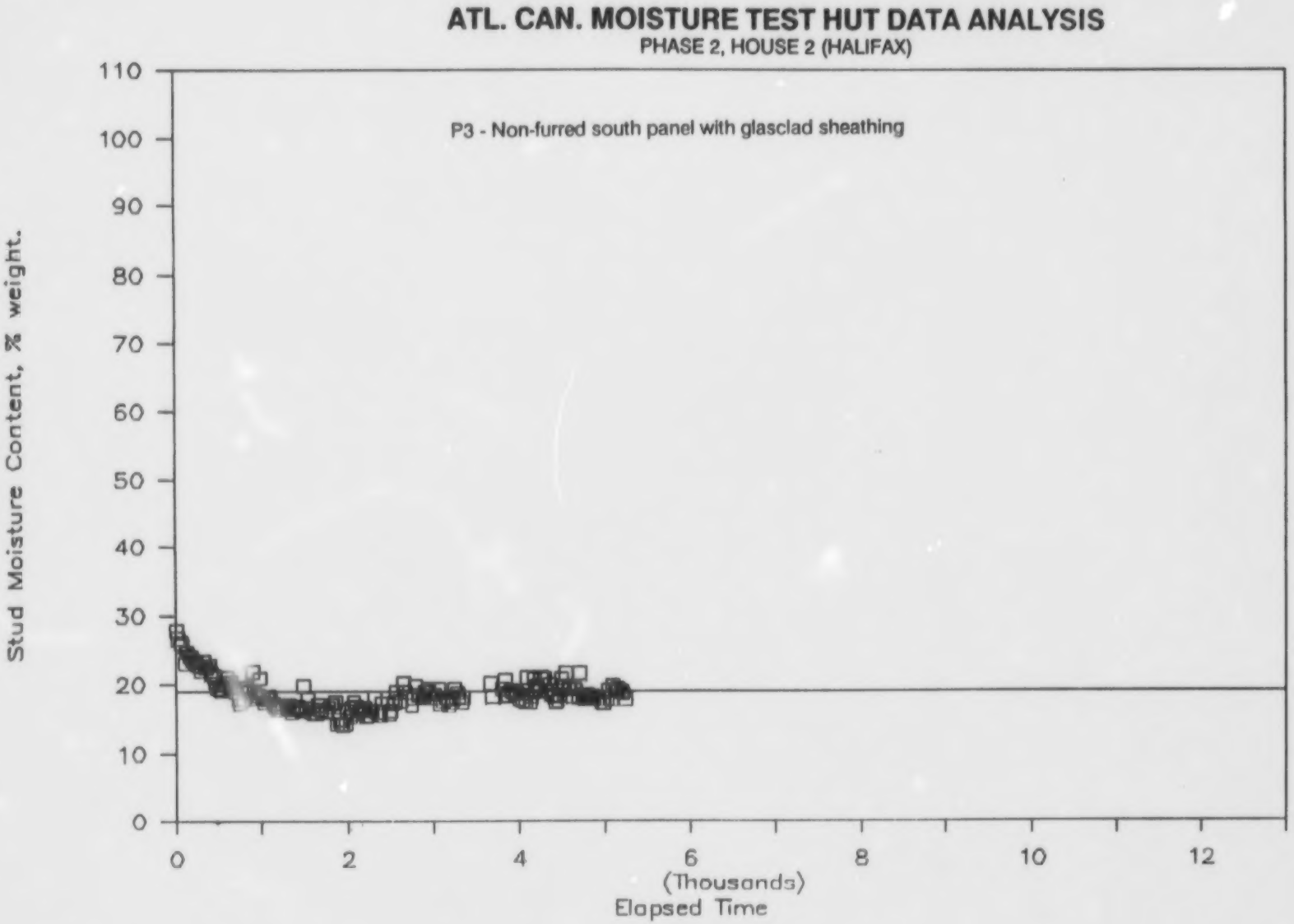
ATL. CAN. MOISTURE TEST HUT DATA ANALYSIS
PHASE 2, HOUSE 2 (HALIFAX)
P3 - Non-furred south panel with glasclad sheathing
Stud Moisture Content, % weight.
110
100
90
80
70
60
50
40
30
20
10
0
0
2
4
6
8
10
12
(Thousands)
Elapsed Time

Figure 41

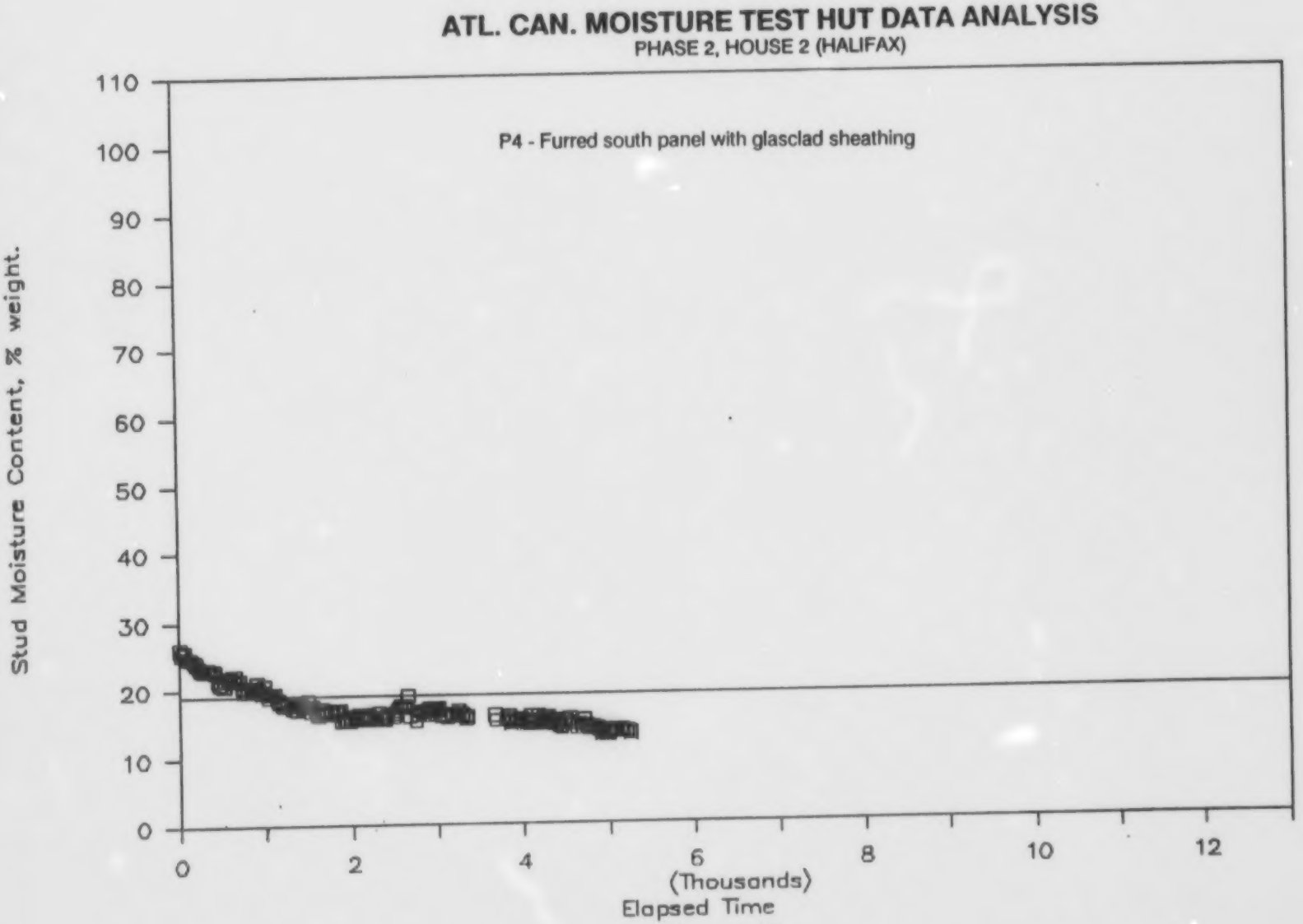
ATL. CAN. MOISTURE TEST HUT DATA ANALYSIS
PHASE 2, HOUSE 2 (HALIFAX)
P4 - Furred south panel with glasclad sheathing
Stud Moisture Content, % weight.
110
100
90
80
70
60
50
40
30
20
10
0
0
2
4
6
8
10
12
(Thousands)
Elapsed Time

Figure 42

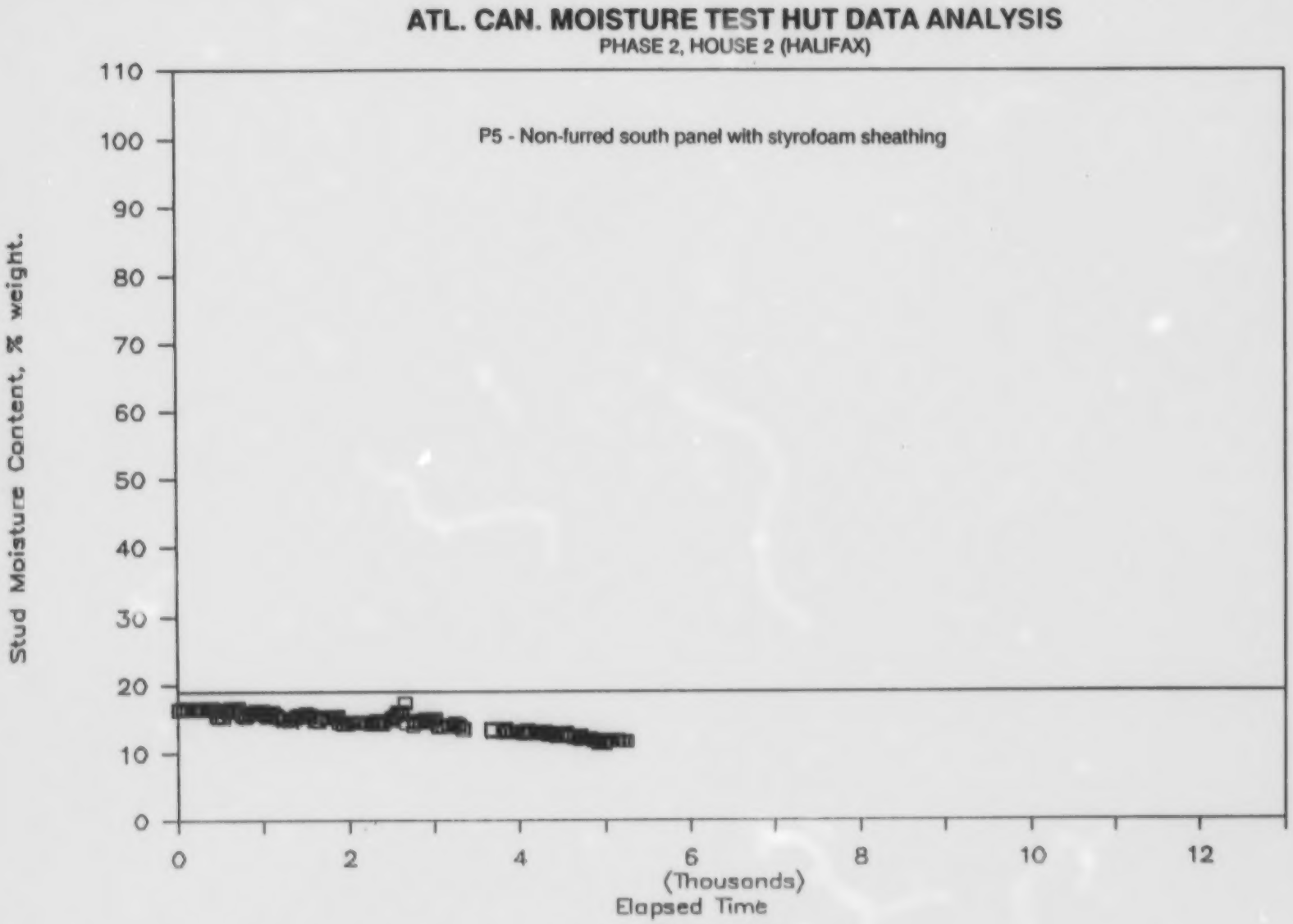
ATL. CAN. MOISTURE TEST HUT DATA ANALYSIS
PHASE 2, HOUSE 2 (HALIFAX)
P5 - Non-furred south panel with styrofoam sheathing
Stud Moisture Content, % weight.
110
100
90
80
70
60
50
40
30
20
10
0
0
2
4
6
8
10
12
(Thousands)
Elapsed Time

Figure 43

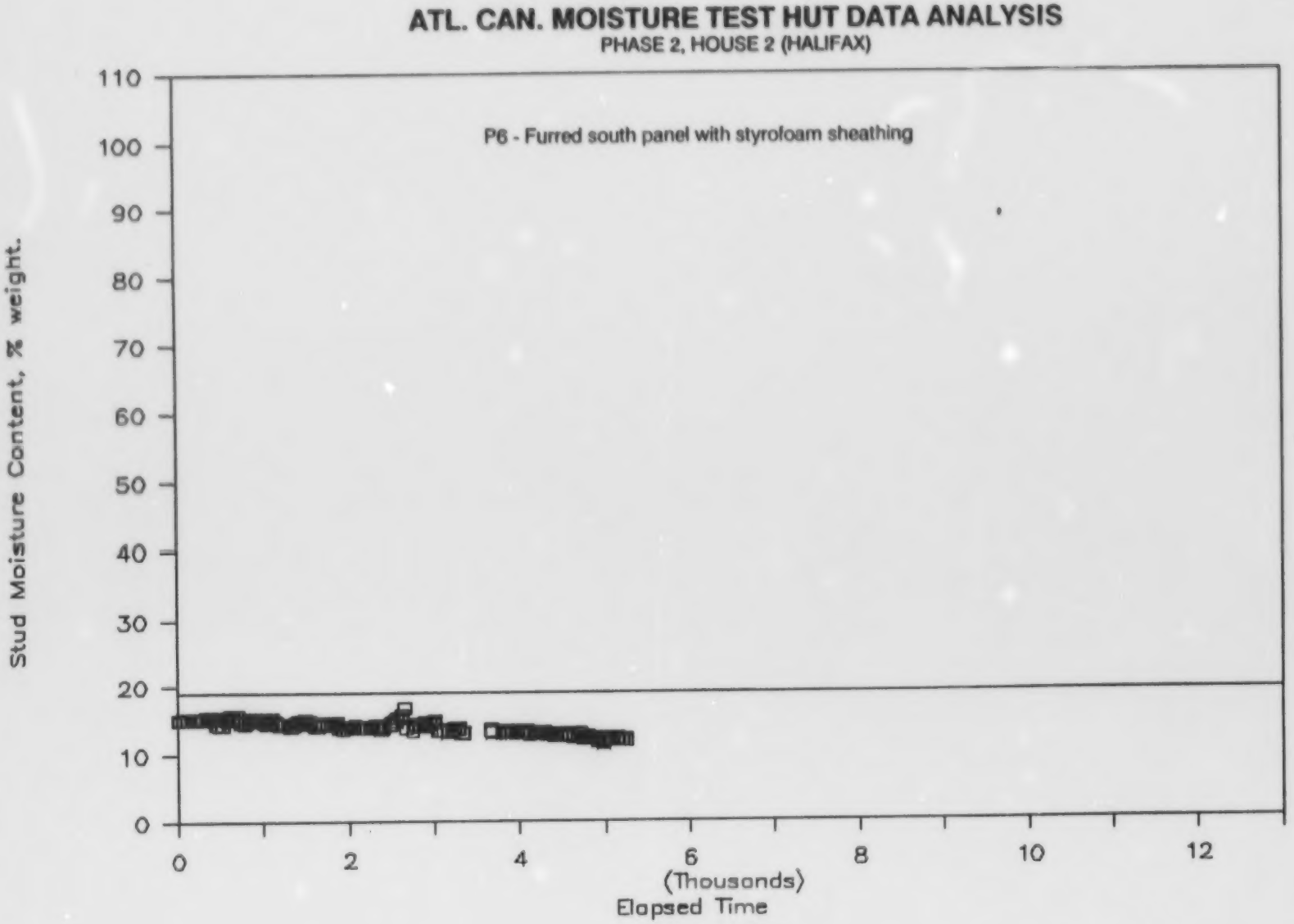
ATL. CAN. MOISTURE TEST HUT DATA ANALYSIS
PHASE 2, HOUSE 2 (HALIFAX)
P6 - Furred south panel with styrofoam sheathing
Stud Moisture Content, % weight.
110
100
90
80
70
60
50
40
30
20
10
0
0
2
4
6
8
10
12
(Thousands)
Elapsed Time

Figure 44

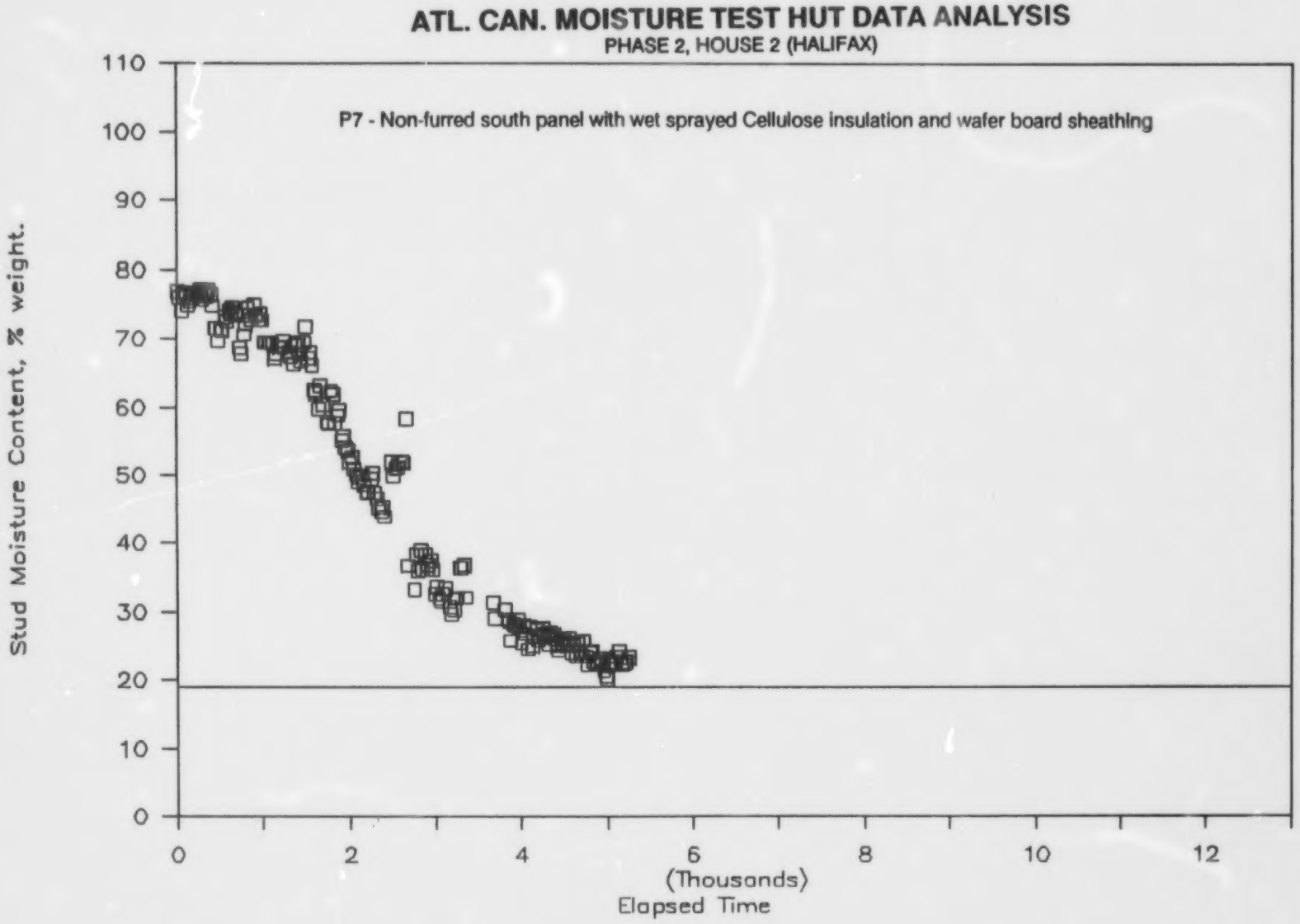
ATL. CAN. MOISTURE TEST HUT DATA ANALYSIS
PHASE 2, HOUSE 2 (HALIFAX)
P7 - Non-furred south panel with wet sprayed Cellulose insulation and wafer board sheathing
Stud Moisture Content, % weight.
110
100
90
80
70
60
50
40
30
20
10
0
0
2
4
6
8
10
12
(Thousands)
Elapsed Time

Figure 45

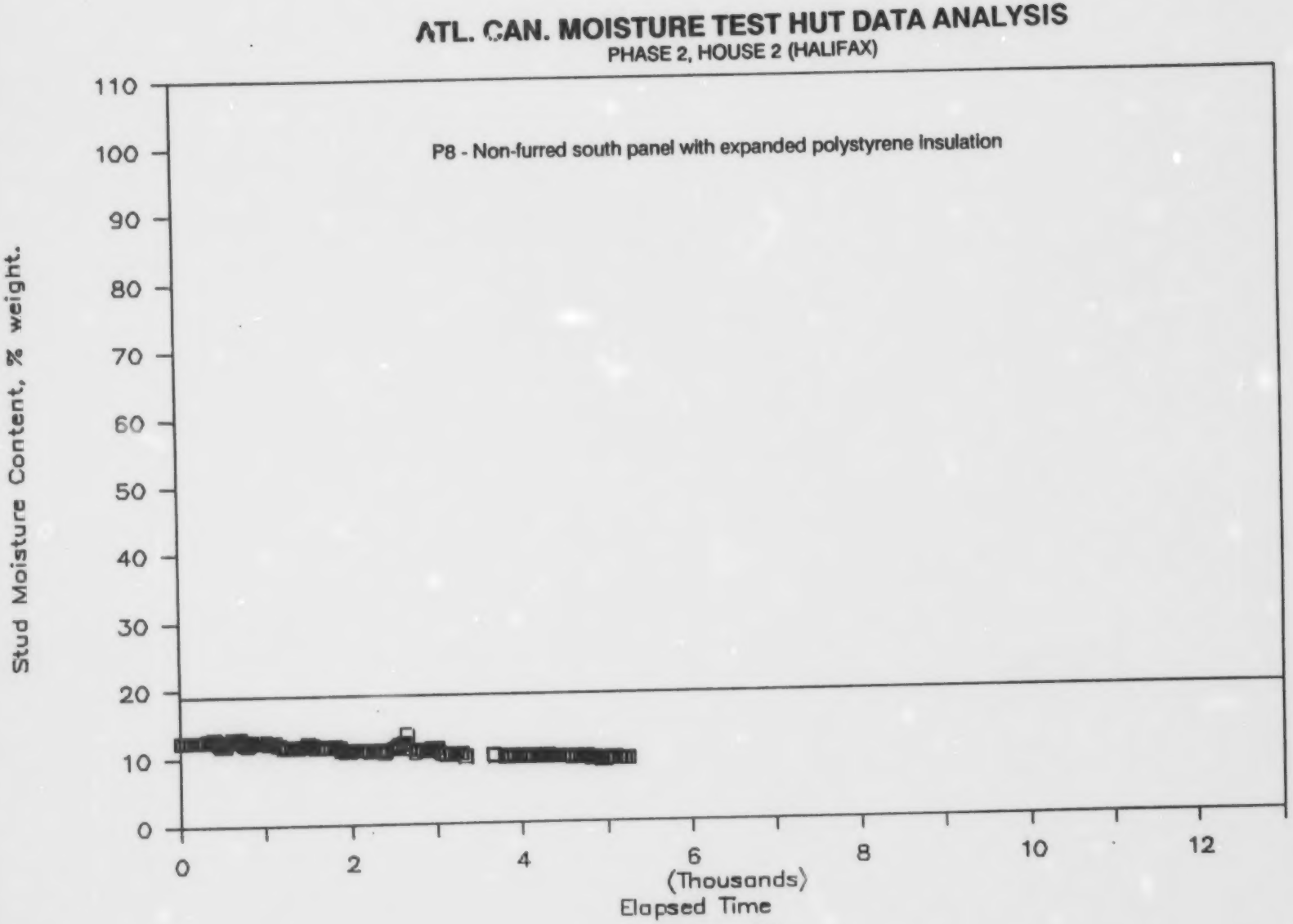
ATL. CAN. MOISTURE TEST HUT DATA ANALYSIS
PHASE 2, HOUSE 2 (HALIFAX)
P8 - Non-furred south panel with expanded polystyrene insulation
Stud Moisture Content, % weight.
110
100
90
80
70
60
50
40
30
20
10
0
0
2
4
6
8
10
12
(Thousands)
Elapsed Time

Figure 46

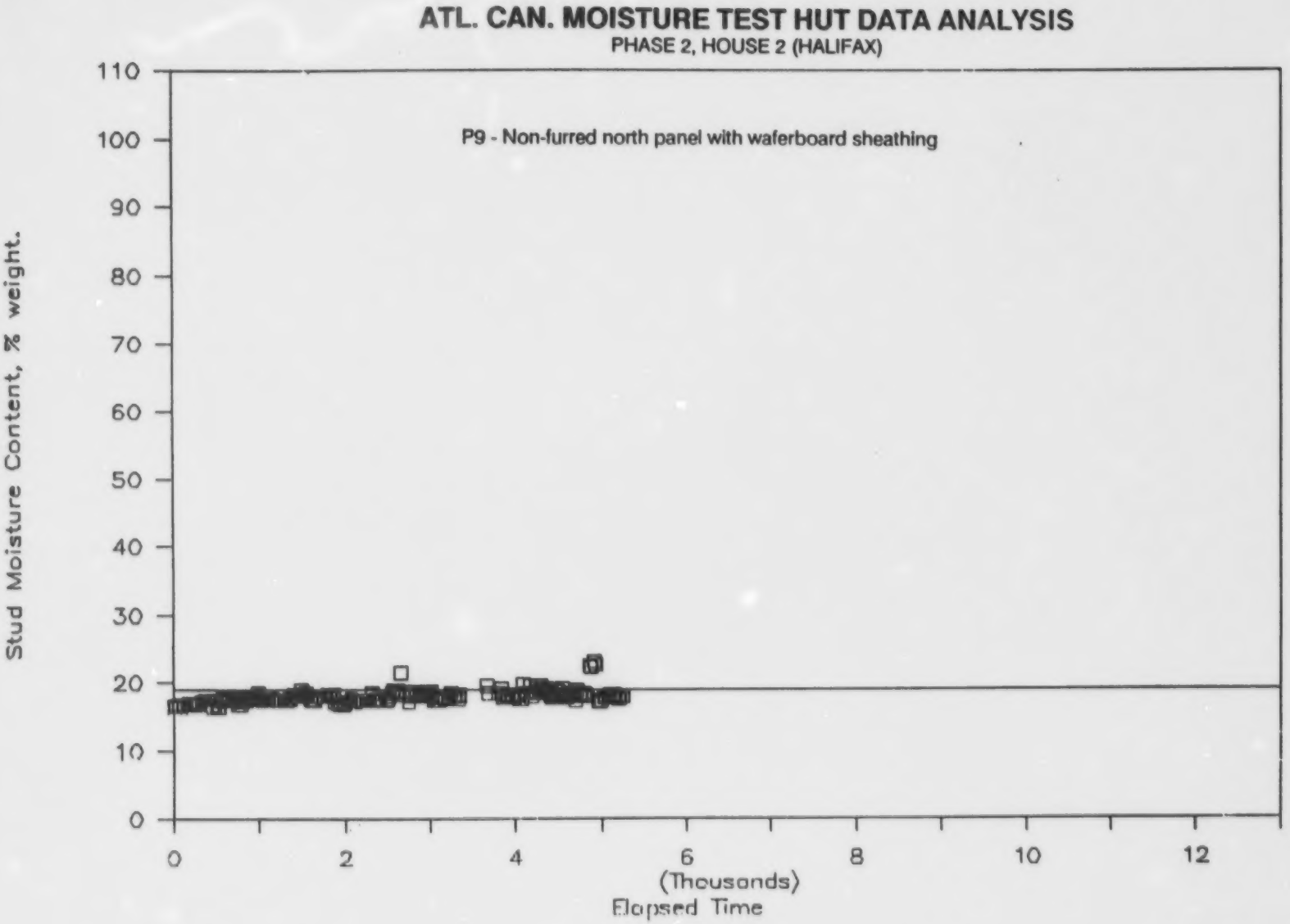
ATL. CAN. MOISTURE TEST HUT DATA ANALYSIS
PHASE 2, HOUSE 2 (HALIFAX)
P9 - Non-furred north panel with waferboard sheathing
Stud Moisture Content, % weight.
110
100
90
80
70
60
50
40
30
20
10
0
0
2
4
6
8
10
12
(Thousands)
Elapsed Time

Figure 47

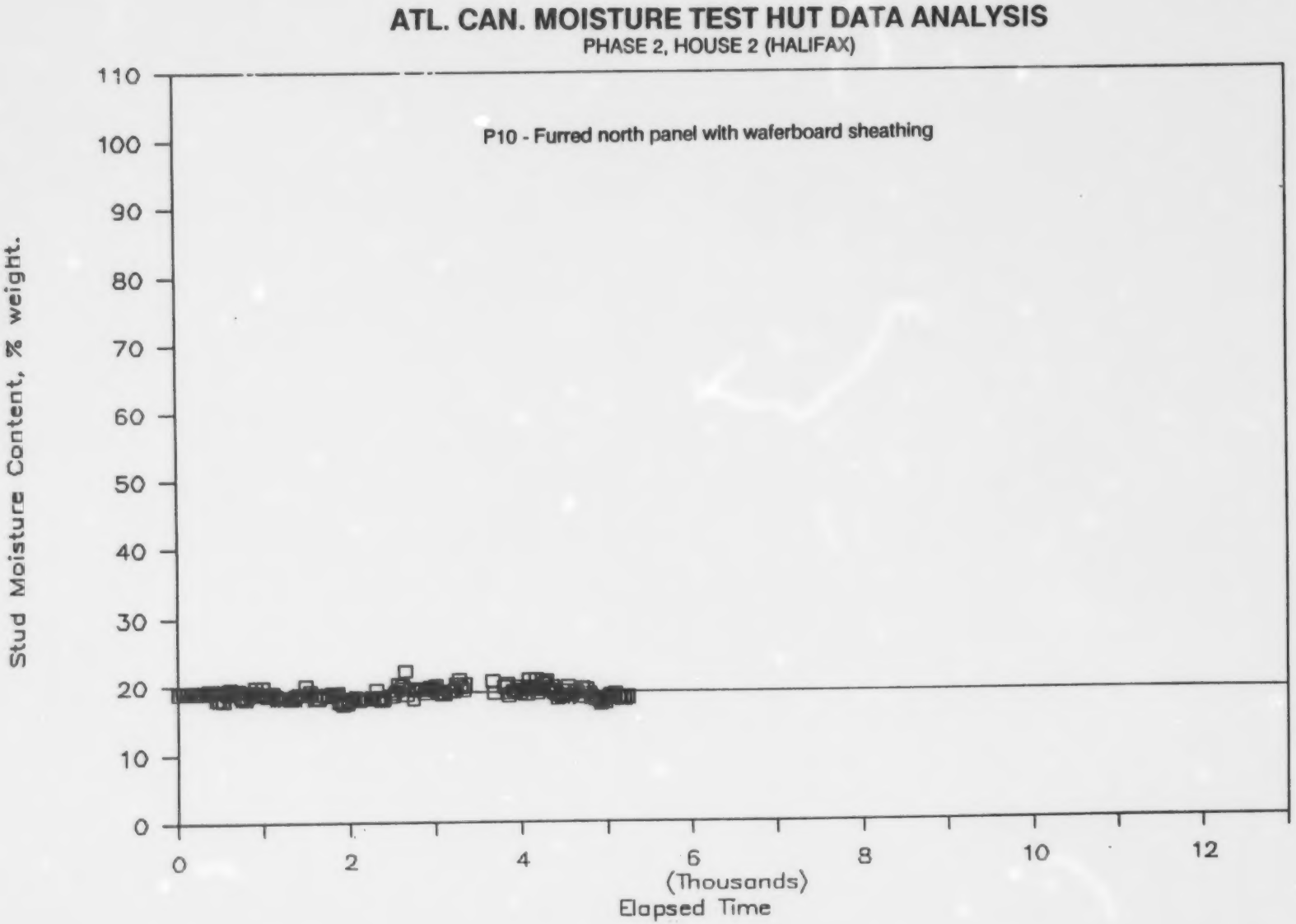
ATL. CAN. MOISTURE TEST HUT DATA ANALYSIS
PHASE 2, HOUSE 2 (HALIFAX)
P10 - Furred north panel with waferboard sheathing
Stud Moisture Content, % weight.
110
100
90
80
70
60
50
40
30
20
10
0
0
2
4
6
8
10
12
(Thousands)
Elapsed Time

Figure 48

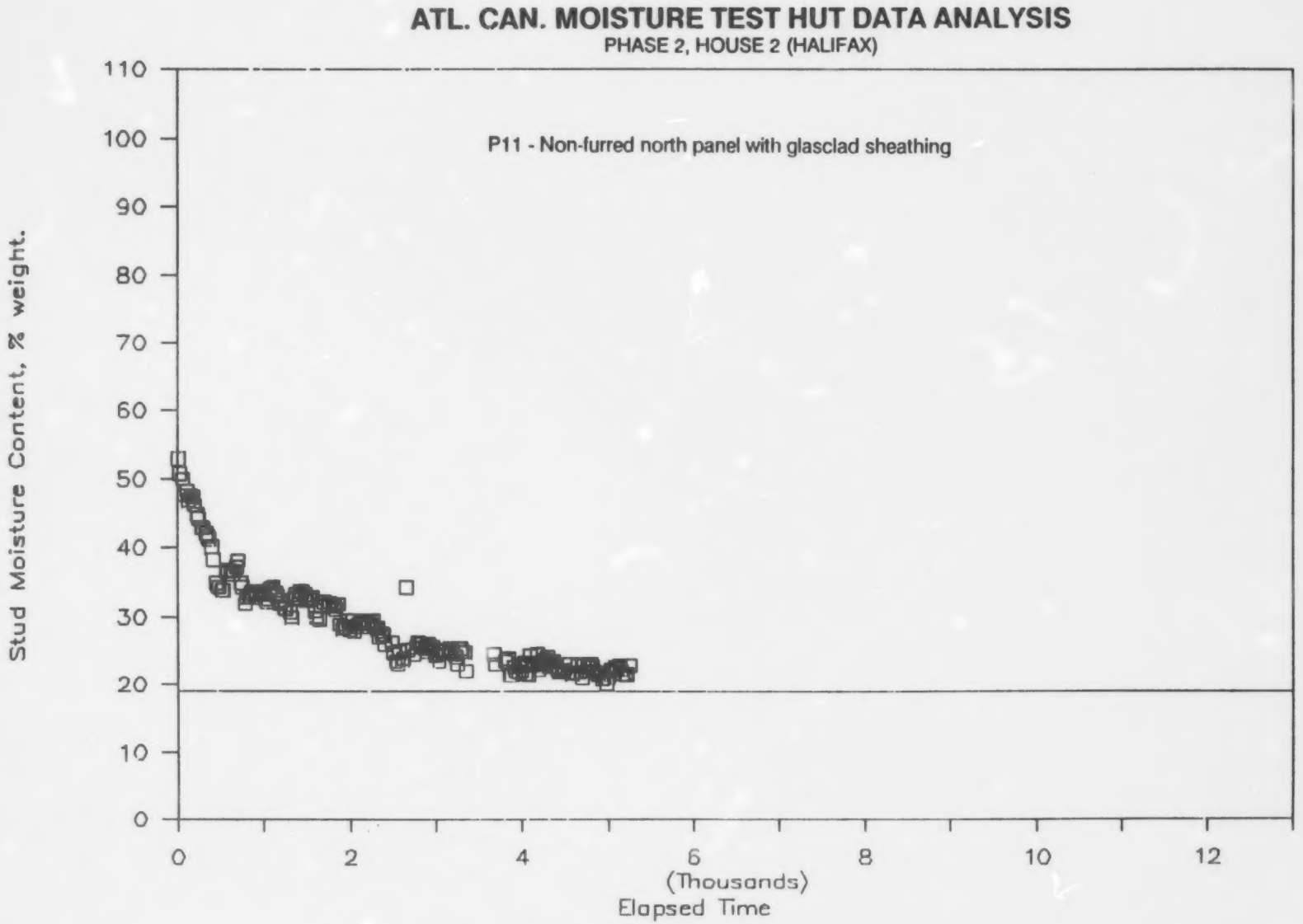
ATL. CAN. MOISTURE TEST HUT DATA ANALYSIS
PHASE 2, HOUSE 2 (HALIFAX)
P11 - Non-furred north panel with glasclad sheathing
Stud Moisture Content, % weight.
110
100
90
80
70
60
50
40
30
20
10
0
0
2
4
6
8
10
12
(Thousands)
Elapsed Time

Figure 49

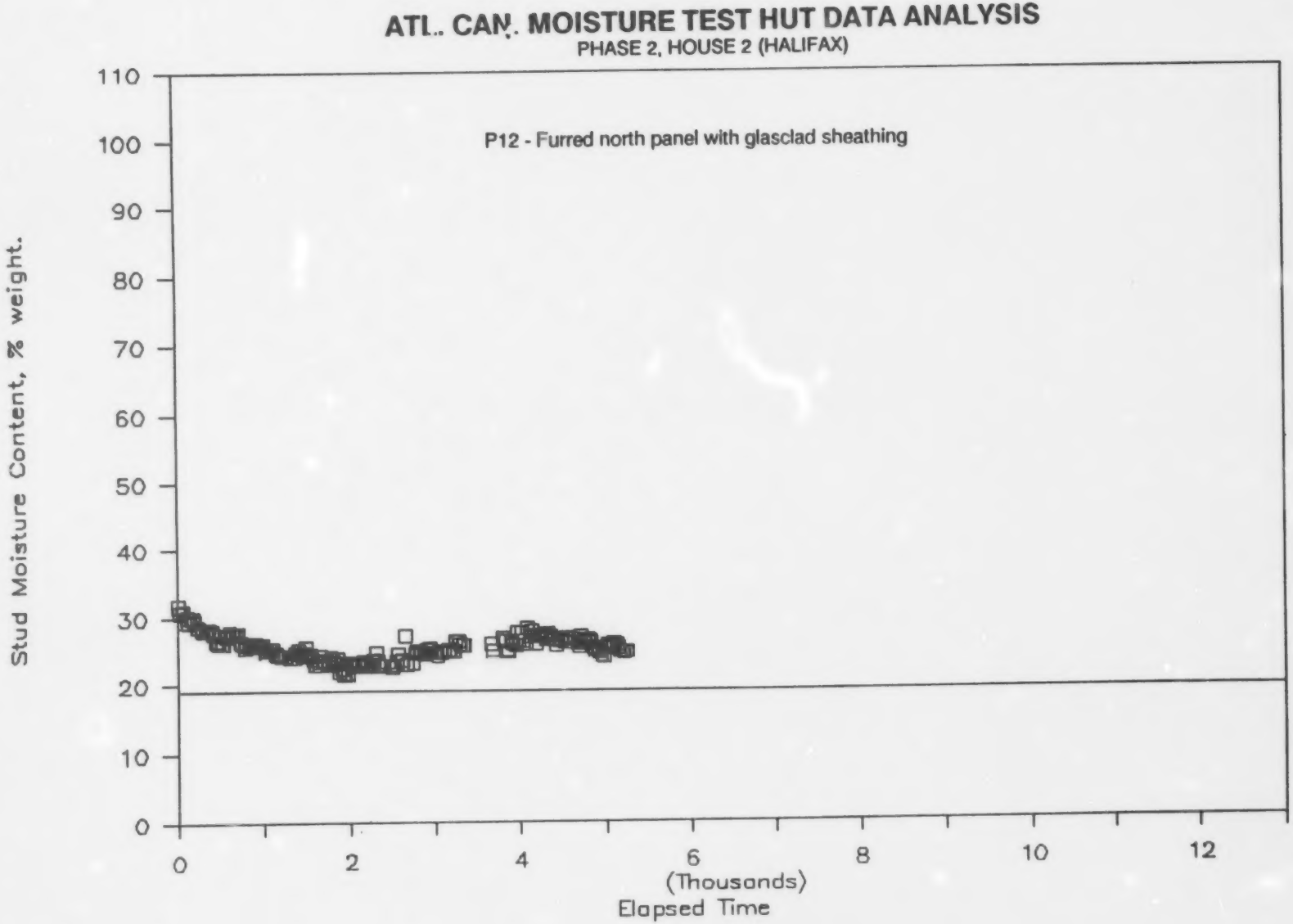
ATL. CAN. MOISTURE TEST HUT DATA ANALYSIS
PHASE 2, HOUSE 2 (HALIFAX)
P12 - Furred north panel with glasclad sheathing
Stud Moisture Content, % weight.
110
100
90
80
70
60
50
40
30
20
10
0
0
2
4
6
8
10
12
(Thousands)
Elapsed Time

Figure 50

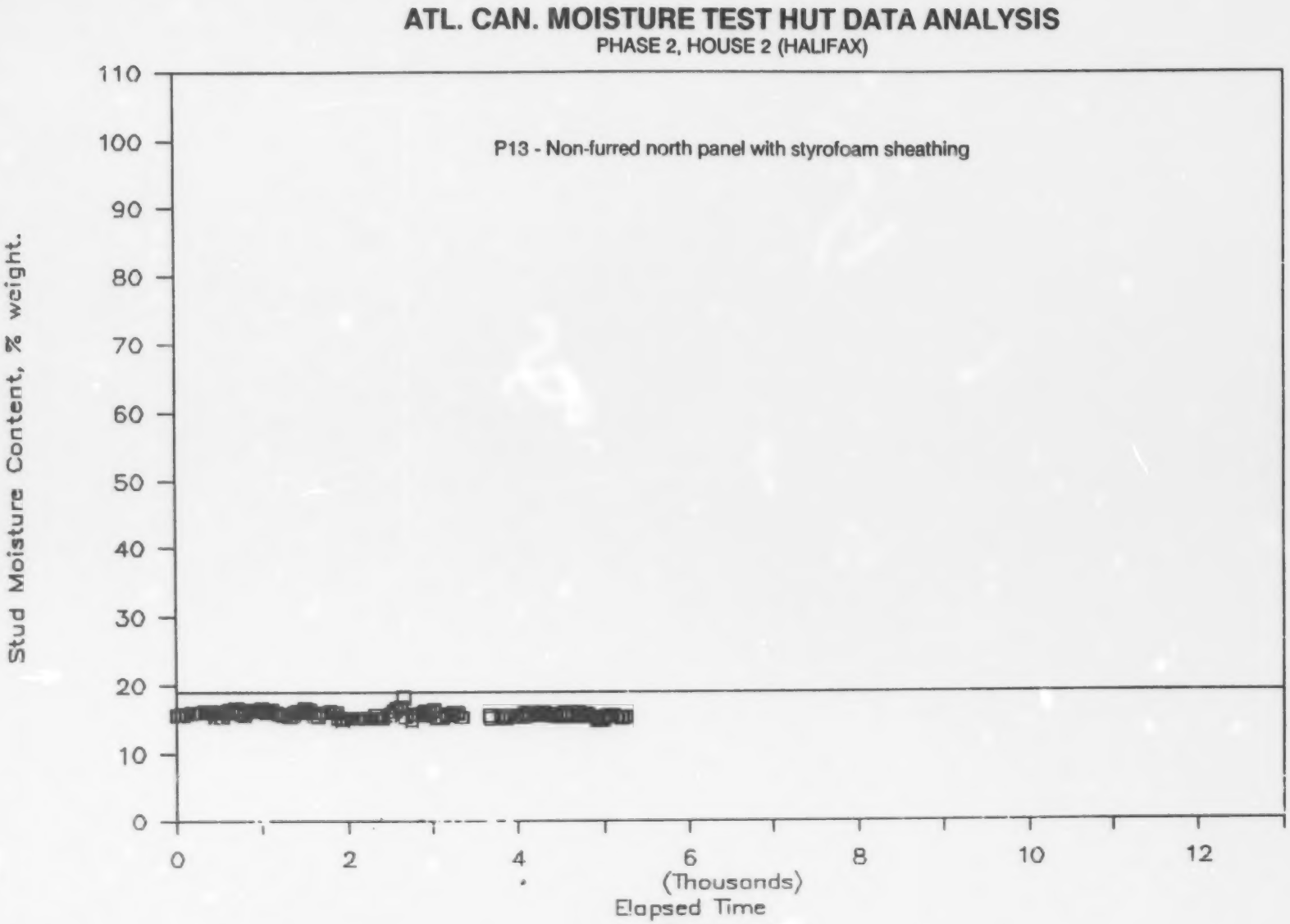
ATL. CAN. MOISTURE TEST HUT DATA ANALYSIS
PHASE 2, HOUSE 2 (HALIFAX)
P13 - Non-furred north panel with styrofoam sheathing
Stud Moisture Content, % weight.
110
100
90
80
70
60
50
40
30
20
10
0
0
2
4
6
8
10
12
(Thousands)
Elapsed Time

Figure 51

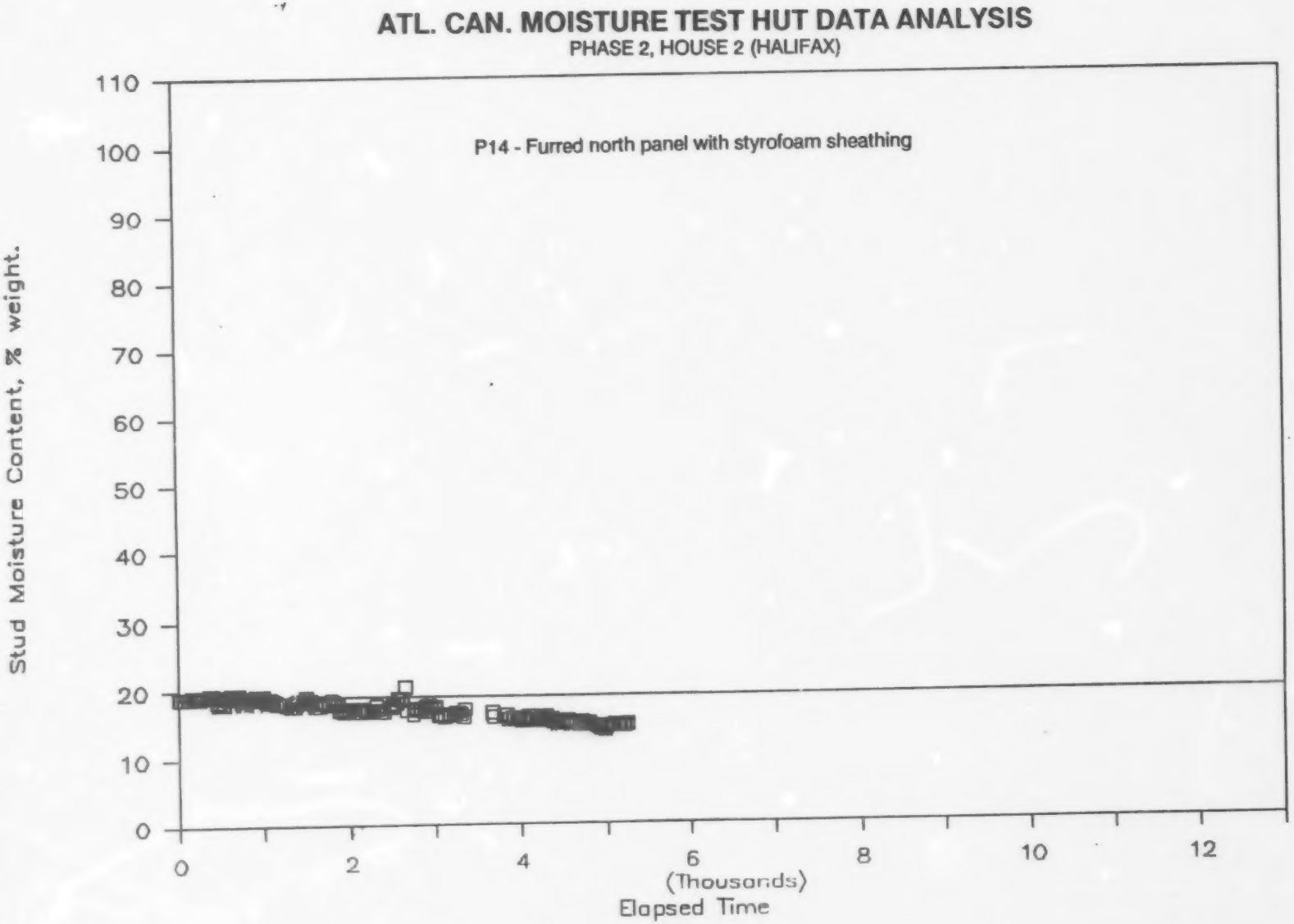
ATL. CAN. MOISTURE TEST HUT DATA ANALYSIS
PHASE 2, HOUSE 2 (HALIFAX)
P14 - Furred north panel with styrofoam sheathing
Stud Moisture Content, % weight.
110
100
90
80
70
60
50
40
30
20
10
0
0
2
4
6
8
10
12
(Thousands)
Elapsed Time

Figure 52

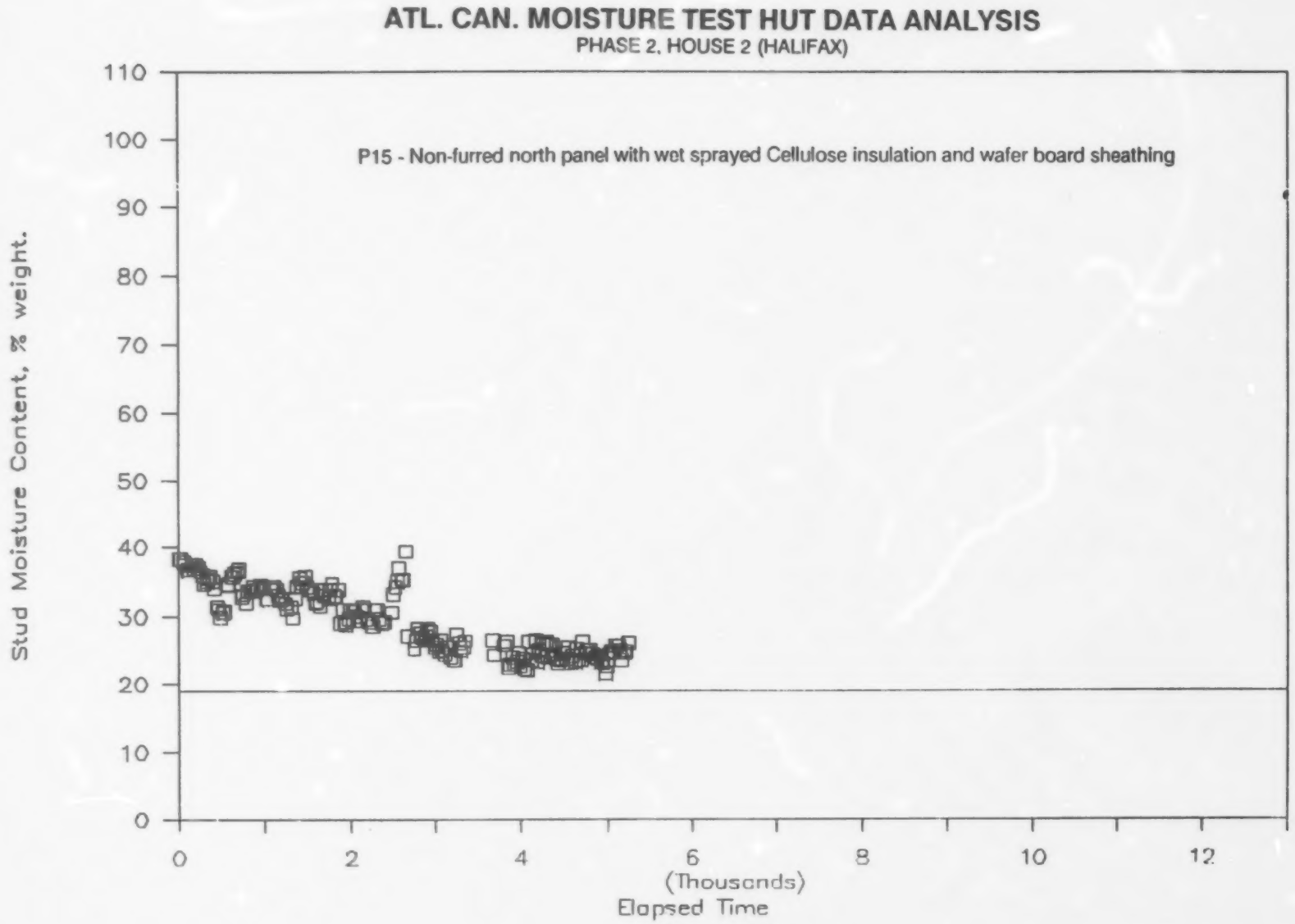
ATL. CAN. MOISTURE TEST HUT DATA ANALYSIS
PHASE 2, HOUSE 2 (HALIFAX)
P15 - Non-furred north panel with wet sprayed Cellulose insulation and wafer board sheathing
Stud Moisture Content, % weight.
110
100
90
80
70
60
50
40
30
20
10
0
0
2
4
6
8
10
12
(Thousands)
Elapsed Time

Figure 53

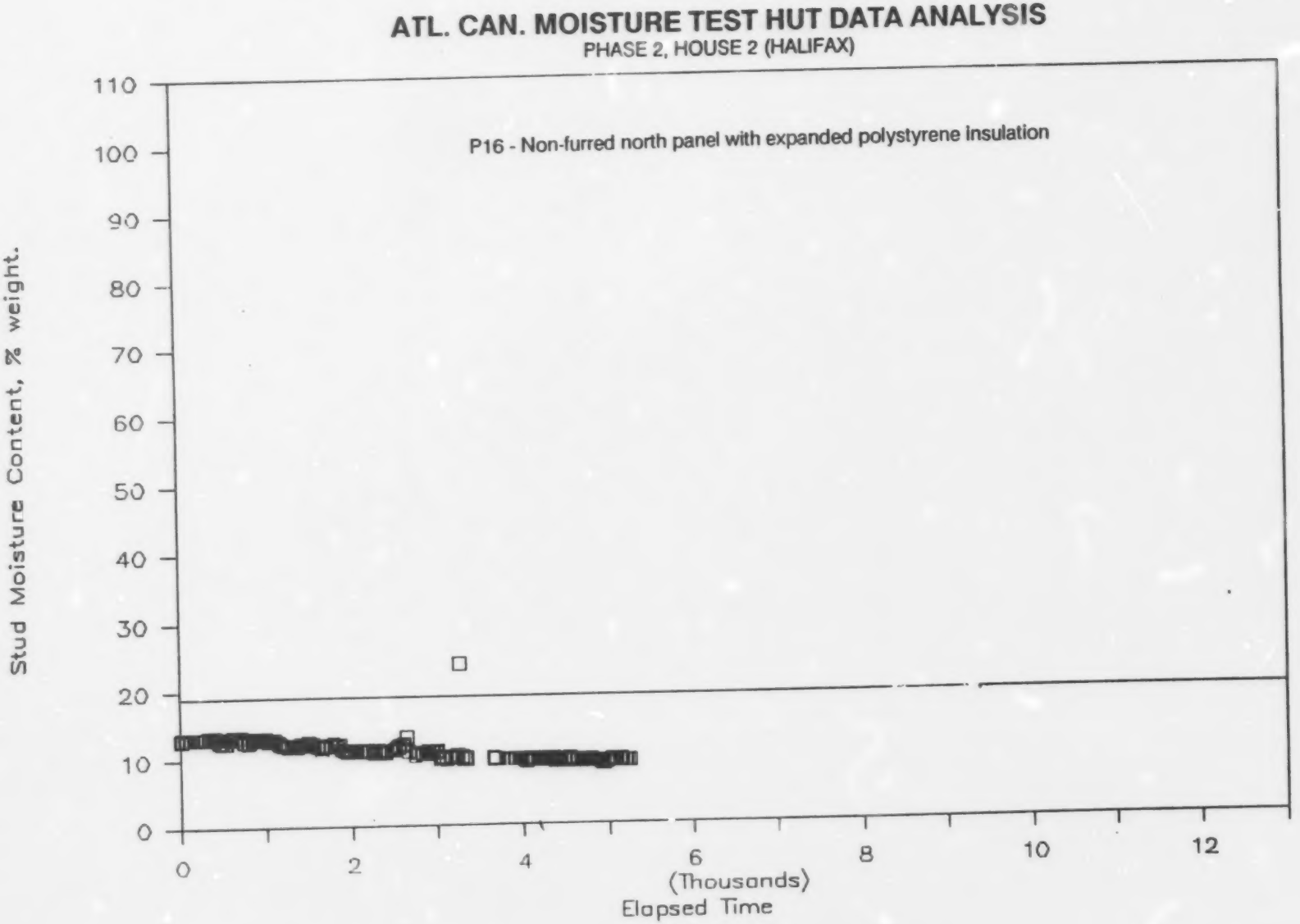
ATL. CAN. MOISTURE TEST HUT DATA ANALYSIS
PHASE 2, HOUSE 2 (HALIFAX)
P16 - Non-furred north panel with expanded polystyrene insulation
Stud Moisture Content, % weight.
110
100
90
80
70
60
50
40
30
20
10
0
0
2
4
6
8
10
12
(Thousands)
Elapsed Time

Figure 54

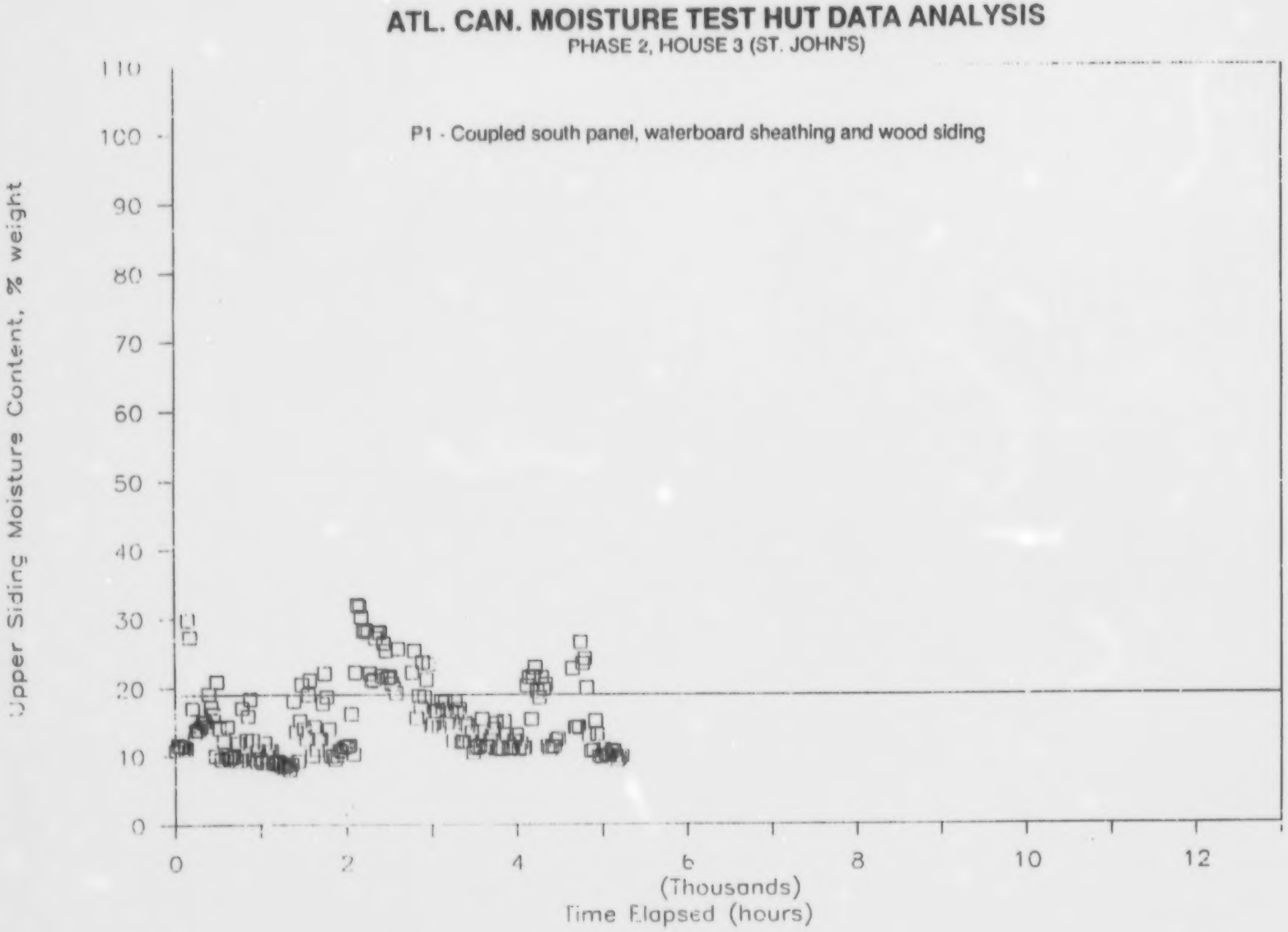
ATL. CAN. MOISTURE TEST HUT DATA ANALYSIS
PHASE 2, HOUSE 3 (ST. JOHN'S)
P1 - Coupled south panel, waterboard sheathing and wood siding
Upper Siding Moisture Content, % weight
110
100
90
80
70
60
50
40
30
20
10
0
0
2
4
6
8
10
12
(Thousands)
Time Elapsed (hours)

Figure 55

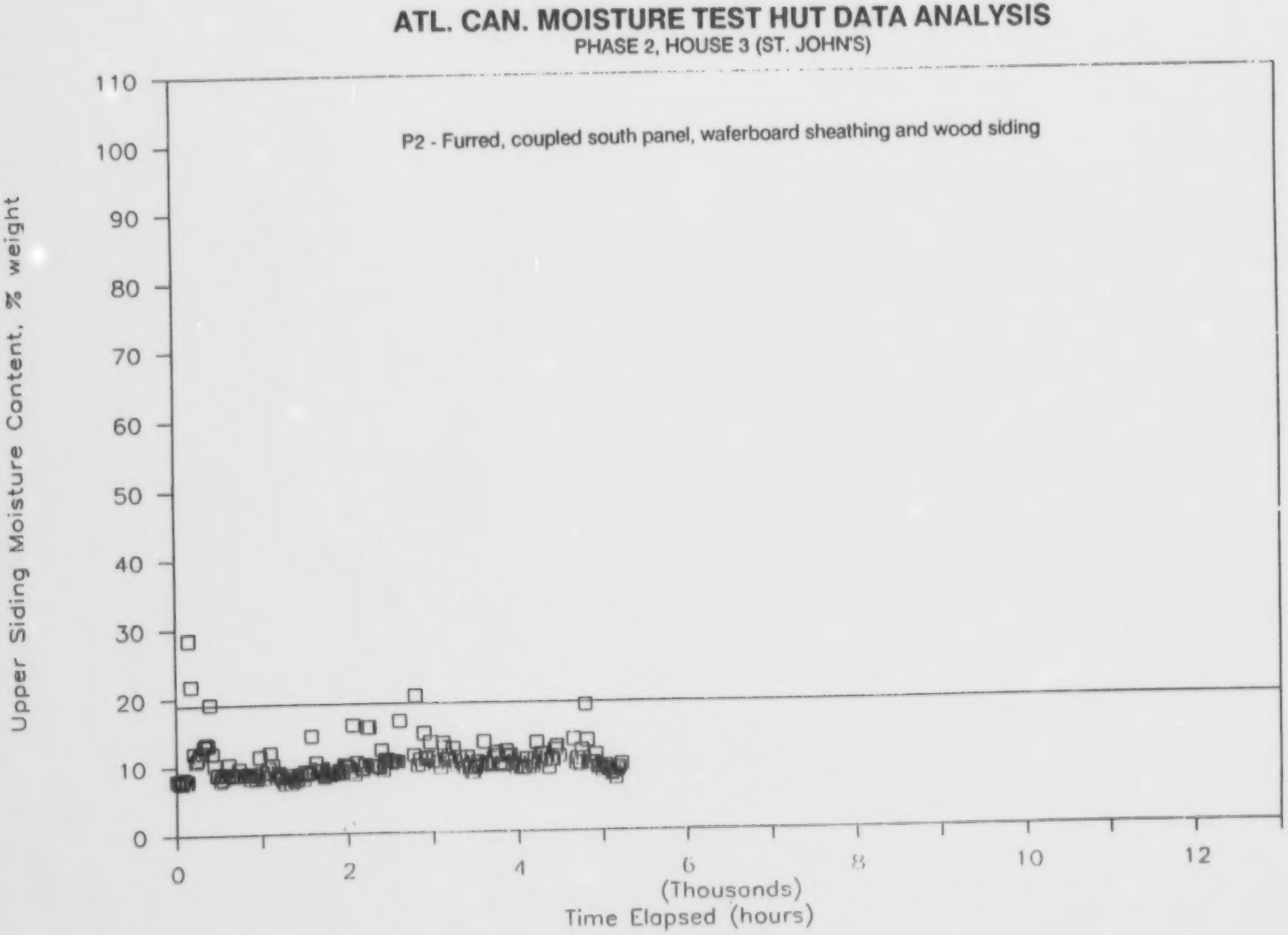
ATL. CAN. MOISTURE TEST HUT DATA ANALYSIS
PHASE 2, HOUSE 3 (ST. JOHN'S)
P2 - Furred, coupled south panel, waferboard sheathing and wood siding
Upper Siding Moisture Content, % weight
110
100
90
80
70
60
50
40
30
20
10
0
0
2
4
6
8
10
12
(Thousands)
Time Elapsed (hours)

Figure 56

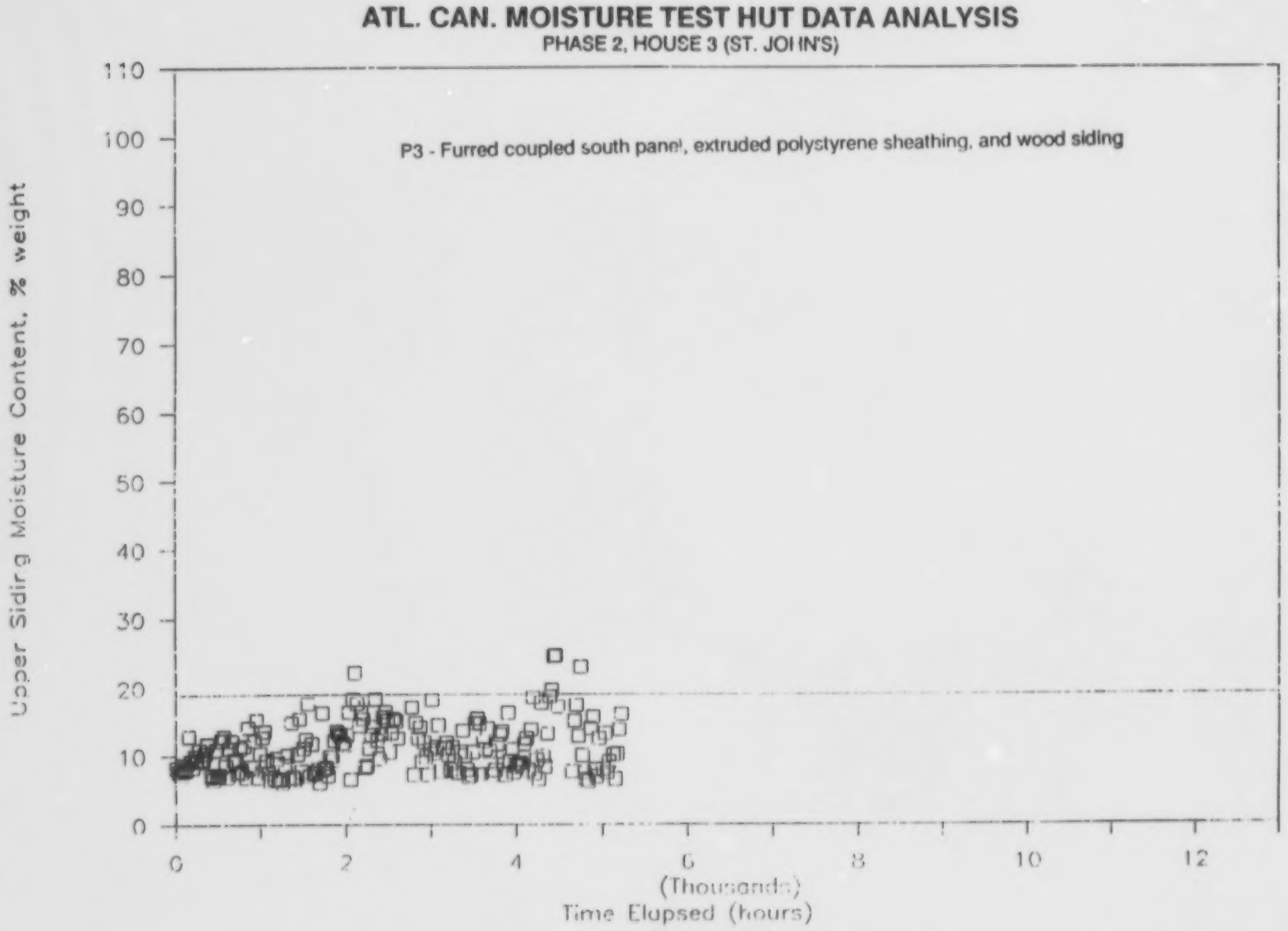
ATL. CAN. MOISTURE TEST HUT DATA ANALYSIS
PHASE 2, HOUSE 3 (ST. JOHN'S)
P3 - Furred coupled south panel, extruded polystyrene sheathing, and wood siding
Upper Siding Moisture Content, % weight
110
100
90
80
70
60
50
40
30
20
10
0
0
2
4
6
8
10
12
(Thousands)
Time Elapsed (hours)

Figure 57

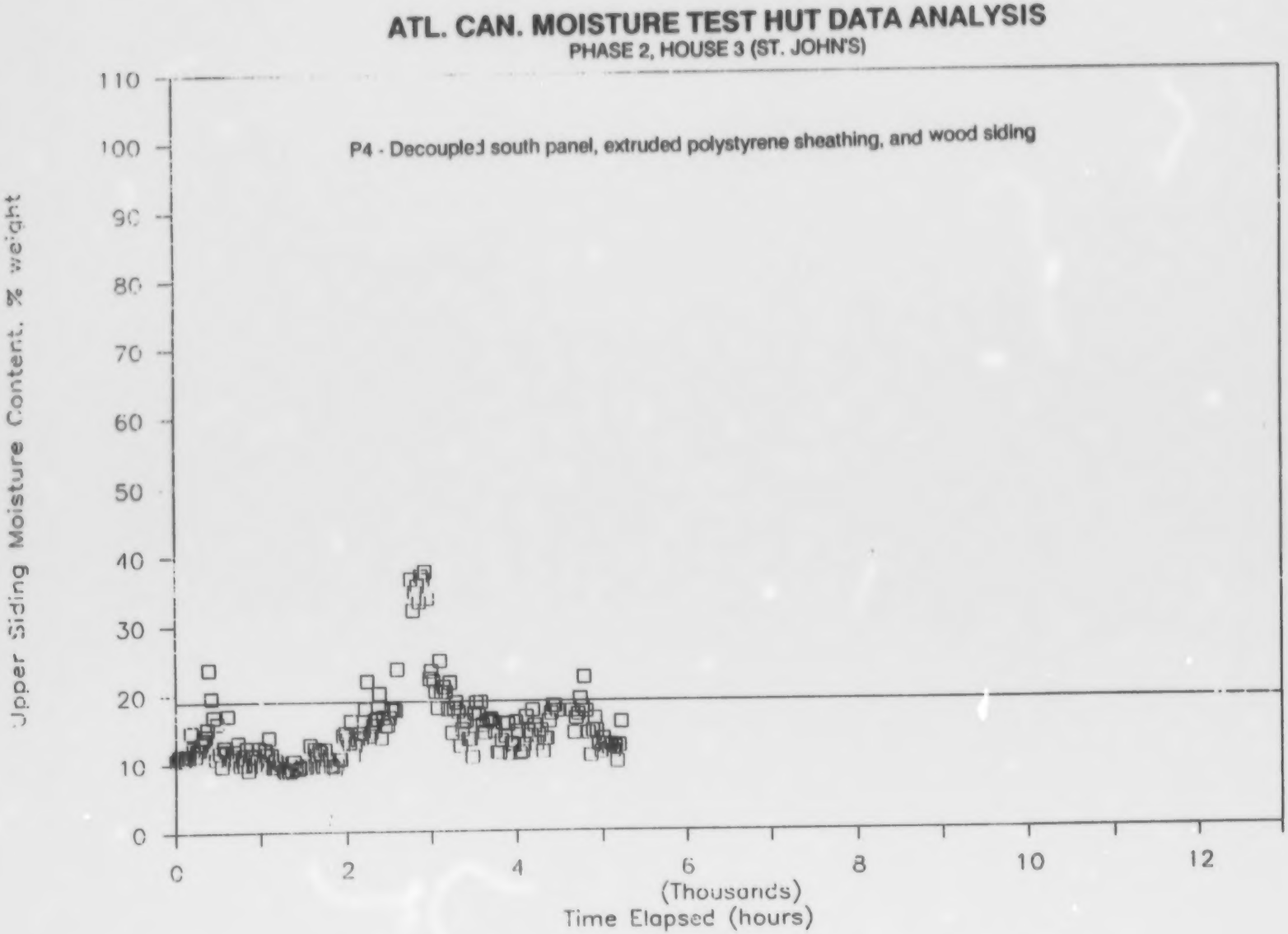
ATL. CAN. MOISTURE TEST HUT DATA ANALYSIS
PHASE 2, HOUSE 3 (ST. JOHN'S)
P4 - Decoupled south panel, extruded polystyrene sheathing, and wood siding
Upper Siding Moisture Content, % weight
110
100
90
80
70
60
50
40
30
20
10
0
0
2
4
6
8
10
12
(Thousands)
Time Elapsed (hours)

Figure 58

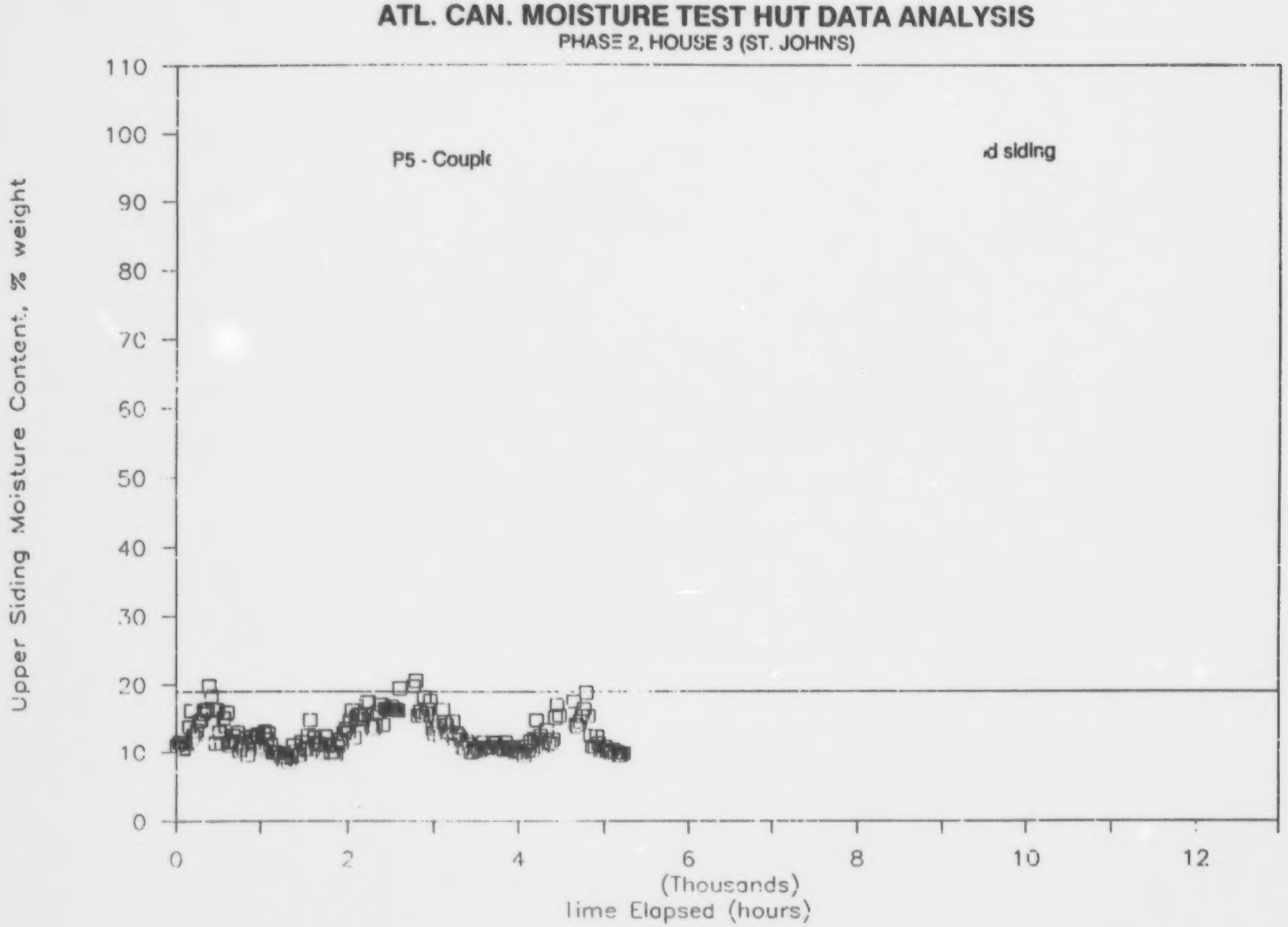
ATL. CAN. MOISTURE TEST HUT DATA ANALYSIS
PHASE 2, HOUSE 3 (ST. JOHN'S)
P5 - Couple
d siding
Upper Siding Moisture Content, % weight
110
100
90
80
70
60
50
40
30
20
10
0
0
2
4
6
8
10
12
(Thousands)
Time Elapsed (hours)

Figure 59

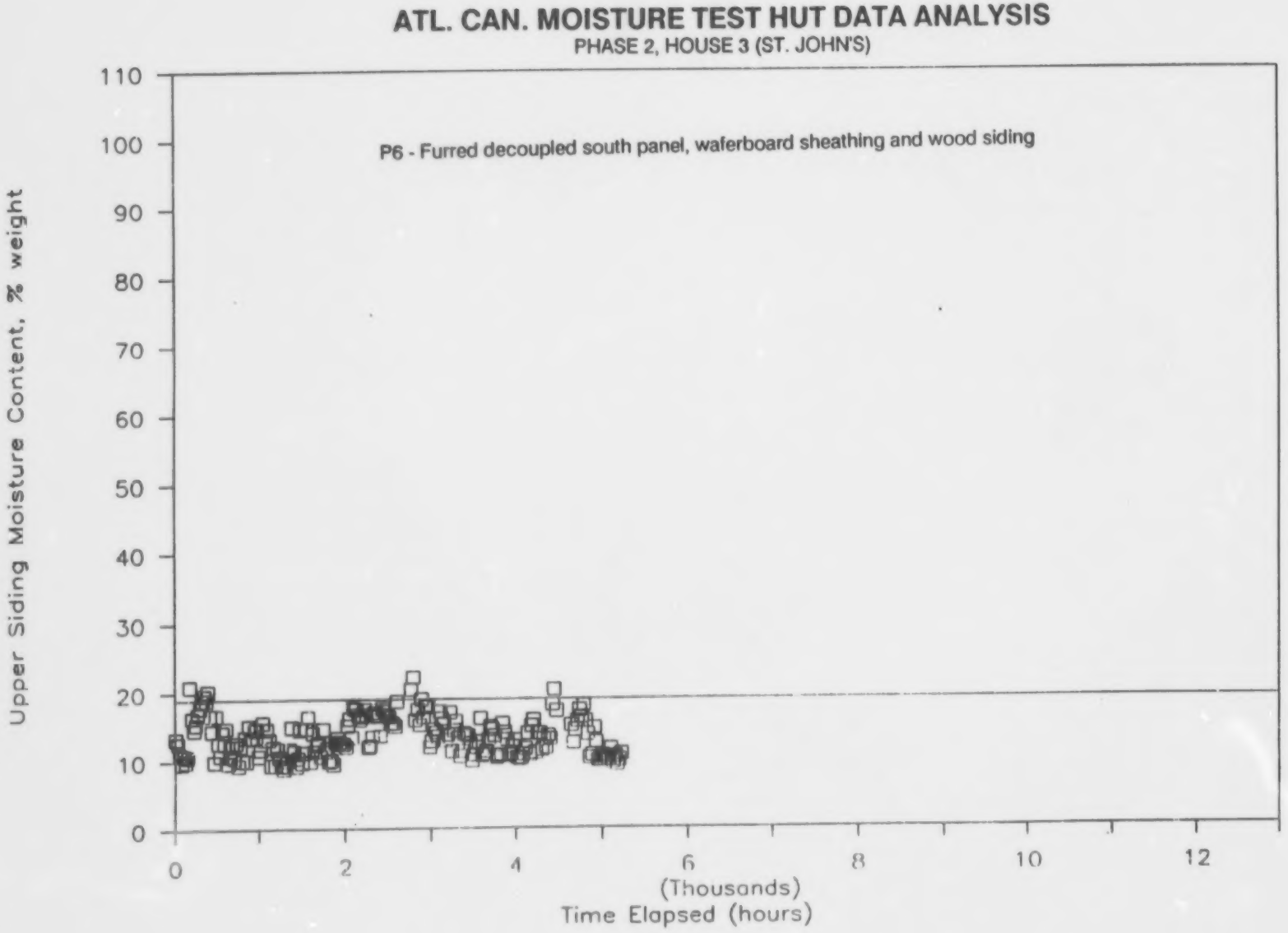
ATL. CAN. MOISTURE TEST HUT DATA ANALYSIS
PHASE 2, HOUSE 3 (ST. JOHN'S)
P6 - Furred decoupled south panel, waferboard sheathing and wood siding
Upper Siding Moisture Content, % weight
110
100
90
80
70
60
50
40
30
20
10
0
0
2
4
6
8
10
12
(Thousands)
Time Elapsed (hours)

Figure 60

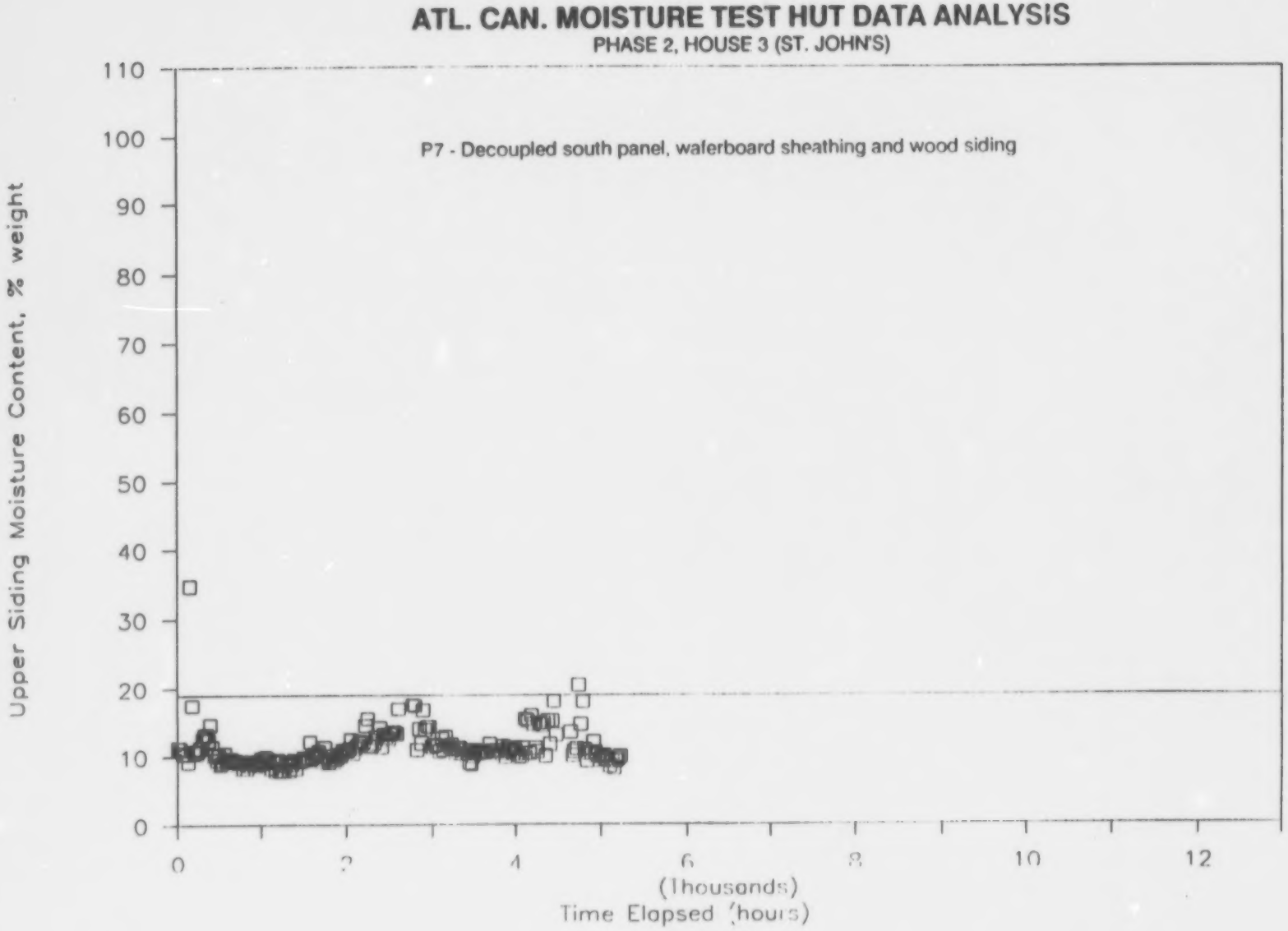
ATL. CAN. MOISTURE TEST HUT DATA ANALYSIS
PHASE 2, HOUSE 3 (ST. JOHN'S)
P7 - Decoupled south panel, waterboard sheathing and wood siding
Upper Siding Moisture Content, % weight
110
100
90
80
70
60
50
40
30
20
10
0
0
2
4
6
8
10
12
(Thousands)
Time Elapsed (hours)

Figure 61

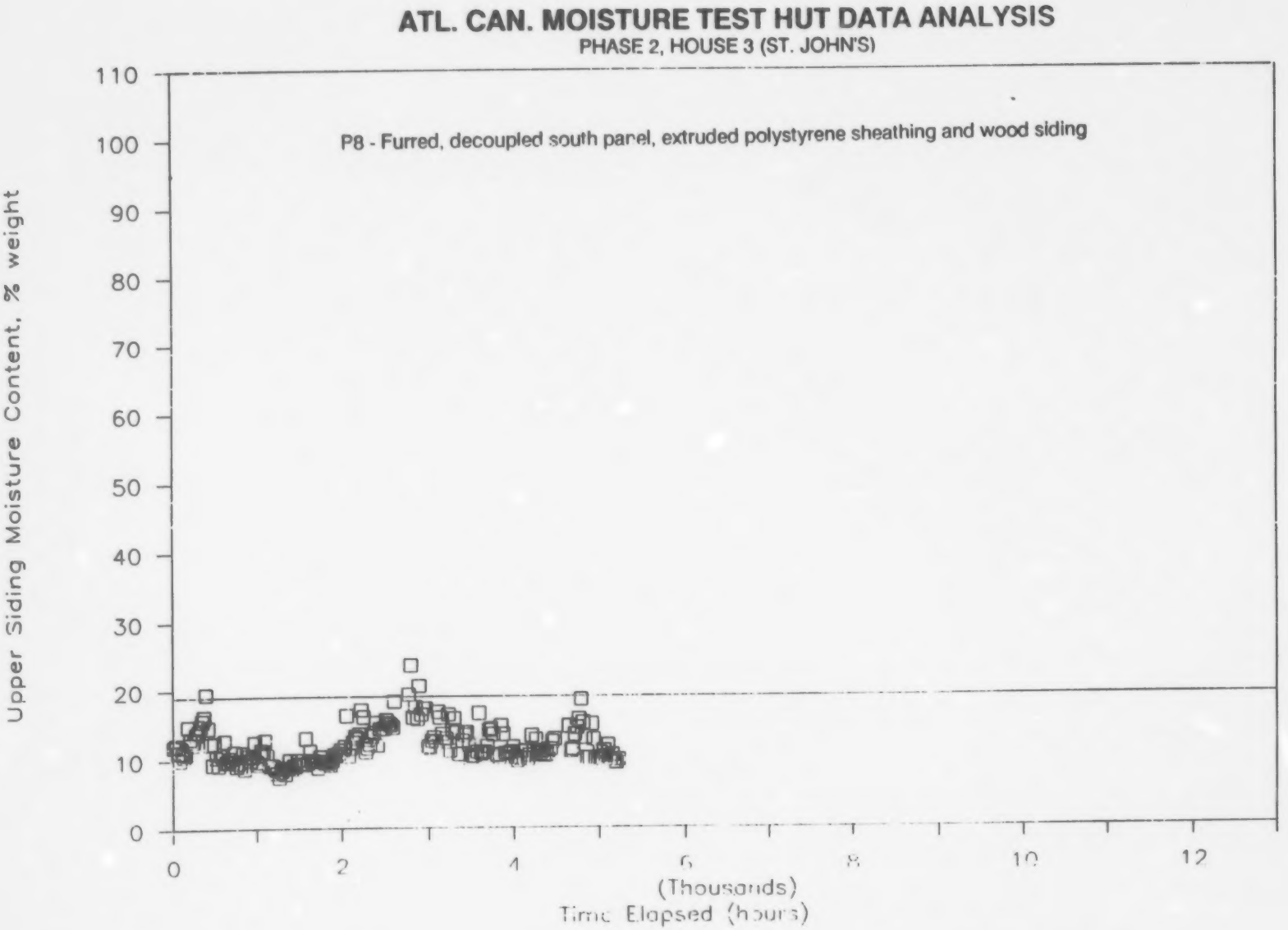
ATL. CAN. MOISTURE TEST HUT DATA ANALYSIS
PHASE 2, HOUSE 3 (ST. JOHN'S)
P8 - Furred, decoupled south panel, extruded polystyrene sheathing and wood siding
Upper Siding Moisture Content, % weight
110
100
90
80
70
60
50
40
30
20
10
0
0
2
4
6
8
10
12
(Thousands)
Time Elapsed (hours)

Figure 62

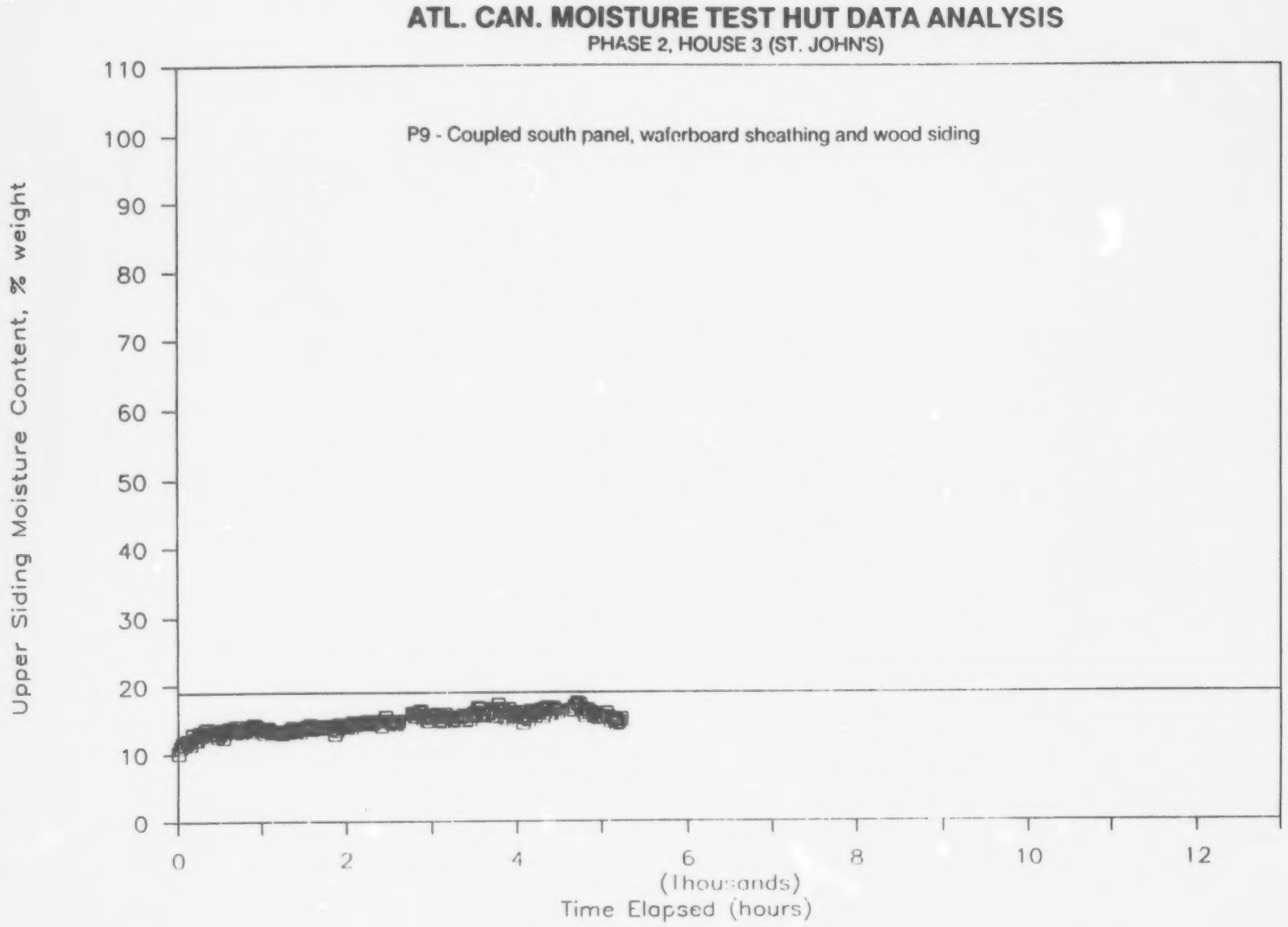
ATL. CAN. MOISTURE TEST HUT DATA ANALYSIS
PHASE 2, HOUSE 3 (ST. JOHN'S)
P9 - Coupled south panel, waferboard sheathing and wood siding
Upper Siding Moisture Content, % weight
110
100
90
80
70
60
50
40
30
20
10
0
0
2
4
6
8
10
12
(Thousands)
Time Elapsed (hours)

Figure 63

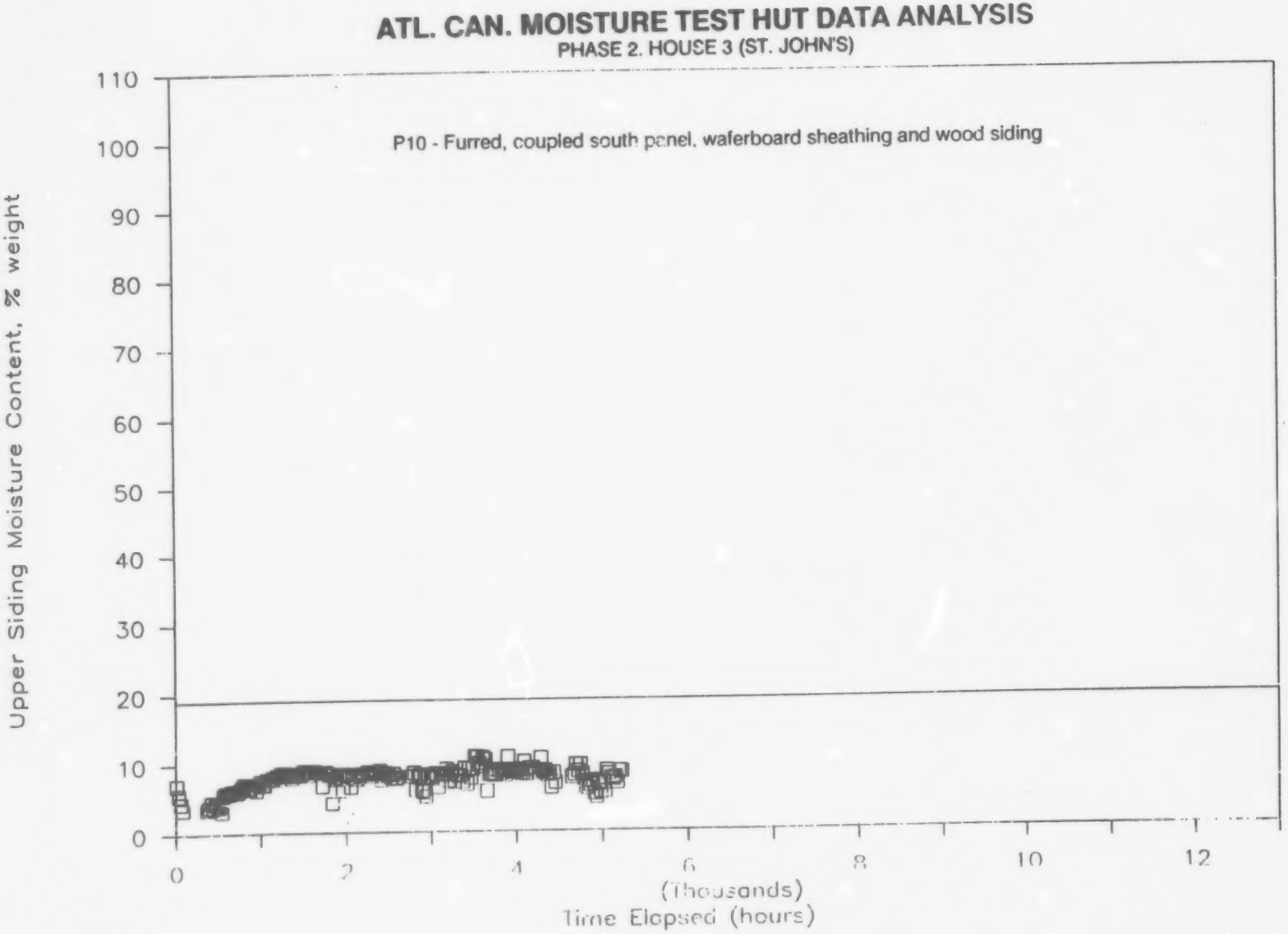
ATL. CAN. MOISTURE TEST HUT DATA ANALYSIS
PHASE 2. HOUSE 3 (ST. JOHN'S)
P10 - Furred, coupled south panel, waferboard sheathing and wood siding
Upper Siding Moisture Content, % weight
110
100
90
80
70
60
50
40
30
20
10
0
0
2
4
6
8
10
12
(Thousands)
Time Elapsed (hours)

Figure 64

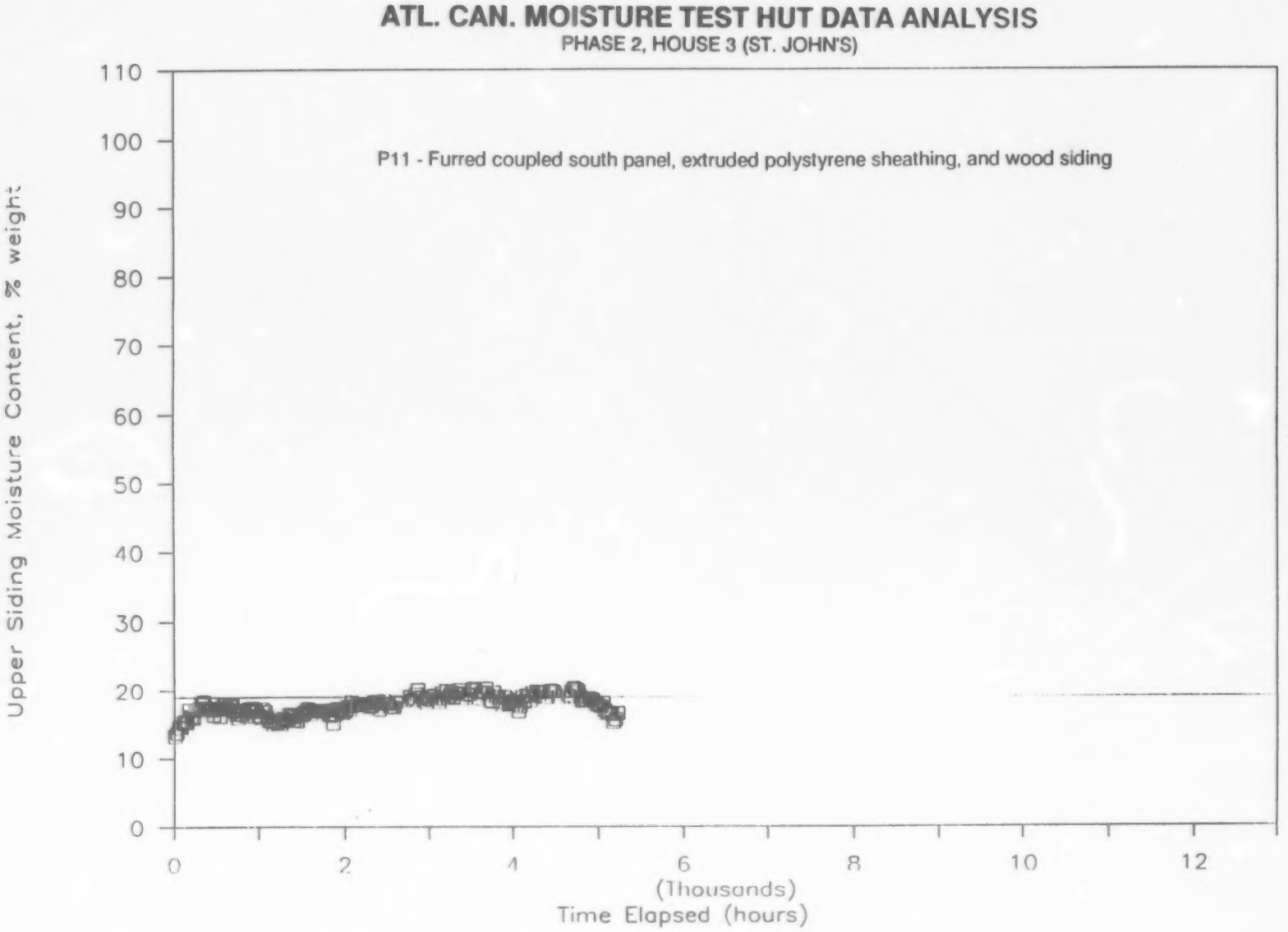
ATL. CAN. MOISTURE TEST HUT DATA ANALYSIS
PHASE 2, HOUSE 3 (ST. JOHN'S)
P11 - Furred coupled south panel, extruded polystyrene sheathing, and wood siding
Upper Siding Moisture Content, % weight
110
100
90
80
70
60
50
40
30
20
10
0
0
2
4
6
8
10
12
(Thousands)
Time Elapsed (hours)

Figure 65

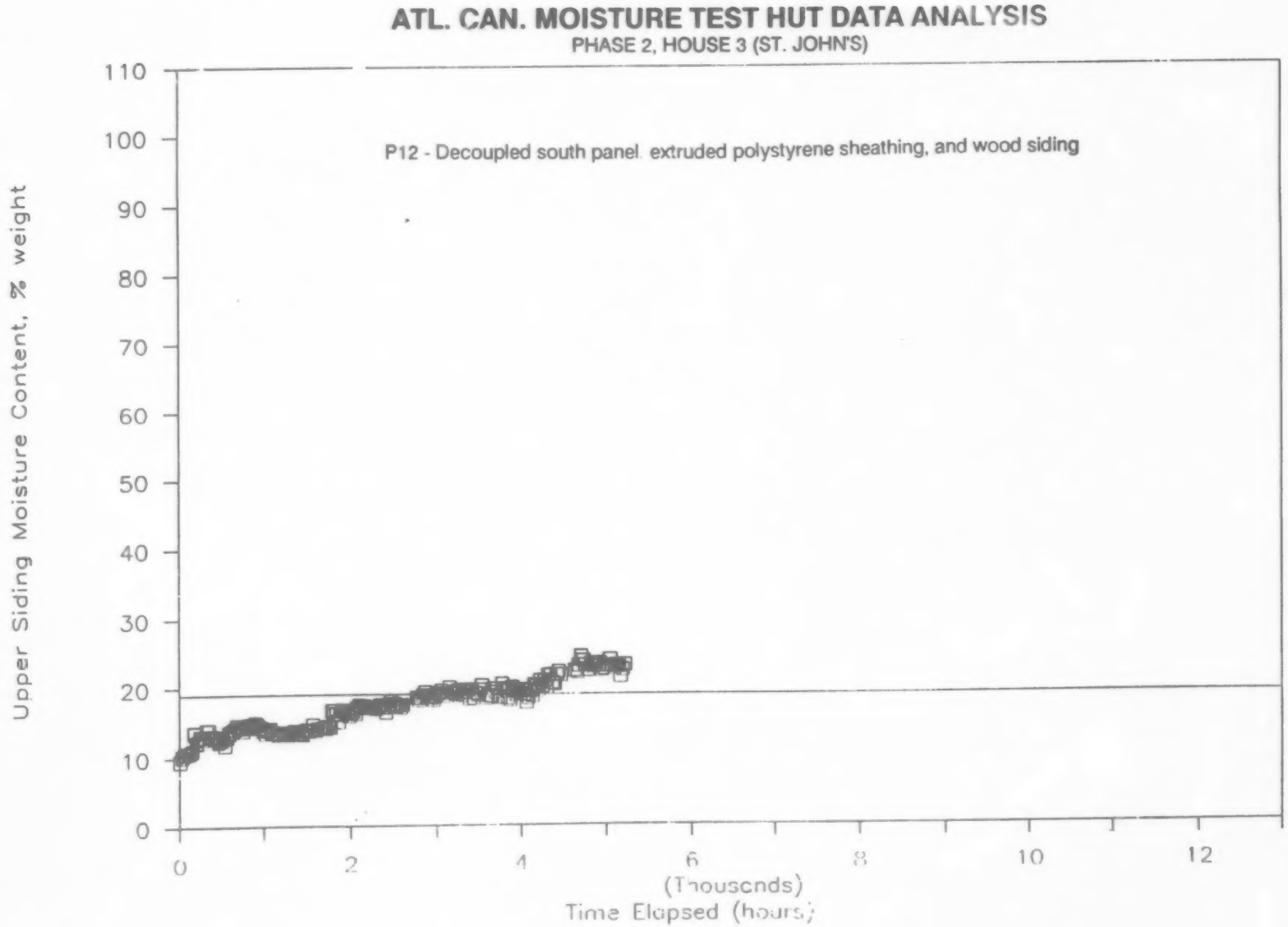
ATL. CAN. MOISTURE TEST HUT DATA ANALYSIS
PHASE 2, HOUSE 3 (ST. JOHN'S)
P12 - Decoupled south panel. extruded polystyrene sheathing, and wood siding
Upper Siding Moisture Content, % weight
110
100
90
80
70
60
50
40
30
20
10
0
0
2
4
6
8
10
12
(Thousands)
Time Elapsed (hours)

Figure 66

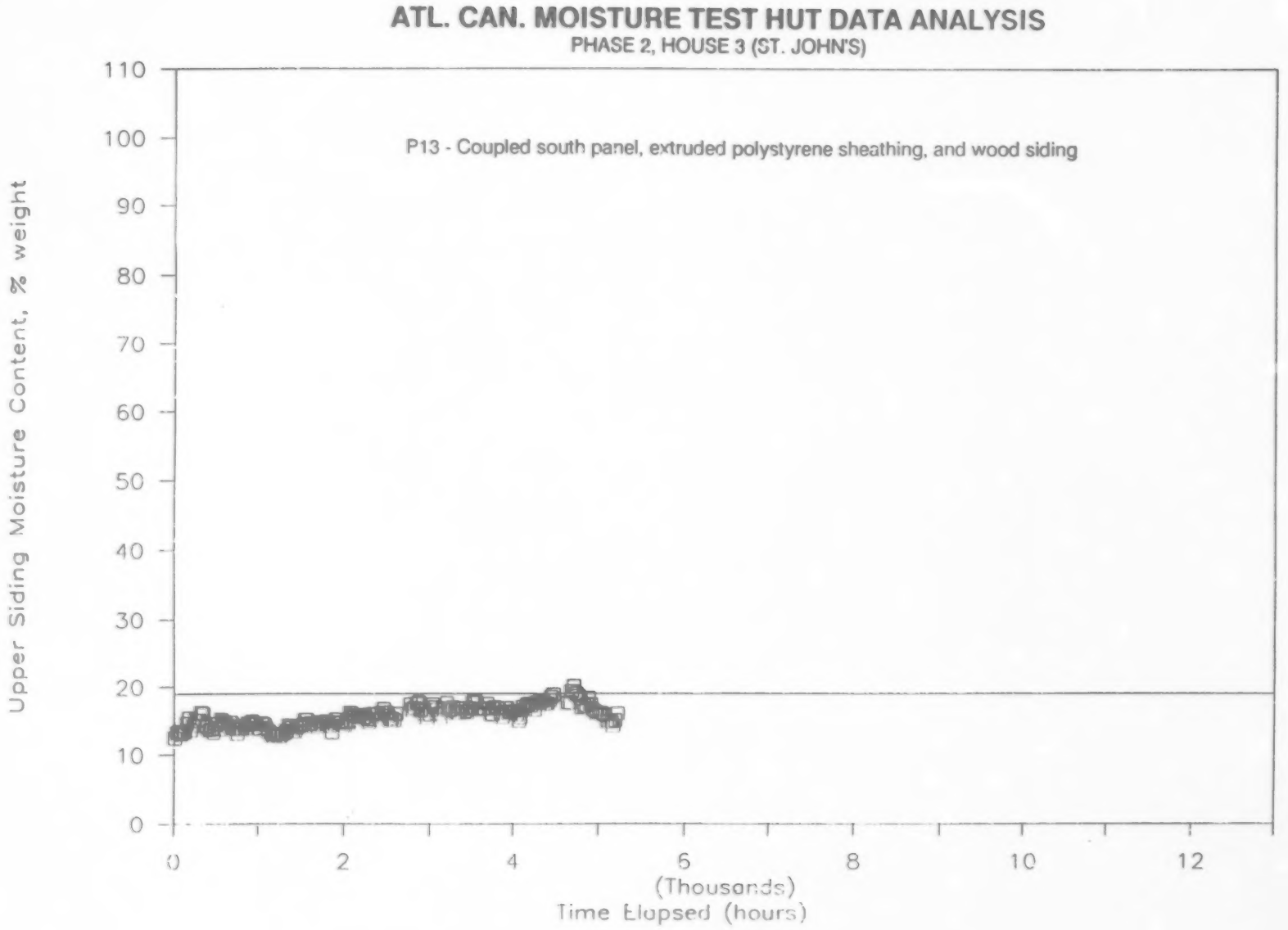
ATL. CAN. MOISTURE TEST HUT DATA ANALYSIS
PHASE 2, HOUSE 3 (ST. JOHN'S)
P13 - Coupled south panel, extruded polystyrene sheathing, and wood siding
Upper Siding Moisture Content, % weight
110
100
90
80
70
60
50
40
30
20
10
0
0
2
4
6
8
10
12
(Thousands)
Time Elapsed (hours)

Figure 67

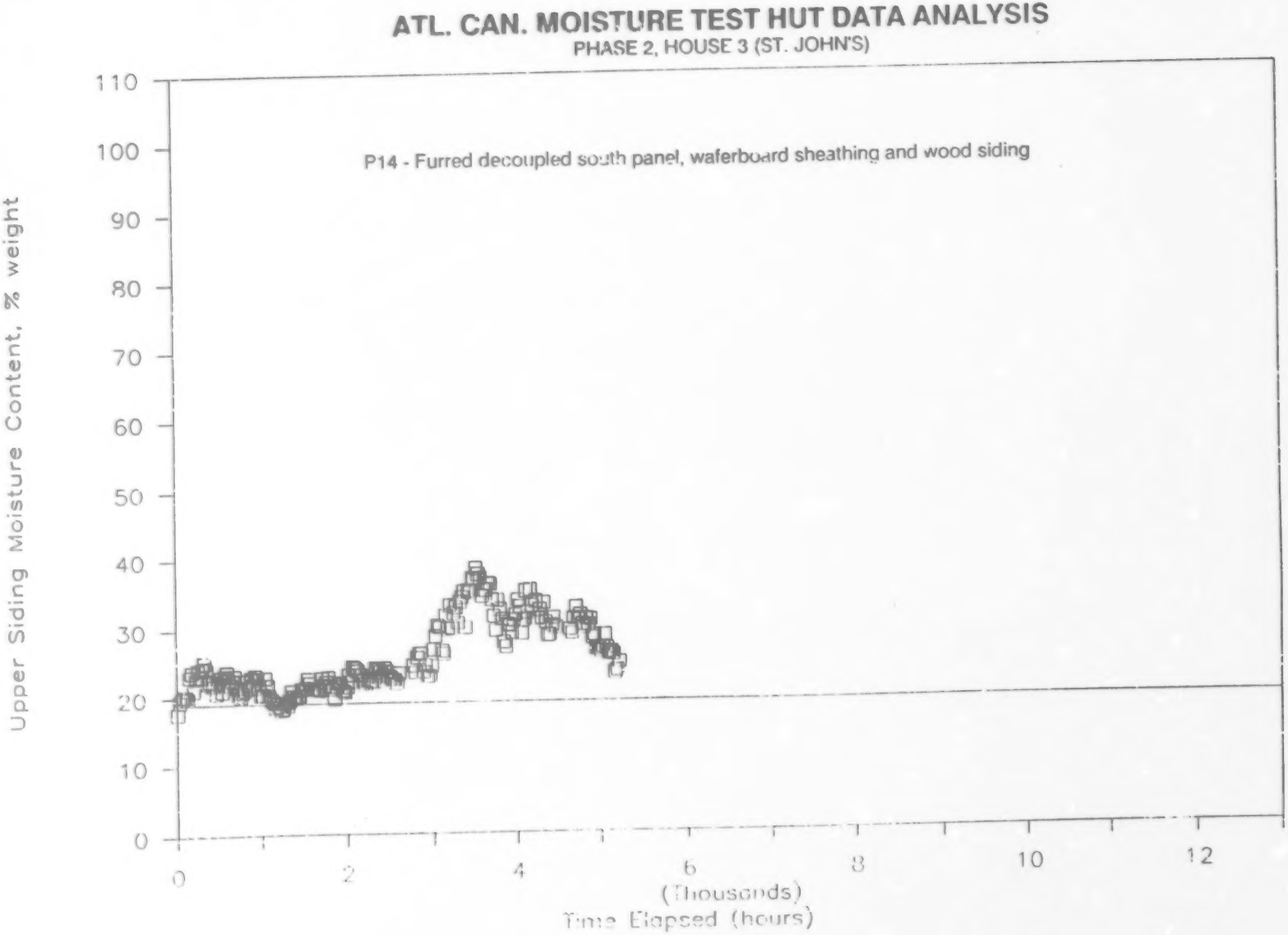
ATL. CAN. MOISTURE TEST HUT DATA ANALYSIS
PHASE 2, HOUSE 3 (ST. JOHN'S)
P14 - Furred decoupled south panel, waferboard sheathing and wood siding
Upper Siding Moisture Content, % weight
110
100
90
80
70
60
50
40
30
20
10
0
0
2
4
6
8
10
12
(Thousands)
Time Elapsed (hours)

Figure 68

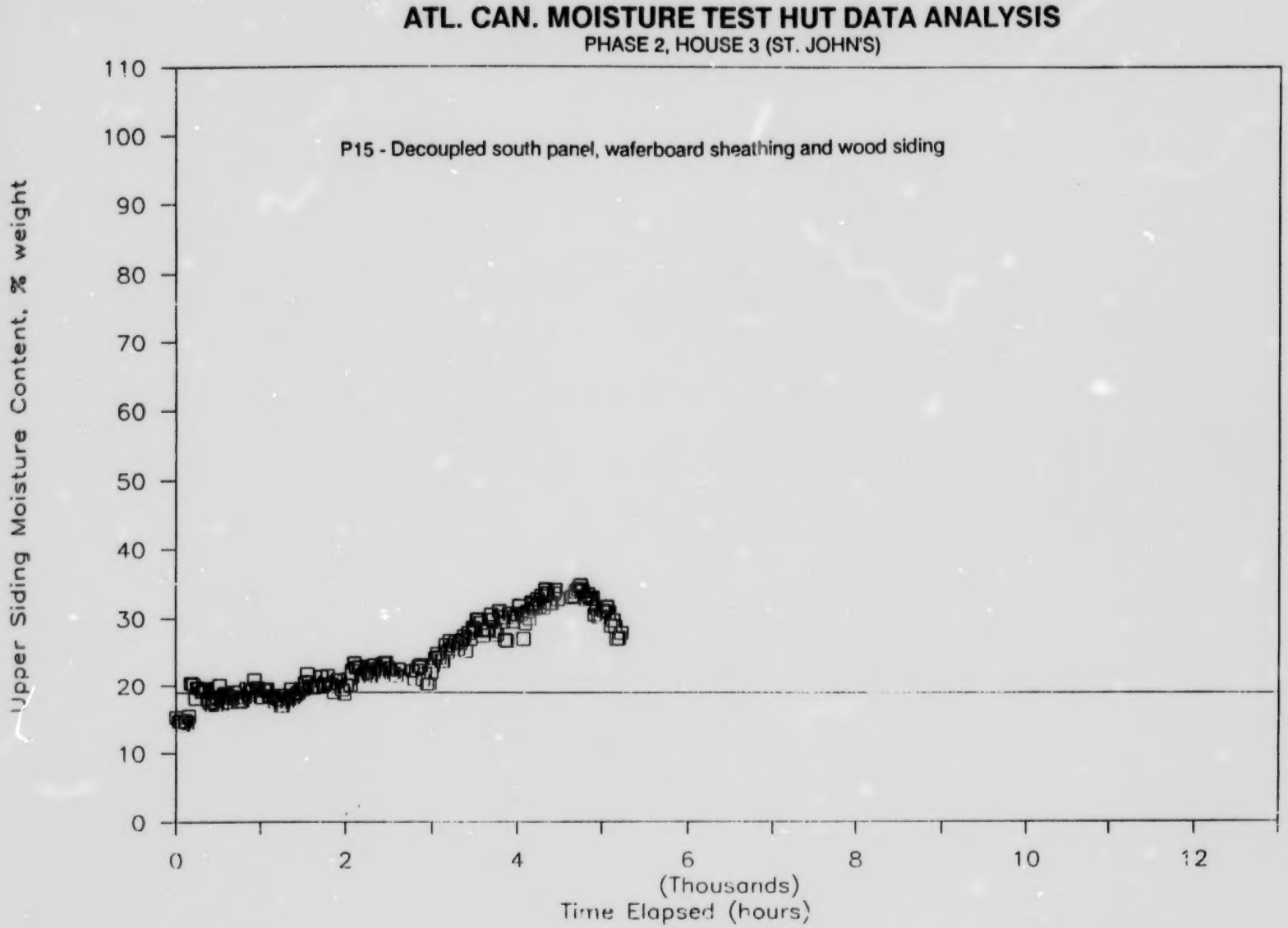
ATL. CAN. MOISTURE TEST HUT DATA ANALYSIS
PHASE 2, HOUSE 3 (ST. JOHN'S)
P15 - Decoupled south panel, waferboard sheathing and wood siding
Upper Siding Moisture Content, % weight
110
100
90
80
70
60
50
40
30
20
10
0
0
2
4
6
8
10
12
(Thousands)
Time Elapsed (hours)

Figure 69

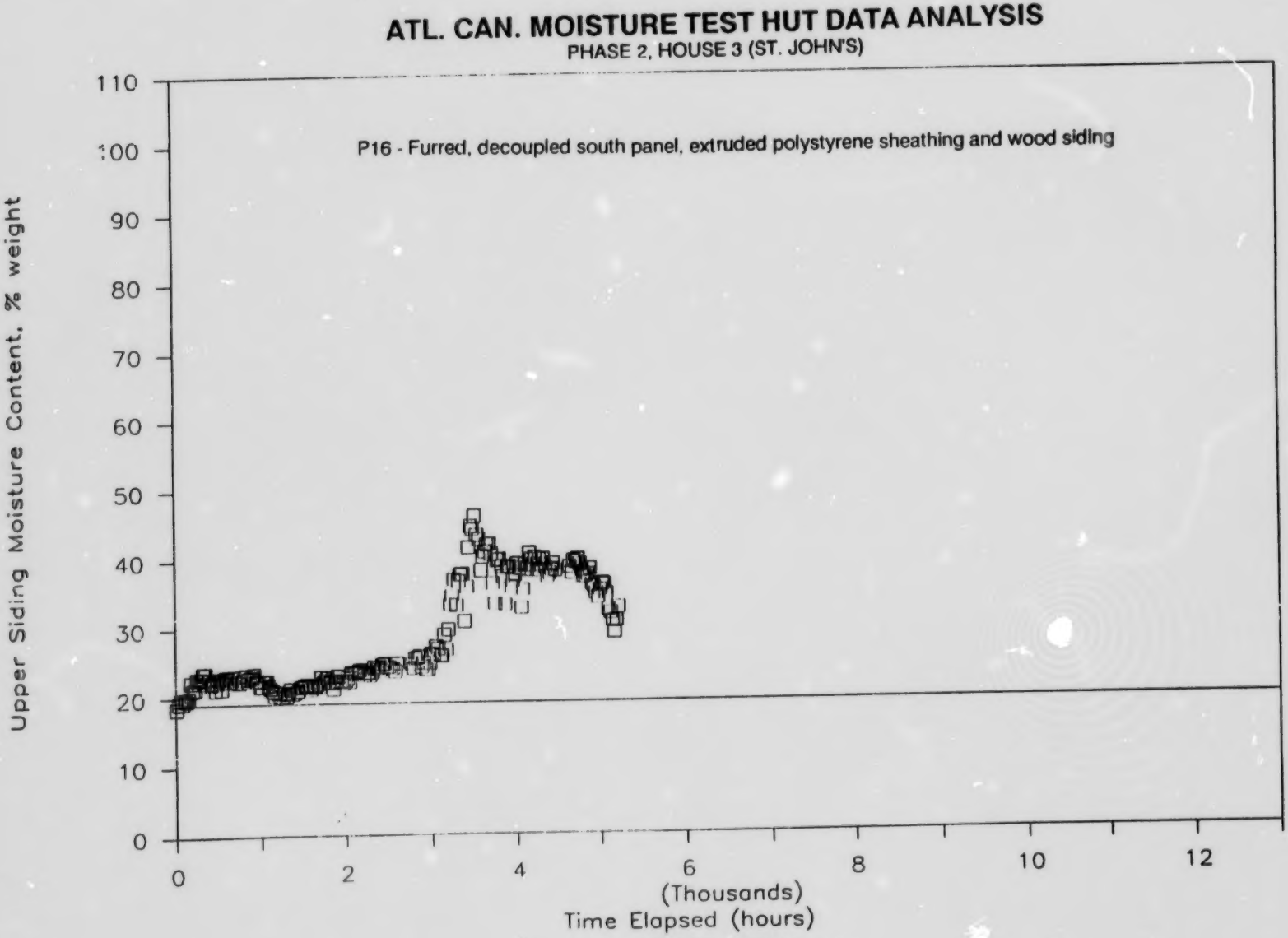
ATL. CAN. MOISTURE TEST HUT DATA ANALYSIS
PHASE 2, HOUSE 3 (ST. JOHN'S)
P16 - Furred, decoupled south panel, extruded polystyrene sheathing and wood siding
Upper Siding Moisture Content, % weight
110
100
90
80
70
60
50
40
30
20
10
0
0
2
4
6
8
10
12
(Thousands)
Time Elapsed (hours)

Figure 70

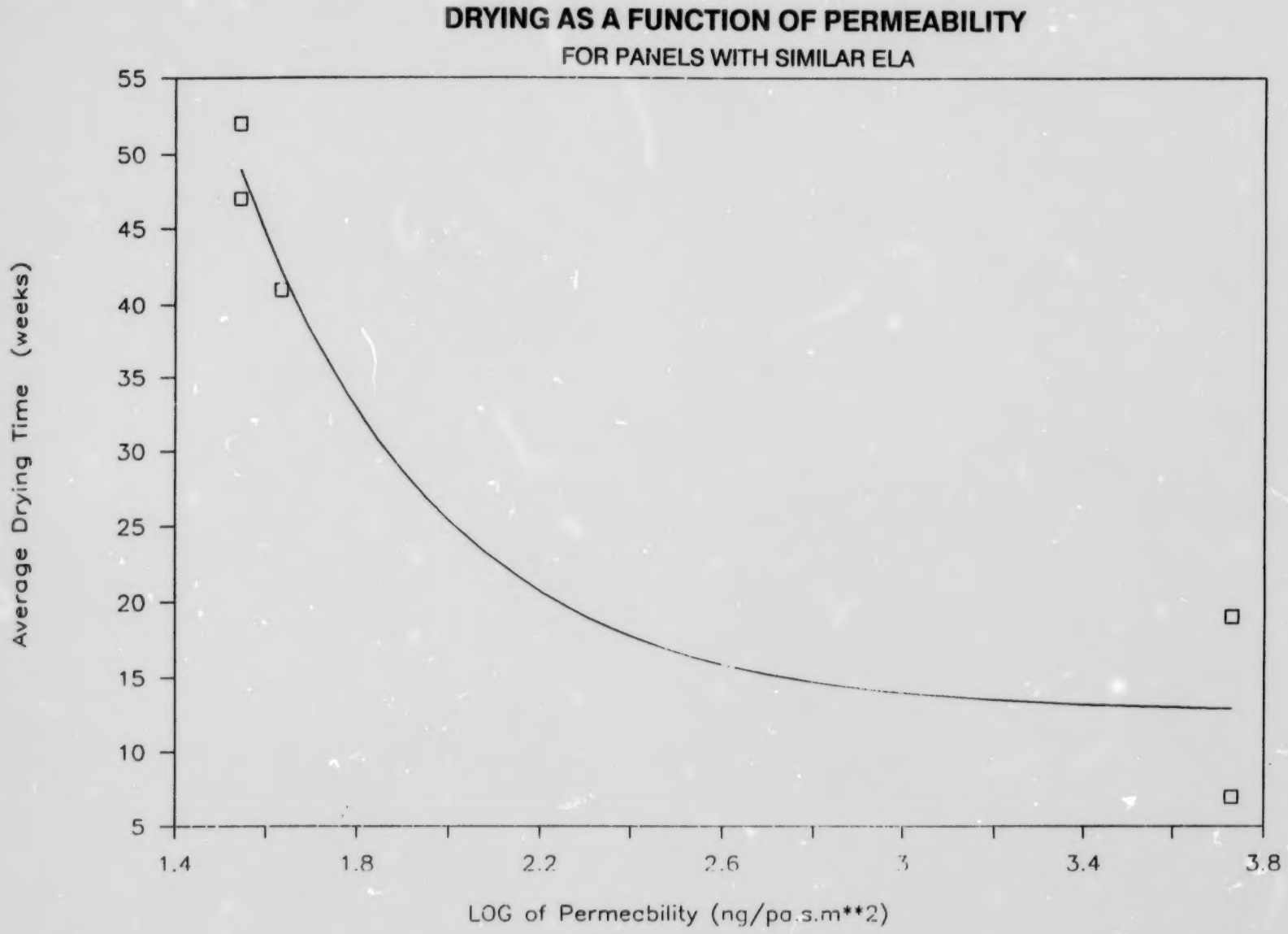
DRYING AS A FUNCTION OF PERMEABILITY
FOR PANELS WITH SIMILAR ELA
Average Drying Time (weeks)
55
50
45
40
35
30
25
20
15
10
5
1.4
1.8
2.2
2.6
3
3.4
3.8
LOG of Permecbility (ng/pa.s.m**2)

Figure 71

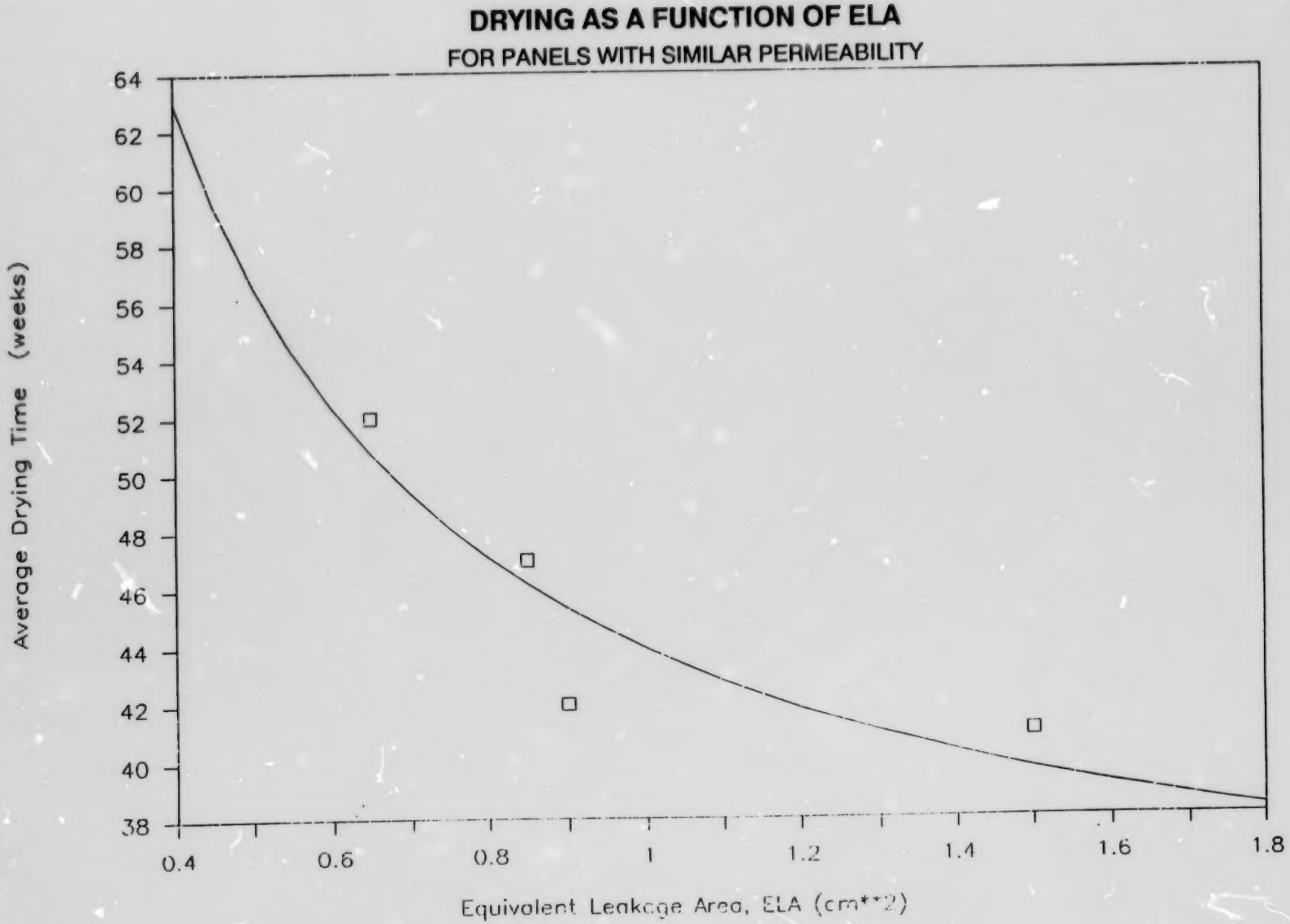
DRYING AS A FUNCTION OF ELA
FOR PANELS WITH SIMILAR PERMEABILITY
Average Drying Time (weeks)
64
62
60
58
56
54
52
50
48
46
44
42
40
38
0.4
0.6
0.8
1
1.2
1.4
1.6
1.8
Equivalent Leakage Area, ELA (cm**2)

Figure 72

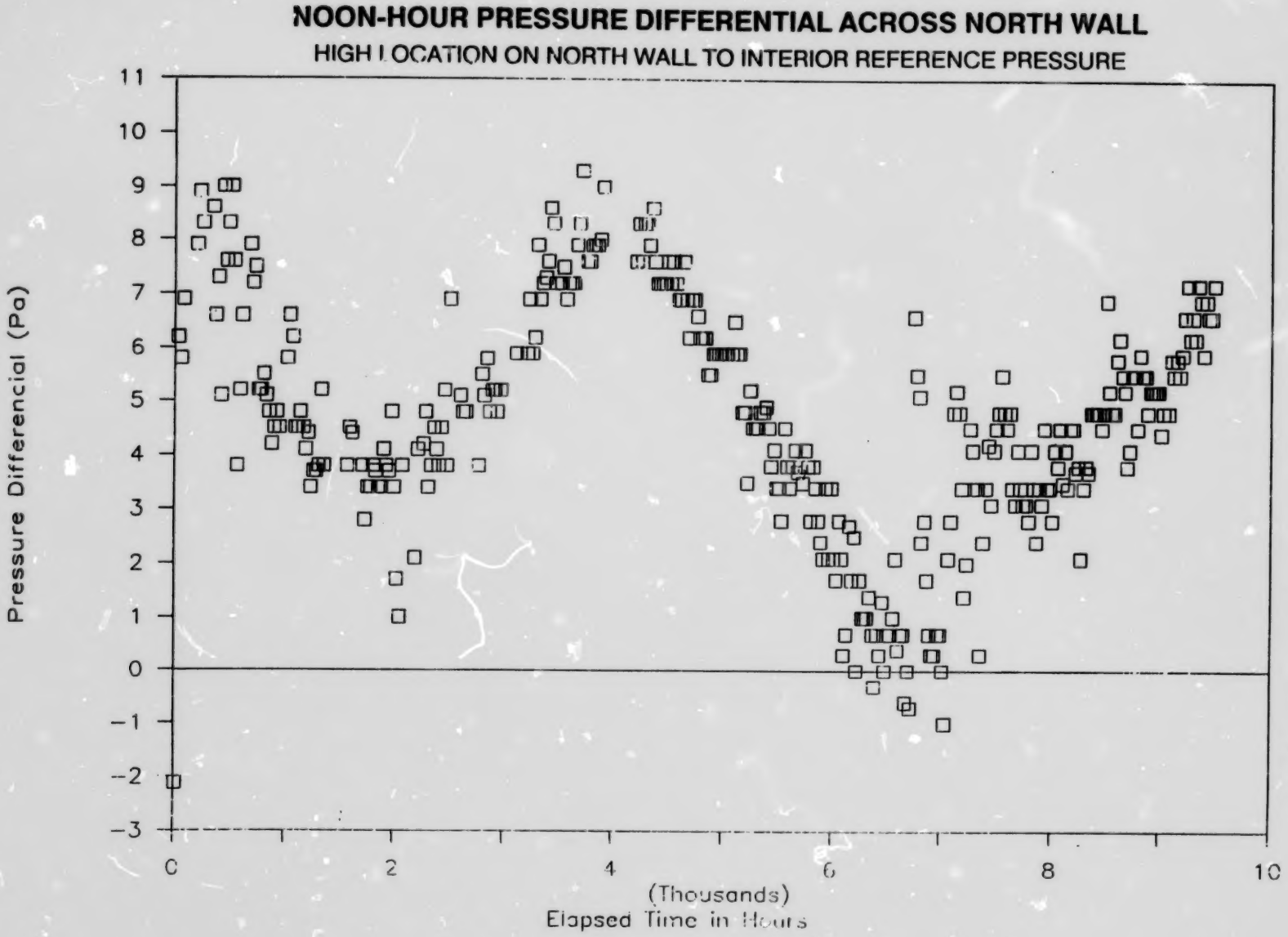
NOON-HOUR PRESSURE DIFFERENTIAL ACROSS NORTH WALL
HIGH LOCATION ON NORTH WALL TO INTERIOR REFERENCE PRESSURE
Pressure Differencial (Pa)
11
10
9
8
7
6
5
4
3
2
1
0
−1
−2
−3
0
2
4
6
8
10
(Thousands)
Elapsed Time in Hours

Figure 73

NOON-HOUR PRESSURE DIFFERENTIAL ACROSS SOUTH WALL

HIGH LOCATION ON SOUTH WALL TO INTERIOR REFERENCE PRESSURE

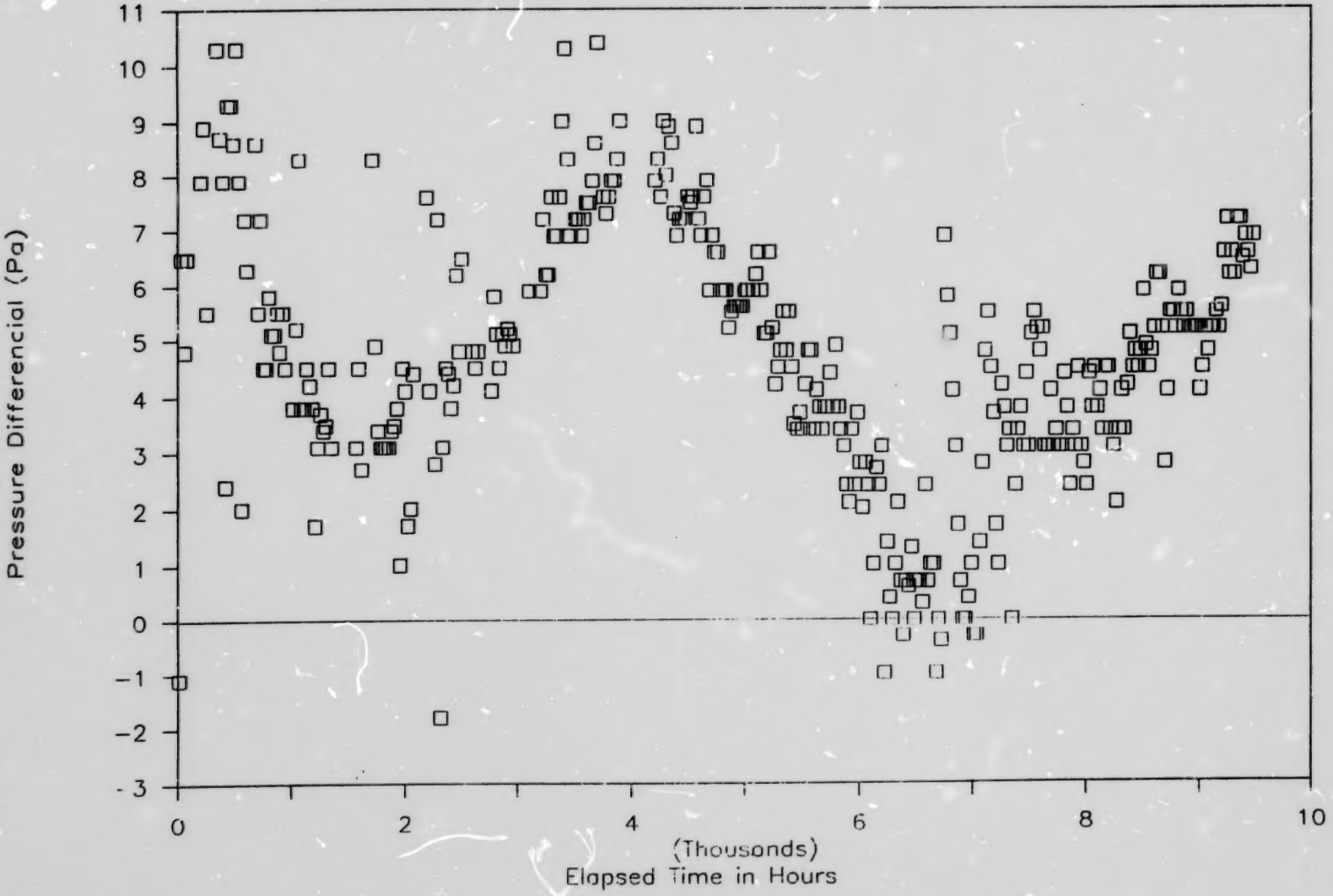

Figure 74

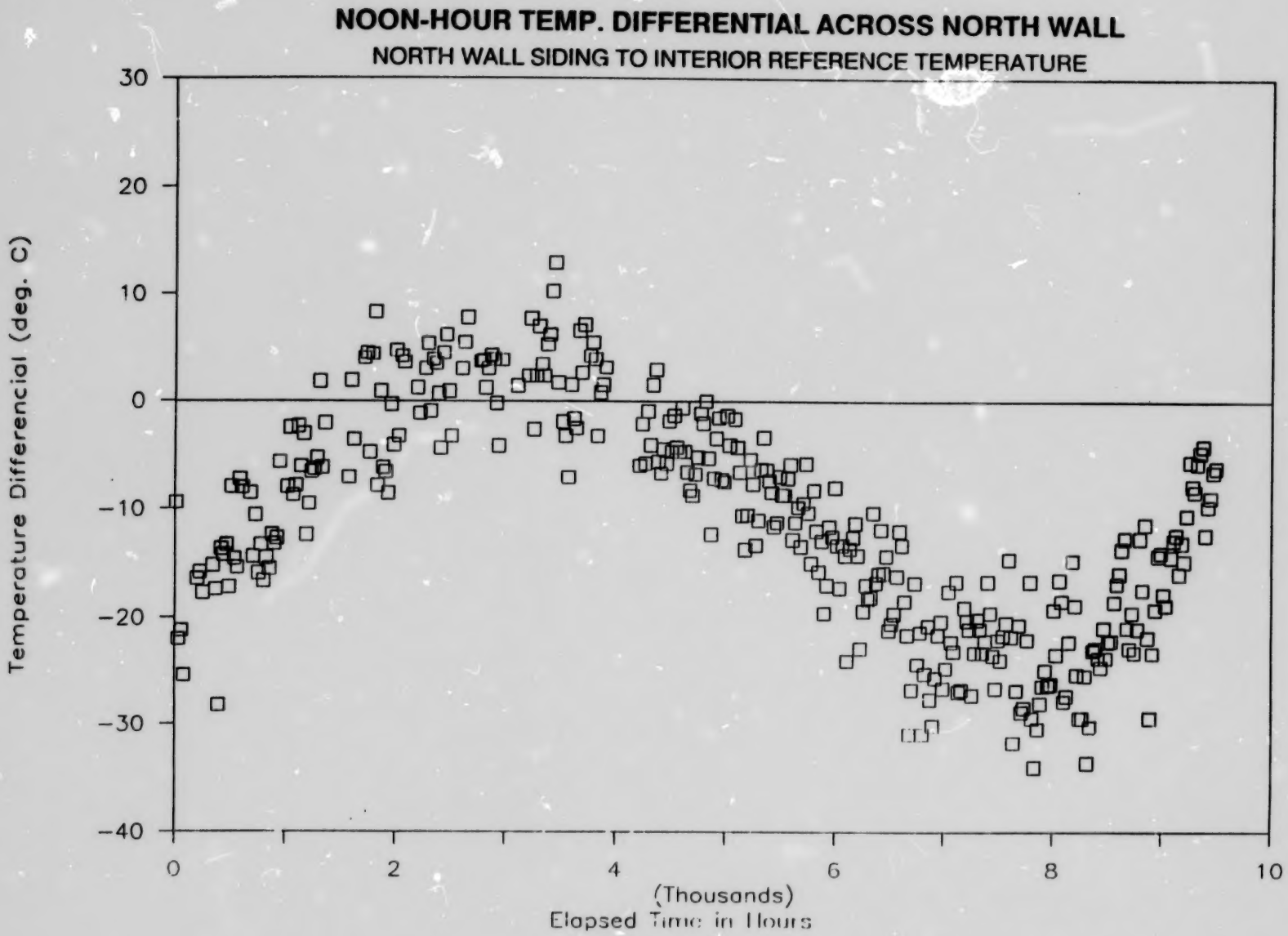
NOON-HOUR TEMP. DIFFERENTIAL ACROSS NORTH WALL
NORTH WALL SIDING TO INTERIOR REFERENCE TEMPERATURE
Temperature Differencial (deg. C)
30
20
10
0
-10
-20
-30
-40
0
2
4
6
8
10
(Thousands)
Elapsed Time in Hours

Figure 75

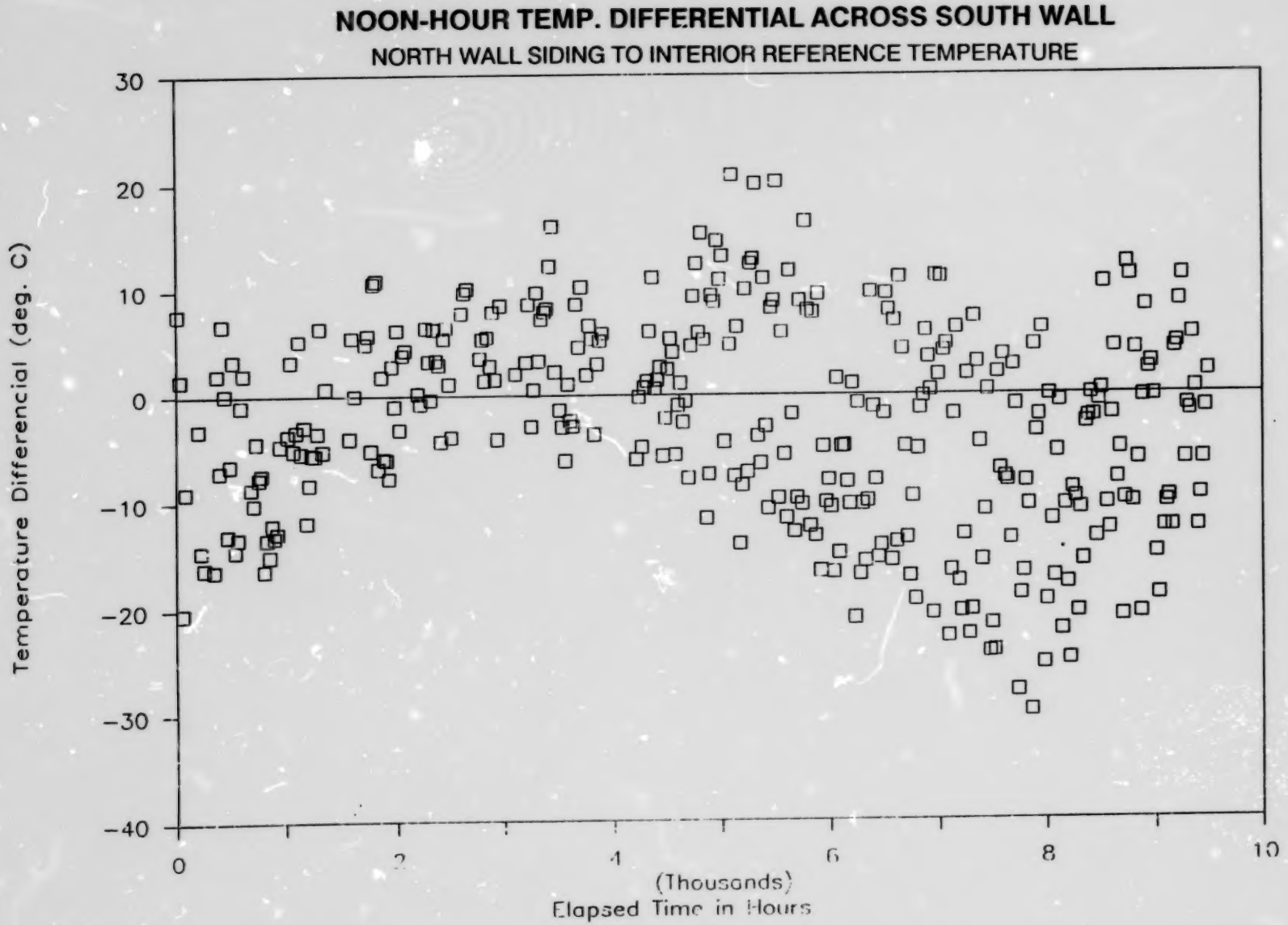
NOON-HOUR TEMP. DIFFERENTIAL ACROSS SOUTH WALL
NORTH WALL SIDING TO INTERIOR REFERENCE TEMPERATURE
Temperature Differencial (deg. C)
30
20
10
0
-10
-20
-30
-40
0
2
4
6
8
10
(Thousands)
Elapsed Time in Hours

Figure 76

PHASE II - VALIDATION OF WALLDRY COMPUTER PROGRAM

1.0 INTRODUCTION

The objectives of the second phase of this project were:

a) to obtain and convert airport weather data to WALLDRY format,
b) to compare the WALLDRY predictions with the monitored data from the Atlantic Canada moisture test hut project,
c) to validate in detail, the solar model and the moisture model separately,
d) to compare WALLDRY with FEMALP 2.1, a complex moisture transport simulation program,
e) to analyze discrepancies, suggest causes and propose improvements to WALLDRY.

1.1 What is the WALLDRY Program?

The WALLDRY Program is a computer model that dynamically simulates the processes of drying and wetting of wood frame walls over a period of time for which the weather data is available.

WALLDRY takes into account the effect of:

- The material properties of the wall assembly (density, specific heat, thermal resistance moisture, diffusion resistance, and if wood based, the hygroscopic properties of wood).
- A full year of hourly weather data including wind speed and direction, outdoor temperature and relative humidity, solar effects and night sky radiation.
- Overall wall dimensions and orientation.
- The configuration of the wall assembly (materials placement, thicknesses, spacing, airtightness, etc.).
- Initial moisture content of the various materials comprising the wall.

WALLDRY was developed to study the effects of:

- choice of materials and their thicknesses
- siding air tightness

- wall orientation
- climate
- wall configuration (e.g. strapped vs. unstrapped siding)

...on the drying and wetting performance of wood frame walls.

1.2 Validation of WALLDRY

The objective of this project was to validate the WALLDRY program by comparing its simulated predictions with the measured moisture data available from the Atlantic Canada Test Hut Project. It is extremely important to point out that during the monitoring of Atlantic Test Huts, wood moisture pins were incorrectly installed across the isotherms. The reliability of the moisture data, therefore, is questionable. However, this error was expected to be consistent throughout the monitoring period and therefore, the data could still be used for comparing the measured drying trends with the WALLDRY predictions.

The measured data was obtained from three test huts, one each in Fredericton, New Brunswick; Halifax, Nova Scotia; and St. John's, Newfoundland. The huts incorporated eight panels in both the north and south walls each with a different material configuration.

The Atmospheric Environment Service (AES) weather data for each of the three cities was acquired for the period overlapping the monitoring in the test huts. The WALLDRY program was run using a specific wall configuration in a specific city and using the AES weather data for that city. The time and date for the period of simulation were the same as the period for which the measured data from the Atlantic Canada Test Hut project were available. The results of the WALLDRY simulations, therefore, could be compared with the measured Atlantic Canada Moisture Test Hut data, for validating the WALLDRY program. The moisture content of the studs, which was monitored in all the test panels, formed the basis of comparison against the WALLDRY simulations.

The preliminary WALLDRY simulation of the Atlantic Canada Test Huts indicated that there was not a good match between the WALLDRY predictions and the measured data. A number of variations in the WALLDRY input were tried to see their effect on the WALLDRY results and whether or not they reduce the deviation

between the simulation results and the measured data. These variations included changing the permeability of the sheathing material, air-tightness of the siding, gap behind the siding and the solar radiation. These changes did not affect the simulation results. The permeability of the studs, however, was found to be a variable that had a significant effect on the moisture content profiles of the studs as predicted by WALLDRY. The permeability of the studs as an input to WALLDRY was adjusted until the predicted profiles matched most closely to the measured moisture content profiles of the studs in a specific panel of a specific hut. Further fine adjustment was carried out by varying the constant in the equation that relates the moisture content of wood to the relative humidity of the surrounding air. Once the best possible match between the WALLDRY simulation and the measured moisture data was obtained, no more changes would be introduced in the WALLDRY program. The modified model was then tested by simulating the other panels in the three cities. Altogether, four south wall panels and two north wall panels were simulated using WALLDRY and then compared with the measured moisture data. The comparisons for about half the cases were reasonably good whereas the other half were quite poor. However, it is expected that the heat transport subroutine in WALLDRY and the material properties could be further revised to give better comparisons. For instance, the moisture diffusion resistance of the studs could be split up in two regimes; one for wet cup and one for dry cup. One of these suitable regimes could be decided based on the moisture content of the studs.

2.0 WEATHER DATA CONVERSION

The hourly weather data for the three cities, Fredericton, Halifax and St. John's was obtained from the Atmospheric and Environment Services, Canada. This weather data included hourly records of dry bulb temperature, wind speed, wind direction, relative humidity, total horizontal solar radiation and cloud cover data for three years: 1986 to 1988. This data was referred to as the raw weather data because it could not be used directly by the WALLDRY program. The raw weather data was first processed to identify missing or bad data and replaced by reasonable averages based on the previous hour's or months records. In order to make it usable by WALLDRY , the hourly total solar radiation on a horizontal surface was transformed to the components that are received by the vertical walls

facing north, east, south and west respectively. Once all the necessary weather data elements were processed and/or calculated, they were converted into a single binary file which could be used by the WALLDRY computer program.

2.1 Solar Model

This solar model was developed in order to calculate the total radiation received by the vertical walls in the four directions; north, east, south and west respectively. Those data were then incorporated into the binary weather file that can be used to make WALLDRY runs. In order to translate the total horizontal solar radiation into its components normal to each of the four vertical surfaces facing north, east, south and west respectively, the total horizontal solar radiation was first broken down to its direct normal and diffuse radiation components. This was achieved with the help of two models; Hottel's model to estimate clear sky radiation, and, Staufer and Klein's model to get the beam and diffuse components of hourly radiation.

The effects of the atmosphere in scattering and absorbing radiation are variable with time, as atmospheric conditions and air mass change. It is useful to define a standard "clear" sky and calculate the hourly radiation which would be received on a horizontal surface under these standard conditions.

Hottel has presented a convenient method for estimating the beam radiation transmitted through clear atmospheres for four climate types. The atmospheric transmittance for beam radiation, τ_b is G_{cnb}/G_{on} and is given in the form

$$\tau_b = a_o + a_1 e^{(-k/\cos\theta_z)} \qquad (2.1.1)$$

where θ_z is the zenith angle.

The constants a_o, a_1, and k for the standard atmosphere with 23 km visibility are found from a_o^*, a_1^* and k^*, which are given for altitudes less than 2.5 km by

$$a_o^* = 0.4237 - 0.00821\,(6 - A)^2 \qquad (2.1.2)$$

$$a_1^* = 0.5055 + 0.00595\,(6.5 - A)^2 \qquad (2.1.3)$$

$$k^* = 0.2711 + 0.01858\,(2.5 - A)^2 \qquad (2.1.4)$$

Where A is the altitude of the observer in kilometers.

Correlation factors are applied to a_0^*, a_1^* and k to allow for changes in climate types. The conversion factors $r_0 = a_0/a_0^*$, $r_1 = a_1/a_1^*$, and $r_k = k/k^*$ are given in Table 2.1. Thus, the transmittance of this standard atmosphere for beam radiation can be determined for any zenith angle and any altitude up to 2.5 km. The clear sky beam normal radiation is then.

$$G_{cnb} = G_{on}\tau_b \qquad (2.1.5)$$

where $$G_{on} = G_{sc}^* \left[1 + 0.033 \cos\left(\frac{360n}{365}\right)\right]$$

(where G_{sc} is the solar constant (= 1353 W/m²) and n is the day of the year)

The clear sky horizontal beam radiation is:

$$G_{cb} = G_{on}\,\tau_b \cos\theta_z \qquad (2.1.6)$$

For periods of an hour, the clear sky horizontal beam radiation is:

$$I_{cb} = I_{on}\,\tau_b \cos\theta_z \qquad (2.1.7)$$

Table 2.1 Conversion Factors for Climate Types*

Climate Type	r_0	r_1	r_k
Tropical	0.95	0.98	1.02
Mid-Latitude Summer	0.97	0.99	1.02
Subarctic Summer	0.99	0.99	1.01
Mid-Latitude Winter	1.03	1.01	1.00

*From Hottel (1976)

Liu and Jordan (1960) developed an empirical relationship between the transmission coefficient for beam and diffuse radiation for clear days:

$$\tau_d = 0.2710 - 0.2939\,\tau_b \qquad (2.1.8)$$

Therefore, the hourly diffuse radiation for a clear sky is:

$$I_{cd} = I_{bn}\, \tau_d \cos\theta_z \qquad (2.1.9)$$

The total clear sky radiation, therefore, is

$$I_c = I_{cb} + I_{cd} \qquad (2.1.10)$$

The split of measured total solar radiation (I) on a horizontal surface into its beam (I_b) and diffuse (I_d) components was achieved by using a correlation developed by Staufer and Klein.

An equation representing this correlation is:

$$[I_d/I] = \begin{cases} 1.00 - 0.1\,(I/I_c) & \text{for } 0 \le (I/I_c) < 0.48 \\ 1.11 + 0.0396\,(I/I_c) - 0.789\,(I/I_c)^2 & \text{for } 0.48 \le (I/I_c) < 1.10 \\ 0.20 & \text{for } (I/I_c) \ge 1.10 \end{cases} \qquad (2.1.11)$$

$$I_b = I - I_d \qquad (2.1.12)$$

Once the beam and diffuse components of the measured total horizontal solar radiation were obtained, their translation to the four vertical surfaces facing north, east, south and west respectively was done by using simple equations. Total radiation on a tilted surface for an hour is given by the equation:

$$I_T = I_b R_b + 0.5\,(I_d + R_g I)$$

where R_b = $\dfrac{\text{beam radiation on a tilted surface}}{\text{beam radiation on a horizontal surface}}$

$= \cos\theta / \sin\beta$ (see Fig. 2.1 for angles)

R_g = ground reflectance

0.5 = view factor from surface to sky or from surface to ground.

A computer program that incorporated into it the above model, was developed and run for the three cities. The output data from this program was formatted into a large ASCII file. The weather parameters included in the file were: wind speed

(km/hr) at a height of 10 m, wind direction (degrees from the north), temperature (° C), Relative humidity (%), cloud amount (fraction of 1.0), cloud opacity (fraction of 1.0), cloud ceiling height (km), total solar radiation (W/m^2) on a horizontal surface and total solar radiation (W/m^2) on the four vertical surfaces facing north, east, south and west.

2.2 Binary Conversion of Weather Data

The ASCII output file produced above was then converted into binary format so that it could fit on a single (300K) floppy and become portable. Two such binary weather files (for 1986 and 1987) were produced for each of the three cities: Fredericton, Halifax and St. John's. These weather files are now WALLDRY useable.

3.0 WALLDRY VALIDATION

3.1 Preliminary WALLDRY Computer Runs

Preliminary WALLDRY runs were made in order to verify the correct input of weather data into WALLDRY.

WALLDRY program files were edited and some print statements were added in order to echo the input weather data. The echoed output was thoroughly inspected and compared with the ASCII weather files. It was made certain that the binary weather files contain the data that they are supposed to contain and in the proper format readable by WALLDRY.

The order of magnitude check, was done on the graphs prepared from the WALLDRY output. Figures 3.1 and 3.2 show the noon hour profiles of solar radiation on south wall, wind speed, ambient temperature and relative humidity of the outdoor air. The visual inspection of these graphs shows that they have correct order of magnitude and correct seasonal variations. The solar radiation incident on the south wall in March (days = 70 to 90) is 700-800 W/m^2 for the noon hours of the days when the sky is least cloudy. This number dips down during the month of May - June and climbs back up during November - December as was expected. The solar radiation incident on the wall was found to

be comparable with the average solar heat gain factors listed in the tables on pages 27.10 and 27.11 of the 1989 ASHRAE Handbook of Fundamentals. The ambient temperature profile also varied as expected. The wind speed and relative humidity profiles also had the expected range of values.

3.2 Validation of the Solar Model

WALLDRY simulations were carried out for the three test huts in Fredericton, Halifax and St. John's, in order to validate the solar model in the WALLDRY program. A number of print statements were added to the WALLDRY program to print out the temperature profiles of the desired elements of the panel. The simulated temperature of the outside surface of the panel (layer 3) was compared with the measured data from the Atlantic Canada Hut project. The south wall siding temperature excursions relative to the ambient temperature for the three cities Fredericton, Halifax and St. John's are shown in Figures 3.3 to 3.14. It is evident from these graphs that WALLDRY underpredicts the daily peaks and overpredicts the night sky radiation. There could be a number of reasons for this discrepancy. One reason could be the constant value of thermal resistance of the exterior air film next to the siding surface, which is used by the WALLDRY program. In reality this value is not constant. It varies according to the wind speed and the wind direction incident on the panel under investigation. Another reason could be the unsteady temperature of the test hut indoor air. The WALLDRY simulation assumes a steady temperature of 20° C during summer and 25° C during winter months. The same is true for the relative humidity.

A hand calculation was carried out to estimate the solar radiation incident on the wall panel that would produce the same wall temperature as measured in the test hut. The wall temperature of St. John's test hut 324 hours after the monitoring commenced was measured at 26.5° C and the ambient temperature measured at the test hut site was 0.5° C. The algorithm provided in the WALLDRY subroutine, RefTempProfile, was used to perform the hand calculation. The following two equations constitute this model;

$$T_{wall} = \frac{G_{uf}(T_{film}) + G_{wi}(T_{in})}{(G_{uf} + G_{ui})} \qquad (3.1)$$

$$T_{film} = \frac{G_{ro}(T_{out} + G_{ri}T_{in} + SG}{(G_{ro} + G_{ri})} \quad (3.2)$$

where T_{wall} = wall temperature

T_{film} = temperature of exterior air film next to the outside surface of siding

T_{in} = indoor air temperature

T_{out} = outdoor air temperature

G_{uf} = conductance of the layers between wall and exterior air film

G_{ui} = conductance of the layers between wall and the interior air film

G_{ro} = conductance of the layers between the exterior air film and outside air

G_{ri} = conductance of the layers between the exterior air film and the indoor air

For the test panel with unstrapped vinyl siding and waferboard sheathing, the conductance values are:

$$G_{uf} = 11.642 \frac{W}{m^2 \cdot C},$$

$$G_{ui} = 0.0487 \frac{W}{m^2 \cdot C},$$

$$G_{ro} = 12.44 \frac{W}{m^2 \cdot C},$$

$$G_{ri} = 0.0485 \frac{W}{m^2 \cdot C}.$$

For $T_w = 26.5^\circ C$; $T_{out} = 0.5^\circ C$ and $T_{in} = 20^\circ C$ the solar gain (SG) of the panel would be:

$$SG = 1736.2 \frac{W}{m^2}$$

$$= 6.25 \frac{MJ}{m^2\ hr.}$$

SG is the estimated solar radiation incident on the panel that would cause the outside surface temperature of the siding to climb to 26.5° C when the ambient temperature is 0.5° C. However, the value estimated is unrealistically high; the maximum possible value is 3.7 MJ/m² hr. Therefore, either the solar model in WALLDRY's subroutine, RefTempProfile, needs to be corrected or the material properties of the exterior air film should be adjusted. For example, the thermal resistance of the exterior layer could be adjusted so that the measured wall excursion temperatures match more closely with the WALLDRY predictions. In actuality, the thermal resistance of the exterior air film is controlled by the movement of air caused by the wind (speed and direction), and also (when the wind is low) by free convection.

3.3 Checking the Moisture Model

In order to validate the long-term moisture content of the studs, the following analytical validation procedure was carried out. The WALLDRY source code was modified to output the noon-hour relative humidity and temperature of the outdoor air, and the temperature of studs as well. The vapour pressure of the outdoor air was calculated using the algorithm provided in the WALLDRY subroutine "Partial pressure":

$$PSAT_{air} = f(\text{Temp of outdoor air})$$

$$PVAP_{air} = PSAT_{air} * RH_{air}/100 \qquad (3.3)$$

Assuming that the vapor pressure of the outdoor air is the same as the vapor pressure of the air surrounding the studs, the relative humidity of the air surrounding the studs was calculated as following:

$$RH_{stud} = PSAT_{air} * RH_{air}/100 \qquad (3.4)$$

where:

$PSAT_{air}$ = saturation pressure of the outdoor air

$PVAP_{air}$ = vapor pressure of the outdoor air

$PSAT_{stud}$ = saturation pressure of the studs

= f (Temp. of studs)

RH_{air} = relative humidity of the air

RH_{stud} = relative humidity of the air surrounding the studs

The stud moisture content was calculated using the Equilibrium Moisture Content (EMC) equation:

MC = EXP(10/6) * RH * 6/K for RH≤ 28% (3.5)

MC = 10/(LN(RH/K)) for RH> 28% (3.6)

where RH = relative humidity of the air in equilibrium with the studs

K = a constant

The calculated equilibrium stud moisture content was plotted against the WALLDRY predictions and the measured stud moisture content data and is shown in Figure 3.20 and Figure 3.23. As the calculated stud moisture content profile assumes no diffusion resistance between the air surrounding the studs and the outdoor air, the two profiles deviate from each other. This deviation seems to be getting smaller and smaller with time. If WALLDRY could be run for a longer period of time, the two profiles would be expected to coincide each other. Therefore, it can be concluded that the WALLDRY has an adequate moisture model. The moisture content predictions of wall components are highly dependent on the material properties used by the WALLDRY simulator.

3.4 Overall Validation Criteria

The overall validation of WALLDRY was carried out by comparing the WALLDRY's upper stud moisture content predictions with those from the Atlantic Canada Test Hut project measurements. The reason for selecting the stud moisture content was that this is the only measured parameter common in all panels of the three houses and that studs are the structural component of a house.

The comparison of noon-hour measured moisture data with that of WALLDRY predictions was thought to be a reasonable basis for validating the WALLDRY program.

3.5 WALLDRY Simulations of the Atlantic Canada Test Hut Panels

A number of preliminary WALLDRY runs were made and the stud moisture content profiles were compared with the measured stud moisture content profiles. The comparison was found to be very poor. This is evident from Figures 3.15 to 3.19. Further runs were carried out to determine the effect of siding airtightness, gap behind the siding, sheathing diffusion resistance and panel orientation on the stud moisture content profiles. It was discovered that these parameters had little or no effect on the stud moisture content predicted by WALLDRY. The above preliminary simulations were made using the default value of stud diffusion resistance of 800 x 10^9 (Pa m² s/kg)/m. However, when this value of stud diffusion resistance was changed to 400 x 10^9 (Pa m² s/kg)/m, the WALLDRY simulation predicted the stud moisture content profile much better than the previous simulation. It was realized that the stud diffusion resistance has a major influence on the stud moisture content profiles predicted by WALLDRY. Another WALLDRY run made using a value of 200 x 10^9 (Pa m² s/kg)/m for the stud diffusion resistance predicted the stud moisture content profile even closer to the measured data. This is evident from Figures 3.19 - 3.21.

Another parameter in WALLDRY that was found to be critical and needed attention was the constant in the Equilibrium Moisture Content (EMC) equation for wood (sometimes also referred to as sorption isotherms).

The EMC equation appears in the WALLDRY program in the following form:

RH = (MC/6)*150/(EXP(10/6)) for MC ≤ 6 (3.7)

RH = 150/(EXP(10/MC)) for MC > 6 (3.8)

This relationship was developed using data from the Handbook of wood. In these two equations, the relative humidity is related to the moisture content of wood. "K = 150" is the parameter whose effect on the stud moisture content profiles was studied by varying it. The test hut panel with high density fibreglass sheathing (panel 3) in St. Johns, was simulated with K = 150, 140 and 120 respectively. The effect of this variation on the stud moisture content predictions of WALLDRY is shown in Figures 3.21 to 3.23. It is evident from these runs that lowering K from

150 down to 120 reduced the deviation between the WALLDRY prediction and the measured stud moisture content profiles.

Based on the conclusions drawn from the above analysis, it was decided that the WALLDRY simulations of the remaining panels would be made using a stud diffusion resistance of 200×10^9 (Pa m² s/kg)/m and K = 120.

After making the adjustments to the WALLDRY model (constant "K" in the EMC equation) and material properties database, the following panels were simulated:

a) south panels 1 - 4 in each of the three test huts
b) north panels 9 and 10 in each of the three test huts.

The WALLDRY predicted stud moisture content profiles for the above cases were compared with the measured stud moisture content profiles. The comparisons are shown in Figures 3.20 to 3.41. It should be noted that the WALLDRY simulation was started after the time when the measured stud moisture content profiles became regular. The initial period when the measured stud moisture content profiles were irregular (varying up and down without a trend) was not included in the simulation. That is why the simulation starting dates are different from one panel to another. The initial stud moisture content for WALLDRY simulation was taken from the upper stud moisture content measurements in each case. The initial moisture content of the siding was normally taken as 30% and that of glasclad sheathing also as 30% which is the maximum limit in each case. The initial moisture content of the wood sheathing was taken from the measured data for respective panels. The gap behind the siding was 3mm when not strapped and 19mm when strapped. The thickness of vinyl siding was taken as 1mm. The indoor air conditions of temperature and relative humidity were 20° C, 40% during winter and 25° C, 60 % during summer. A sample WALLDRY input file listing is included in the Appendix "A".

3.6 Validation of WALLDRY Using Alp Keresteciogiu's Model (FEMALP 2.1)

The Validation of WALLDRY was performed using the "evaporation and condensation" model developed by Dr. Alp Keresteciogiu of Florida Solar Energy Center[4]. If WALLDRY and "evaporation and condensation" model use similar heat and moisture transfer equations then they must produce similar results.

In the validation, a hypothetical material was used. The properties of the hypothetical material are as follows:

TABLE 3.6

Symbol	Value	Units	Name
k	0.262	W/m.K	Thermal conductivity
C_p	1085	J/kg.K	Specific heat
ρ	725	kg/m^3	Density
ρ_b	725	kg/m^3	Bulk density
D_v	5.5×10^{-6}	m^2/s	Vapor diffusivity
Λ	0.7	-	Porosity
A_T	1.1602	m^3/kg	Isothermal moisture capacity
B_ρ	8.794×10^{-4}	kg/kg.K	Thermo-gradient coefficient
λ	$2.5 \times 10^{+6}$	J/kg	Heat of sorption

For the hypothetical sample a linearized equilibrium moisture sorption isotherm was used. The sorption isotherm is defined by the following equation:

$$EMC = 0.322 + 1.1602\rho_V - 8.794 \times 10^{-4}\ T$$

where T = temperature of the sample slab

ρ_V = water vapor density (kg/m^3)

EMC = Equilibrium moisture content of the sample slab (kg/kg)

If a small range of temperatures around 300° K is considered, then the above equation can be reduced to:

$$EMC = 0.322 + 1.602\rho_V - 8.794 \times 10^{-4}\ (300) \qquad (3.61)$$

now relative humidity $\phi = \rho_V/\rho_{V,sat}$

and $\rho_{V,sat} = [EXP\ [23.7093 - 4111/(T-35.45)]]/(461.5(300))$

$\rho_{V,sat})_{300k} = 0.0255$

$\rho_V = \phi * \rho_{V,sat}$

$\therefore EMC = 0.0582 + 1.1602 * 0.0255\phi$

or $EMC = 0.0582 + 0.0296\phi \qquad (3.62)$

Maximum water absorption is the equilibrium moisture content at a 100% relative humidity = 8.78%

Equation (2) can also be expressed in the form:

$$\phi = (EMC - 0.0582)/0.0296$$

or in terms of %:

$$\phi = (EMC - 5.82)/0.0296 \qquad (3.63)$$

where ϕ and EMC are in %.

The sorption isotherm developed above in equation 3.63 was incorporated into WALLDRY by replacing the original equations 3.5 and 3.6. The sheathing material in WALLDRY's material properties data base was assigned the new material properties as for the hypothetical material chosen above as in Table 3.6. The WALLDRY computer program was then run assuming the same initial and boundary conditions as in Alp's model run listed in Appendix B. In an attempt to simulate Alp's model case 2, the following modifications were made to the WALLDRY computer program:

(i) the diffusion resistivity and the thermal resistivity of all the materials between the sheathing and the indoors were made the largest possible in order to make interior surface of the sheathing impermeable and adiabatic,

(ii) the gap between the sheathing and siding was made the largest,

(iii) the temperature and the relative humidity of the air in the gap was made same as the outdoor air at the same ambient conditions as in Alp's model case 2.

The moisture content and temperature profiles of the sheathing from the WALLDRY simulation in Figures 3.42 and 3.43 did not compare well with the

moisture content and temperature profiles from Alp's model Figure 3.44 and 3.45. It can only be concluded from the above comparison that WALLDRY could not be properly set up to produce the simulation parallel to Alp's case 2. It appears that the only way to compare the two models is by extracting the pertinent subroutines from WALLDRY and run them separately.

In order to validate the wood moisture isotherm used by WALLDRY, Alp Keresteciogiu's model "Theoretical and Computational Investigation of Algorithms for Simultaneous Heat and Moisture Transport in Buildings," was used. The comparison of the sorption isotherms from the two models is shown in Figure 3.46. The two models compare very well varifying that the sorption isotherm equations used in WALLDRY are satisfactory.

4.0 DISCUSSION OF RESULTS

A number of preliminary WALLDRY runs were carried out in order to determine the effect of various parameters on the stud moisture content profiles of the test hut being simulated.

The south wall siding temperature excursions relative to ambient for Fredericton, Halifax and St. Johns are shown in Figures 3.3 to 3.11. Similar excursions for north wall are shown in Figures 3.12 to 3.14. It can be seen from these graphs that WALLDRY underpredicted the siding temperature excursions as compared with the measured data. Also it can be observed from these graphs that the night sky radiation affect is overpredicted by WALLDRY. One reason for the underprediction of daily peaks could be the inappropriate value of thermal resistance of the exterior air film next to the siding. In WALLDRY, the thermal resistance of the exterior siding air film during the day time is kept constant while at night it is a function of wind speed and wind direction. Other reasons include error in the technique for the measurement of wall temperature and data error. The probable reason for the overprediction of night sky radiation effect could be that an inappropriate wall emmissivity value (0.8) was used by WALLDRY. The north wall siding temperature excursion comparisons were much better than the south siding because of low solar radiation received by the north wall. Figure 3.18a shows, however, that the WALLDRY predictions of stud moisture content

profiles of north and south panels were very close to being coincidental. This does not agree with the results of the measured data from the Test Huts.

Two hypotheses are discussed in order to explain the effect of solar radiation on the migration of moisture in the walls of a building. According to a first theory, the moisture content of the wall components is dependent on the temperature of the wall components. Since the solar radiation received by the south wall is more than that of the north wall, the average temperature of the south wall is higher than that of the north wall. Therefore, the south wall should dry faster than the north wall. This hypotheses is supported by the conclusion based on the analysis of the Atlantic Moisture data that states that the south walls dry faster than the north walls. However, WALLDRY appears to employ the second theory which is based on the thermal gradient across the wall. During the day, when the solar radiation incident on the wall raises the temperature of the surface on the outside of the wall, the thermal gradient across the wall becomes very low or even negative. The negative thermal gradient across the wall means, that the moisture migrates from the outside of the wall towards the studs. Conversely, during the night, the movement of moisture would be outwards from the studs. This would mean that the drying of walls takes place in the absence of solar radiation. Also, the north walls should dry faster than the south walls. WALLDRY simulates this effect correctly (Figure 3.18a), however, the magnitude of the difference in the drying rates of north and south walls is insignificant.

To study the impact of this process in WALLDRY two simulations were carried out on the north panel in St. John's having strapped vinyl siding and waferboard sheathing: one with actual solar radiation incident on the panel and the other with no radiation incident on the panel. The plots from these runs are shown in Figures 3.17a and 3.17b. It is quite evident that in the simulation without solar radiation the panel dries faster than in the one with solar radiation. This means that the phenomenon of wall drying is primarily a nightly occurrence while the long term drying is impeded by the moisture driven back into the wall during the day when solar insolation causes negative temperature gradients.

Another parameter that affects the drying of walls is the relative humidity of the outdoor air. The relative humidity of the outdoor air and the temperature gradient across the wall determine the drying potential of the wall panels.

The effect of siding airtightness on the drying rate of the wall was analyzed by simulating two panels differing only in the siding airtightness. Figure 3.18b shows that changing the siding airtightness from K_1 = 38.574 and K_2 = 7.668 to K_1 = 25.0 and K_2 = 4.5 (Pa/(L/s))/m had only a small effect on the drying profiles. The wall with a looser siding dries slightly faster than the one with tighter siding.

The thermal resistance of the exterior air film showed an insignificant effect on the drying of panels as evident from Figure 3.18c. Changing the thermal resistance of the exterior air film from 15 ((m².C/W) to 25 (m².C/W) only slightly shifted the stud moisture content profile downwards.

The WALLDRY simulation of panel 3 in St. John's formed the basis of a validation technique called calibrated modelling. In this technique we assumed probable values of the unknown parameters such as diffusion resistance of the siding, sheathing and studs, air tightness of the siding, gap behind the siding etc., ran WALLDRY and compared its predictions with measured data. Several adjustments to the values of the unknown parameters, within the range of probable values, were made until the WALLDRY predictions closely matched the measured data. It was found that the WALLDRY program was sensitive only to the diffusion resistance of the studs and the sorption isotherm. The variations in the values of other parameters had no effect on the stud moisture content profiles predicted by WALLDRY. The effect of stud diffusion resistance on the moisture content profiles of the studs is evident from Figures 3.19, 3.20 and 3.21. The best comparison between WALLDRY simulation and the measured data was achieved when the value of stud diffusion resistance was 200 x 10^9 (Pa m² s/kg)/m. This comparison is shown in Figure 3.21. Further fine tuning of the simulation profiles was done by changing the constant K in the equation for the sorption isotherms for wood. The default value of K in those equations (3.7 and 3.8) was first replaced by 140 and then by 120. The stud moisture comparisons of each of these simulations are shown in Figures 3.22 and 3.23. It can be noticed that the simulation with K = 120 compares better with the measured data than the simulations with K = 140 and 150. The horizontal portion of the moisture curve (from hours 105 onwards) shifts upwards as the constant K was changed from 150 to 120. This was expected according to the Equilibrium Moisture Content curve (sorption isotherm curve) for wood. It is speculated that K is a function of

temperature. It is recommended that more research should be done on studying the effect of temperature on the sorption isotherms of wood. Based on the WALLDRY runs made so far, the best agreement between the simulation results and measured data was obtained when the stud diffusion resistance was 200 x 10^9 (Pa m^2 s/kg)/m and the constant (K) in the equilibrium moisture content equation was 120. The rest of the WALLDRY simulations were carried out with the above changes incorporated into materials properties database and WALLDRY program code.

Initial moisture content values assigned to the various components of the wall at the beginning of the simulation were picked up from the corresponding hours of the measured moisture hut data. The effect of initial moisture content on the resulting stud moisture content profiles is evident from Figures 3.32 and 3.33. The initial stud moisture content establishes the initial moisture transfer gradient. The simulations with higher initial moisture content will dry faster in the early stages of the simulation period. But the equilibrium moisture contents obtained in long run would be the same for both the cases.

The starting point of the simulation (starting time of the year and the initial moisture content) was selected after reviewing the measured stud moisture content profile of the corresponding panel. During the analysis of the measured data in phase I of this project, it was observed that the initial portions of the stud moisture content profiles were almost flat for as much as 8 months in some cases. A logical explanation for this occurrence could be the false moisture data collected with the wood moisture pins installed incorrectly across the isotherms. Also it is understood that the moisture content measurements in wood become highly unreliable over 30%. WALLDRY was unable to simulate this behavior. Therefore, the starting point for WALLDRY simulations was the point on the measured profiles when the irregularity ends and the moisture content starts to decline in a regular fashion.

The results of the simulations carried out using the modified WALLDRY program and materials properties database with appropriate starting point are graphed in Figures 3.24 to 3.41. In more than half the cases, the simulated stud moisture content profiles were found to agree reasonably well with the measured data. The agreement was particularly good for the huts in St. John's and Halifax. WALLDRY

best simulated the panels with glasclad sheathing (panels 3 and 4). Glasclad has a very low diffusion resistance and therefore makes the moisture transport phenomenon simple as compared with the waferboard sheathing (in panels 1 and 2). WALLDRY needs to be modified in order to better simulate the panels with high diffusion resistivity.

The probable reasons for poor agreement between WALLDRY simulations and the measured data are listed as following:

i) the model's inability to respond well to the variations in solar radiation (north vs. south) walls),
ii) the model's inability to respond well to the variations in the diffusion resistivity of various components of the panel,
iii) the model's inability to respond well to the variations in the gap behind the siding, airtightness of the siding and the strapping behind the siding,
iv) non-uniform properties of the building materials,
v) possible inconsistency in the mounting of the moisture pins, calibration of moisture pins and other errors that could have occurred during the collection and processing of data.
vi) all the runs were made with indoor air conditions of 20° C, 40% rh and 25° C, 60% for the winter and summer respectively, whereas a review of the indoor monitored data suggested that the indoor conditions were maintained at 20 ± 5° C and 60 ± 2% rh,
vii) the maximum water absorption limit for the glass fibre batt insulation was assumed to be 30% (by weight) in all simulations,
viii) WALLDRY does not allow assigning different initial moisture content values for the upper and the lower parts of the siding, sheathing and studs for use with measured data.

CONCLUSION

The analysis of the results of the preliminary simulations indicated that WALLDRY did not adequately model the test panels with respect to the orientation (north vs. south), the airtightness of the siding, the gap behind the siding and the diffusion resistivity of the siding and the sheathing. The overall comparison of WALLDRY

predictions of the stud moisture content profiles with the measured data was quite poor. The parameter that highly influenced the stud moisture content predictions of WALLDRY was found to be the diffusion resistivity of the studs. The value of the stud diffusion resistivity was adjusted to 200 x 10^9 (Pa.m2.s/kg)/m in the materials properties database.

The WALLDRY simulation of the test panels with this stud diffusion resistivity produced stud moisture content profiles which best agreed with the measured data. Also the constant "K" in the sorption isotherms of wood was adjusted to 120 (from 150). All the WALLDRY runs were carried out with these changes incorporated.

Using these modified property values, the WALLDRY simulations of more than half the panels predicted stud moisture content profiles that agreed reasonably well with the measured data. The agreement was particularly good for the test panels containing glasclad sheathing (low diffusion resistivity), where the transfer of moisture is basically a diffusion phenomenon. The test panels with high diffusion resistivity showed poor results probably because in this case condensation on the interior of the sheathing is an important element in the process, and this phenomenon seems to be inadequately modeled in WALLDRY. The moisture diffusion resistivity of wood should be a function of the wood moisture content.

The solar model responded poorly with respect to the wall orientation. WALLDRY underpredicted the wall surface temperature (during the day) and overpredicted the nightsky radiation. The removal of heat from the wall surface (exterior) via convection was not modelled adequately by WALLDRY. The convective heat transfer co-efficient during day should be made to vary with the direction and speed of wind incident on the wall surface.

The overall validation of WALLDRY suggested that it can simulate the drying of walls reasonably well if suitable material properties of wall components are utilized. The program should be modified by making the suggested improvements to the solar and moisture models.

REFERENCES

1. Oboe Engineering Ltd. — Final Report on the Drying of Walls - Atlantic Canada, November 26, 1987.

2. Oboe Engineering Ltd. — Manual for Atlantic Canada Hut Project, March 6, 1989.

3. Canadian Mortgage and Housing Corporation — CMHC/CHBA Task force on moisture problems in Atlantic Canada.

4 A Keresteciogiu, L Gu — Theoretical and Computational Investigation of Simultaneous Heat and Moisture Transfer in Buildings: "Evaporation and Condensation" Theory.

Table 3.1

TITLE

05-Oct-89

DAY FROM START	DAY	TEMP(C) OUT	RH OUT	WIND (km/hr)	NOON SOLAR (W/m2)	MC(%) (3,5)	SHEATHING MOISTURE CONTENT (11,5)	(12,5)	(13,5)	STUD MOISTURE CONTENT(%) (21,1)	(21,5)	(21,9)	AIR SPACE VELOCITY(m/s) (7,1)	(7,5)	(7,9)	STUD MOISTURE CONTENT(%) (22,1)	(22,5)	(22,9)	SHEATHING FILM THICKNESS (11,1)	(11,5)	(11,9)
129	129	0.8	85	30	277	29.99	36.99	37.00	37.06	53.96	53.96	53.96	0.00	0.00	0.00	54.00	54.00	54.00	0.00	0.00	0.00
130	130	4.4	88	22	281	29.94	36.72	37.01	38.52	53.14	53.14	53.14	0.00	0.00	0.00	54.00	54.00	54.00	0.00	0.00	0.00
131	131	3.4	75	7	535	29.84	36.47	37.02	39.94	52.33	52.33	52.33	0.00	0.00	0.00	53.99	53.99	53.99	0.00	0.00	0.00
132	132	2.6	75	33	444	29.68	36.21	37.05	41.33	51.54	51.54	51.54	-0.01	0.00	0.00	53.98	53.98	53.98	0.00	0.00	0.00
133	133	3.0	82	19	255	29.55	35.95	37.08	42.71	50.76	50.76	50.76	0.00	0.01	0.00	53.96	53.96	53.96	0.00	0.00	0.00
134	134	12.4	52	4	537	29.36	35.72	37.12	43.98	50.04	50.04	50.04	0.00	0.00	0.00	53.94	53.94	53.94	0.00	0.00	0.00
135	135	21.7	25	28	535	28.13	35.34	37.20	44.71	49.59	49.60	49.59	0.01	0.00	-0.01	53.90	53.90	53.90	0.00	0.00	0.00
136	136	22.1	25	30	534	26.65	34.92	37.30	45.24	49.24	49.27	49.24	0.01	0.00	-0.01	53.85	53.85	53.85	0.00	0.00	0.00
137	137	8.1	67	19	532	26.06	34.58	37.37	46.20	48.68	48.71	48.67	0.01	0.00	-0.01	53.81	53.81	53.81	0.00	0.00	0.00
138	138	18.7	56	37	531	25.74	34.33	37.45	47.13	48.13	48.17	48.13	0.02	0.01	-0.02	53.76	53.76	53.76	0.00	0.00	0.00
139	139	16.3	78	41	485	25.56	33.97	37.56	47.75	47.75	47.79	47.75	0.02	0.01	-0.03	53.70	53.70	53.70	0.00	0.00	0.00
140	140	1.4	100	15	50	25.41	33.69	37.63	48.68	47.21	47.26	47.20	0.00	0.00	0.00	53.64	53.64	53.64	0.00	0.00	0.00
141	141	1.4	99	22	127	25.56	33.54	37.67	49.96	46.50	46.55	46.50	0.00	0.01	0.00	53.60	53.60	53.60	0.00	0.00	0.00
142	142	5.8	100	4	134	25.72	33.39	37.72	51.20	45.82	45.86	45.81	0.00	0.00	0.00	53.55	53.55	53.55	0.00	0.00	0.00
143	143	7.9	80	33	365	25.83	33.22	37.79	52.31	45.20	45.24	45.19	-0.01	0.00	0.00	53.48	53.48	53.48	0.00	0.00	0.00
144	144	7.9	69	24	522	25.70	33.06	37.87	53.34	44.62	44.66	44.61	0.00	0.01	0.01	53.41	53.41	53.41	0.00	0.00	0.00
145	145	3.6	84	35	253	25.61	32.89	37.94	54.46	44.00	44.04	43.99	-0.01	0.00	0.00	53.34	53.34	53.34	0.00	0.00	0.00
146	146	5.6	71	13	519	25.49	32.76	38.01	55.58	43.39	43.43	43.39	0.00	0.00	0.00	53.26	53.26	53.26	0.00	0.00	0.00
147	147	10.0	72	13	518	25.38	32.63	38.08	56.62	42.83	42.86	42.82	0.00	0.00	0.00	53.18	53.18	53.18	0.00	0.00	0.00
148	148	11.0	86	19	355	25.37	32.48	38.17	57.54	42.33	42.36	42.32	0.01	0.00	-0.01	53.08	53.08	53.08	0.00	0.00	0.00
149	149	14.5	71	17	502	25.41	32.35	38.25	58.42	41.86	41.89	41.85	0.00	0.00	0.00	52.97	52.98	52.97	0.00	0.00	0.00
150	150	14.0	56	19	490	25.22	32.23	38.34	59.26	41.41	41.45	41.41	0.01	0.00	-0.01	52.86	52.86	52.86	0.00	0.00	0.00
151	151	20.6	39	22	419	24.63	32.14	38.44	59.83	41.13	41.17	41.12	0.01	0.00	-0.01	52.73	52.74	52.73	0.00	0.00	0.00
152	152	13.6	66	19	468	24.51	31.99	38.54	60.50	40.77	40.81	40.76	0.01	0.00	-0.01	52.60	52.61	52.60	0.00	0.00	0.00
153	153	21.7	75	37	324	24.14	31.91	38.66	60.78	40.[illegible]	40.68	40.62	0.03	-0.01	-0.06	52.45	52.46	52.45	0.00	0.00	0.00
154	154	16.2	90	41	135	24.25	31.76	38.78	60.99	40.54	40.58	40.53	0.03	-0.01	-0.07	52.29	52.30	52.29	0.00	0.00	0.00
155	155	9.6	53	41	544	24.25	31.67	38.85	61.86	40.09	40.14	40.07	0.02	0.01	-0.03	52.18	52.18	52.17	0.00	0.00	0.00
156	156	10.1	96	46	145	23.90	31.56	38.92	62.67	39.68	39.73	39.66	0.03	0.01	-0.04	52.04	52.05	52.04	0.00	0.00	0.00
157	157	11.6	86	15	508	23.98	31.50	38.99	63.52	39.25	39.31	39.24	0.00	0.00	0.00	51.91	51.92	51.91	0.00	0.00	0.00
158	158	14.0	30	19	507	23.44	31.44	39.06	64.11	38.97	39.03	38.96	0.01	0.00	-0.02	51.77	51.77	51.76	0.00	0.00	0.00
159	159	15.1	26	24	509	22.60	31.39	39.14	64.66	38.71	38.77	38.70	0.01	0.00	-0.01	51.61	51.62	51.61	0.00	0.00	0.00

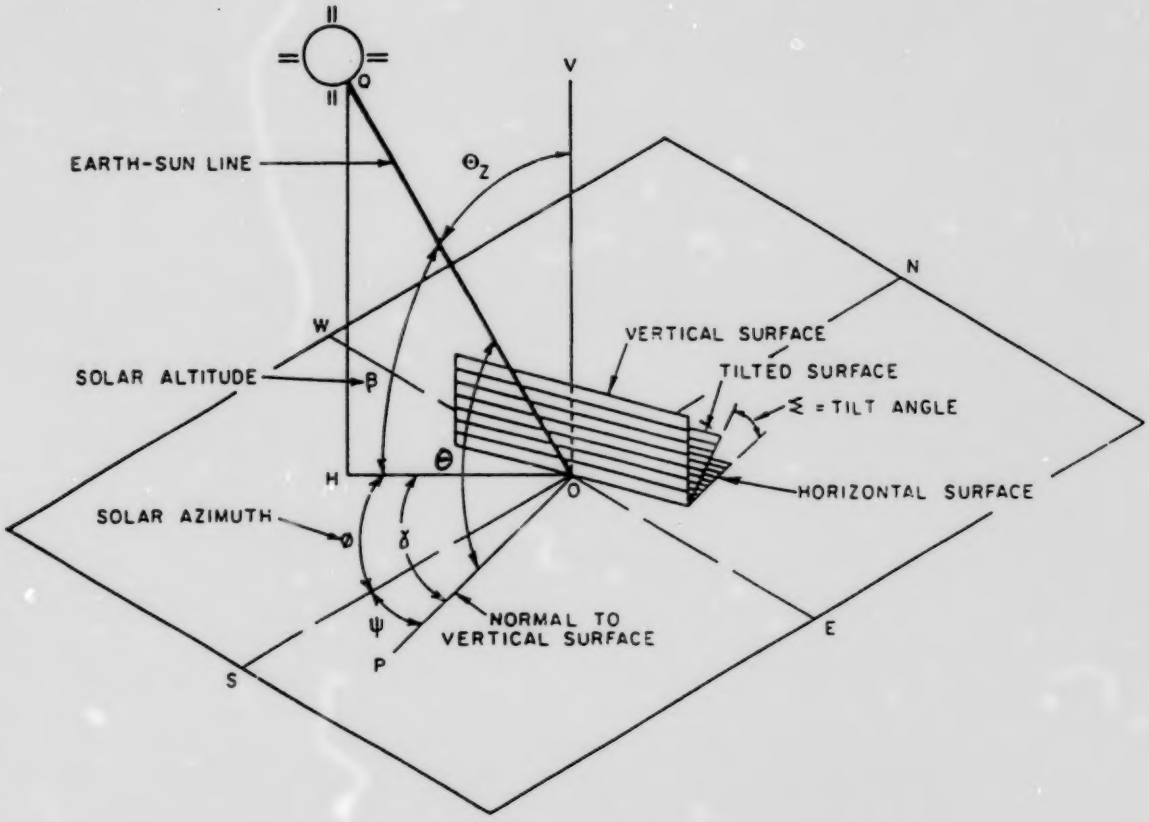

Figure 2.1 Solar Angles for Vertical and Horizontal Surfaces.

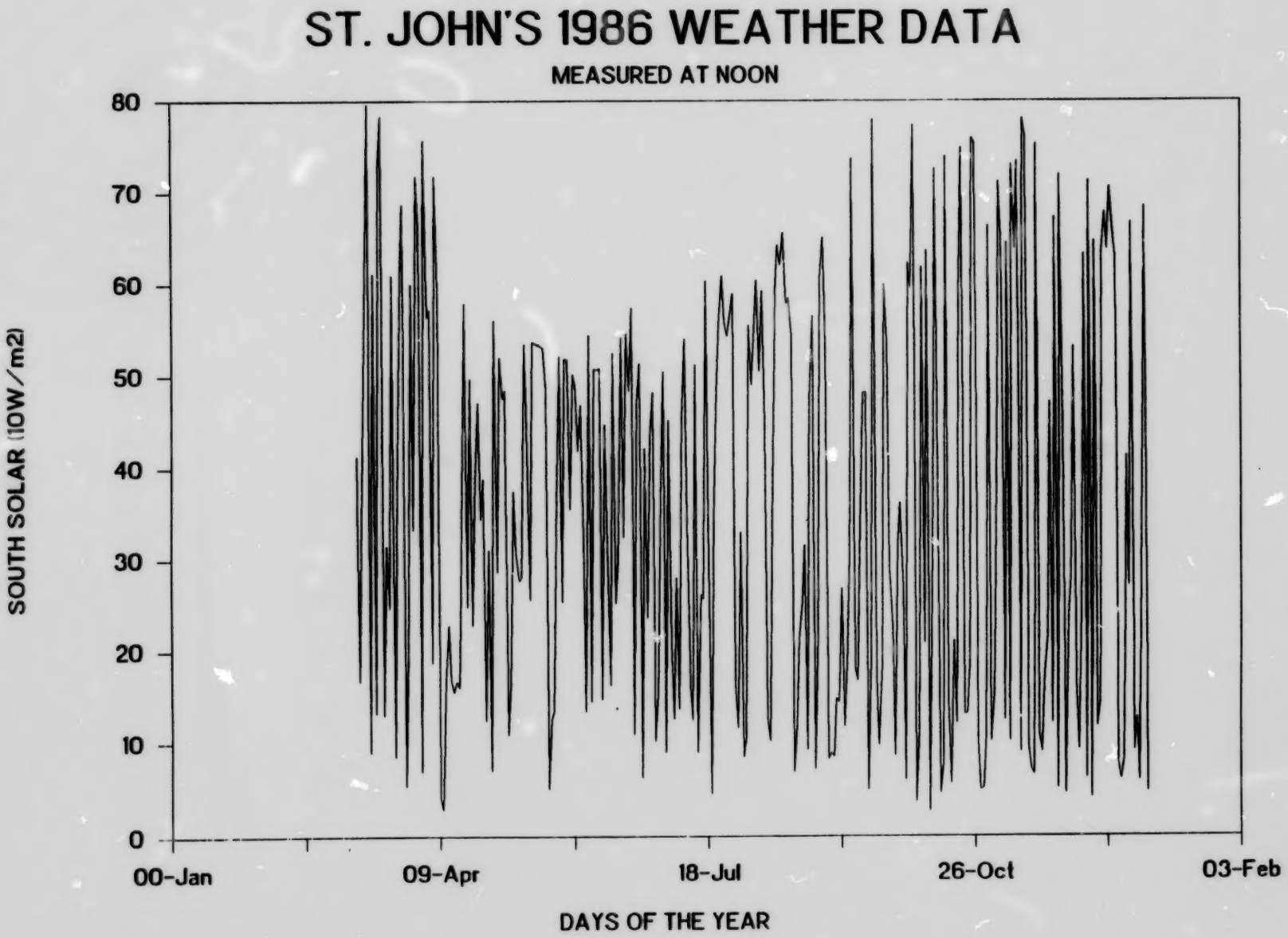
ST. JOHN'S 1986 WEATHER DATA
MEASURED AT NOON
SOUTH SOLAR (10W/m2)
80
70
60
50
40
30
20
10
0
00-Jan
09-Apr
18-Jul
26-Oct
03-Feb
DAYS OF THE YEAR

Figure 3.1

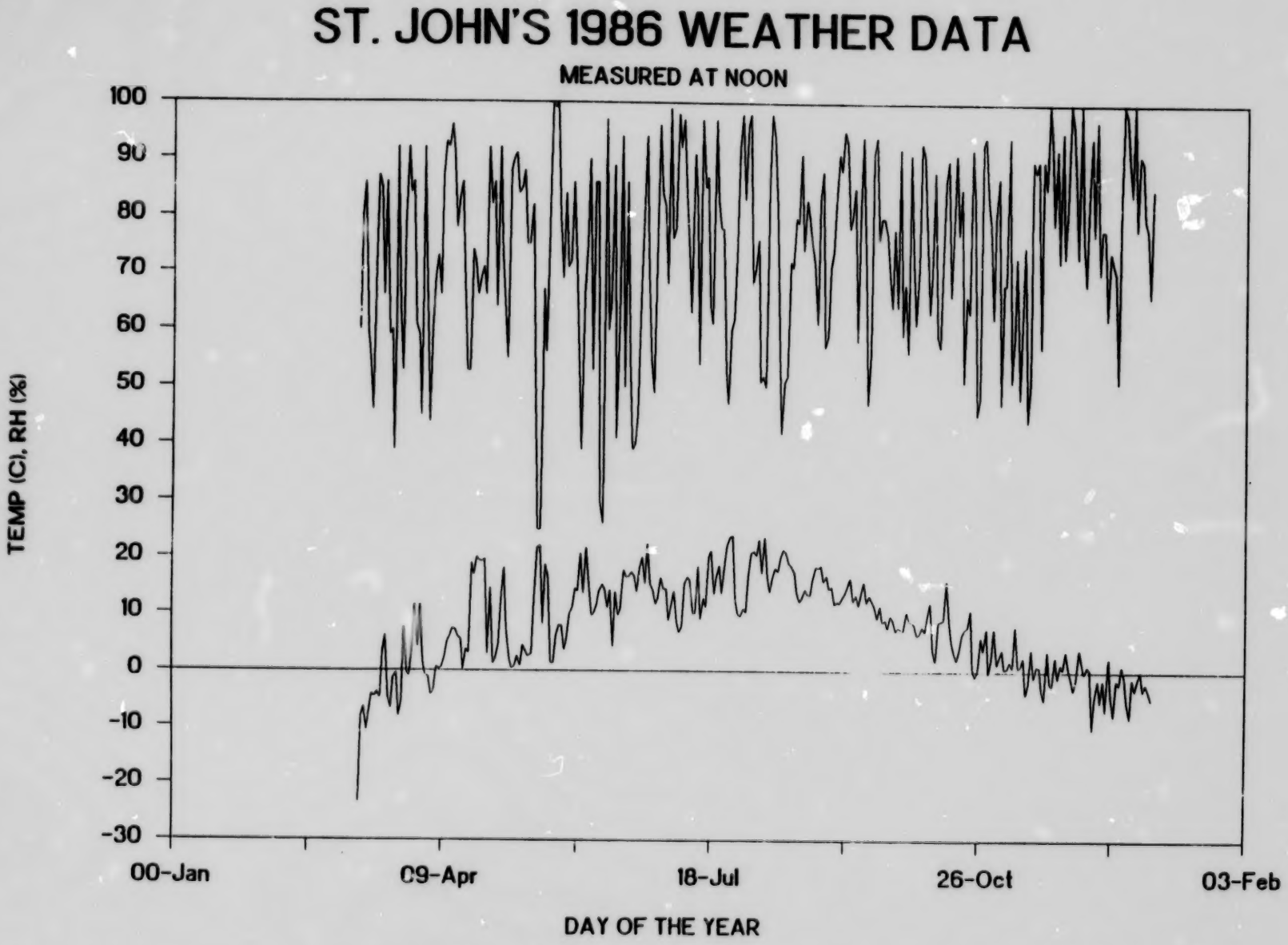
ST. JOHN'S 1986 WEATHER DATA
MEASURED AT NOON
TEMP (C), RH (%)
100
90
80
70
60
50
40
30
20
10
0
-10
-20
-30
00-Jan
09-Apr
18-Jul
26-Oct
03-Feb
DAY OF THE YEAR

Figure 3.2

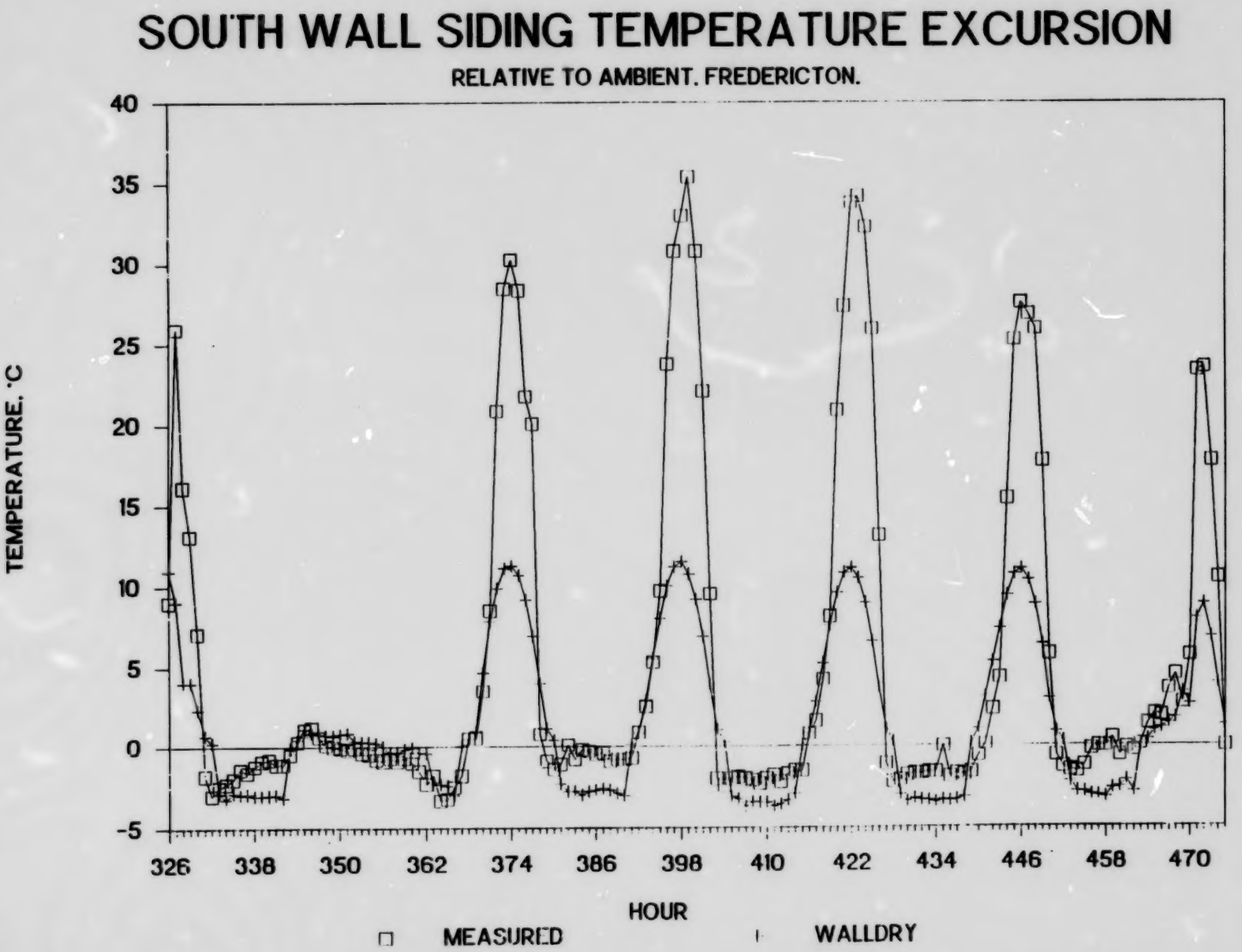
SOUTH WALL SIDING TEMPERATURE EXCURSION
RELATIVE TO AMBIENT. FREDERICTON.
TEMPERATURE. °C
40
35
30
25
20
15
10
5
0
-5
326
338
350
362
374
386
398
410
422
434
446
458
470
HOUR
MEASURED
WALLDRY

Figure 3.3

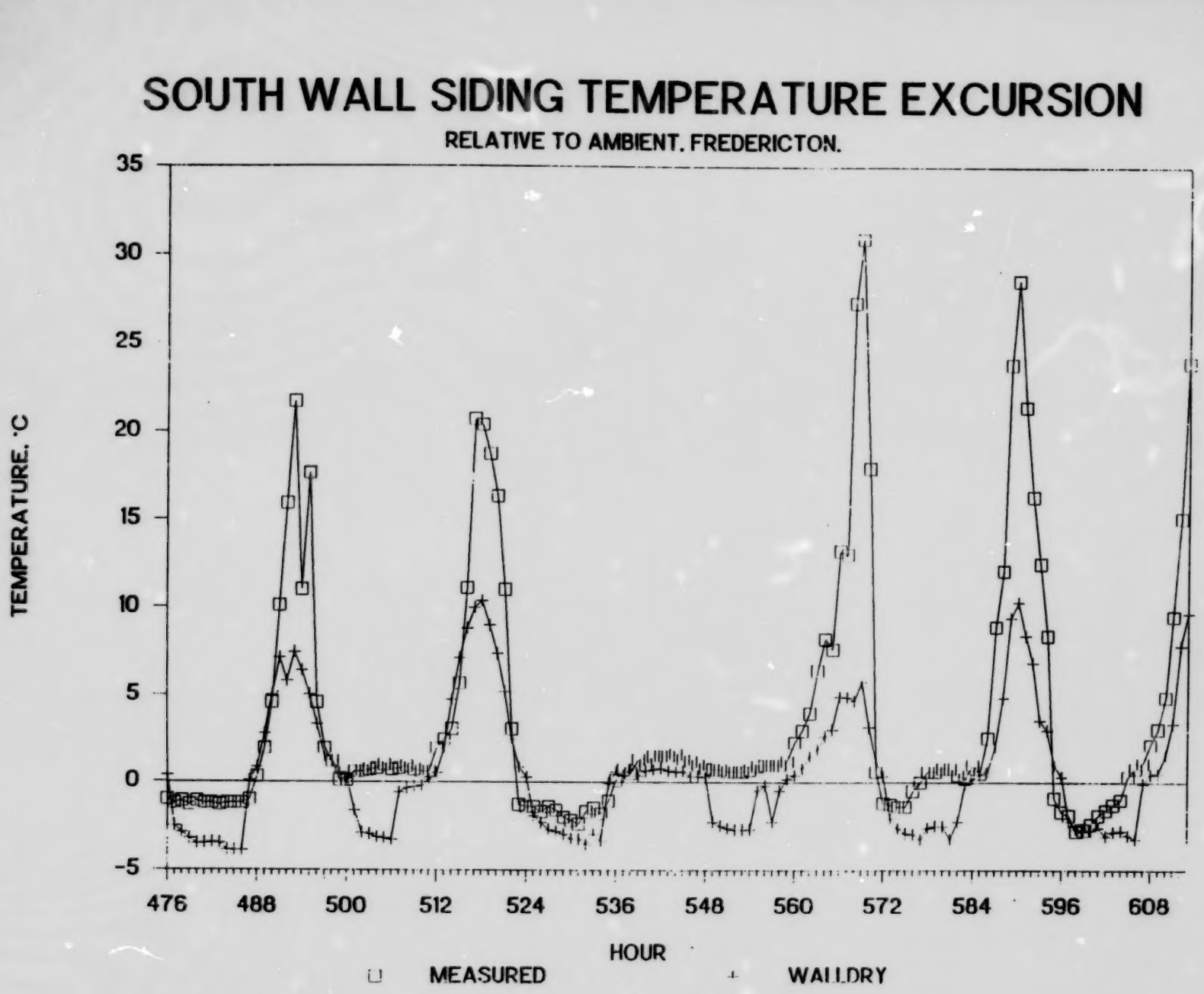
SOUTH WALL SIDING TEMPERATURE EXCURSION
RELATIVE TO AMBIENT. FREDERICTON.
TEMPERATURE, °C
35
30
25
20
15
10
5
0
-5
476
488
500
512
524
536
548
560
572
584
596
608
HOUR
MEASURED
WALLDRY

Figure 3.4

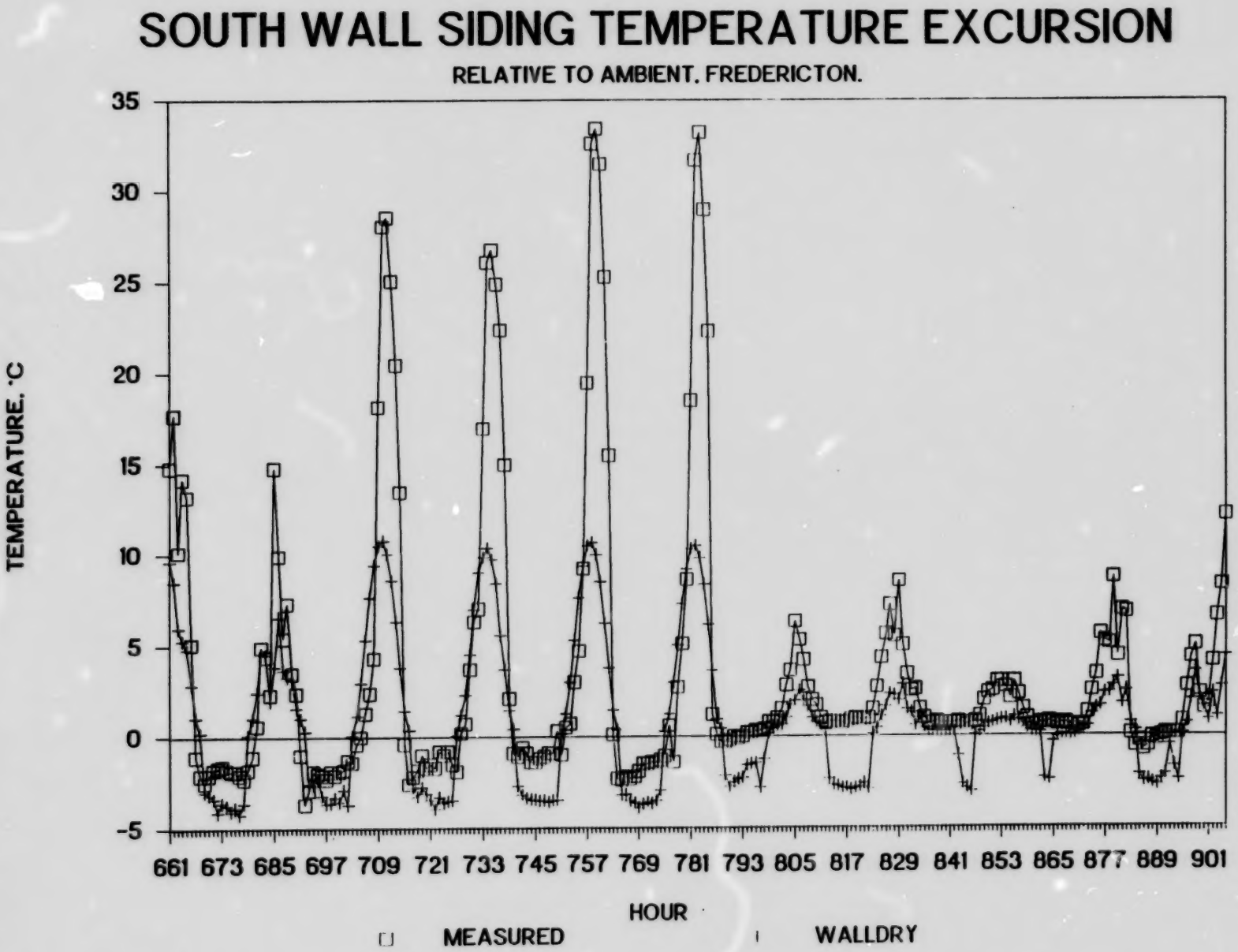
SOUTH WALL SIDING TEMPERATURE EXCURSION
RELATIVE TO AMBIENT. FREDERICTON.
TEMPERATURE, °C
35
30
25
20
15
10
5
0
-5
661 673 685 697 709 721 733 745 757 769 781 793 805 817 829 841 853 865 877 889 901
HOUR
MEASURED
WALLDRY

Figure 3.5

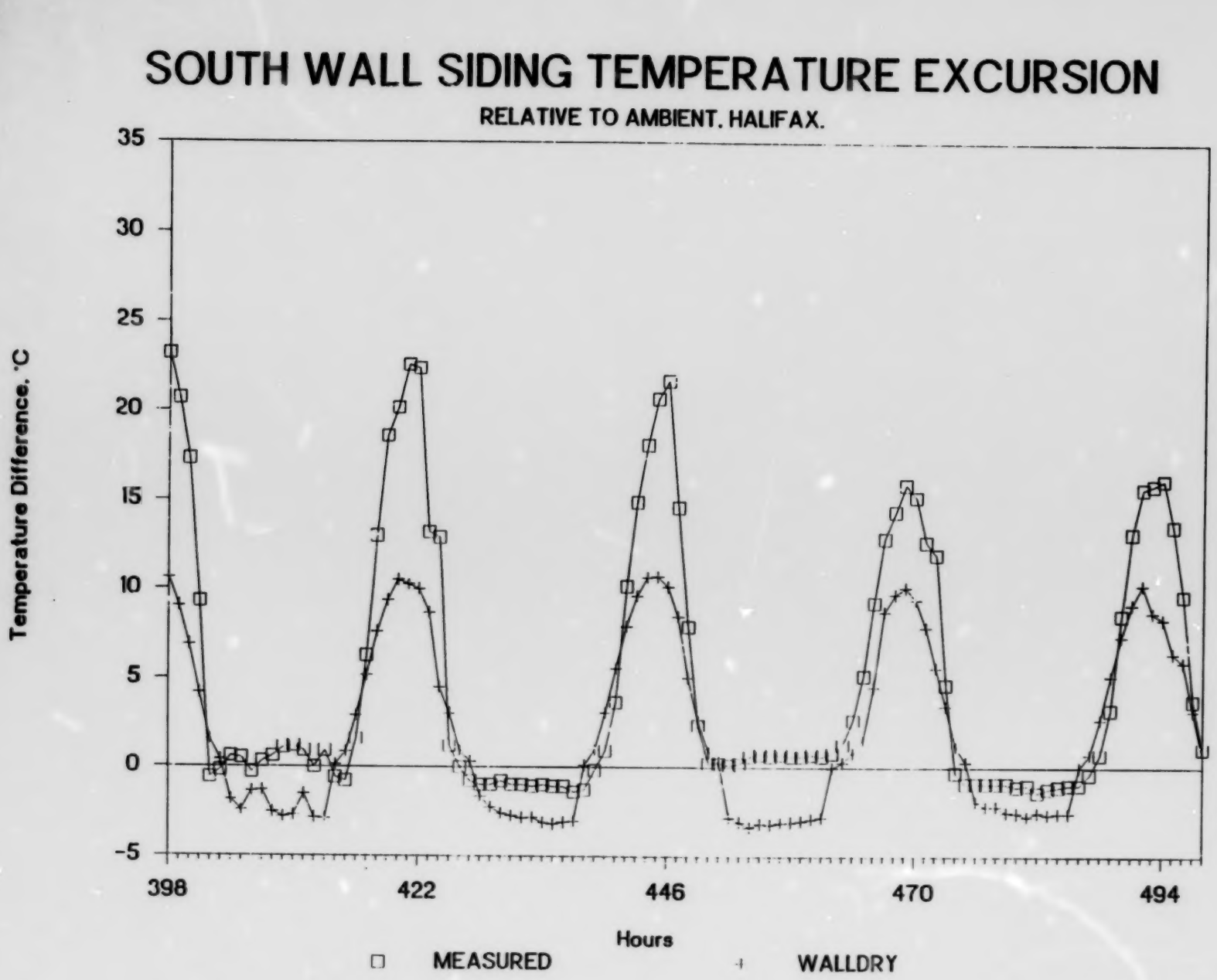
SOUTH WALL SIDING TEMPERATURE EXCURSION
RELATIVE TO AMBIENT. HALIFAX.
Temperature Difference, °C
35
30
25
20
15
10
5
0
-5
398
422
446
470
494
Hours
MEASURED
WALLDRY

Figure 3.6

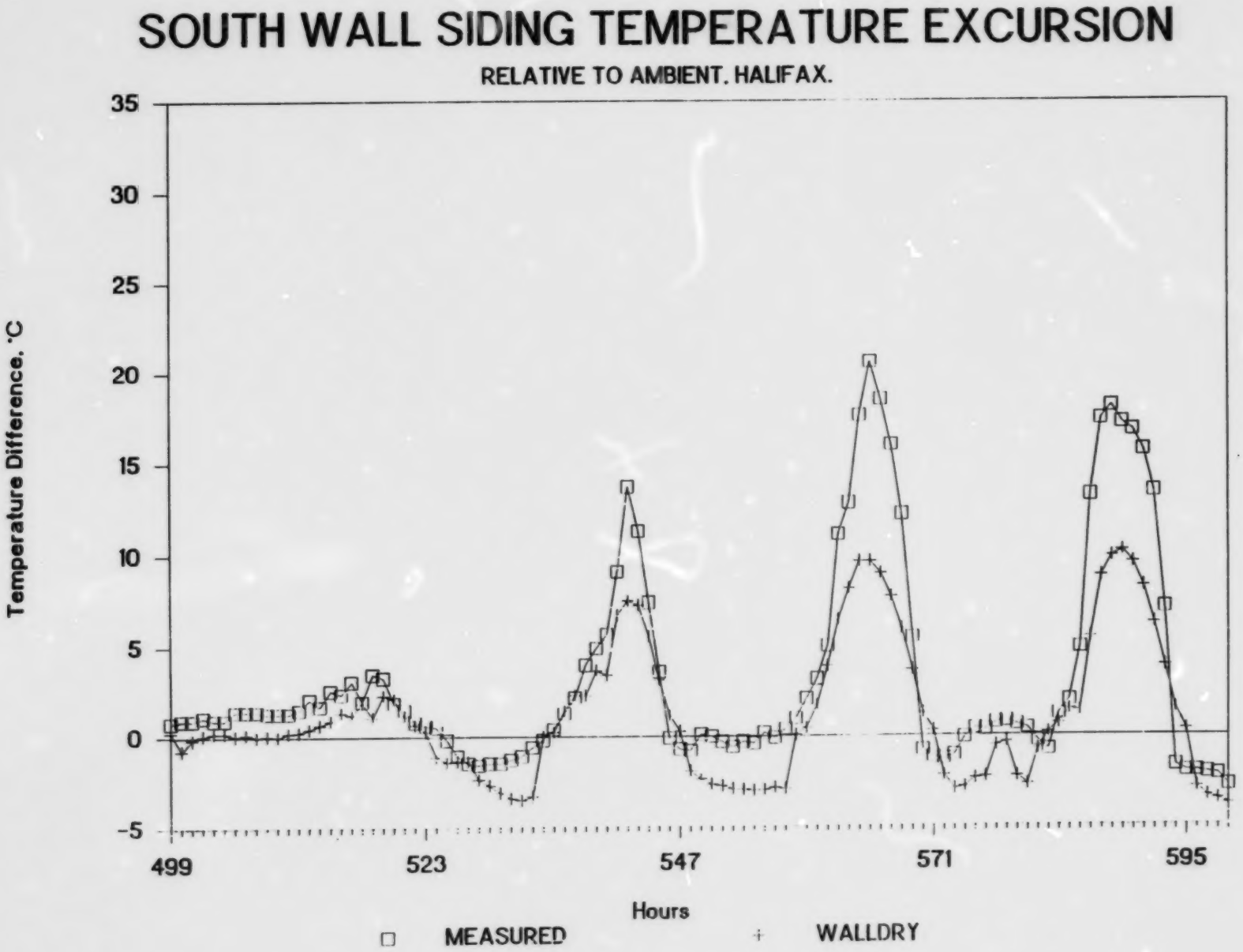
SOUTH WALL SIDING TEMPERATURE EXCURSION
RELATIVE TO AMBIENT. HALIFAX.
Temperature Difference, °C
35
30
25
20
15
10
5
0
-5
499
523
547
571
595
Hours
MEASURED
WALLDRY

Figure 3.7

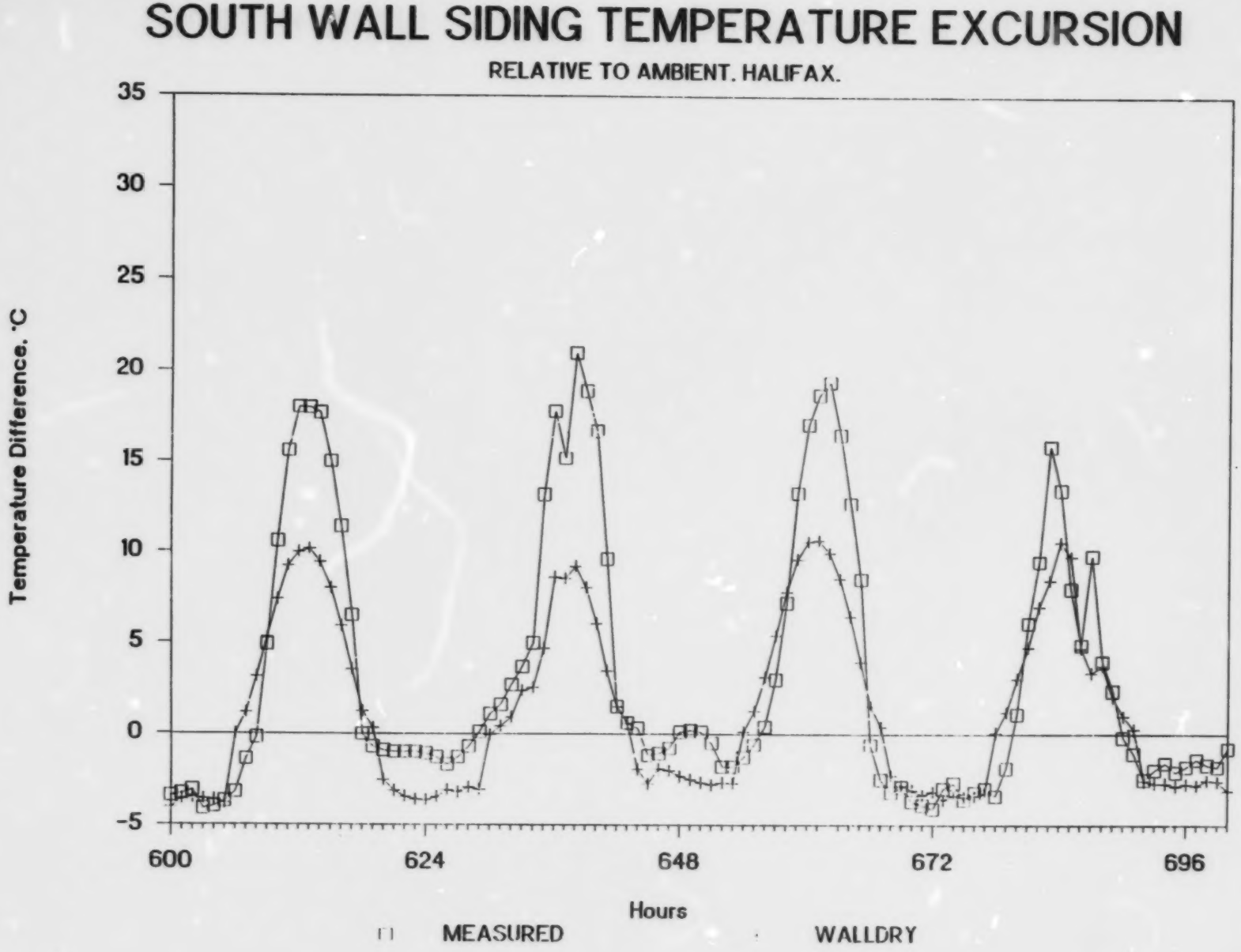
SOUTH WALL SIDING TEMPERATURE EXCURSION
RELATIVE TO AMBIENT. HALIFAX.
Temperature Difference, °C
35
30
25
20
15
10
5
0
-5
600
624
648
672
696
Hours
MEASURED
WALLDRY

Figure 3.8

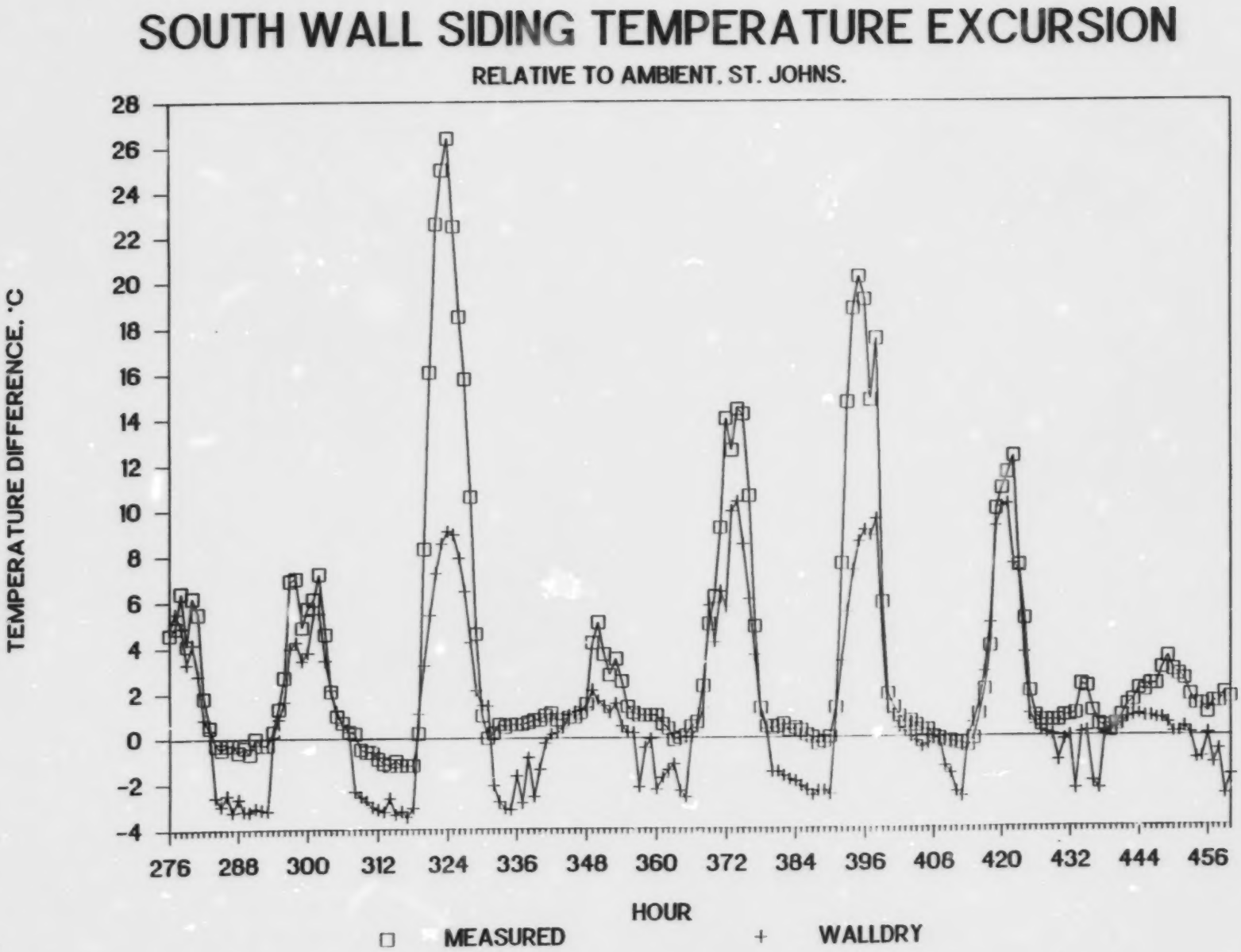
SOUTH WALL SIDING TEMPERATURE EXCURSION
RELATIVE TO AMBIENT, ST. JOHNS.
TEMPERATURE DIFFERENCE, °C
28
26
24
22
20
18
16
14
12
10
8
6
4
2
0
-2
-4
276
288
300
312
324
336
348
360
372
384
396
406
420
432
444
456
HOUR
MEASURED
WALLDRY

Figure 3.9

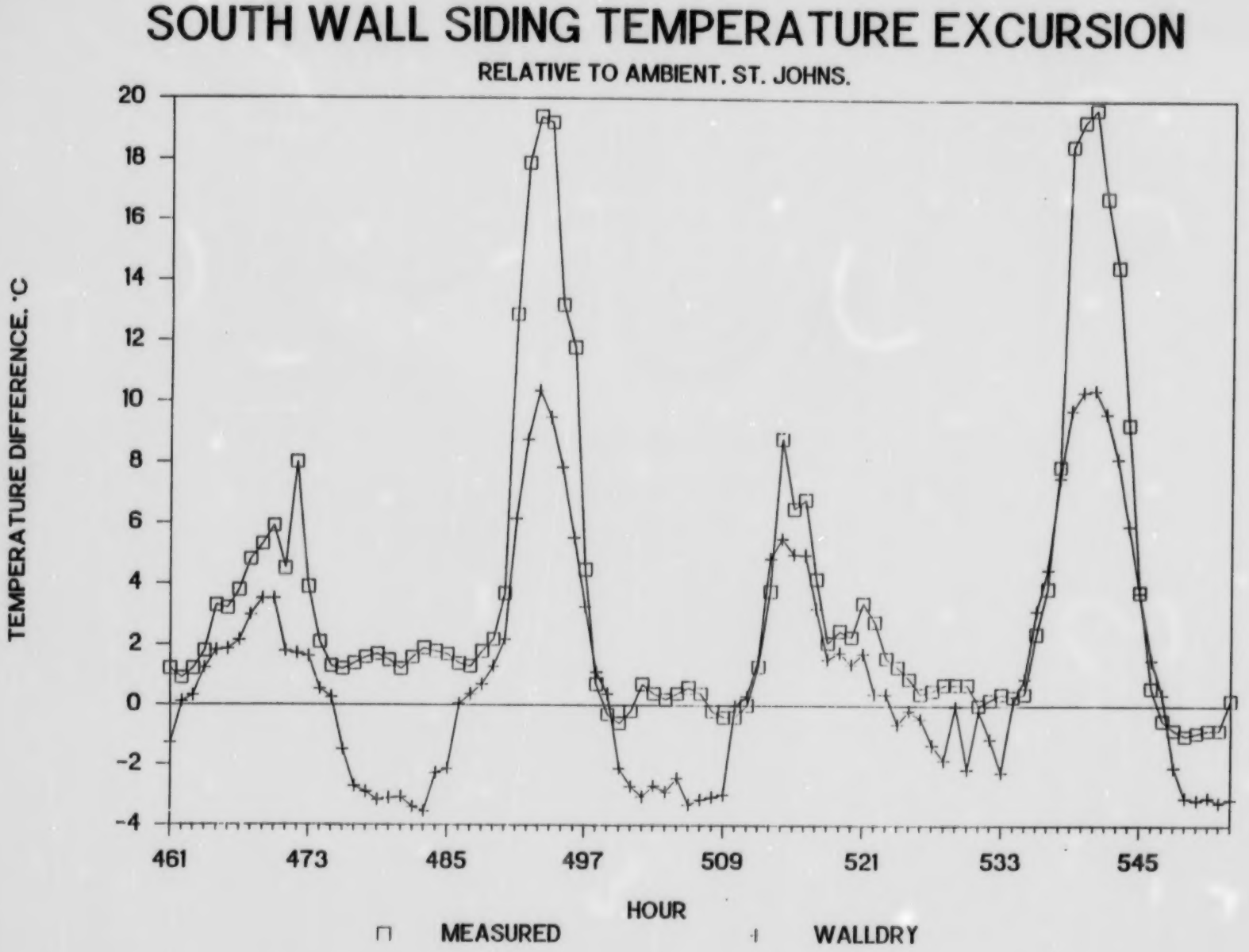
SOUTH WALL SIDING TEMPERATURE EXCURSION
RELATIVE TO AMBIENT, ST. JOHNS.
TEMPERATURE DIFFERENCE, °C
20
18
16
14
12
10
8
6
4
2
0
-2
-4
461
473
485
497
509
521
533
545
HOUR
MEASURED
WALLDRY

Figure 3.10

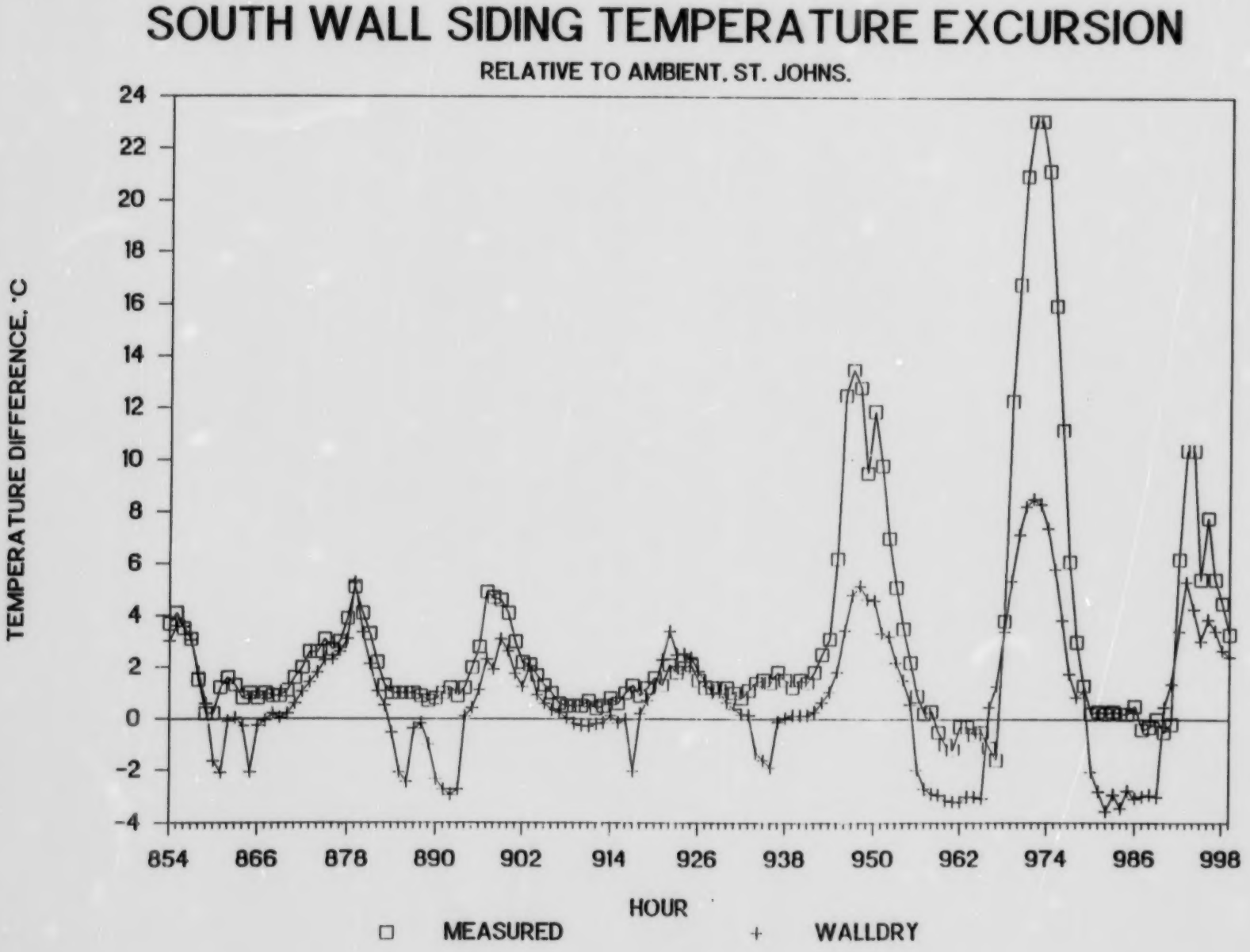
SOUTH WALL SIDING TEMPERATURE EXCURSION
RELATIVE TO AMBIENT. ST. JOHNS.
TEMPERATURE DIFFERENCE, °C
24
22
20
18
16
14
12
10
8
6
4
2
0
-2
-4
854
866
878
890
902
914
926
938
950
962
974
986
998
HOUR
MEASURED
WALLDRY

Figure 3.11

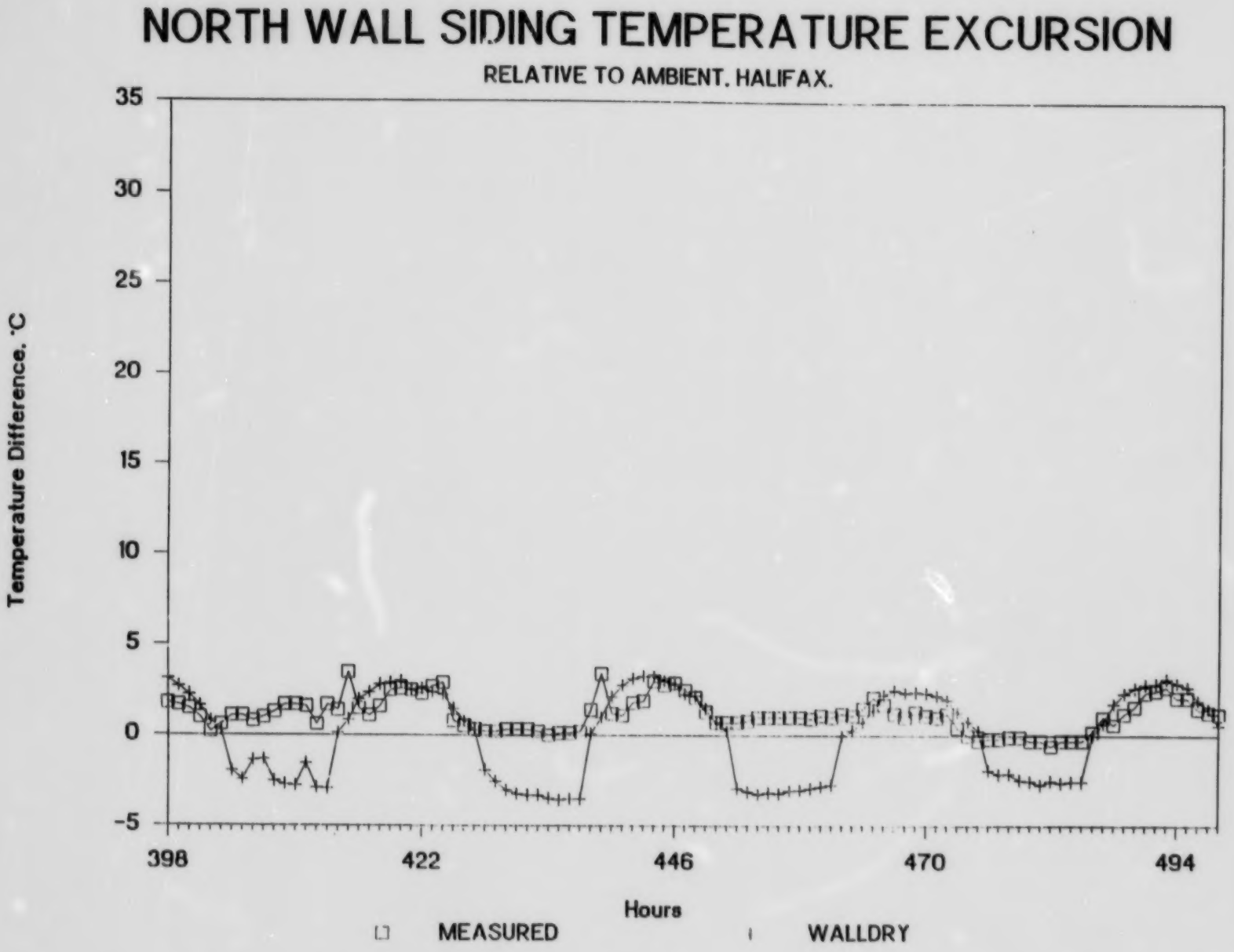
NORTH WALL SIDING TEMPERATURE EXCURSION
RELATIVE TO AMBIENT, HALIFAX.
Temperature Difference, °C
35
30
25
20
15
10
5
0
-5
398
422
446
470
494
Hours
MEASURED
WALLDRY

Figure 3.12

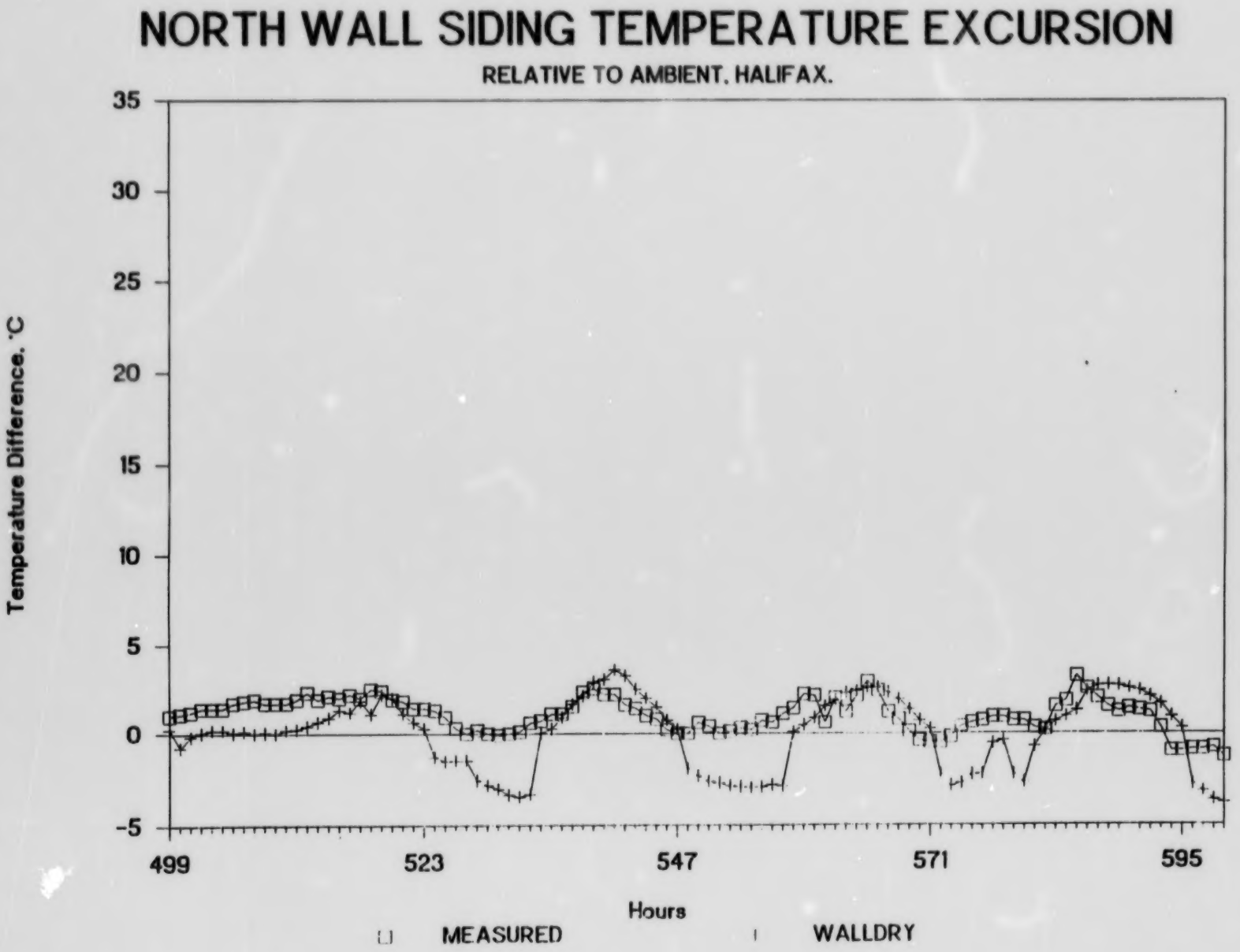
NORTH WALL SIDING TEMPERATURE EXCURSION
RELATIVE TO AMBIENT, HALIFAX.
Temperature Difference, °C
35
30
25
20
15
10
5
0
-5
499
523
547
571
595
Hours
MEASURED
WALLDRY

Figure 3.13

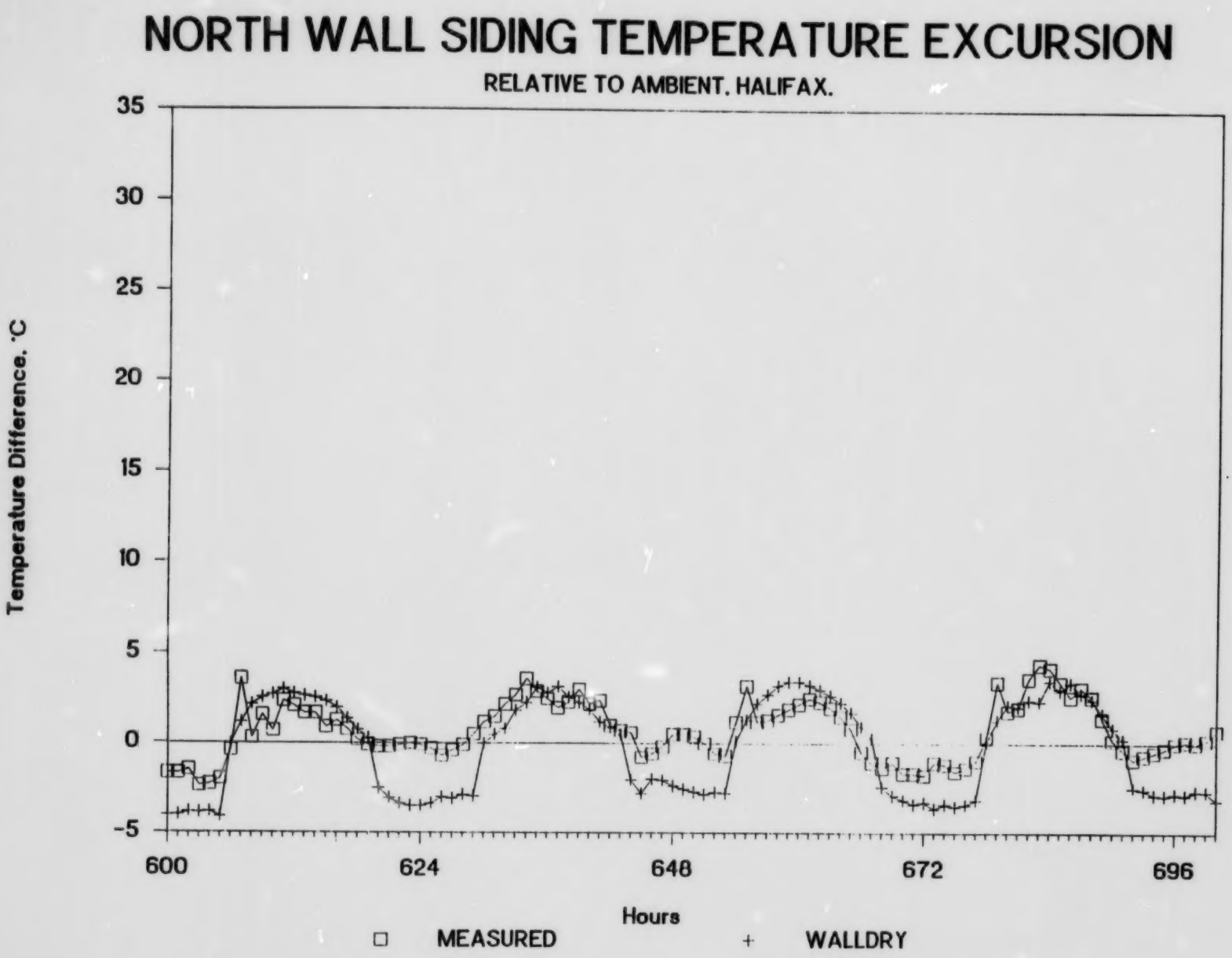
NORTH WALL SIDING TEMPERATURE EXCURSION
RELATIVE TO AMBIENT. HALIFAX.
Temperature Difference. °C
35
30
25
20
15
10
5
0
-5
600
624
648
672
696
Hours
MEASURED
WALLDRY

Figure 3.14

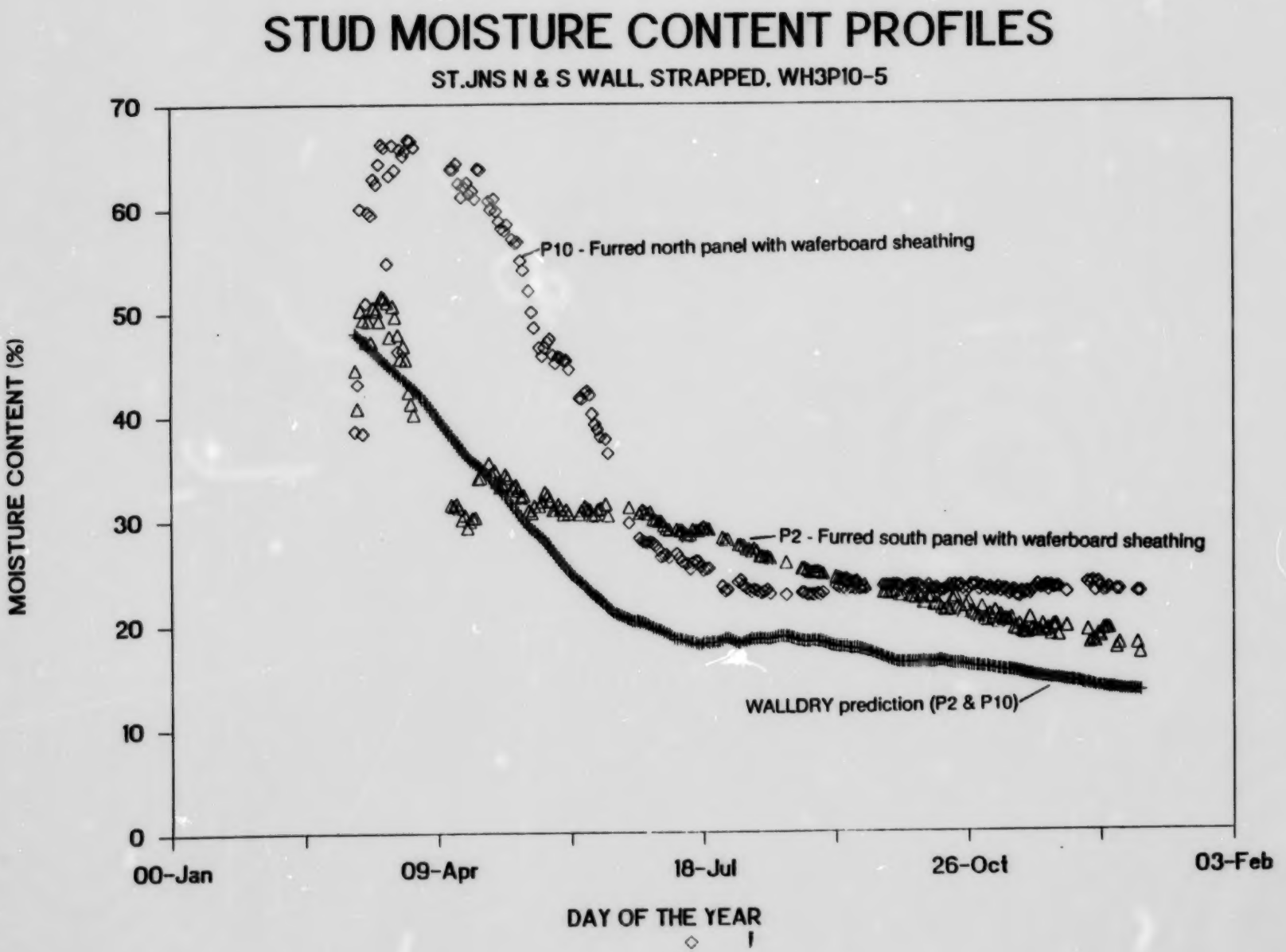
STUD MOISTURE CONTENT PROFILES
ST.JNS N & S WALL. STRAPPED. WH3P10-5
MOISTURE CONTENT (%)
70
60
50
40
30
20
10
0
P10 - Furred north panel with waferboard sheathing
P2 - Furred south panel with waferboard sheathing
WALLDRY prediction (P2 & P10)
00-Jan
09-Apr
18-Jul
26-Oct
03-Feb
DAY OF THE YEAR

Figure 3.15

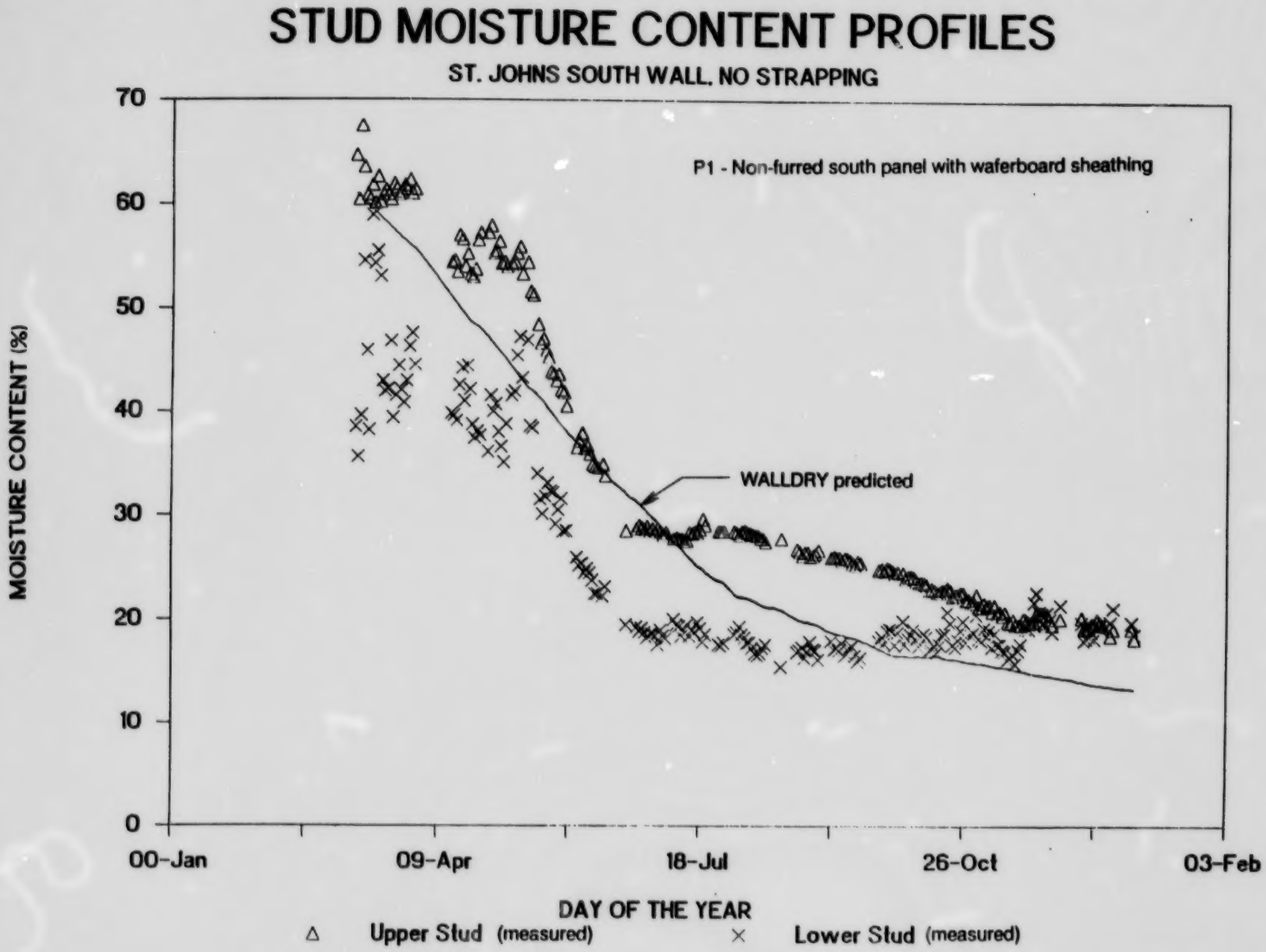
STUD MOISTURE CONTENT PROFILES
ST. JOHNS SOUTH WALL, NO STRAPPING
P1 - Non-furred south panel with waferboard sheathing
WALLDRY predicted
MOISTURE CONTENT (%)
70
60
50
40
30
20
10
0
00-Jan
09-Apr
18-Jul
26-Oct
03-Feb
DAY OF THE YEAR
Upper Stud (measured)
Lower Stud (measured)

Figure 3.16

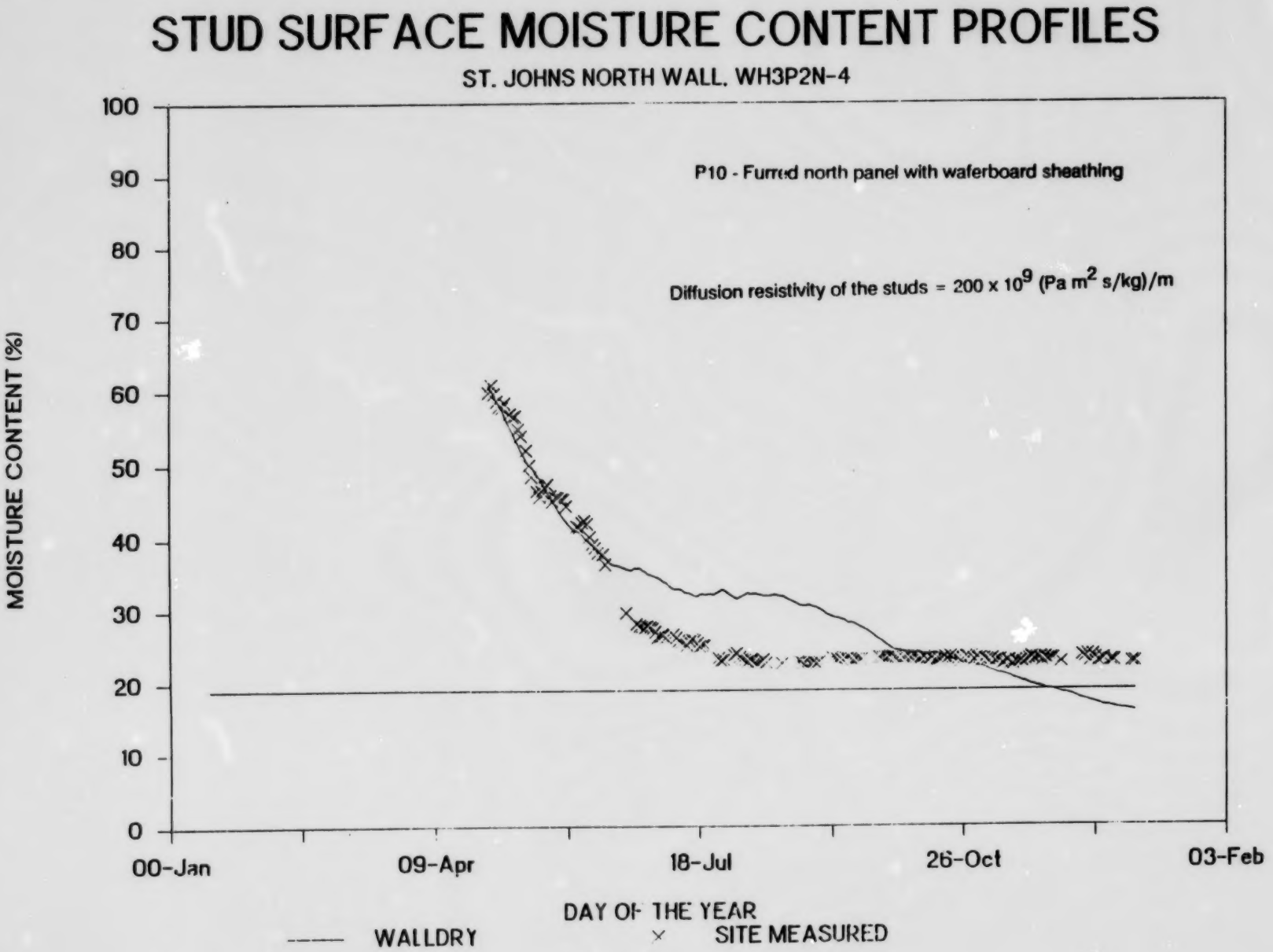
STUD SURFACE MOISTURE CONTENT PROFILES
ST. JOHNS NORTH WALL. WH3P2N-4
P10 - Furred north panel with waferboard sheathing
Diffusion resistivity of the studs = 200 x 10^9 (Pa m^2 s/kg)/m
MOISTURE CONTENT (%)
100
90
80
70
60
50
40
30
20
10
0
00-Jan
09-Apr
18-Jul
26-Oct
03-Feb
DAY OF THE YEAR
WALLDRY
SITE MEASURED

Figure 3.17a

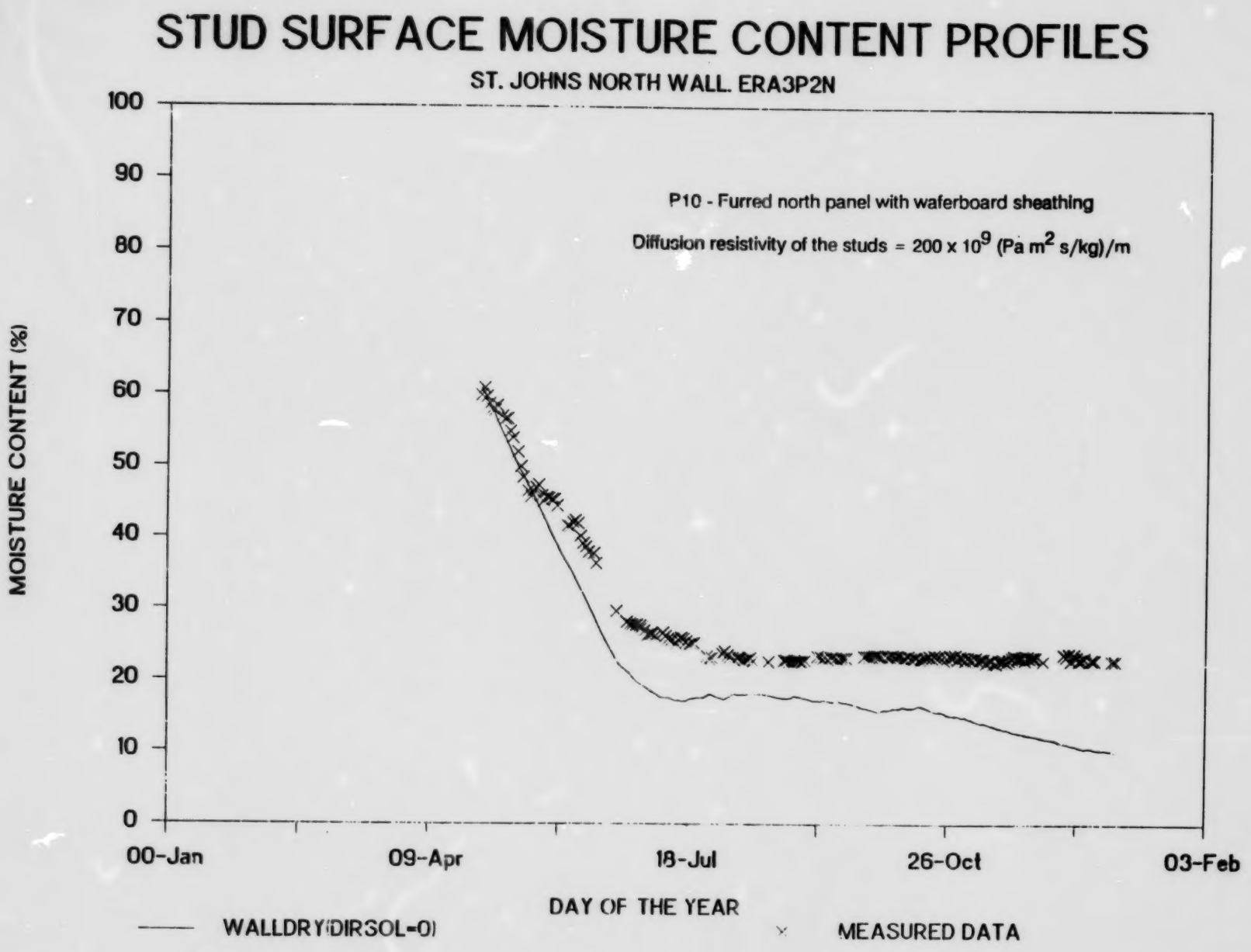
STUD SURFACE MOISTURE CONTENT PROFILES
ST. JOHNS NORTH WALL. ERA3P2N
P10 - Furred north panel with waferboard sheathing
Diffusion resistivity of the studs = 200 x 10^9 (Pa m^2 s/kg)/m
MOISTURE CONTENT (%)
100
90
80
70
60
50
40
30
20
10
0
00-Jan
09-Apr
18-Jul
26-Oct
03-Feb
DAY OF THE YEAR
WALLDRY(DIRSOL=0)
MEASURED DATA

Figure 3.17b

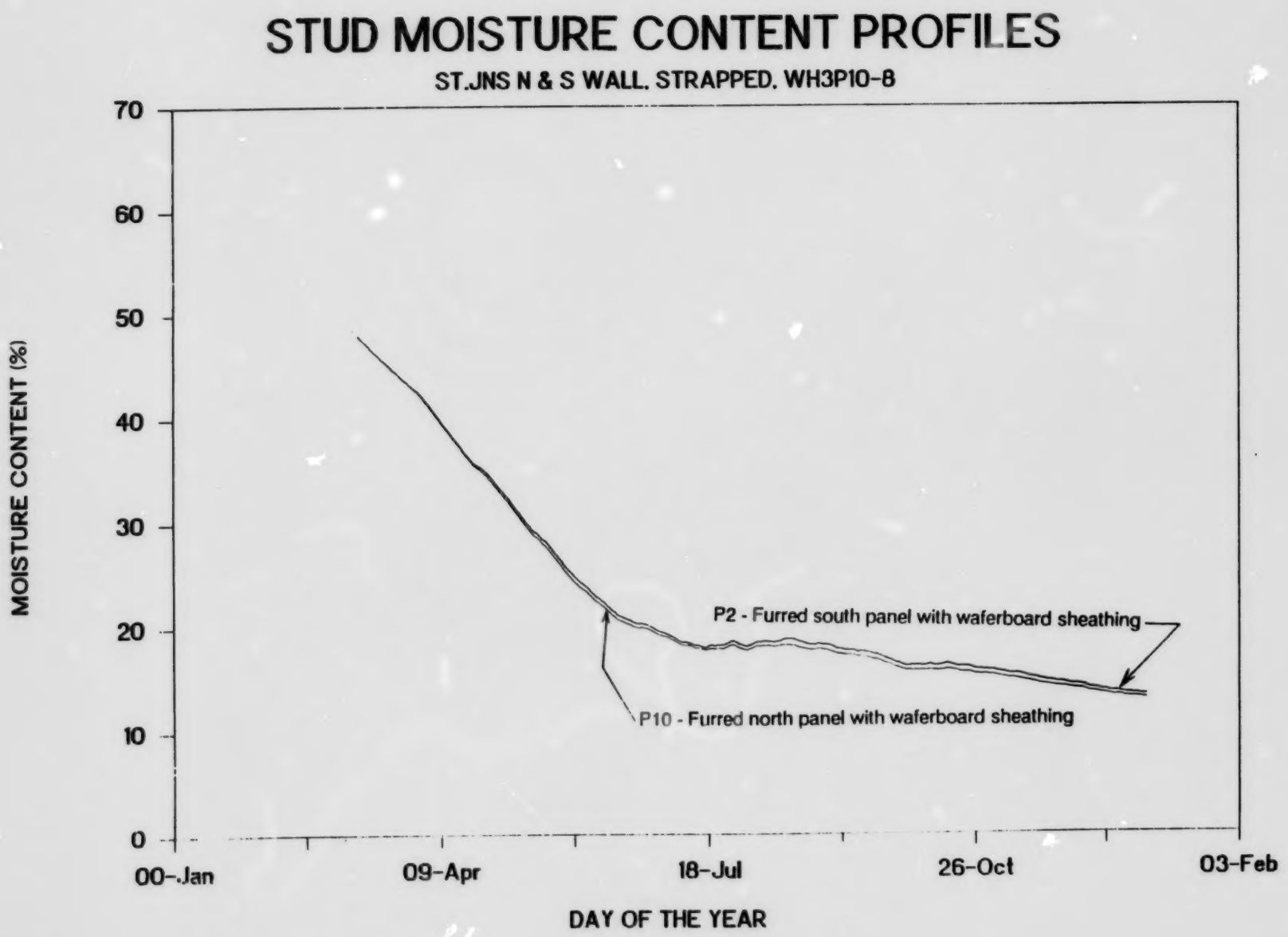
STUD MOISTURE CONTENT PROFILES
ST.JNS N & S WALL. STRAPPED. WH3P10-8
MOISTURE CONTENT (%)
70
60
50
40
30
20
10
0
00-Jan
09-Apr
18-Jul
26-Oct
03-Feb
DAY OF THE YEAR
P2 - Furred south panel with waferboard sheathing
P10 - Furred north panel with waferboard sheathing

Figure 3.18a

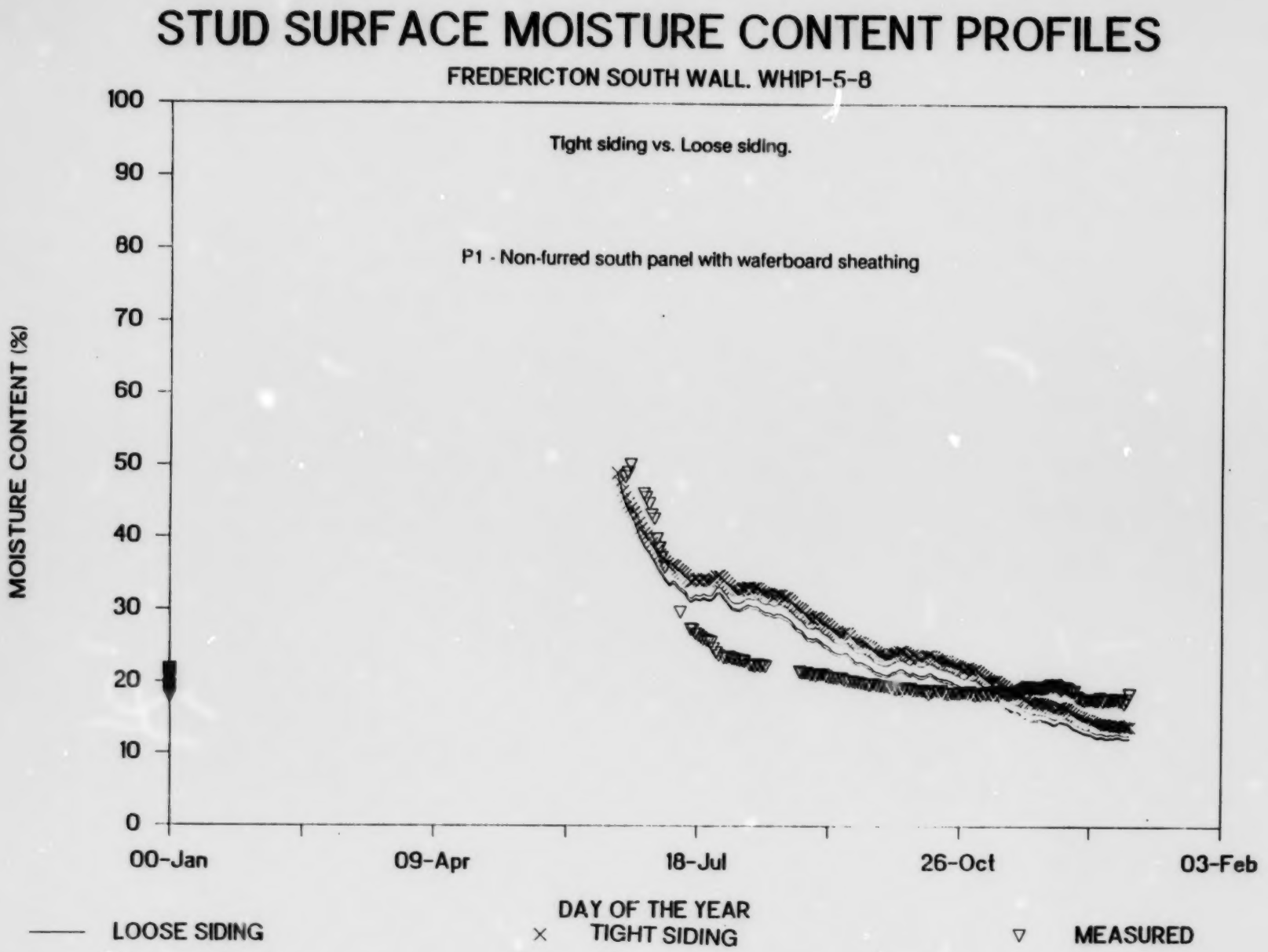
STUD SURFACE MOISTURE CONTENT PROFILES
FREDERICTON SOUTH WALL. WHIP1-5-8
Tight siding vs. Loose siding.
P1 - Non-furred south panel with waferboard sheathing
MOISTURE CONTENT (%)
100
90
80
70
60
50
40
30
20
10
0
00-Jan
09-Apr
18-Jul
26-Oct
03-Feb
DAY OF THE YEAR
LOOSE SIDING
TIGHT SIDING
MEASURED

Figure 3.18b

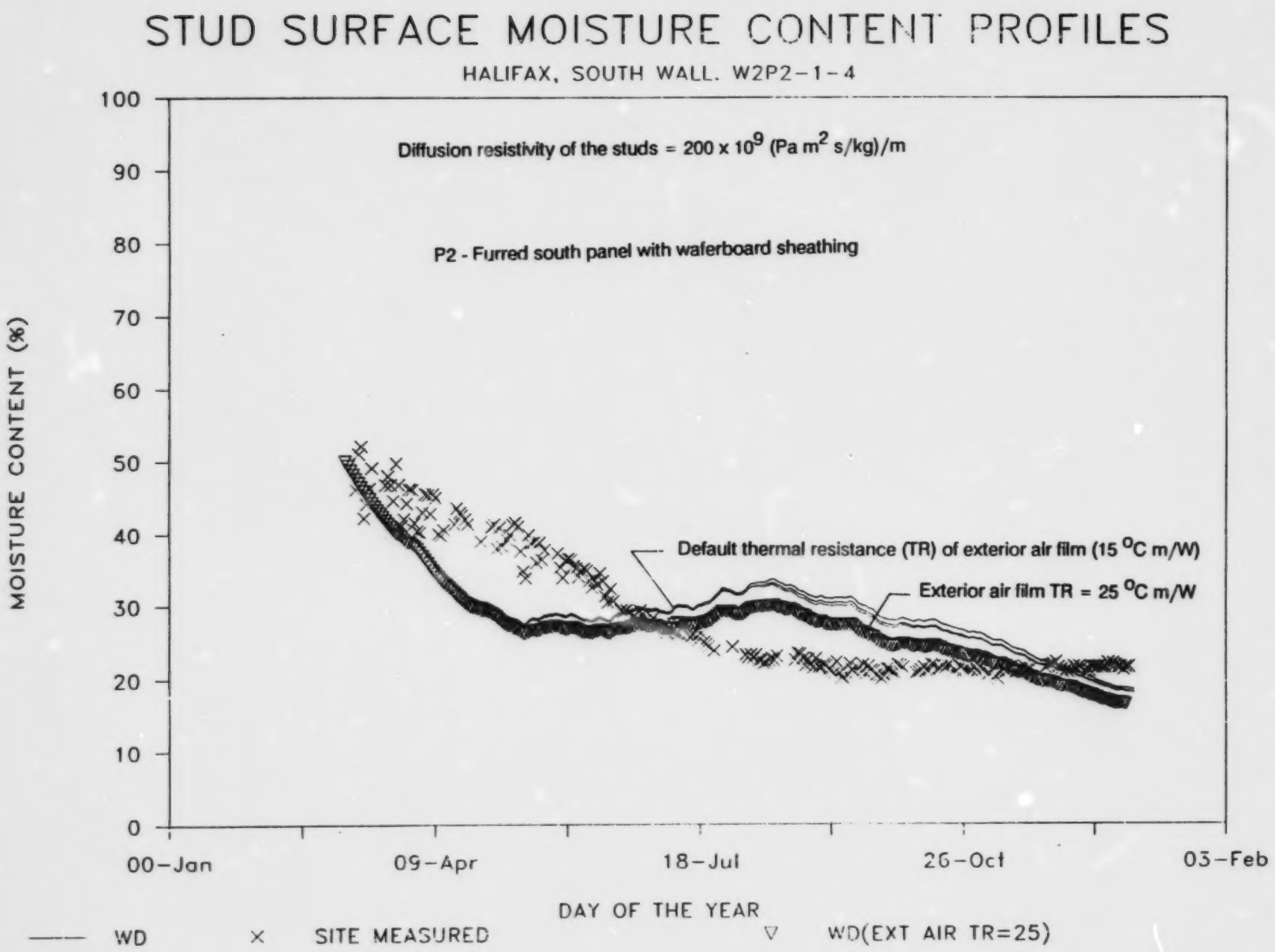
STUD SURFACE MOISTURE CONTENT PROFILES
HALIFAX, SOUTH WALL. W2P2-1-4
Diffusion resistivity of the studs = 200 x 10^9 (Pa m^2 s/kg)/m
P2 - Furred south panel with waferboard sheathing
Default thermal resistance (TR) of exterior air film (15 °C m/W)
Exterior air film TR = 25 °C m/W
MOISTURE CONTENT (%)
100
90
80
70
60
50
40
30
20
10
0
00-Jan
09-Apr
18-Jul
26-Oct
03-Feb
DAY OF THE YEAR
WD
SITE MEASURED
WD(EXT AIR TR=25)

Figure 3.18c

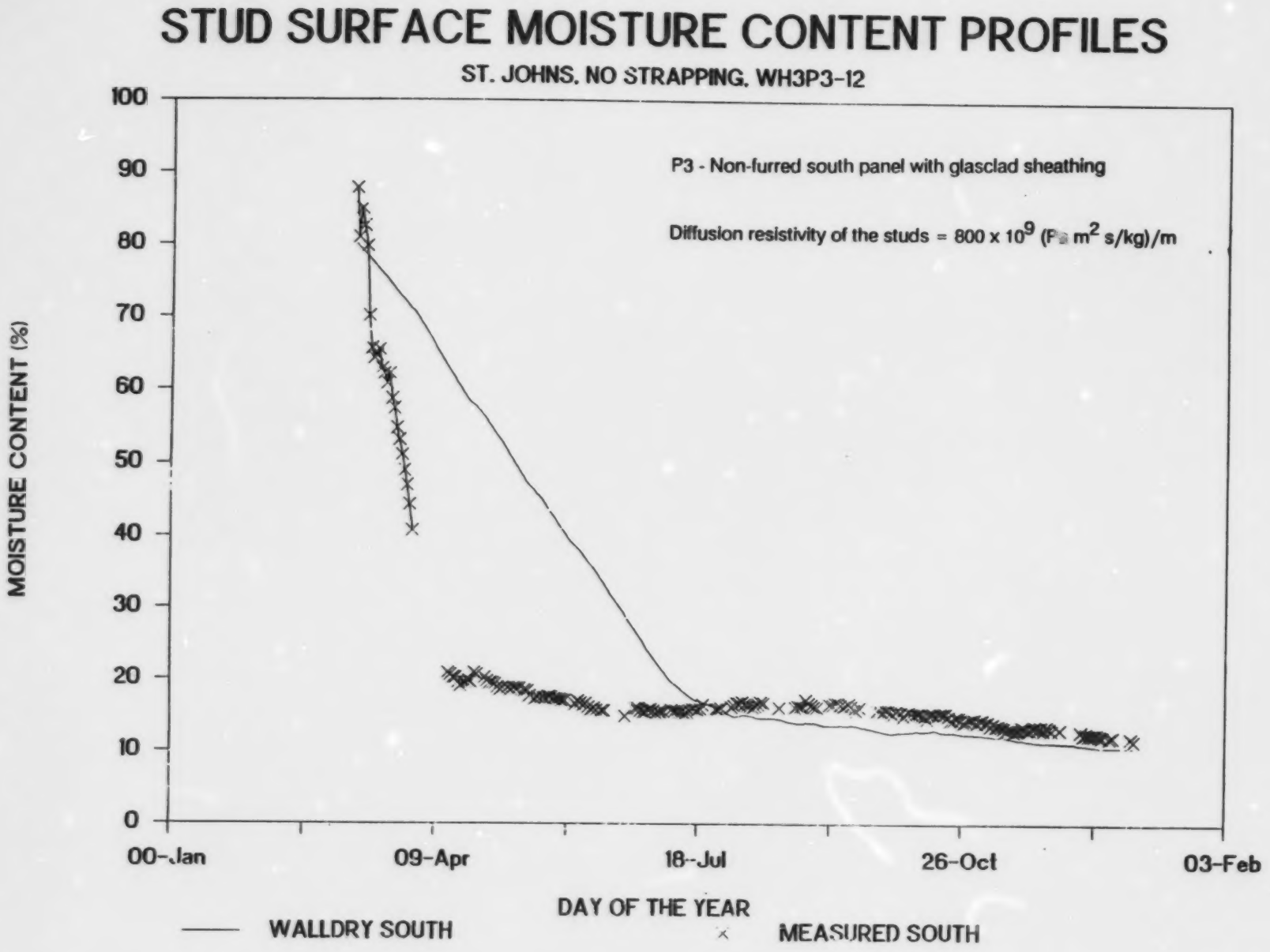
STUD SURFACE MOISTURE CONTENT PROFILES
ST. JOHNS. NO STRAPPING. WH3P3-12
P3 - Non-furred south panel with glasclad sheathing
Diffusion resistivity of the studs = 800 x 10^9 (Pa m^2 s/kg)/m
MOISTURE CONTENT (%)
100
90
80
70
60
50
40
30
20
10
0
00-Jan
09-Apr
18-Jul
26-Oct
03-Feb
DAY OF THE YEAR
WALLDRY SOUTH
MEASURED SOUTH

Figure 3.19

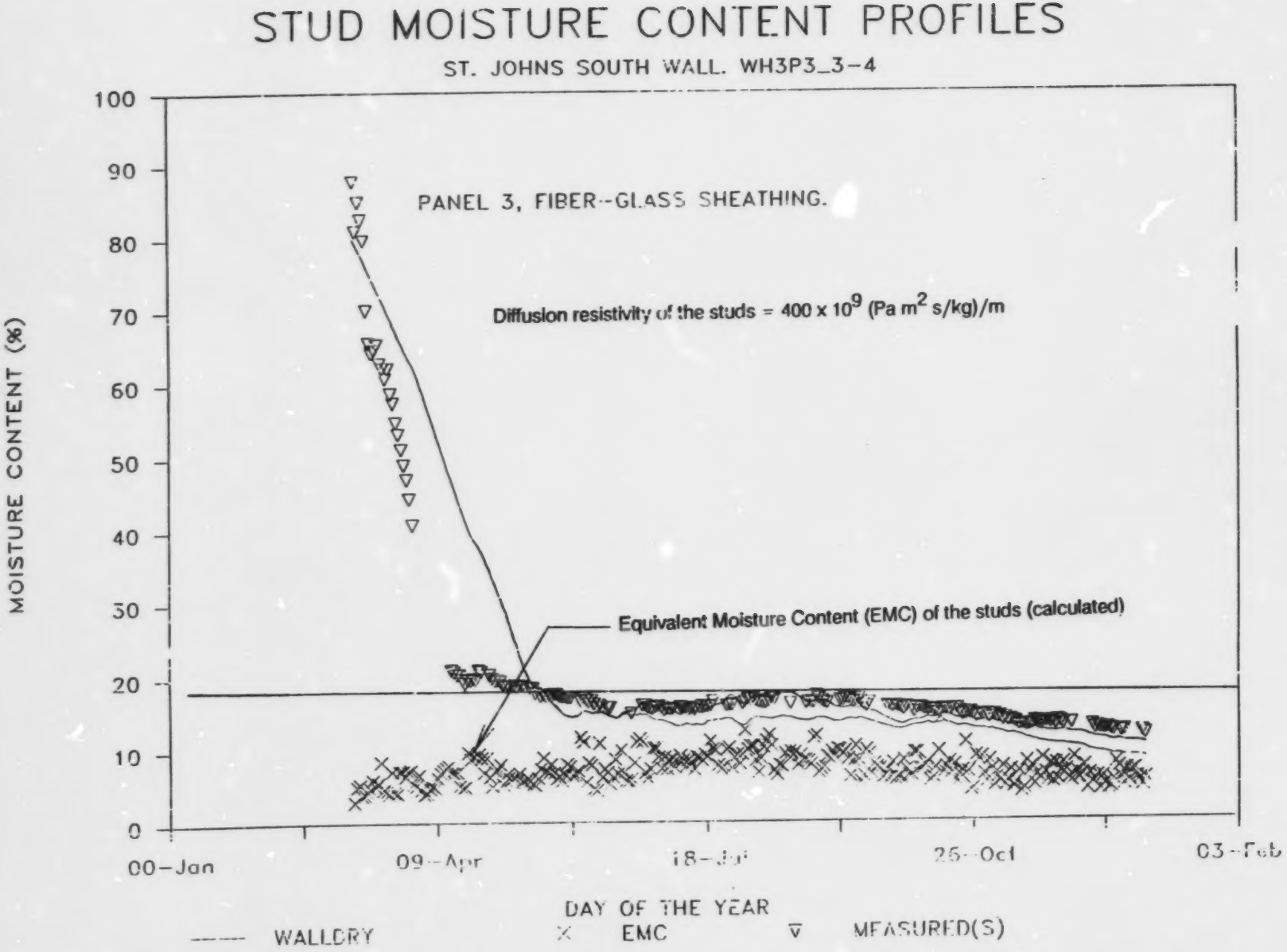
STUD MOISTURE CONTENT PROFILES
ST. JOHNS SOUTH WALL. WH3P3_3-4
PANEL 3, FIBER--GLASS SHEATHING.
Diffusion resistivity of the studs = 400 x 10^9 (Pa m^2 s/kg)/m
Equivalent Moisture Content (EMC) of the studs (calculated)
MOISTURE CONTENT (%)
100
90
80
70
60
50
40
30
20
10
0
00-Jan
09-Apr
18-Jul
26-Oct
03-Feb
DAY OF THE YEAR
WALLDRY
EMC
MEASURED(S)

Figure 3.20

UPPER STUD MOISTURE CONTENT PROFILES

ATLANTIC CANADA HUT PROJECT PANEL 3 SIMULATION

GLASCLAD SHEATHING, ST. JOHNS

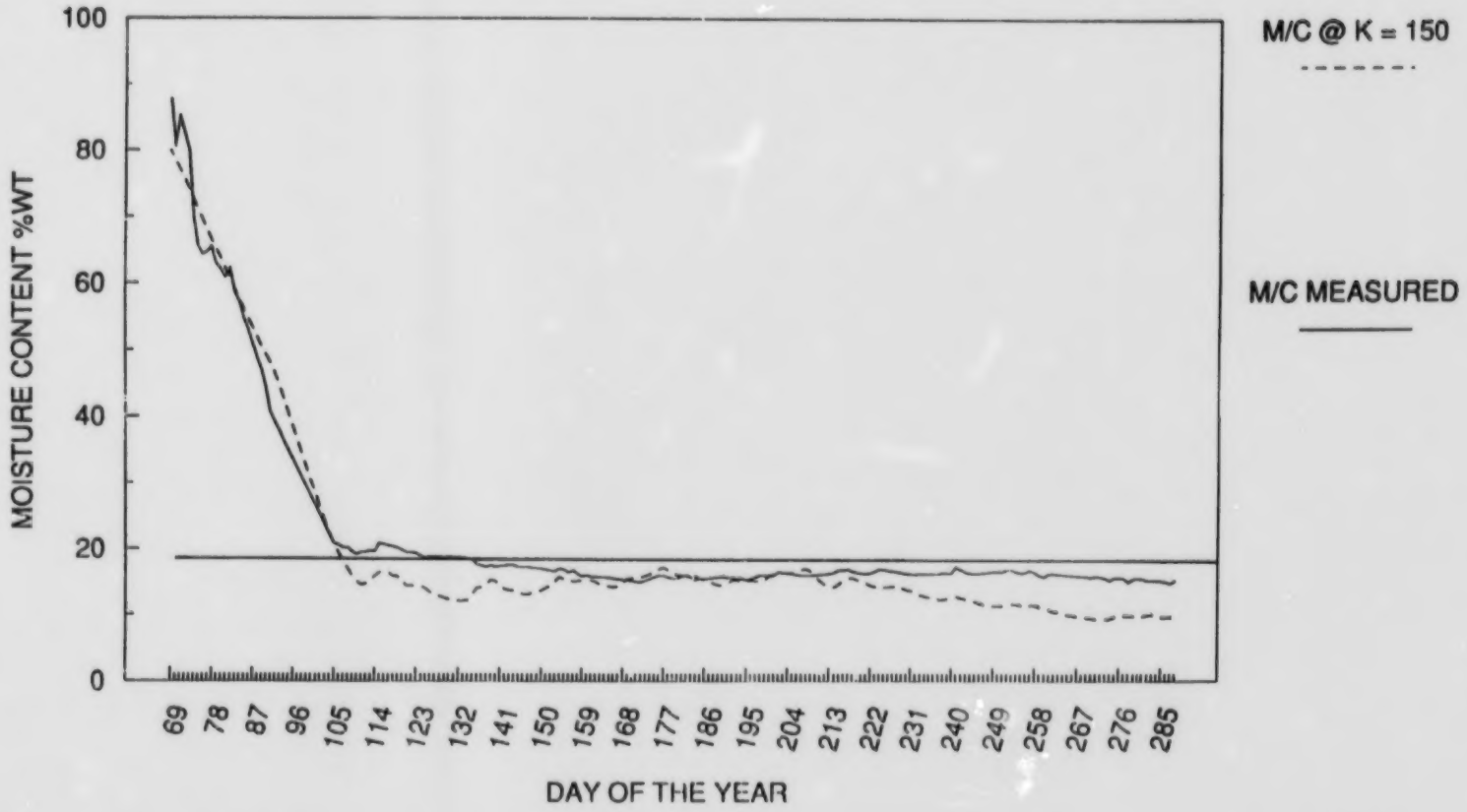

STUD DIFFUSION RESISTANCE = 200E9 (Pa.m2.s/Kg)/m

WH3P3_4-4

Figure 3.21

UPPER STUD MOISTURE CONTENT PROFILES

ATLANTIC CANADA HUT PROJECT PANEL 3 SIMULATION

GLASCLAD SHEATHING, ST. JOHNS

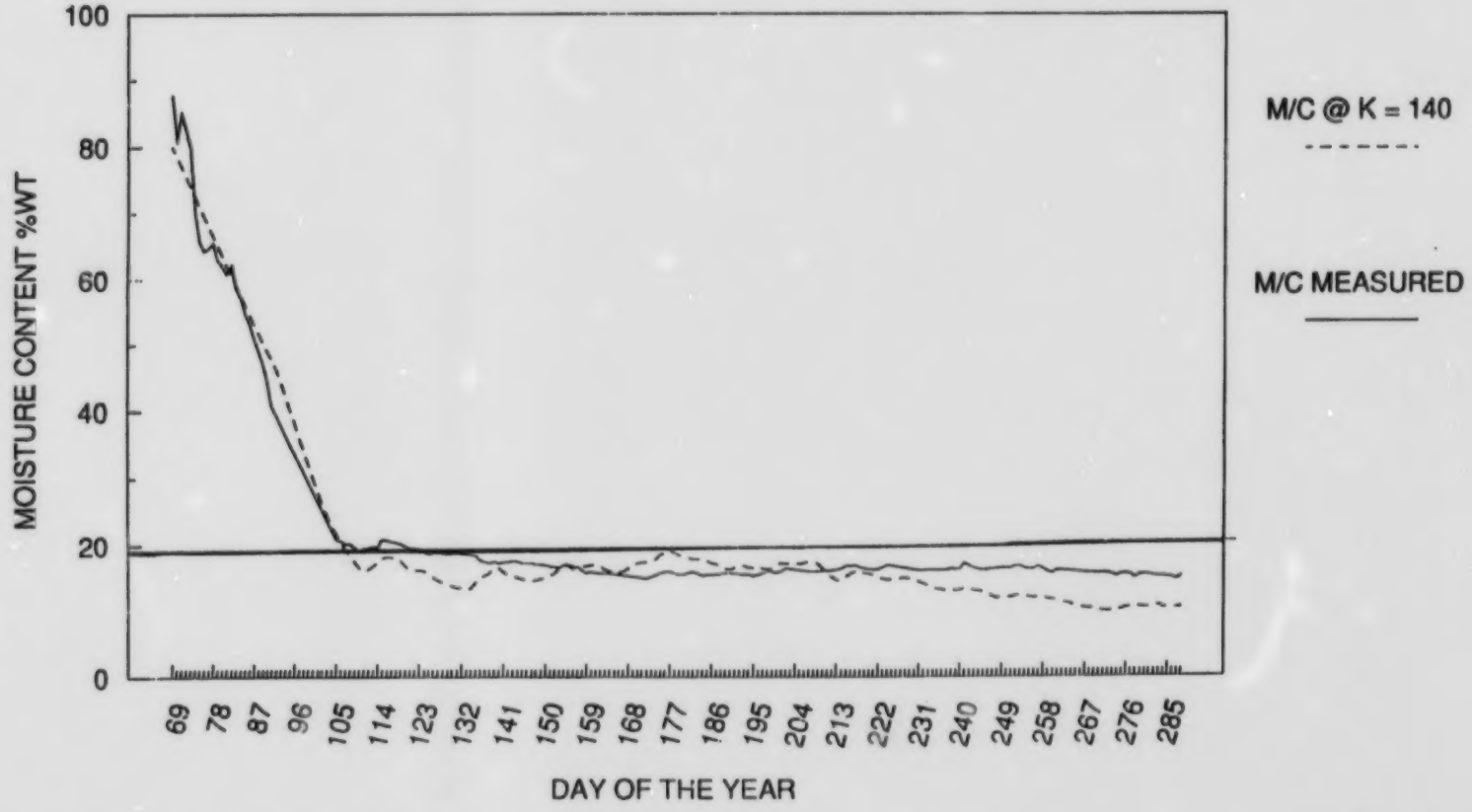

STUD DIFFUSION RESISTANCE = 200E9 (Pa.m2.s/Kg)/m

WH3P3_4-4

Figure 3.22

UPPER STUD MOISTURE CONTENT PROFILES

ATLANTIC CANADA HUT PROJECT PANEL 3 SIMULATION

GLASCLAD SHEATHING, ST. JOHNS

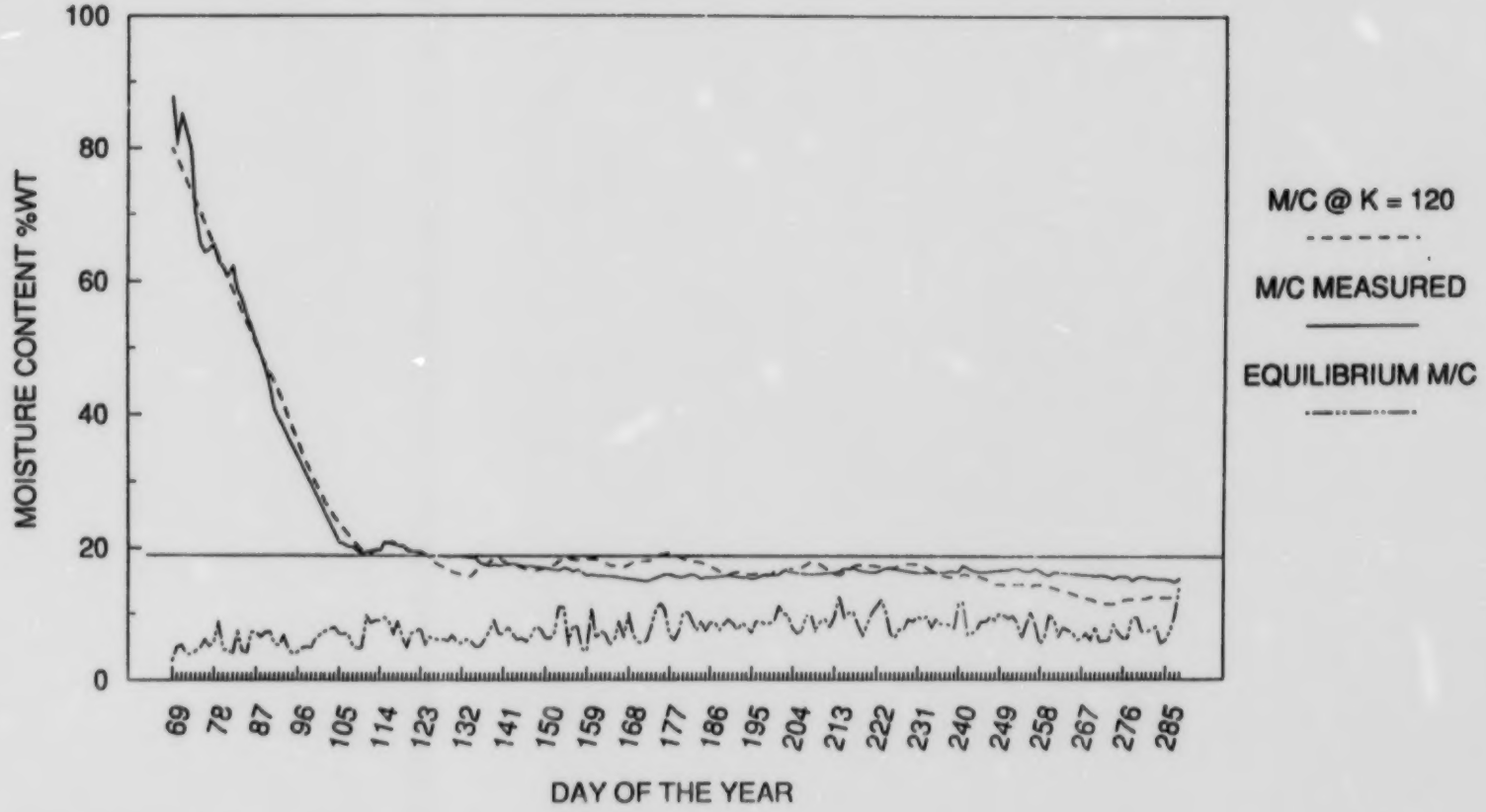

STUD DIFFUSION RESISTANCE = 200E9 (Pa.m2.s/Kg)/m

WH3P3_4-4

Figure 3.23

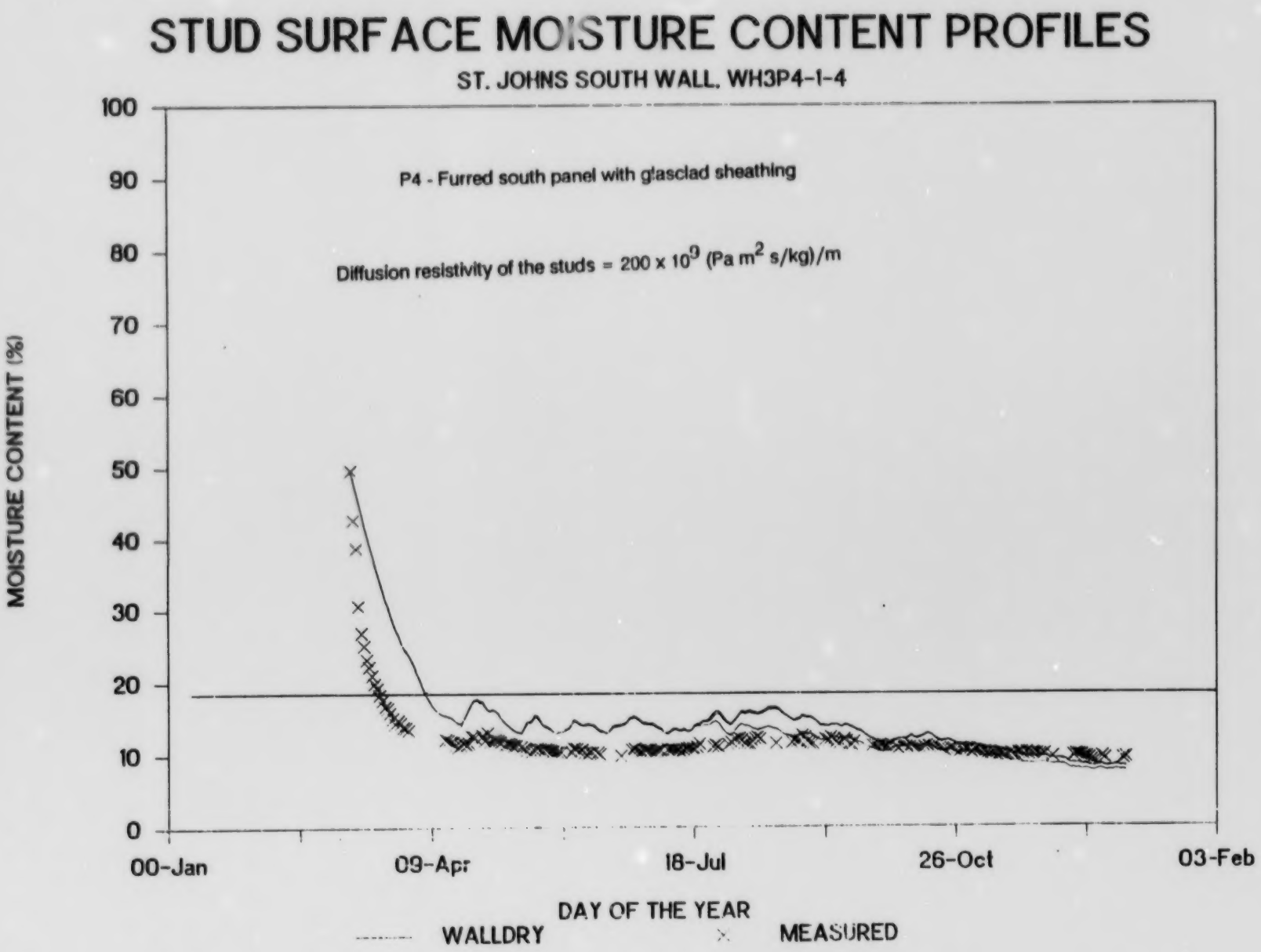
STUD SURFACE MOISTURE CONTENT PROFILES
ST. JOHNS SOUTH WALL. WH3P4-1-4
P4 - Furred south panel with glasclad sheathing
Diffusion resistivity of the studs = 200 x 10^9 (Pa m^2 s/kg)/m
MOISTURE CONTENT (%)
100
90
80
70
60
50
40
30
20
10
0
00-Jan
09-Apr
18-Jul
26-Oct
03-Feb
DAY OF THE YEAR
WALLDRY
MEASURED

Figure 3.24

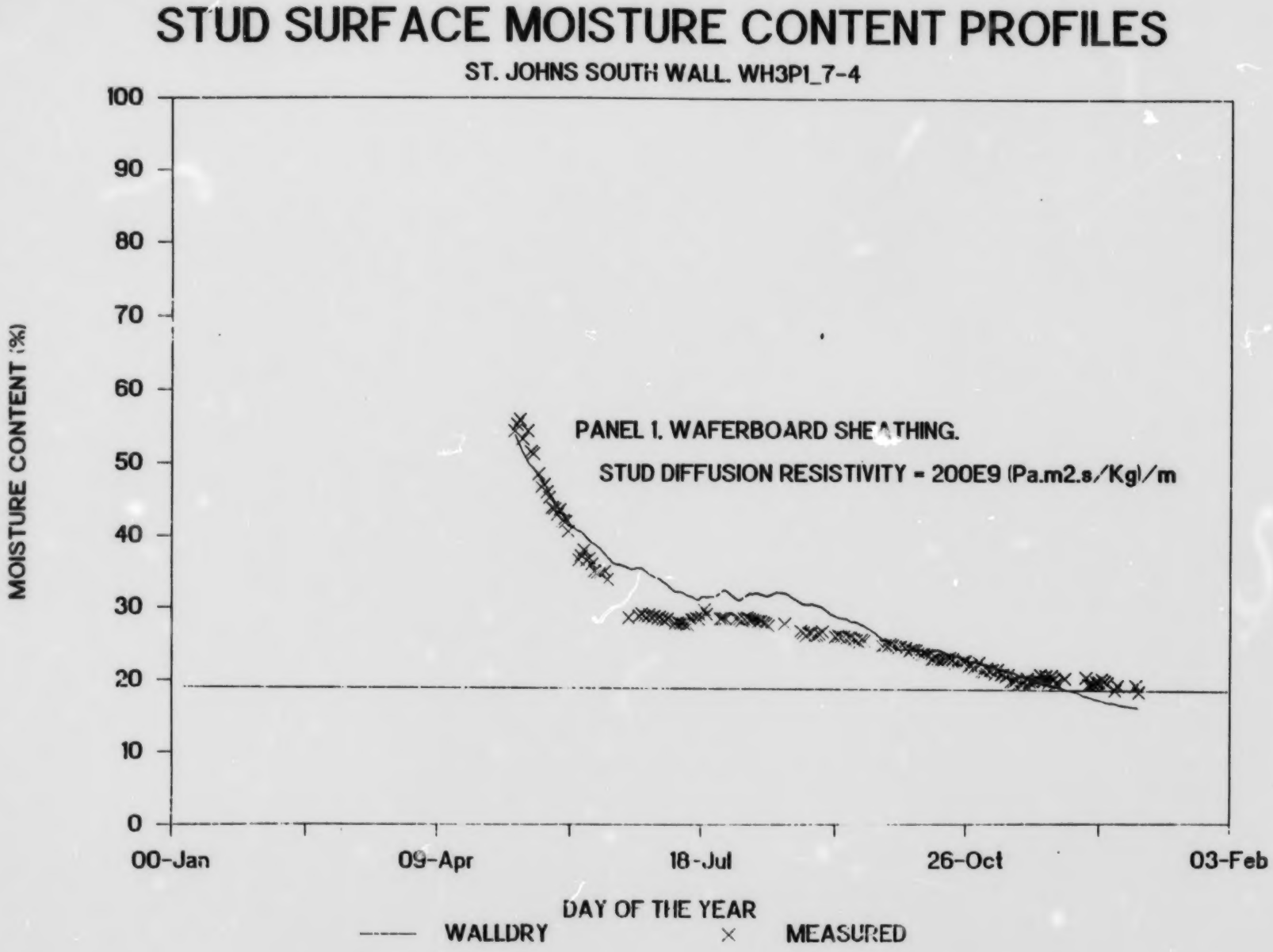
STUD SURFACE MOISTURE CONTENT PROFILES
ST. JOHNS SOUTH WALL. WH3P1_7-4
MOISTURE CONTENT (%)
100
90
80
70
60
50
40
30
20
10
0
PANEL 1. WAFERBOARD SHEATHING.
STUD DIFFUSION RESISTIVITY = 200E9 (Pa.m2.s/Kg)/m
00-Jan
09-Apr
18-Jul
26-Oct
03-Feb
DAY OF THE YEAR
WALLDRY
MEASURED

Figure 3.25

STUD SURFACE MOISTURE CONTENT PROFILES

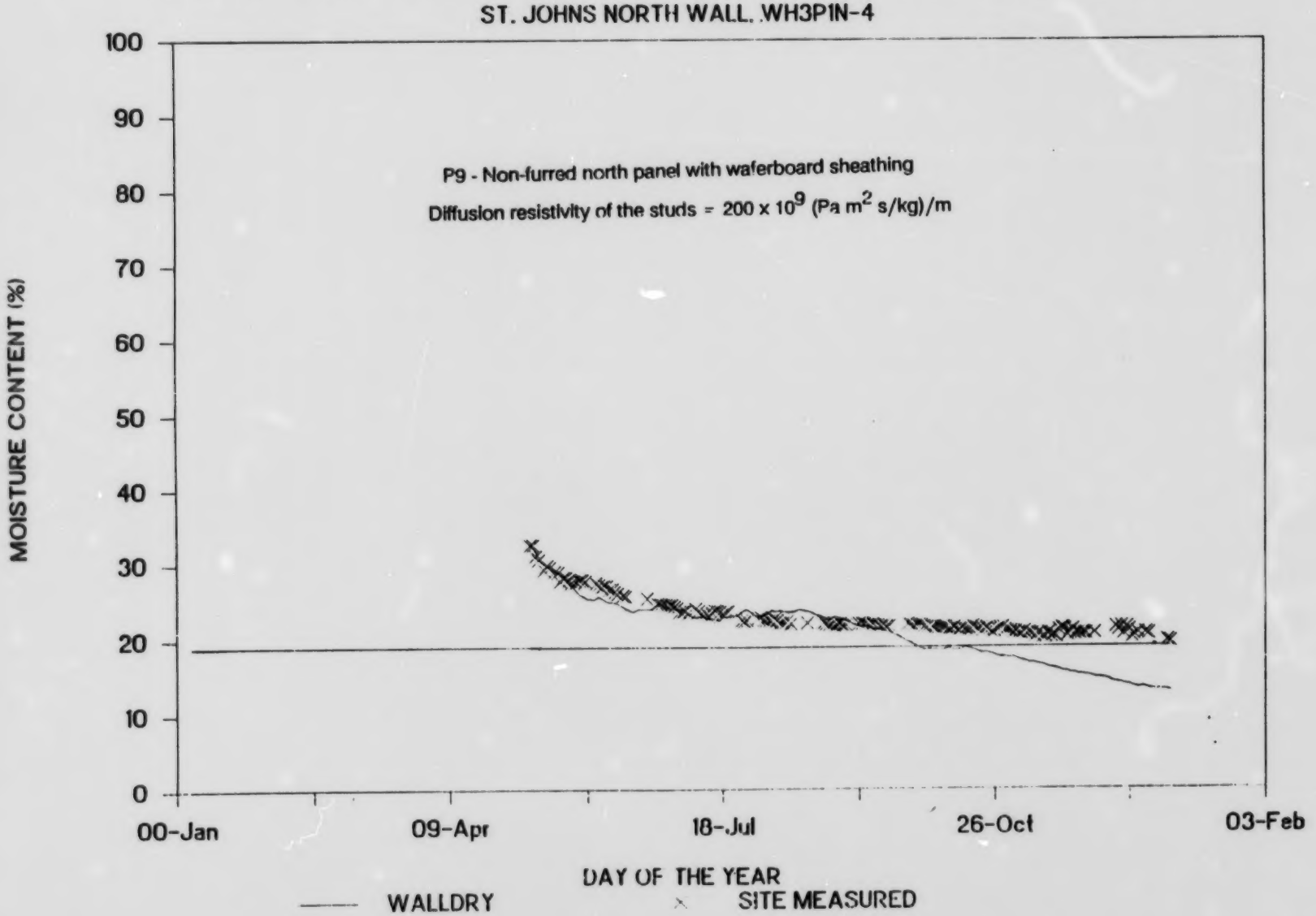

Figure 3.26

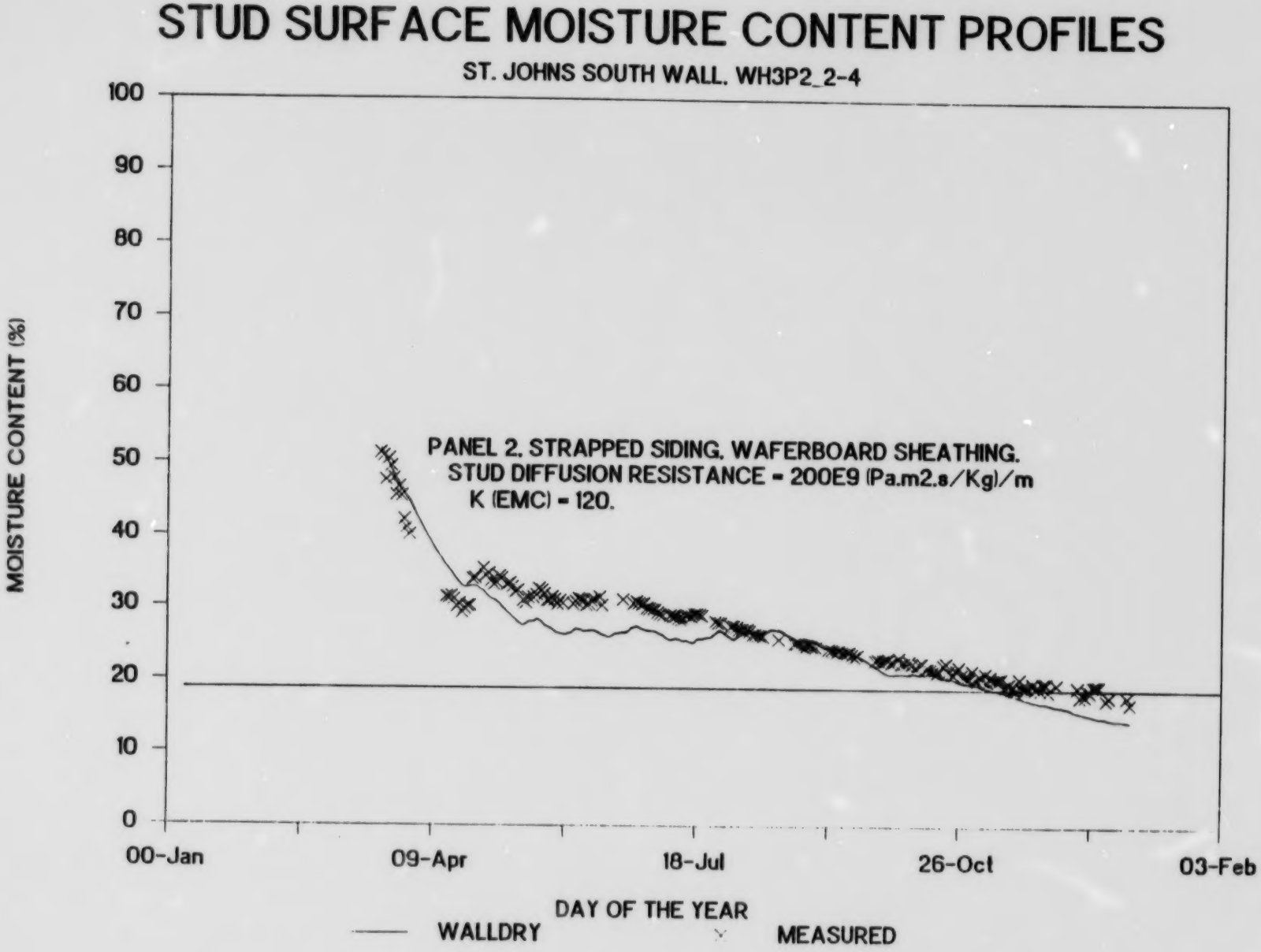
STUD SURFACE MOISTURE CONTENT PROFILES
ST. JOHNS SOUTH WALL. WH3P2_2-4
MOISTURE CONTENT (%)
100
90
80
70
60
50
40
30
20
10
0
PANEL 2. STRAPPED SIDING. WAFERBOARD SHEATHING.
STUD DIFFUSION RESISTANCE = 200E9 (Pa.m2.s/Kg)/m
K (EMC) = 120.
00-Jan
09-Apr
18-Jul
26-Oct
03-Feb
DAY OF THE YEAR
WALLDRY
MEASURED

Figure 3.27

STUD SURFACE MOISTURE CONTENT PROFILES

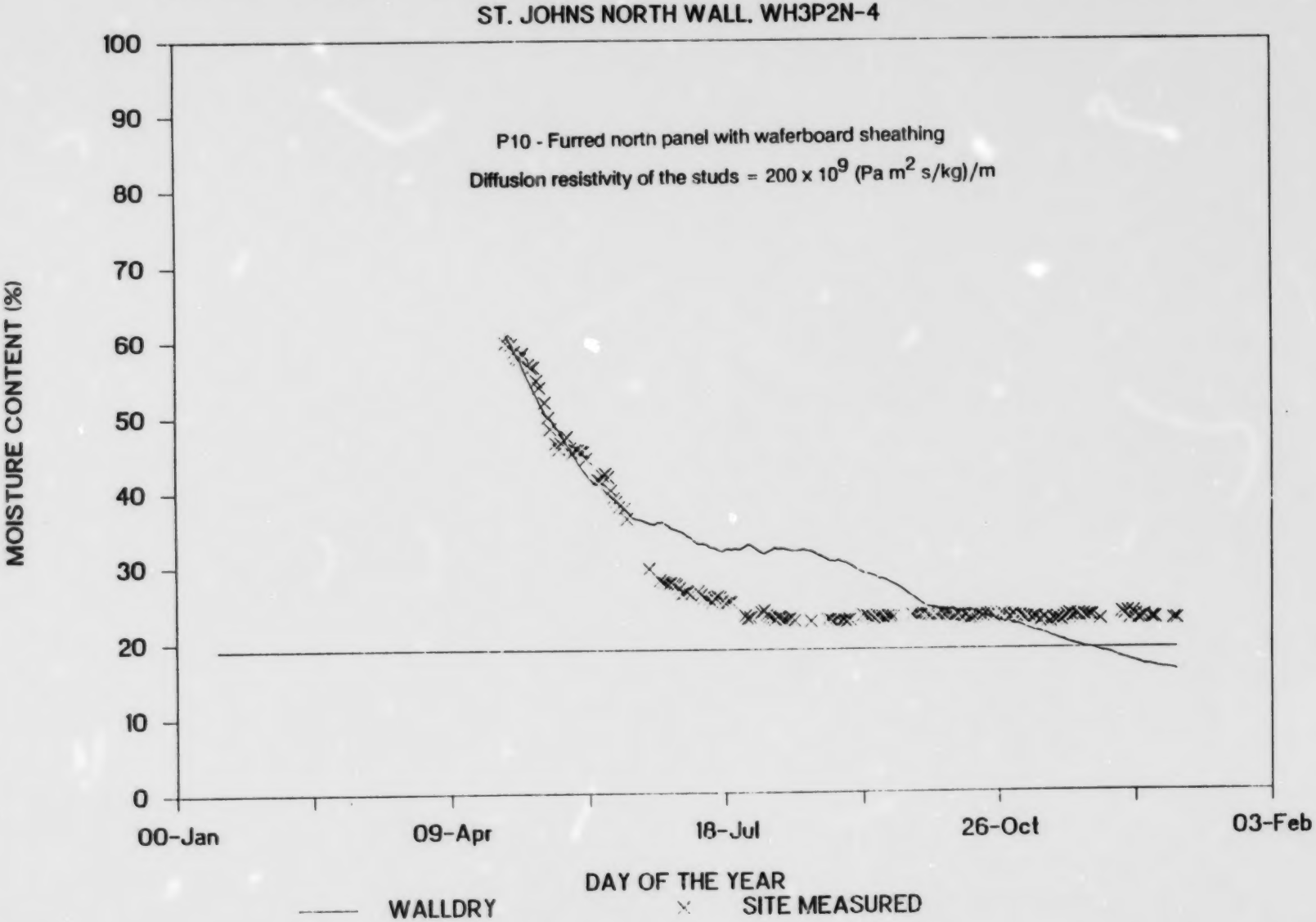

Figure 3.28

STUD SURFACE MOISTURE CONTENT PROFILES

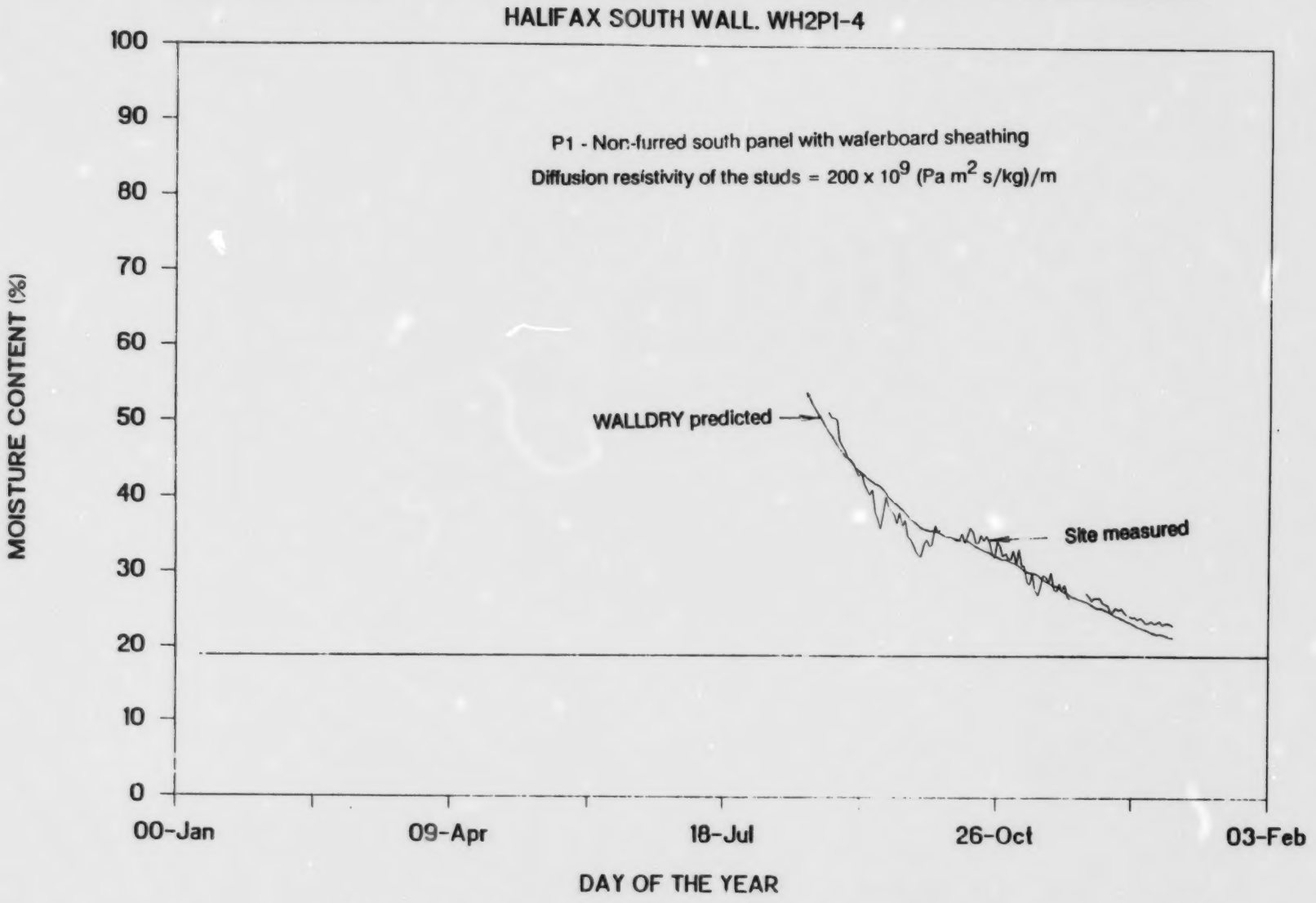

Figure 3.29

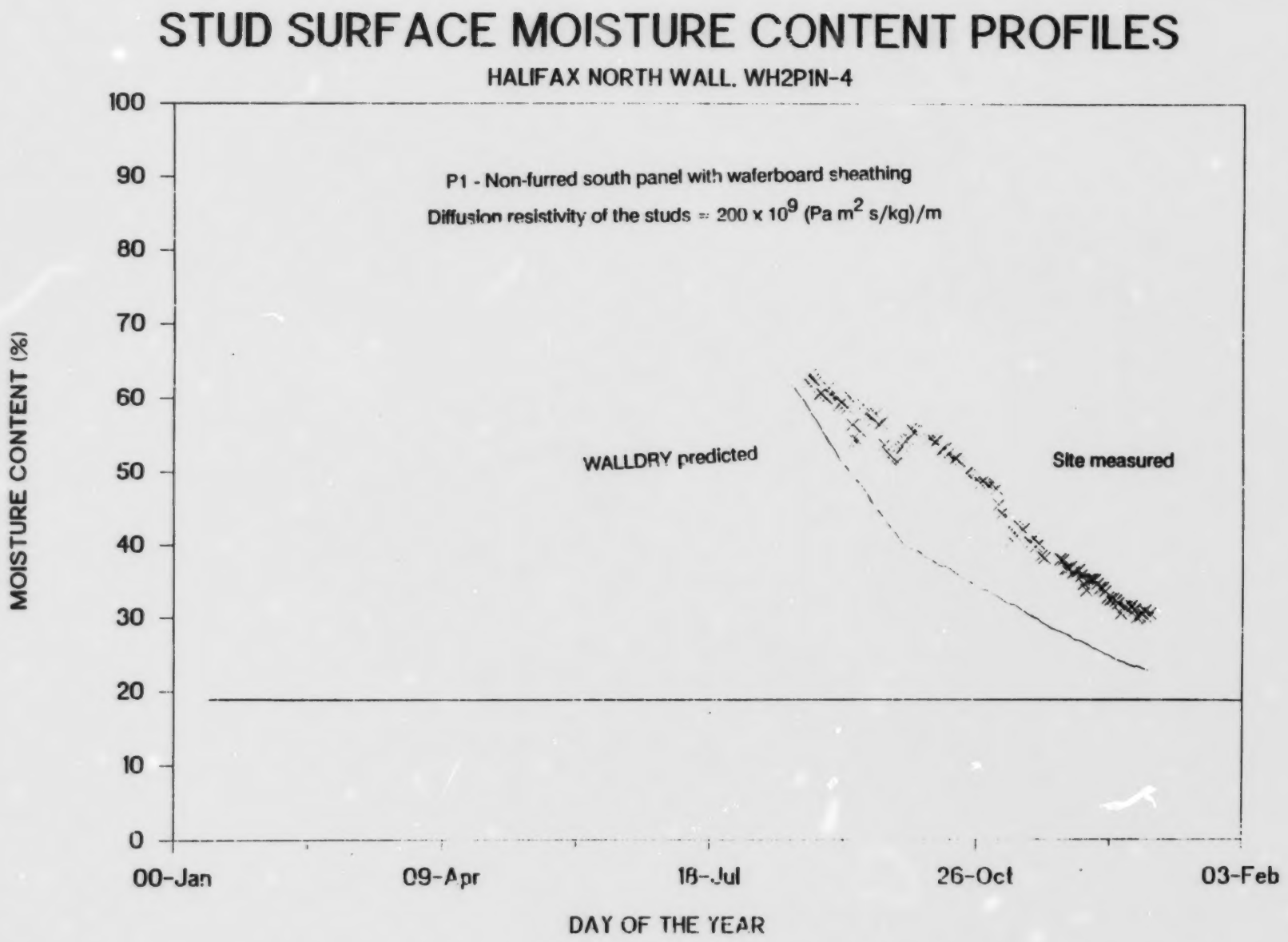
STUD SURFACE MOISTURE CONTENT PROFILES
HALIFAX NORTH WALL. WH2P1N-4
P1 - Non-furred south panel with waferboard sheathing
Diffusion resistivity of the studs = 200 x 10^9 (Pa m^2 s/kg)/m
WALLDRY predicted
Site measured
MOISTURE CONTENT (%)
100
90
80
70
60
50
40
30
20
10
0
00-Jan
09-Apr
18-Jul
26-Oct
03-Feb
DAY OF THE YEAR

Figure 3.30

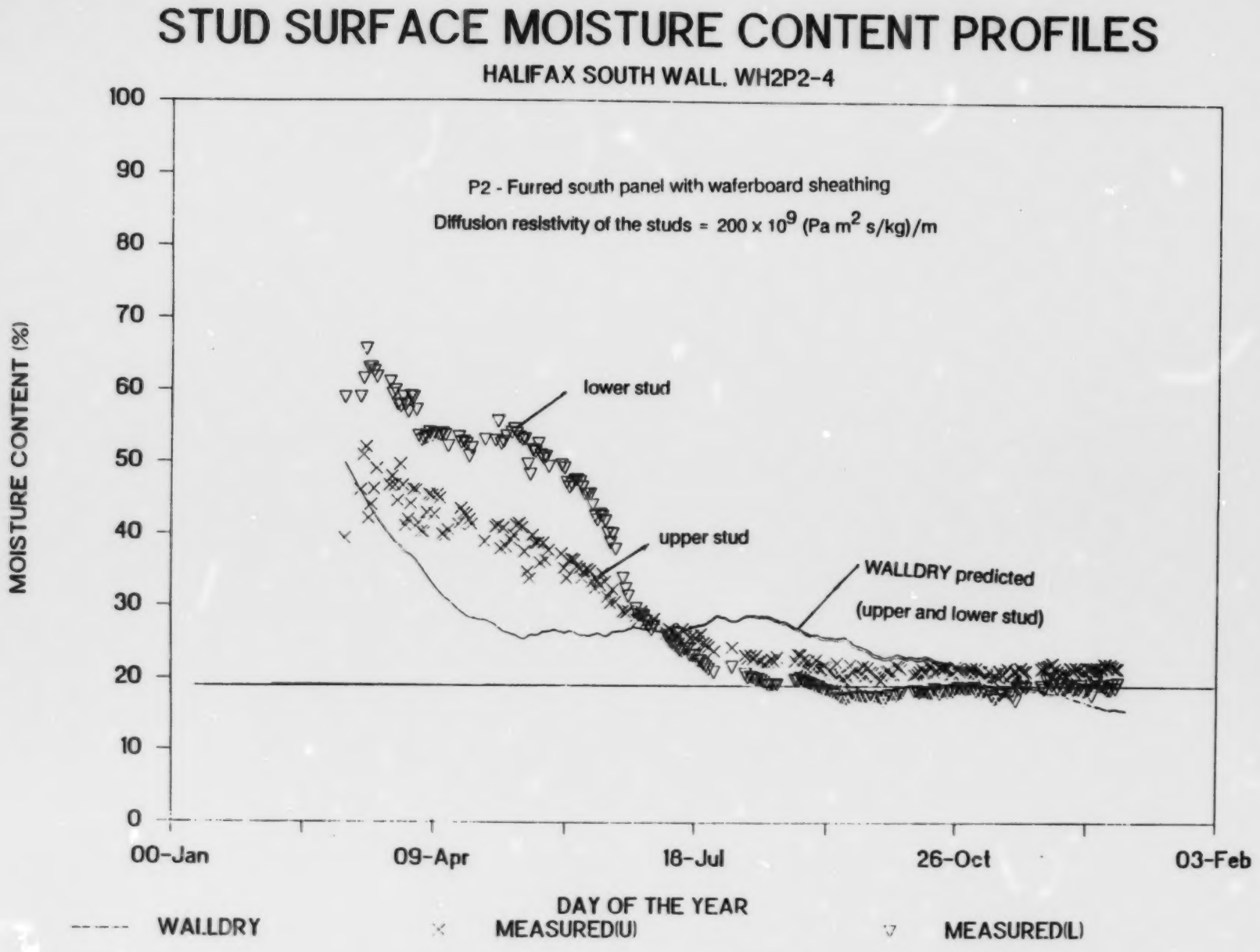
STUD SURFACE MOISTURE CONTENT PROFILES
HALIFAX SOUTH WALL. WH2P2-4
P2 - Furred south panel with waferboard sheathing
Diffusion resistivity of the studs = 200 x 10^9 (Pa m^2 s/kg)/m
MOISTURE CONTENT (%)
100
90
80
70
60
50
40
30
20
10
0
lower stud
upper stud
WALLDRY predicted
(upper and lower stud)
00-Jan
09-Apr
18-Jul
26-Oct
03-Feb
DAY OF THE YEAR
WALLDRY
MEASURED(U)
MEASURED(L)

Figure 3.31

STUD SURFACE MOISTURE CONTENT PROFILES

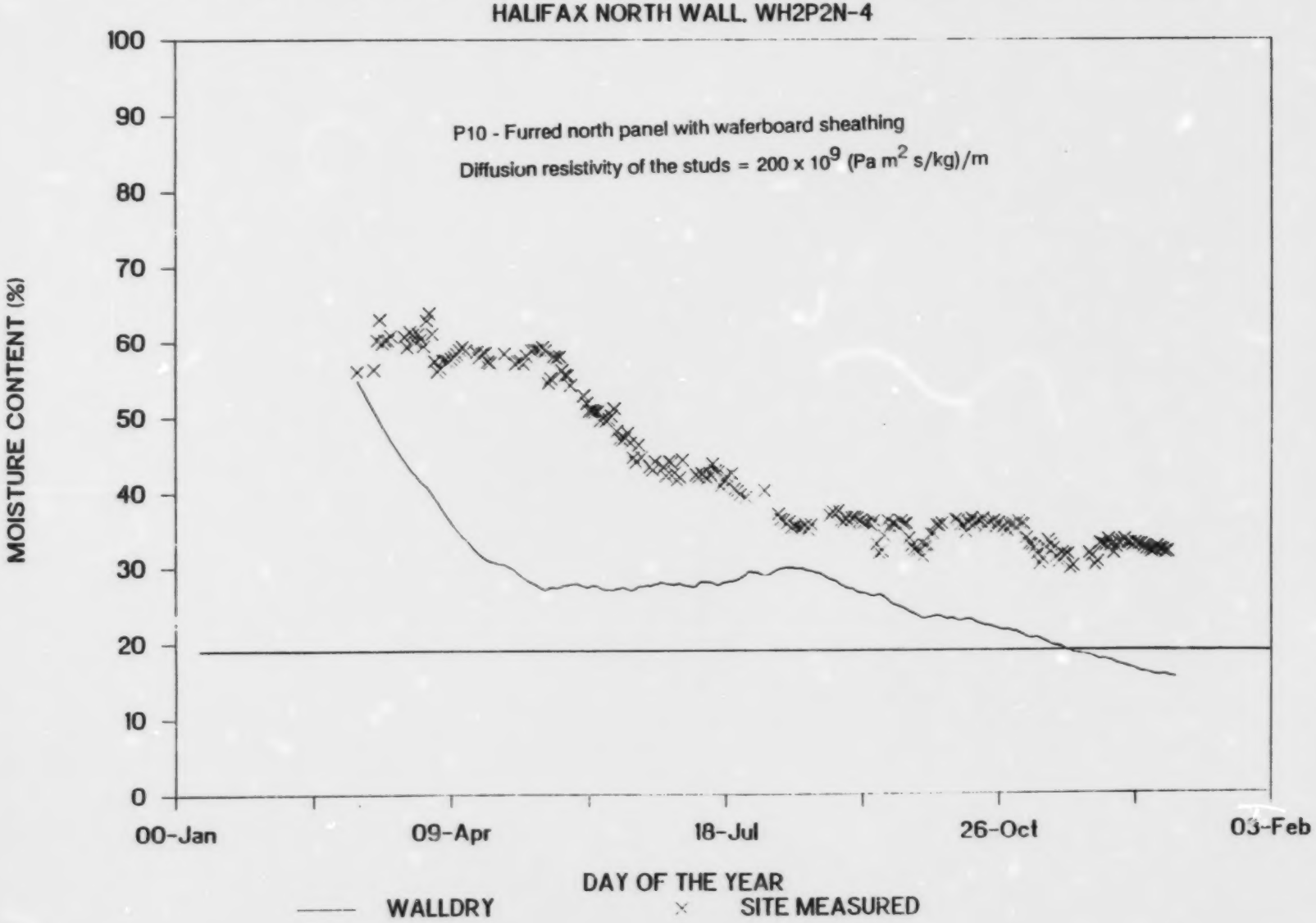

Figure 3.32

STUD SURFACE MOISTURE CONTENT PROFILES

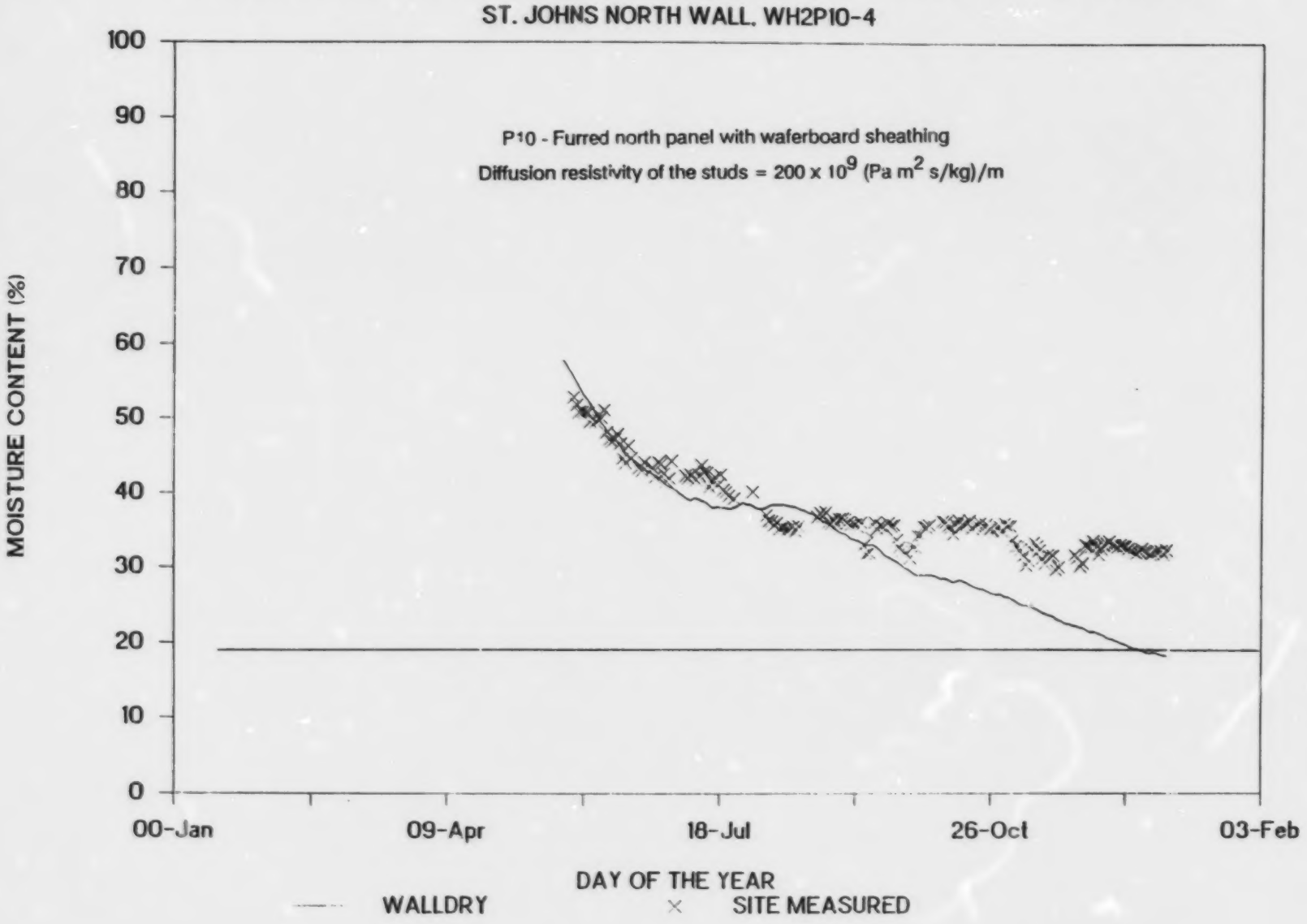

Figure 3.33

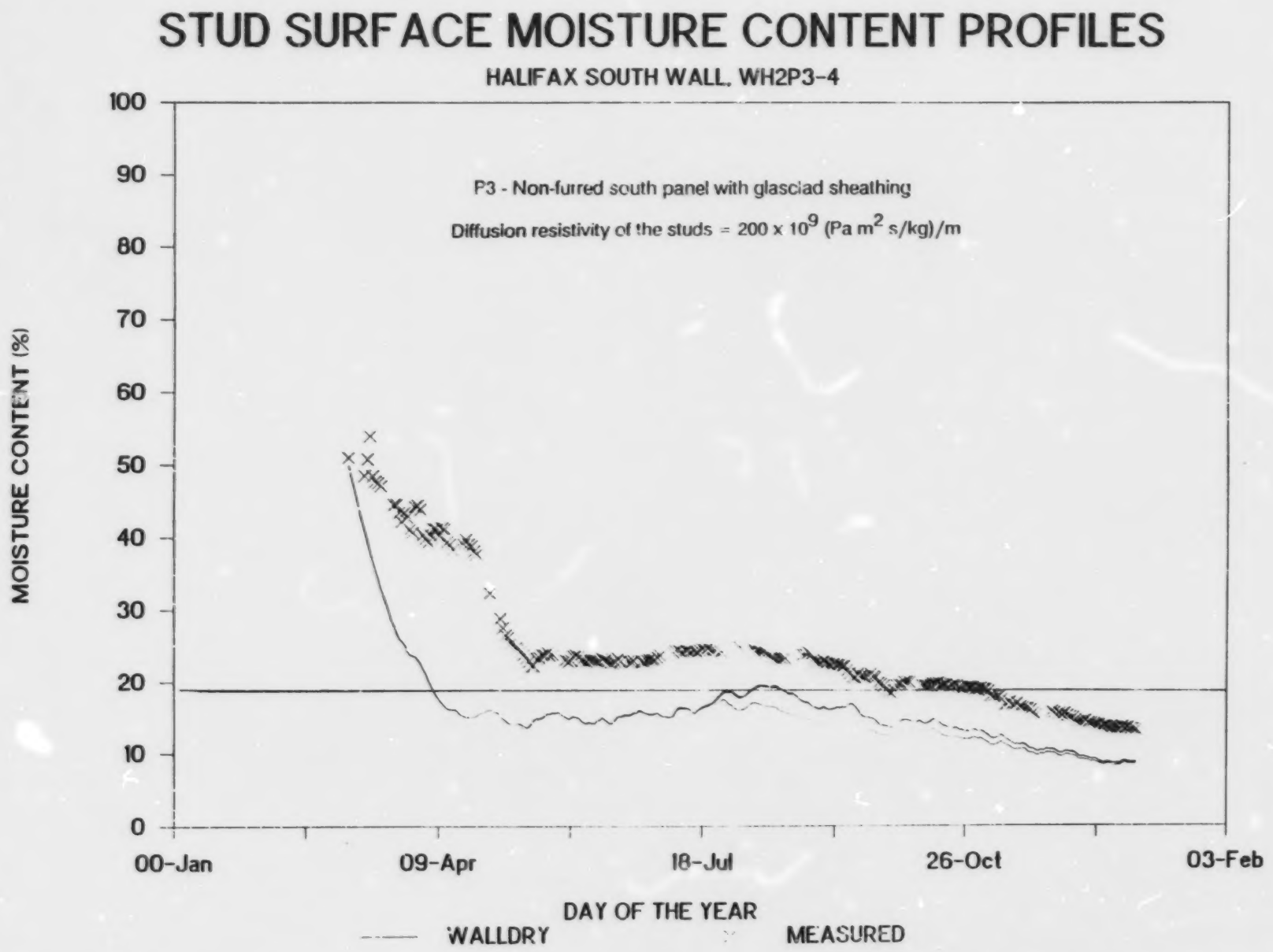
STUD SURFACE MOISTURE CONTENT PROFILES
HALIFAX SOUTH WALL, WH2P3-4
P3 - Non-furred south panel with glasclad sheathing
Diffusion resistivity of the studs = 200 x 10^9 (Pa m^2 s/kg)/m
MOISTURE CONTENT (%)
100
90
80
70
60
50
40
30
20
10
0
00-Jan
09-Apr
18-Jul
26-Oct
03-Feb
DAY OF THE YEAR
WALLDRY
MEASURED

Figure 3.34

STUD SURFACE MOISTURE CONTENT PROFILES

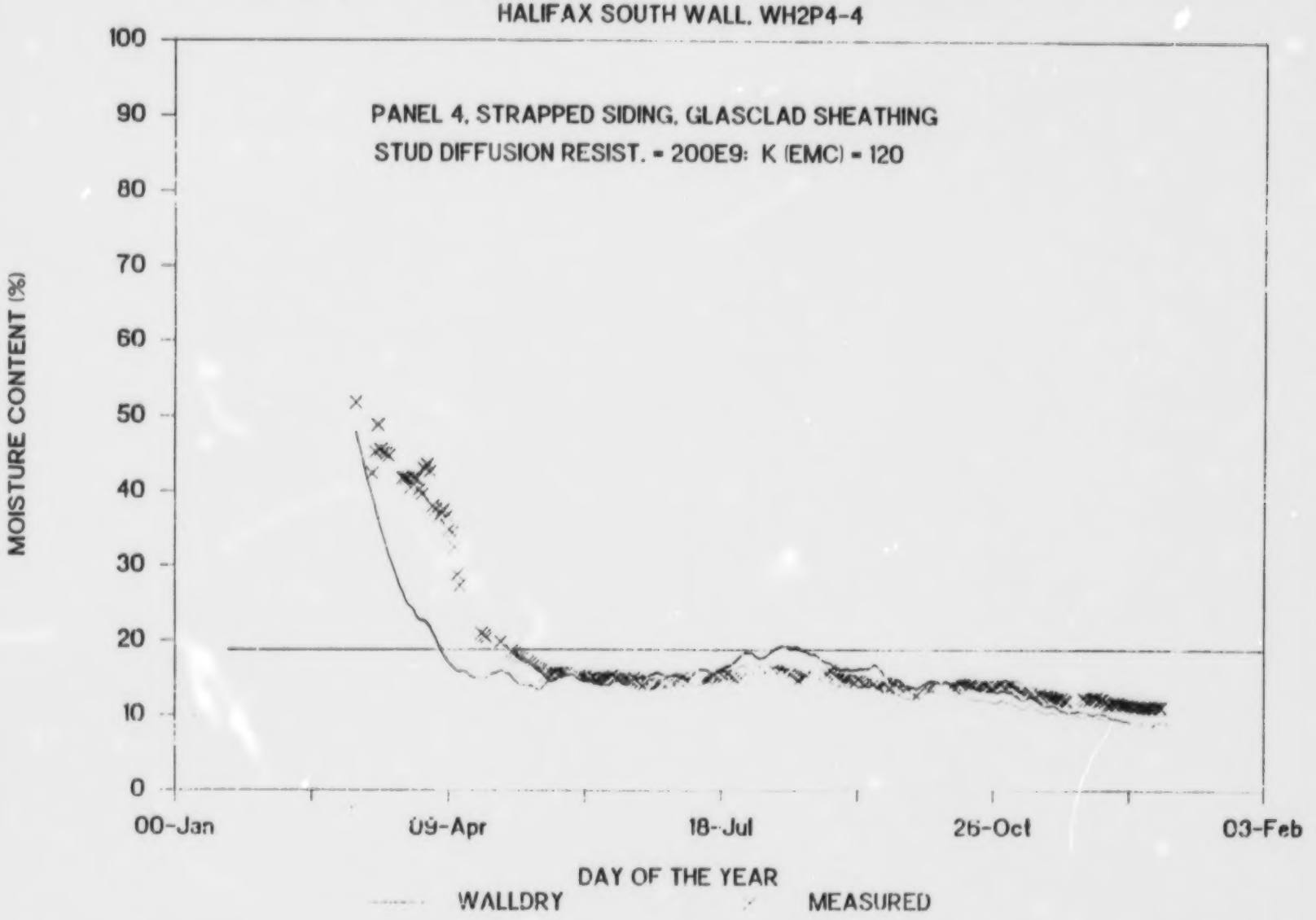

Figure 3.35

STUD SURFACE MOISTURE CONTENT PROFILES

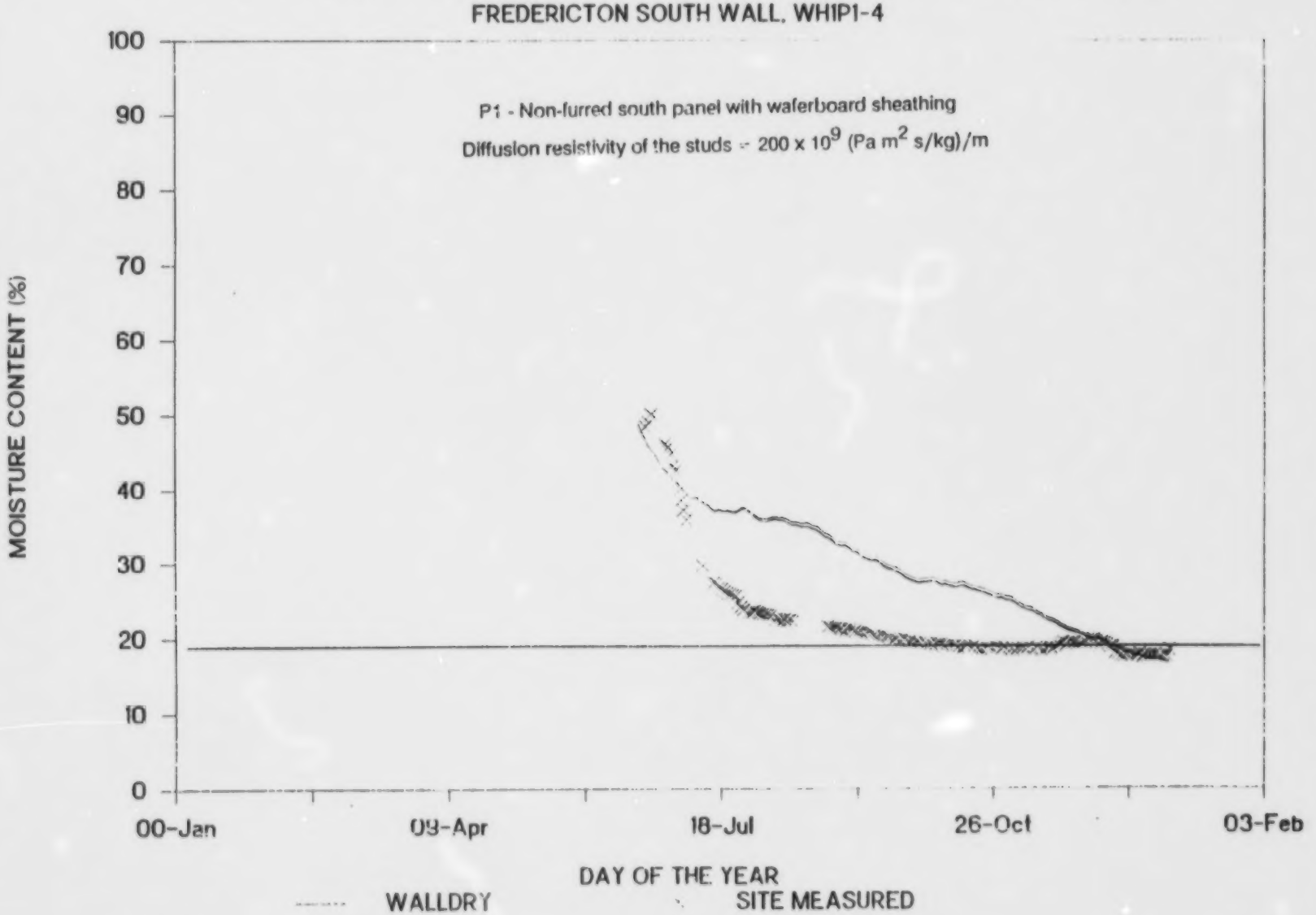

Figure 3.36

STUD SURFACE MOISTURE CONTENT PROFILES

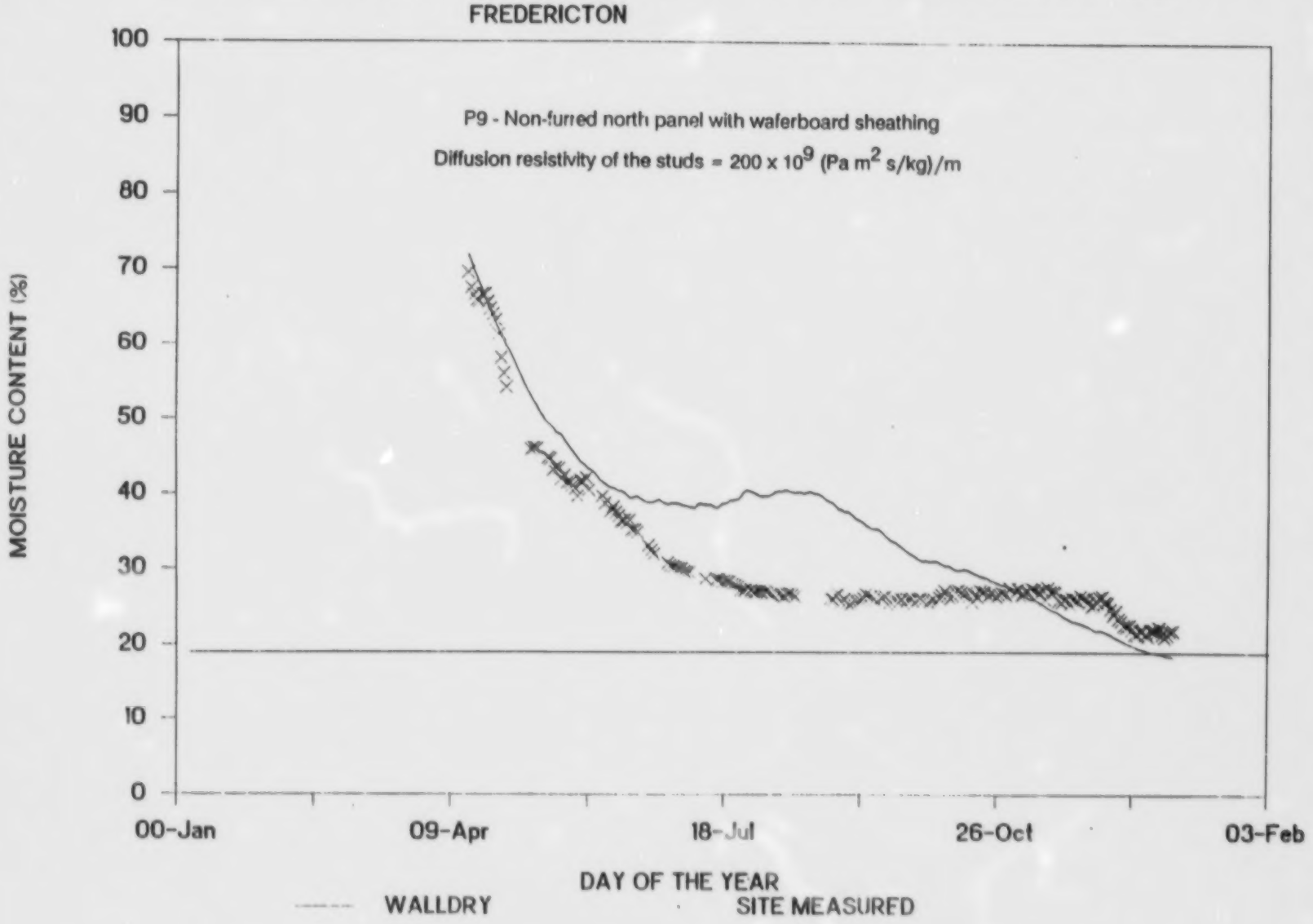

Figure 3.37

STUD SURFACE MOISTURE CONTENT PROFILES

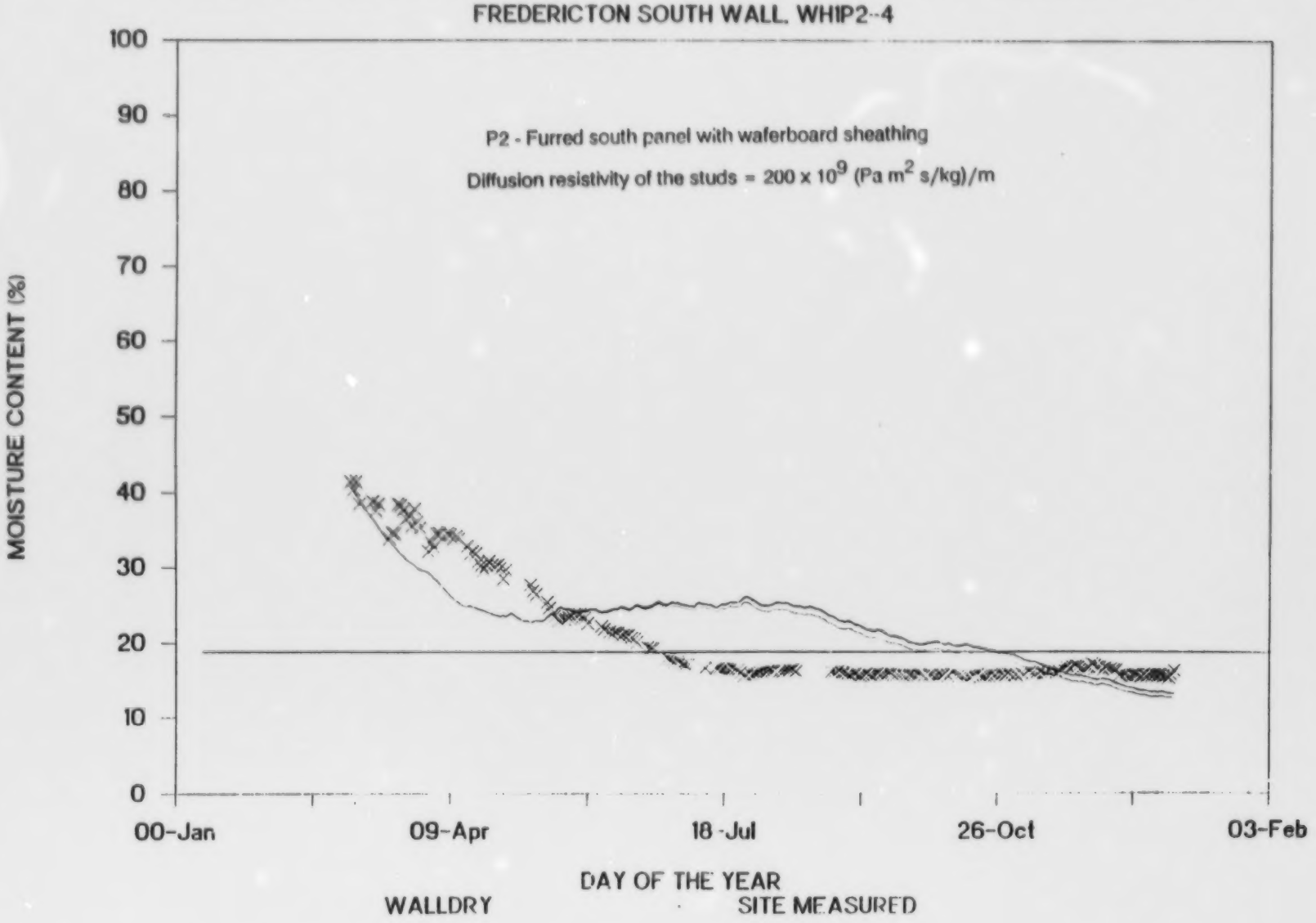

Figure 3.38

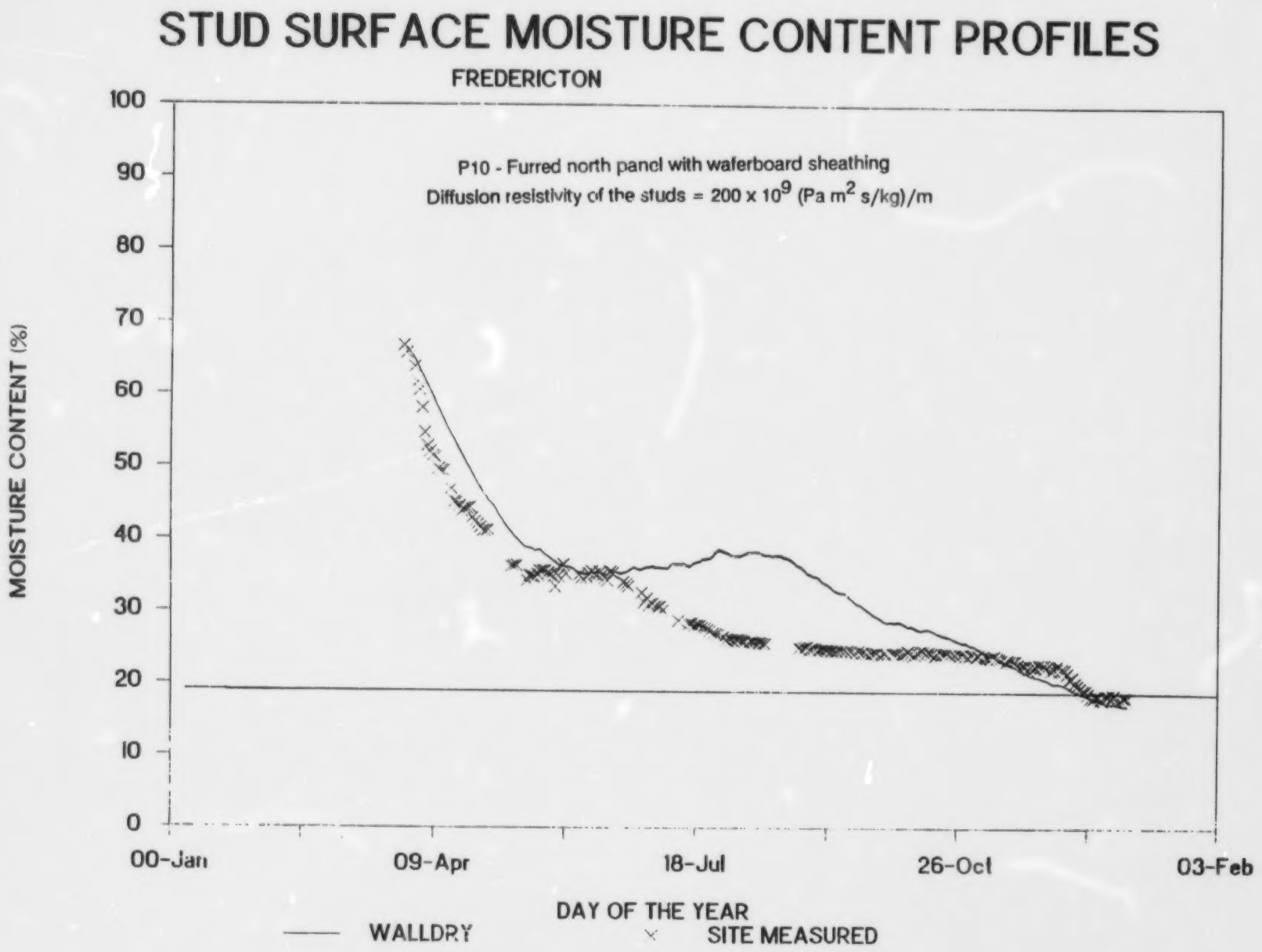
STUD SURFACE MOISTURE CONTENT PROFILES
FREDERICTON
P10 - Furred north panel with waferboard sheathing
Diffusion resistivity of the studs = 200 x 10^9 (Pa m^2 s/kg)/m
MOISTURE CONTENT (%)
100
90
80
70
60
50
40
30
20
10
0
00-Jan
09-Apr
18-Jul
26-Oct
03-Feb
DAY OF THE YEAR
WALLDRY
SITE MEASURED

Figure 3.39

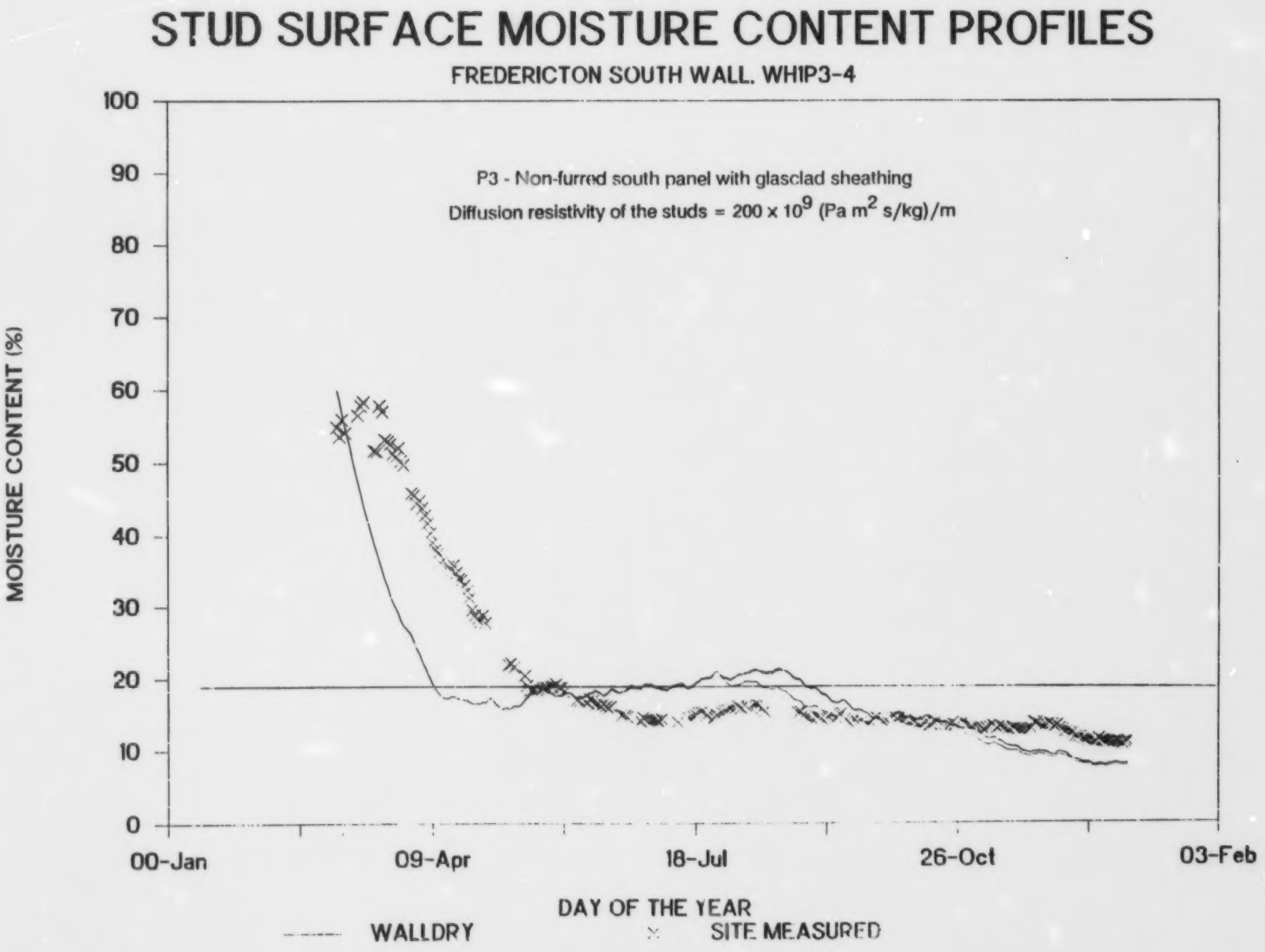
STUD SURFACE MOISTURE CONTENT PROFILES
FREDERICTON SOUTH WALL. WH1P3-4
P3 - Non-furred south panel with glasclad sheathing
Diffusion resistivity of the studs = 200 x 10^9 (Pa m^2 s/kg)/m
MOISTURE CONTENT (%)
100
90
80
70
60
50
40
30
20
10
0
00-Jan
09-Apr
18-Jul
26-Oct
03-Feb
DAY OF THE YEAR
WALLDRY
SITE MEASURED

Figure 3.40

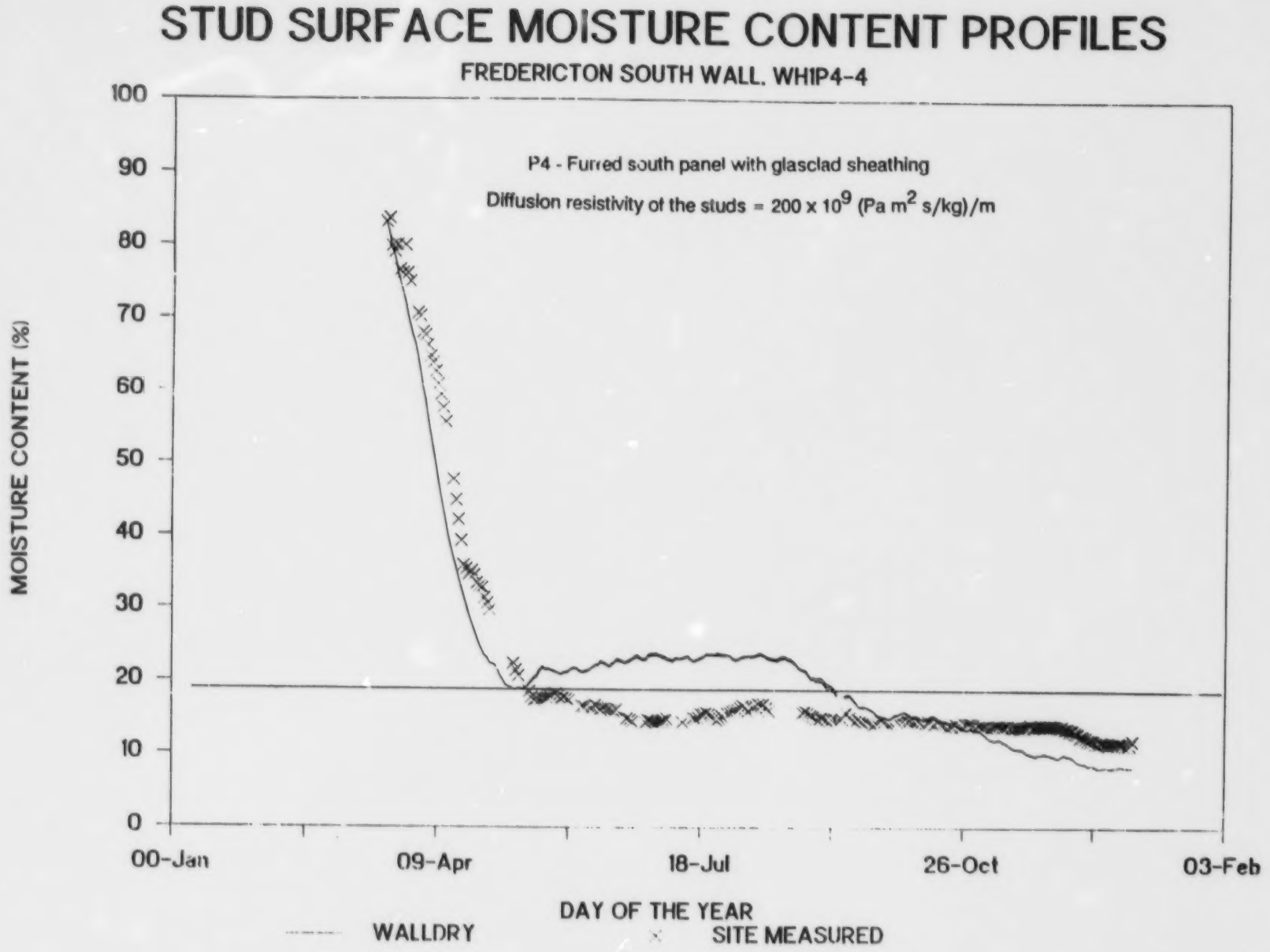
STUD SURFACE MOISTURE CONTENT PROFILES
FREDERICTON SOUTH WALL. WH1P4-4
P4 - Furred south panel with glasclad sheathing
Diffusion resistivity of the studs = 200 x 10^9 (Pa m^2 s/kg)/m
MOISTURE CONTENT (%)
100
90
80
70
60
50
40
30
20
10
0
00-Jan
09-Apr
18-Jul
26-Oct
03-Feb
DAY OF THE YEAR
WALLDRY
SITE MEASURED

Figure 3.41

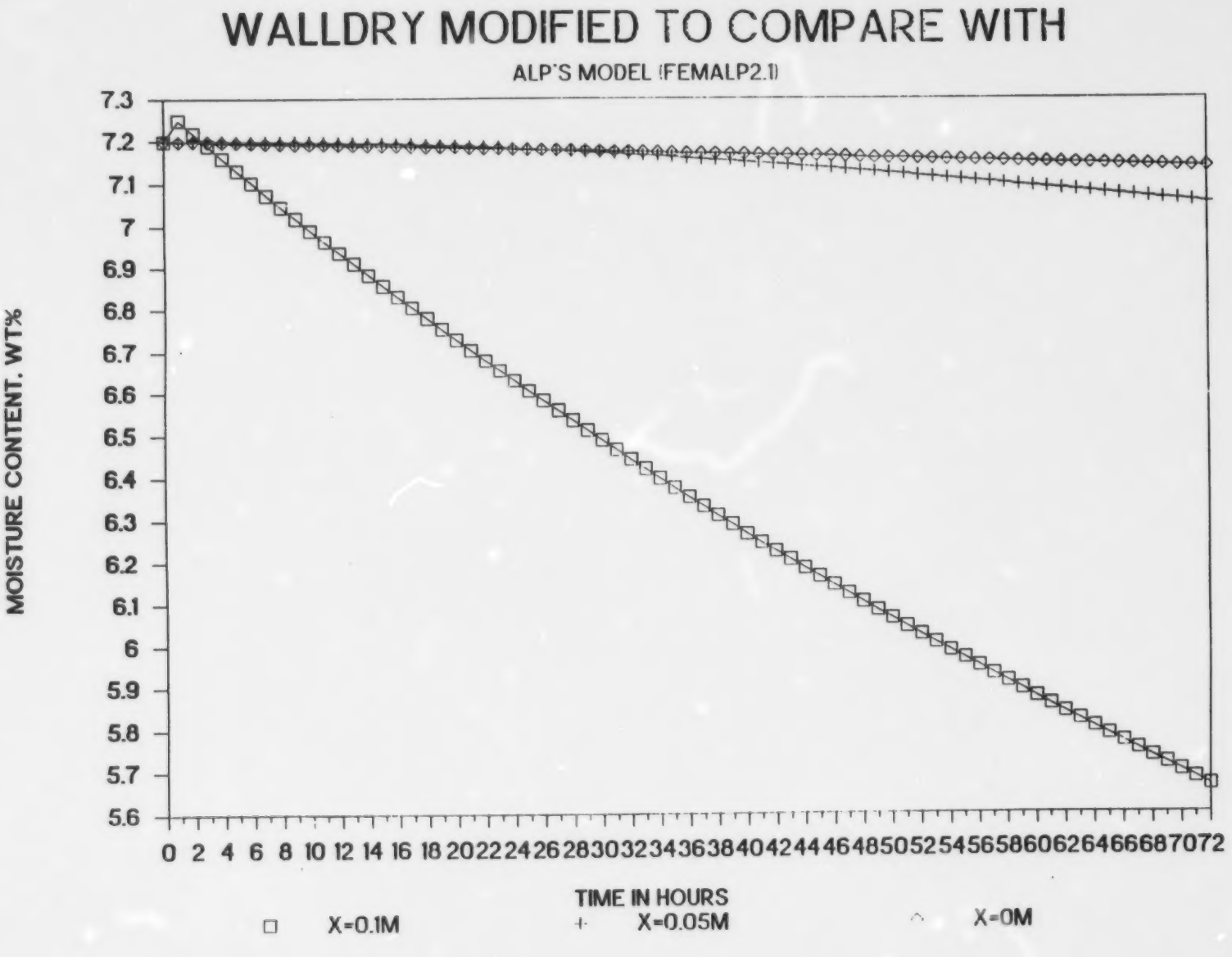
WALLDRY MODIFIED TO COMPARE WITH
ALP'S MODEL (FEMALP2.1)
MOISTURE CONTENT, WT%
7.3
7.2
7.1
7
6.9
6.8
6.7
6.6
6.5
6.4
6.3
6.2
6.1
6
5.9
5.8
5.7
5.6
0 2 4 6 8 10 12 14 16 18 20 22 24 26 28 30 32 34 36 38 40 42 44 46 48 50 52 54 56 58 60 62 64 66 68 70 72
TIME IN HOURS
X=0.1M
X=0.05M
X=0M

Figure 3.42

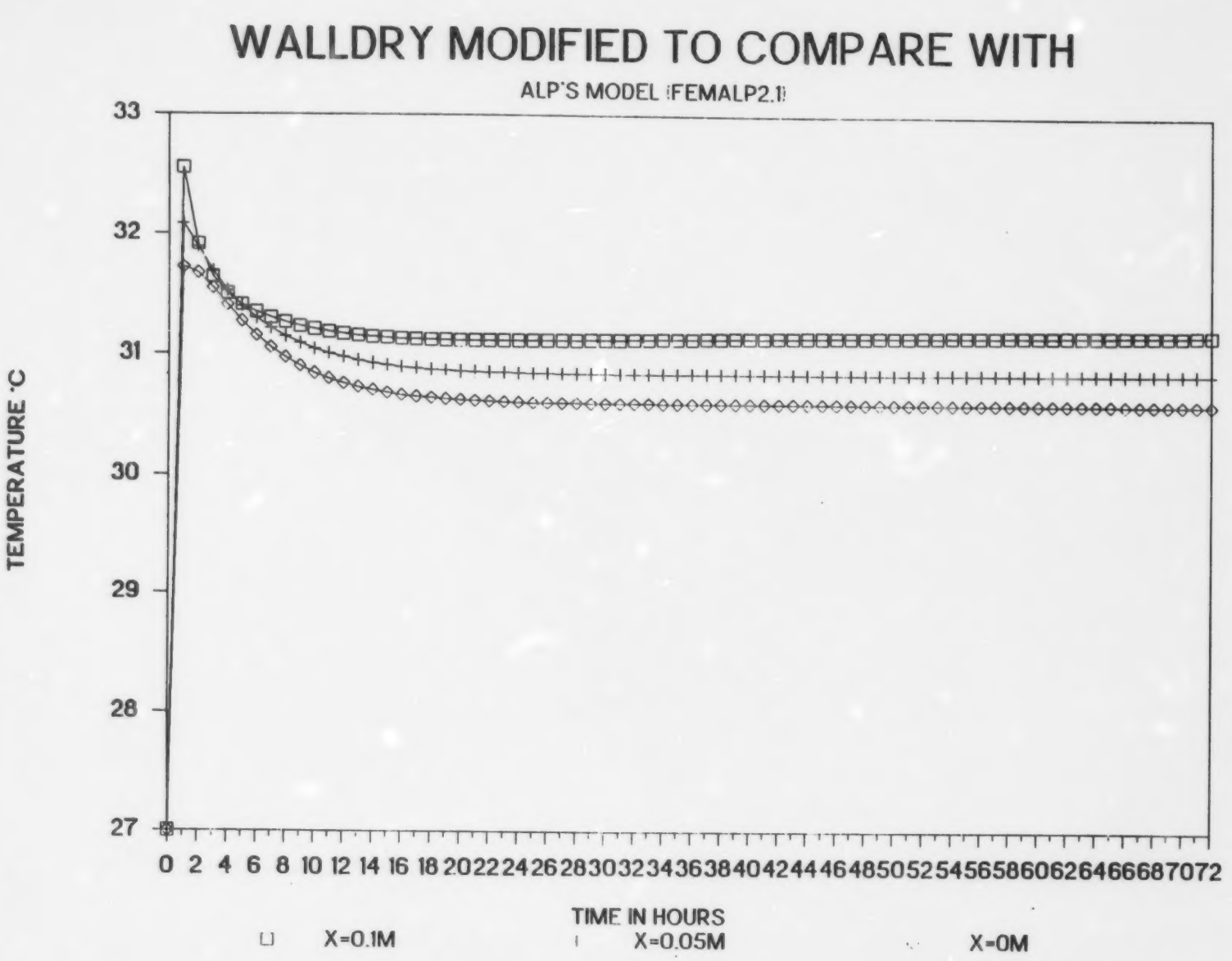
WALLDRY MODIFIED TO COMPARE WITH
ALP'S MODEL (FEMALP2.1)
TEMPERATURE °C
33
32
31
30
29
28
27
0 2 4 6 8 10 12 14 16 18 20 22 24 26 28 30 32 34 36 38 40 42 44 46 48 50 52 54 56 58 60 62 64 66 68 70 72
TIME IN HOURS
X=0.1M
X=0.05M
X=0M

Figure 3.43

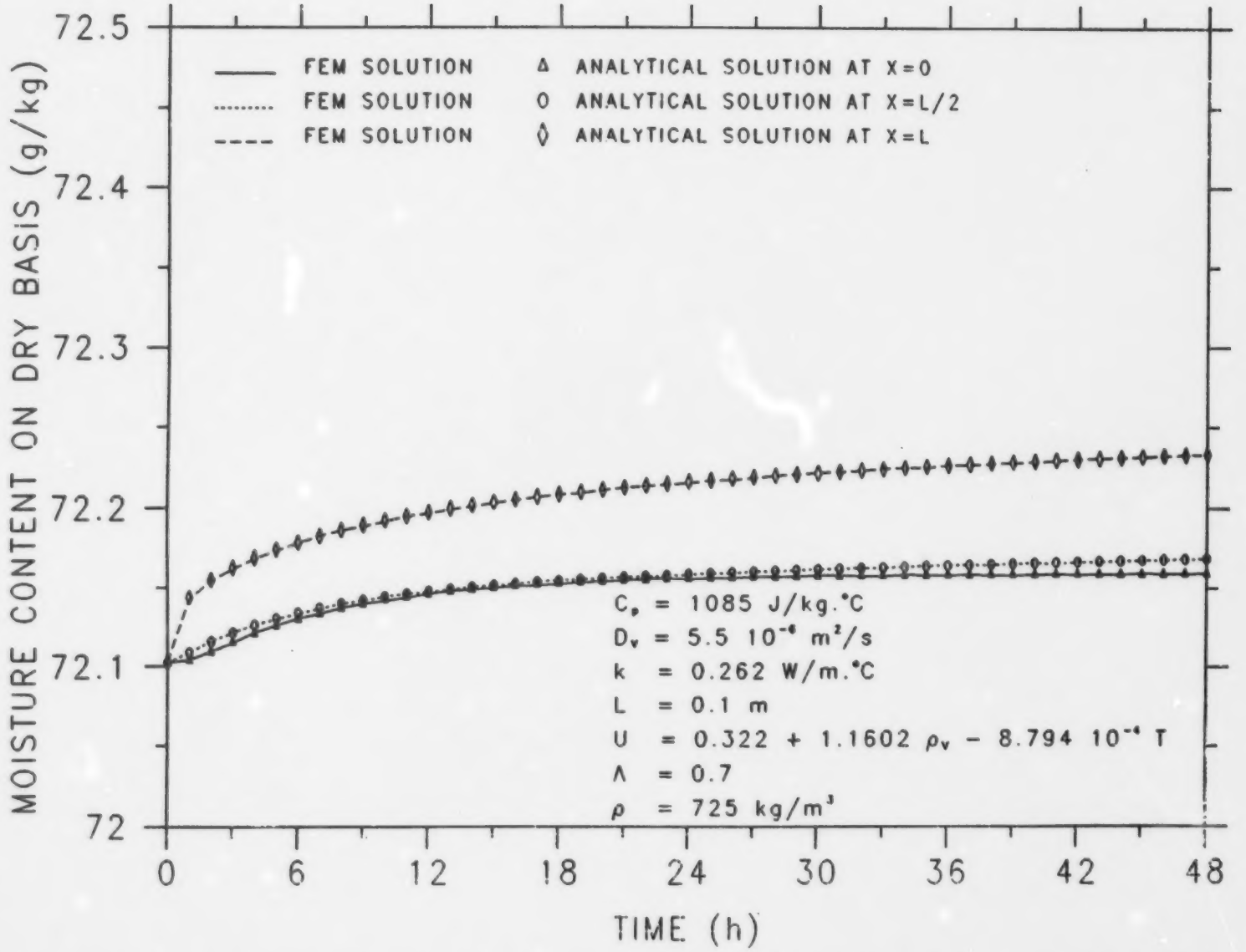

Figure 3.44 Comparison of analytical versus finite element moisture content distribution in a theoretical sample exposed to convective boundary conditions.

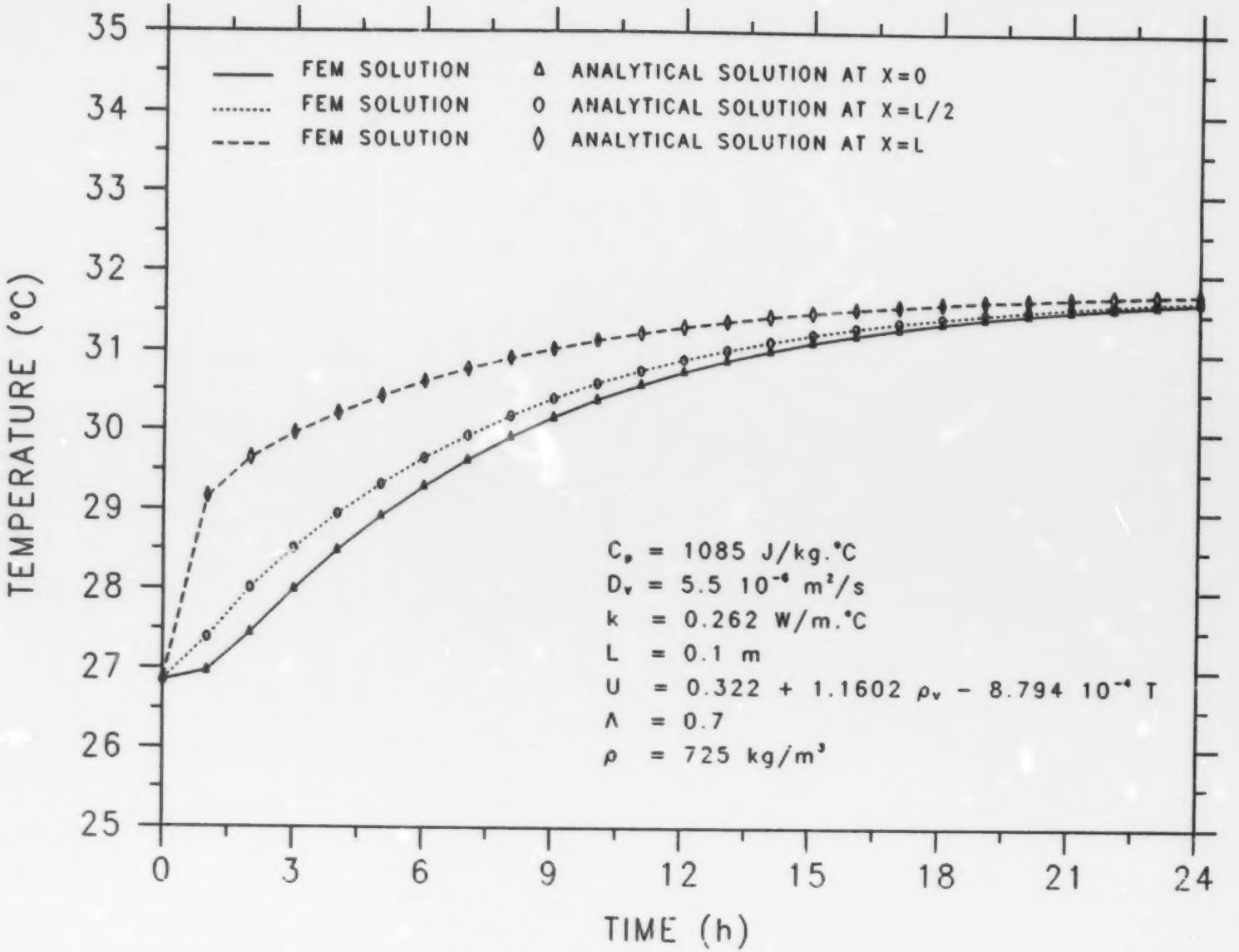

Figure 3.45 Comparison of analytical versus finite element temperature distribution in a theoretical sample exposed to convective boundary conditions.

COMPARISON OF SORPTION ISOTHERMS FOR WOOD WALLDRY VS. ALP KERESTECIOGLU'S MODEL [5] (MOISTURE CONTENT VS. RELATIVE HUMIDITY)

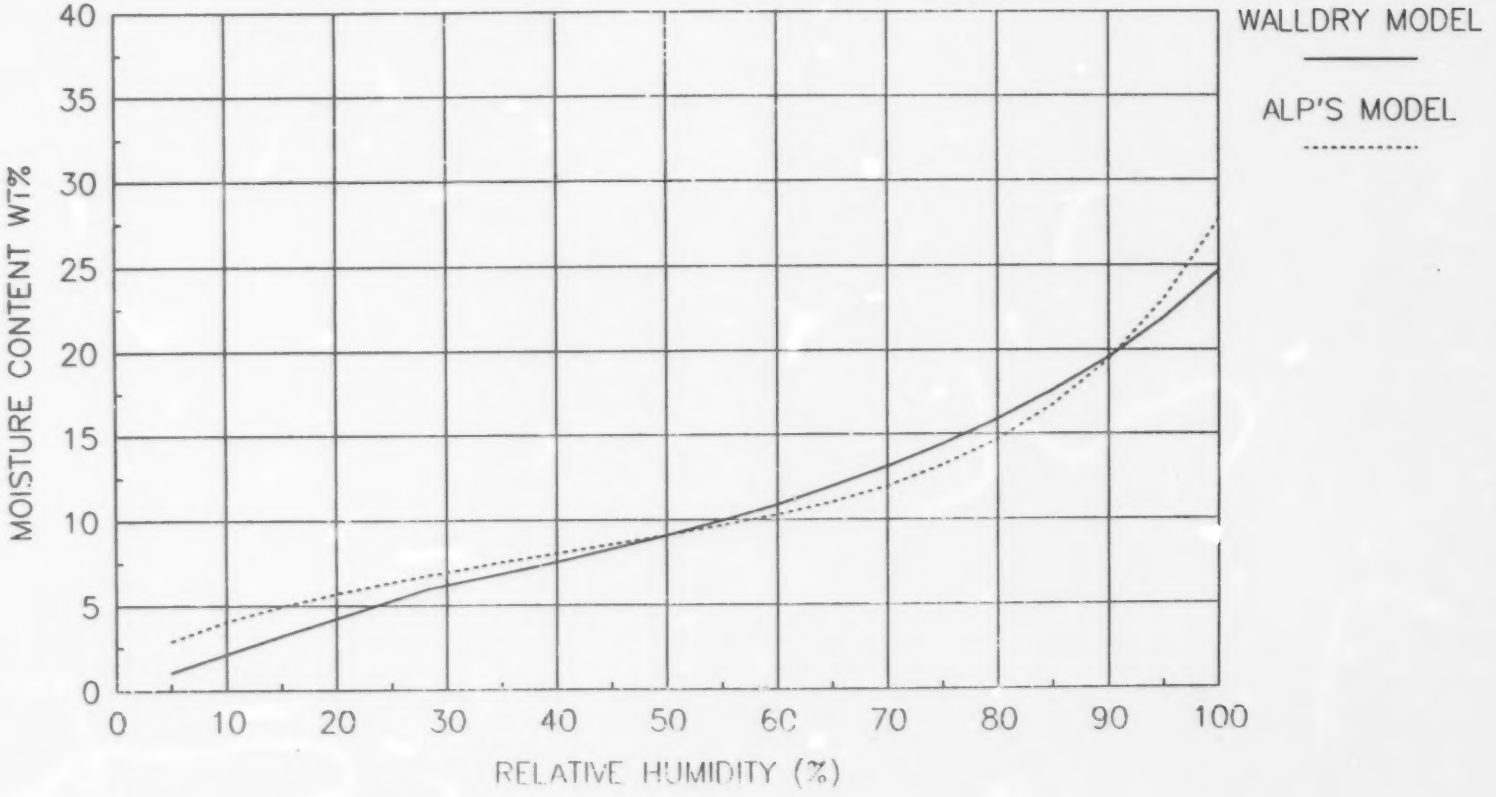

Figure 3.46

APPENDIX A

WH2P4
VINYL SIDING STRAPPING GLASCLAD & 2X4 STUDS

NUMBER OF ROWS OF SIDING UP THE WALL (NV) AND LAYERS THROUGH THE WALL (NE)
12 20

NUMBER OF LAYERS OF SHEATHING: 2 OR 3 (USE 2 FOR LIGHT MATERIAL 3 FOR HEAVY)
3
O
Y
Y
O
Y
Y

SELECTION OF MATERIALS FOR EACH LAYER (SEE PROPERTIES DATABASE FOR #)
1
15
25
25
25
4
5
4
22
6
12
12
12
17
17
17
19
21
4
9

THICKNESS OF EACH LAYER (in m)
1
.002
3.333333E-04
3.333333E-04
3.333333E-04
.0005
.019
.0005
.0005
.0005
1.266667E-02
1.266667E-02
1.266667E-02

2.966667E-02
2.966667E-02
2.966667E-02
.000127
.0127
.002
1

SELECTION OF MATERIALS FOR THE STUD LAYERS (SEE PROPERTIES DATA BASE FOR #)
18
18

LATERAL THICKNESS OF STUD LAYERS
.019
.019

INITIAL MOISTURE CONTENT (%): SIDING, SHEATHING, STUDS
30 30 48

WALL HEIGHT (m), WALL LENGTH (m), No. OF EQUIVALENT FULL LENGTH STUDS, STUD LAYER LOCATION
1.4 1.2 5.669951 15

Siding GAP Characteristics: K1 (Pa/(L/min)/m)) | bottom to top (9 elements + opening)
.6429
.6429
.6429
.6429
.6429
.6429
.6429
.6429
.6429
.6429

Siding GAP Characteristics: K2 (Pa/((L/min)/m)^2) | bottom to top (9 + opening)
.00213
.00213
.00213
.00213
.00213
.00213
.00213
.00213
.00213
.00213

Siding AIR SPACE Characteristics: K1 (Pa/gap)/(L/min/m)) | bottom to top (9 elements + opening)
1.572700042724609D-02
1.572700042724609D-02
1.572700042724609D-02
1.572700042724609D-02
1.572700042724609D-02

1.572700042724609D-02
1.572700042724609D-02
1.572700042724609D-02
1.572700042724609D-02
1.572700042724609D-02

Siding AIR SPACE Characteristics: K2 (Pa/gap)/(L/min/m)^2) | bottom to top (9 + opening)
4.258333E-06
4.258333E-06
4.258333E-06
4.258333E-06
4.258333E-06
4.258333E-06
4.258333E-06
4.258333E-06
4.258333E-06
4.258333E-06

INWARD LEAK: ELEMENT # (0 IF NONE), ORIENTATION OF MAJOR LEAKS, WINTER & SUMMER INDOOR TEMPS & RH
0 360 20 25 40 60

NUMBER OF THE AIR SPACE LAYER
7

(+/- 45) WIND PRESSURE COEFFICIENTS | bottom to top (9 elements + opening)
45
.2
.15
.12
.1
.095
.09
.1
.15
.21
.32

(+/- 90) WIND PRESSURE COEFFICIENTS | bottom to top (9 elements + opening)
90
.02
-.005
-.0225
-.0475
-.0475
-.055
-.06
-.035
-.02
.03

(+/- 135) WIND PRESSURE COEFFICIENTS | bottom to top (9 elements + opening)
135
-.16

-.16
-.165
-.175
-.19
-.2
-.22
-.23
-.25
-.26

(OTHER DIRECTIONS) WIND PRESSURE COEFF | bottom to top (9 elements + opening)
180
-.18
-.17
-.16
-.15
-.15
-.155
-.155
-.16
-.15
-.14

WALL ORIENTATION (DEGREES FROM NORTH): N:360, E:90, S:180, W:270
180

MOISTURE SOURCE STRENGTH IN kg/hr, & LOCATION: LAYER # & ELEMENT NUMBER
0 10 6

INITIAL WATER FILM THICKNESS TRAPPED BETWEEN SHEATHING PAPER & SHEATHING
0

NUMBER OF LAYERS FACING AIR (OR INSULATION), WHICH LAYERS
6
3
5
9
11
13
21

SIMULATION START AND END (DAY OF THE YEAR)
66 12 365 24

NUMBER OF ITERATIONS BETWEEN THE 3 MAJOR SUB MODELS
3

NUMER OF LAYERS DISPLAYED IN SCREEN (MAX 12); SPECIFY LAYER NUMBERS
12
1
2
3
5
6

7
11
12
13
21
22
20

CITY LOCATION (1 - 10) SEE MANUAL
2

NAME OF OUTPUT FILE FOR PLOTTING and TABULAR OUTPUT(e.g. GRAPGH.PRN)
WH2P4 .PRN
WH2P4 .SUM

SIDING TIGHTNESS EQUATION FORM & FLOW COEFFICIENTS & EXPONENTS
3 0 0 0 0 0 0 0 0 0 0
0 0

GRAPHICS AND TABULAR OUTPUT CONTROLS
D
M
3 13 21 5 5 5
3 5
11 5
12 5
13 5
21 1
21 5
21 9
22 1
22 5
22 9
3

For the hypothetical sample a linearized equilibrium moisture sorption isotherm is used. The sorption isotherm is defined by the following equation:

$$U_e = 0.322 + 1.1602\ \rho_v - 8.794\times10^{-4}\ T$$

Where

T -- Temperature (K)
ρ_v -- Water vapor density (kg/m^3)
U_e -- Equilibrium moisture content (kg/kg)

In the validations, a one-dimensional slab is considered. The slab and the coordinate system are shown in Figure 1.

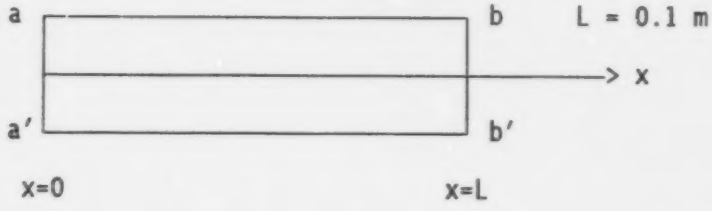

Figure 1. Schematic of the validation case.

In each validation case, aa' is assumed to be impermeable and insulated, and different types of boundary conditions are applied to bb'. The different validation cases are as follows:

Case 1 Prescribed Temperature and water vapor density at x=L.

$$T^* = 305\ K \quad \text{and} \quad \rho^*_v = 0.016\ kg/m^3$$

Case 2 Convective heat and moisture transfer at x=L.

$$T_\alpha = 305\ K \quad \text{and} \quad h_T = 5\ W/m^2.K$$
$$\rho_{v,\alpha} = 0.016\ kg/m^3 \quad \text{and} \quad h_\rho = 7.347\times10^{-5}\ m/s$$

Case 3 Imposed heat and moisture flux at x=L.

$$q''_T = 10\ W/m^2 \quad \text{and} \quad q''_M = 2.78\text{x}10\text{-}8\ kg/m^2.s$$

Where

T^* -- Prescribed surface temperature (K)
ρ^*_v -- Prescribed water vapor density (kg/m^3)
T_α -- Convective ambient temperature (K)
h_T -- Convective heat transfer coefficient ($W/m^2.K$)
h_ρ -- Convective mass transfer coefficient (m/s)
$\rho_{v,\alpha}$ -- Convective ambient water vapor density (kg/m^3)
q''_T -- Imposed heat flux (W/m^2)
q''_M -- Imposed mass flux ($kg/m^2.s$)

In the validations, the following initial conditions are used:

$$T_i = 300 \text{ K}; \quad \rho_{v,i} = 0.012 \text{ kg/m}^3$$

The initial moisture content of the slab can be calculated using the sorption isotherm equation. For the validations the initial moisture content is U_e=0.0721 kg/kg.

RESULTS

Figures 1 through 4 give the temperature, water vapor density, partial water vapor pressure and moisture content distributions for the first validation case (prescribed temperature and water vapor density). The results are given for x=0 (insulated and impermeable end), x=L/2 (0.05 m, middle of the slab), and x=L (where the boundary conditions are applied).

Figures 5 through 8 give the temperature, water vapor density, partial water vapor pressure and moisture content distributions for the second validation case (convective boundary conditions).

Figures 9 through 11 give the temperature, water vapor density and partial water vapor pressure distributions for the third validation case (imposed heat and moisture flux conditions).

PROPERTY RELATIONS

The diffusion resistivity factor (DRF) used by WALLDRY can be related to the vapor diffusivity (D_v) by the following relation:

$$DRF = (R_v\ T)/(D_v\ \Lambda)$$

DRF -- Diffusion resistivity factor (Pa.m.s/kg)
D_v -- Vapor diffusivity (m^2/s)
R_v -- Ideal gas constant (461.52 J/kg.K)
T -- Temperature (K)
Λ -- Porosity (unitless)

The maximum water adsorption may be obtained from the sorption isotherm.

The water vapor density (ρ_v) is related to the partial water vapor pressure through the ideal gas equation.

$$P_v = \rho_v\ R_v\ T$$

P_v -- Partial water vapor pressure (Pa)
ρ_v -- Water vapor density (kg/m^3)
R_v -- Ideal gas constant (461.52 J/kg.K)
T -- Temperature (K)

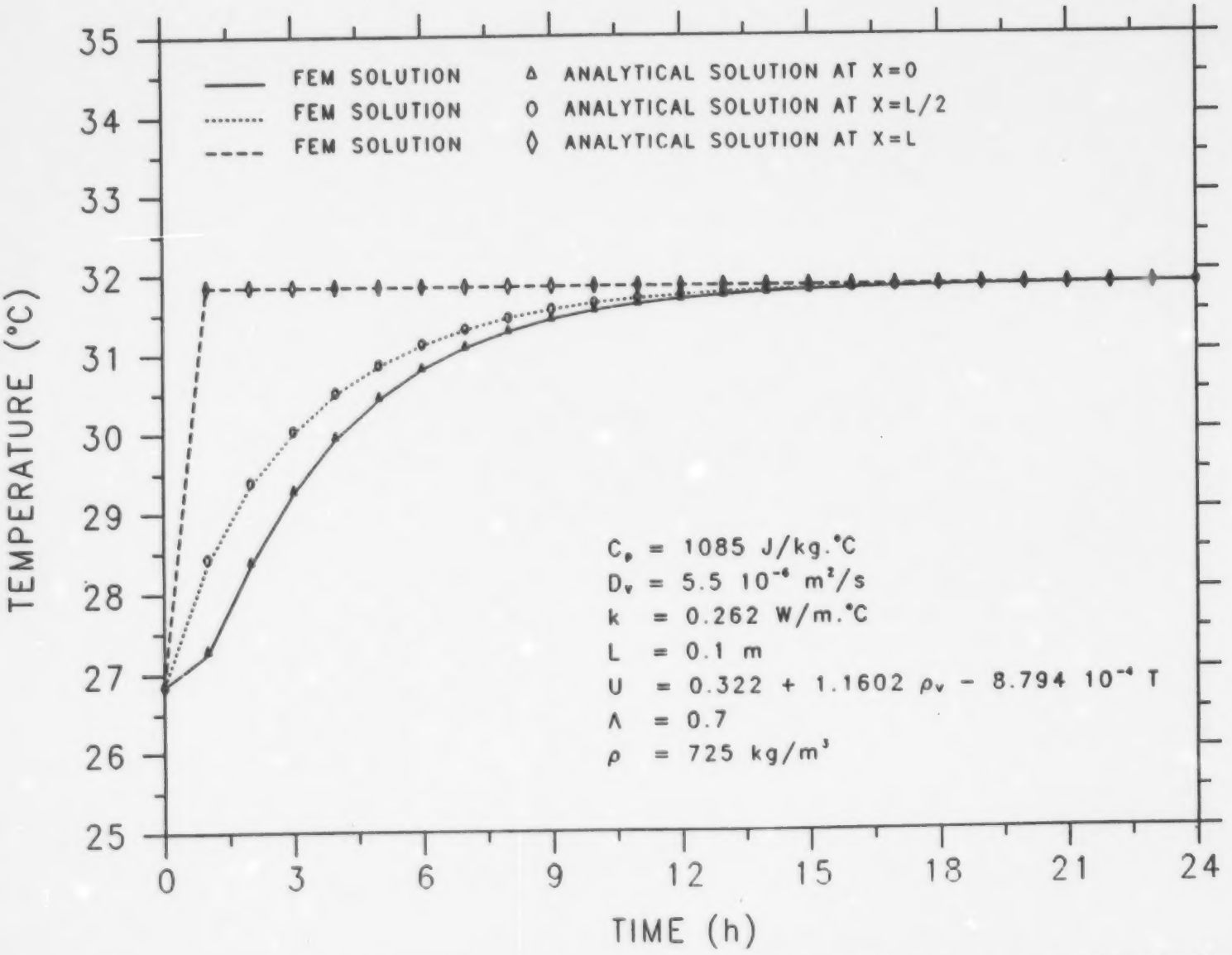

Figure 1. Comparison of analytical versus finite element temperature distribution in a theoretical sample exposed to prescribed boundary conditions.

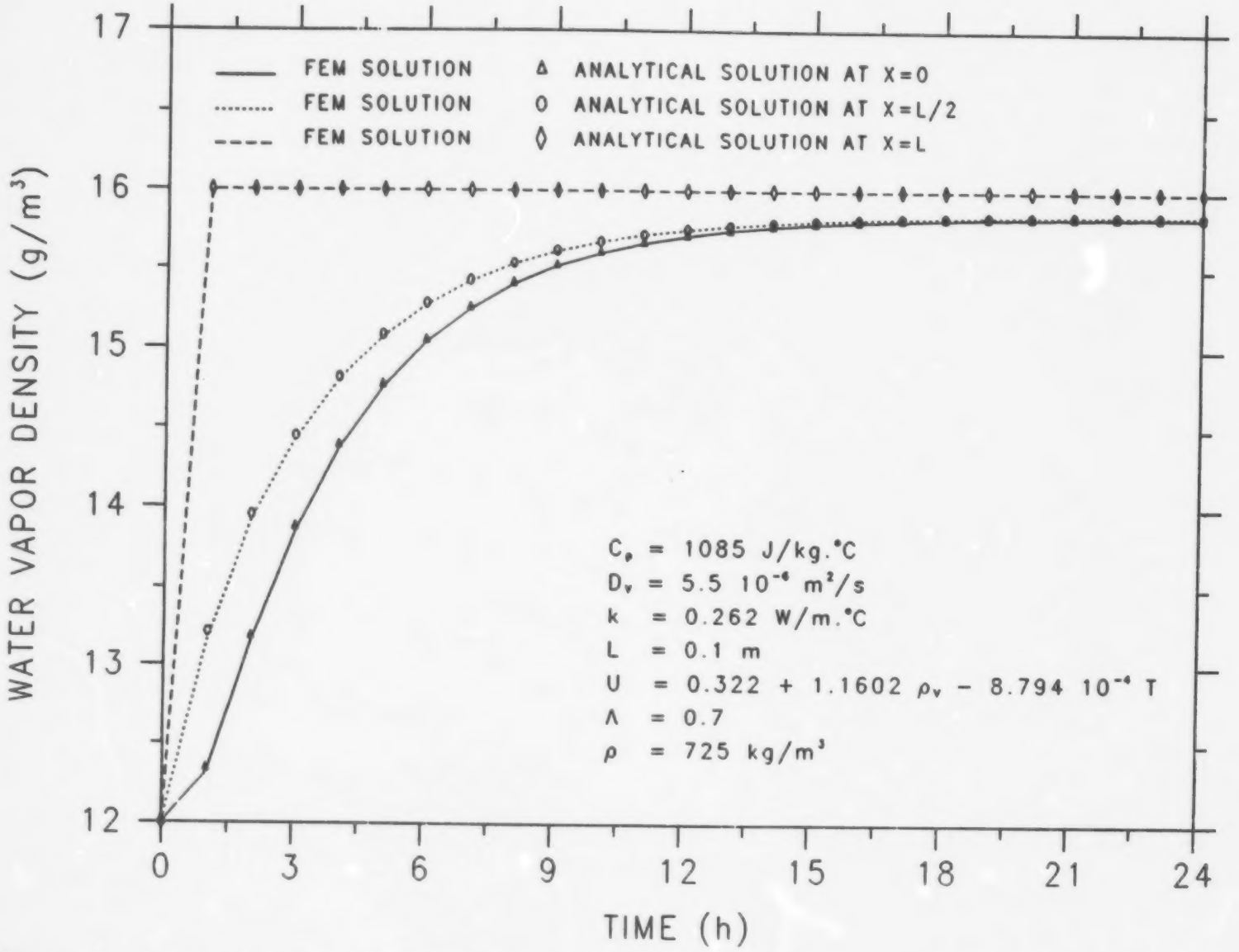

Figure 2. Comparison of analytical versus finite element vapor density distribution in a theoretical sample exposed to prescribed boundary conditions.

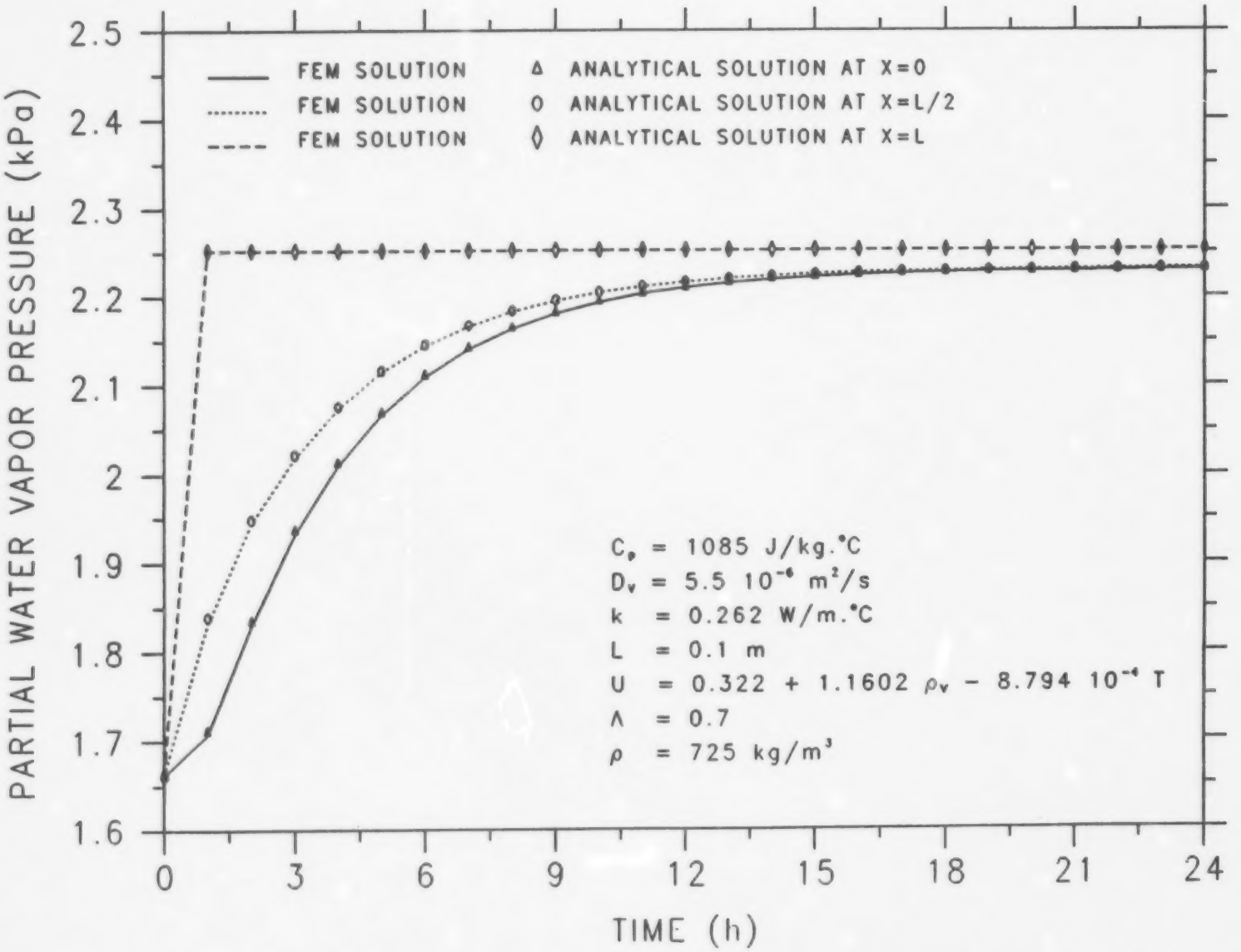

Figure 3. Comparison of analytical versus finite element vapor pressure distribution in a theoretical sample exposed to prescribed boundary conditions.

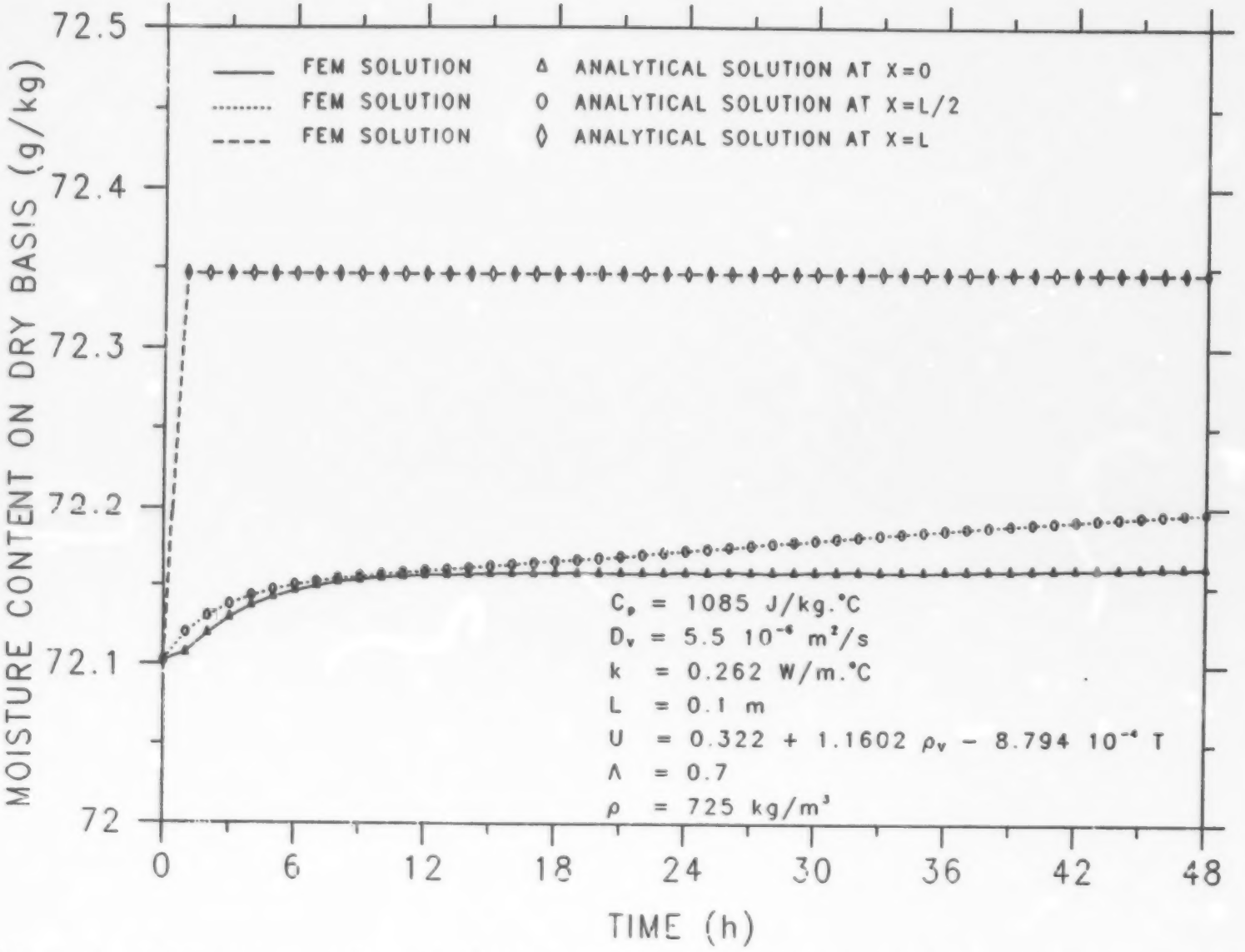

Figure 4. Comparison of analytical versus finite element moisture content distribution in a theoretical sample exposed to prescribed boundary conditions.

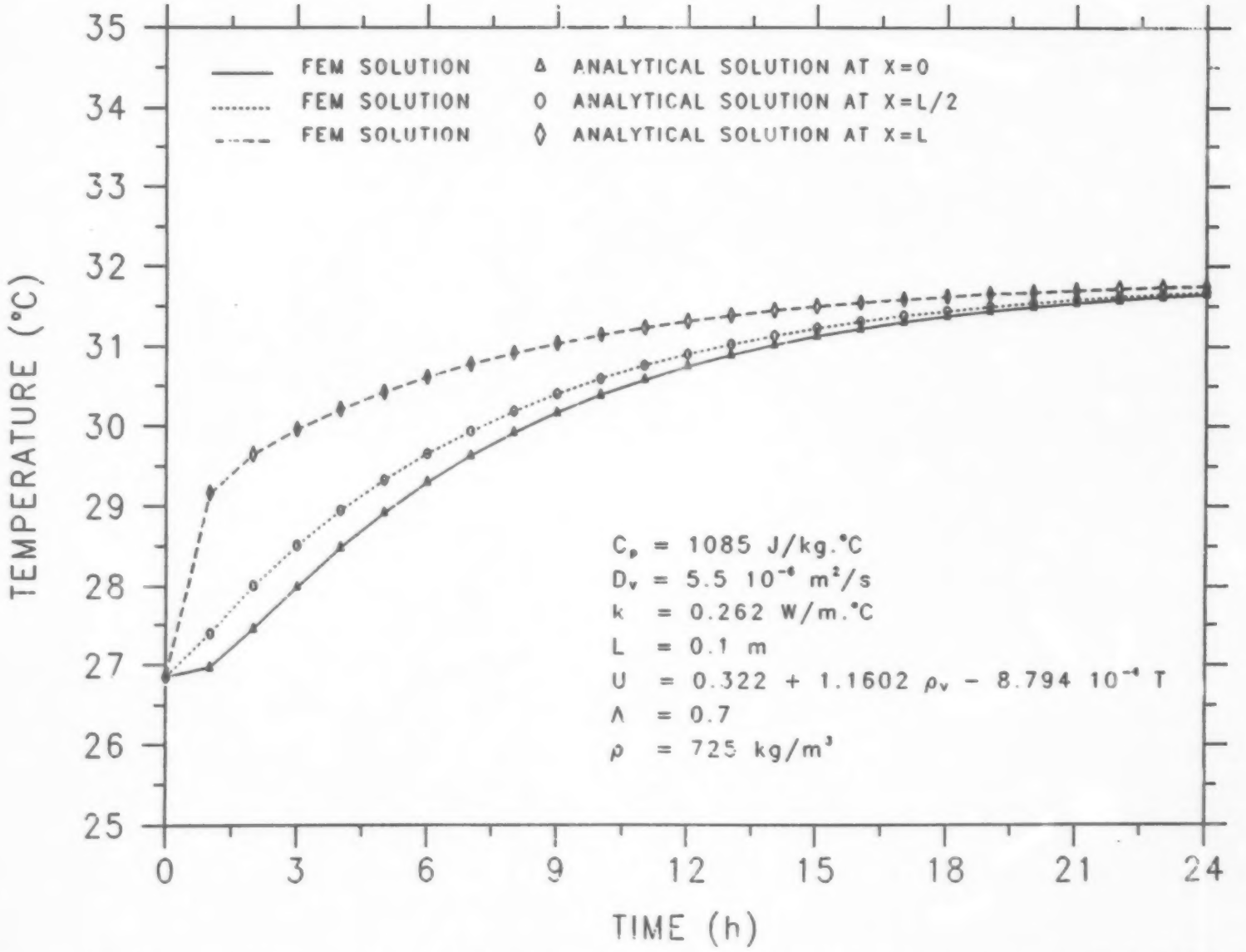

Figure 5. Comparison of analytical versus finite element temperature distribution in a theoretical sample exposed to convective boundary conditions.

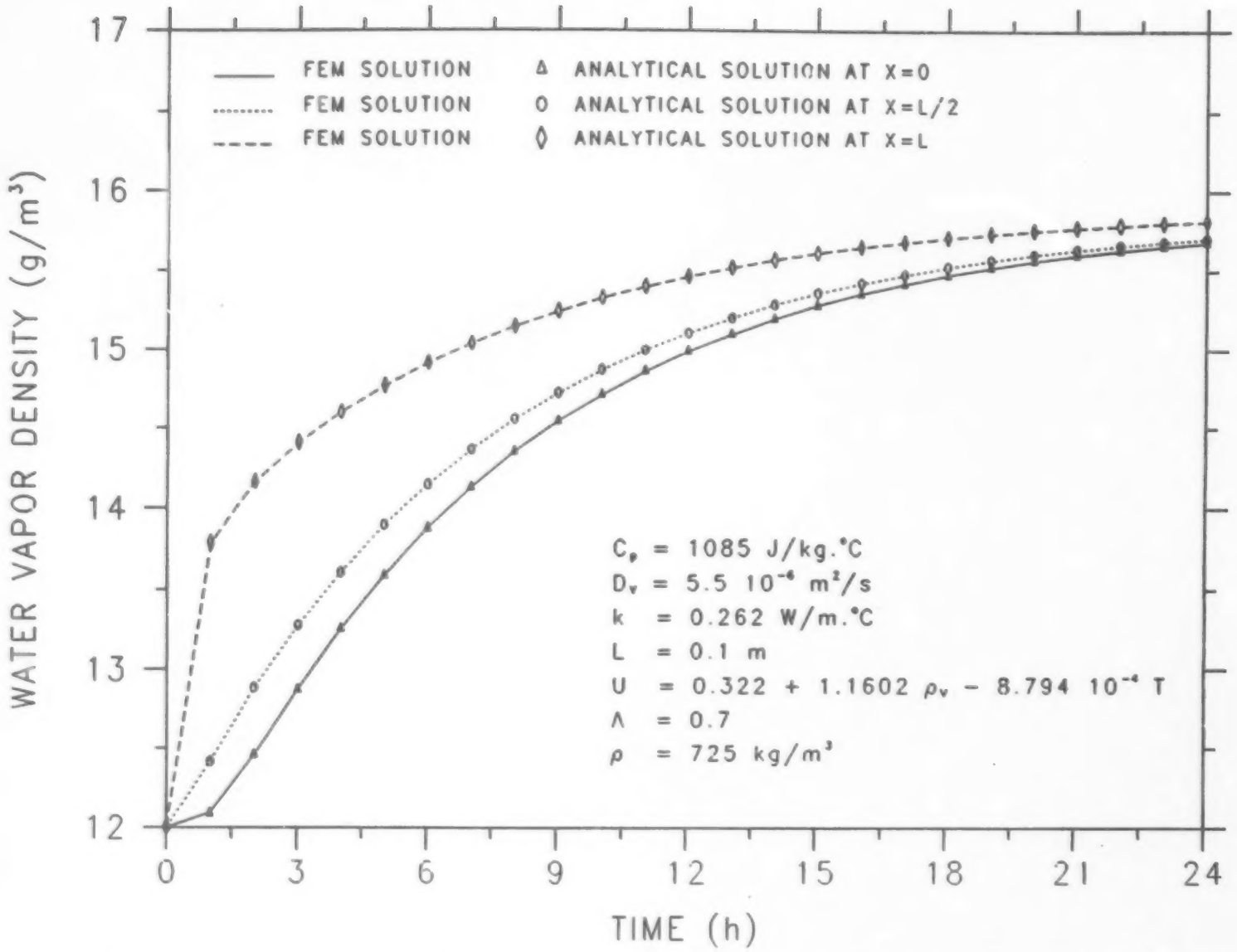

Figure 6. Comparison of analytical versus finite element vapor density distribution in a theoretical sample exposed to convective boundary conditions.

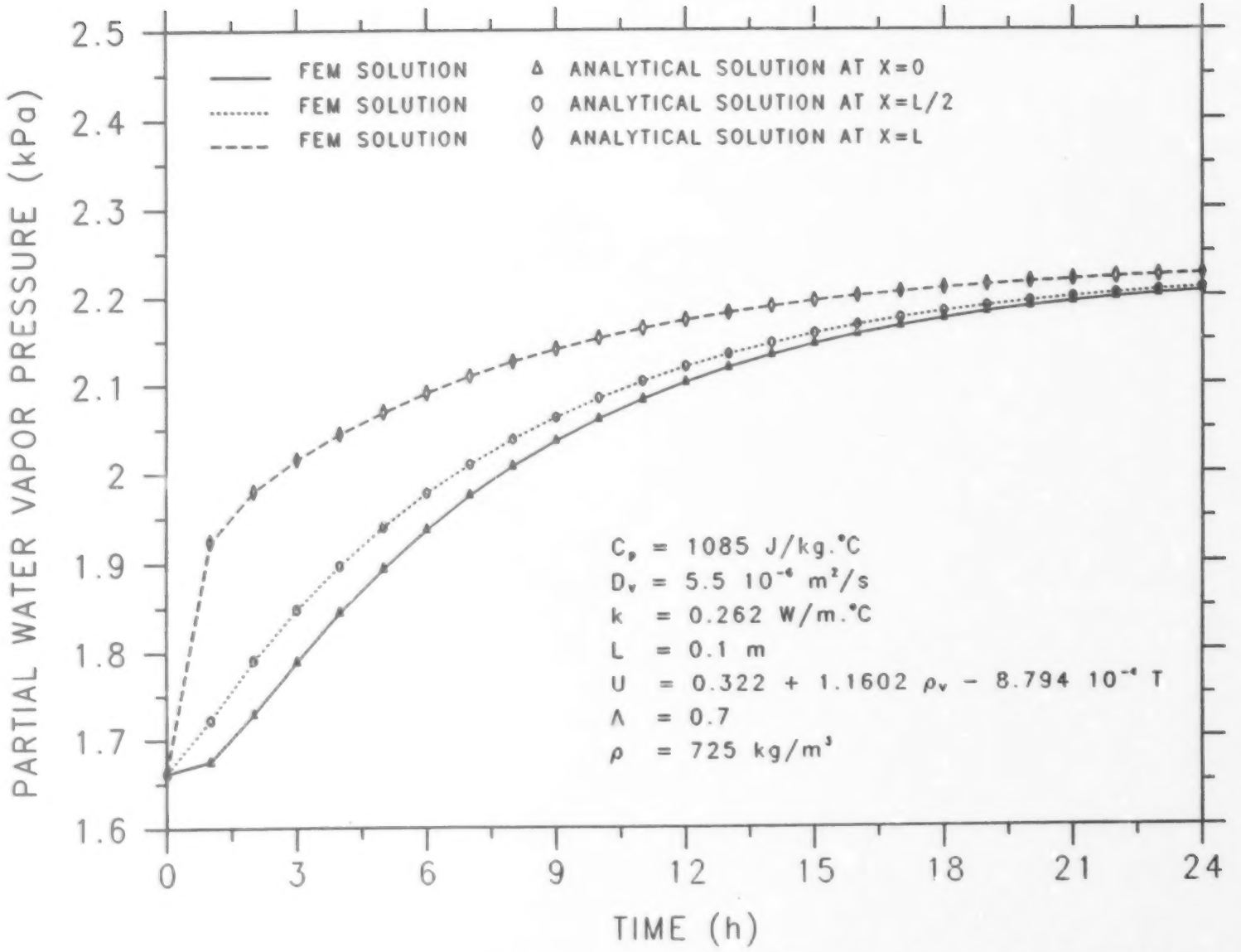

Figure 7. Comparison of analytical versus finite element vapor pressure distribution in a theoretical sample exposed to convective boundary conditions.

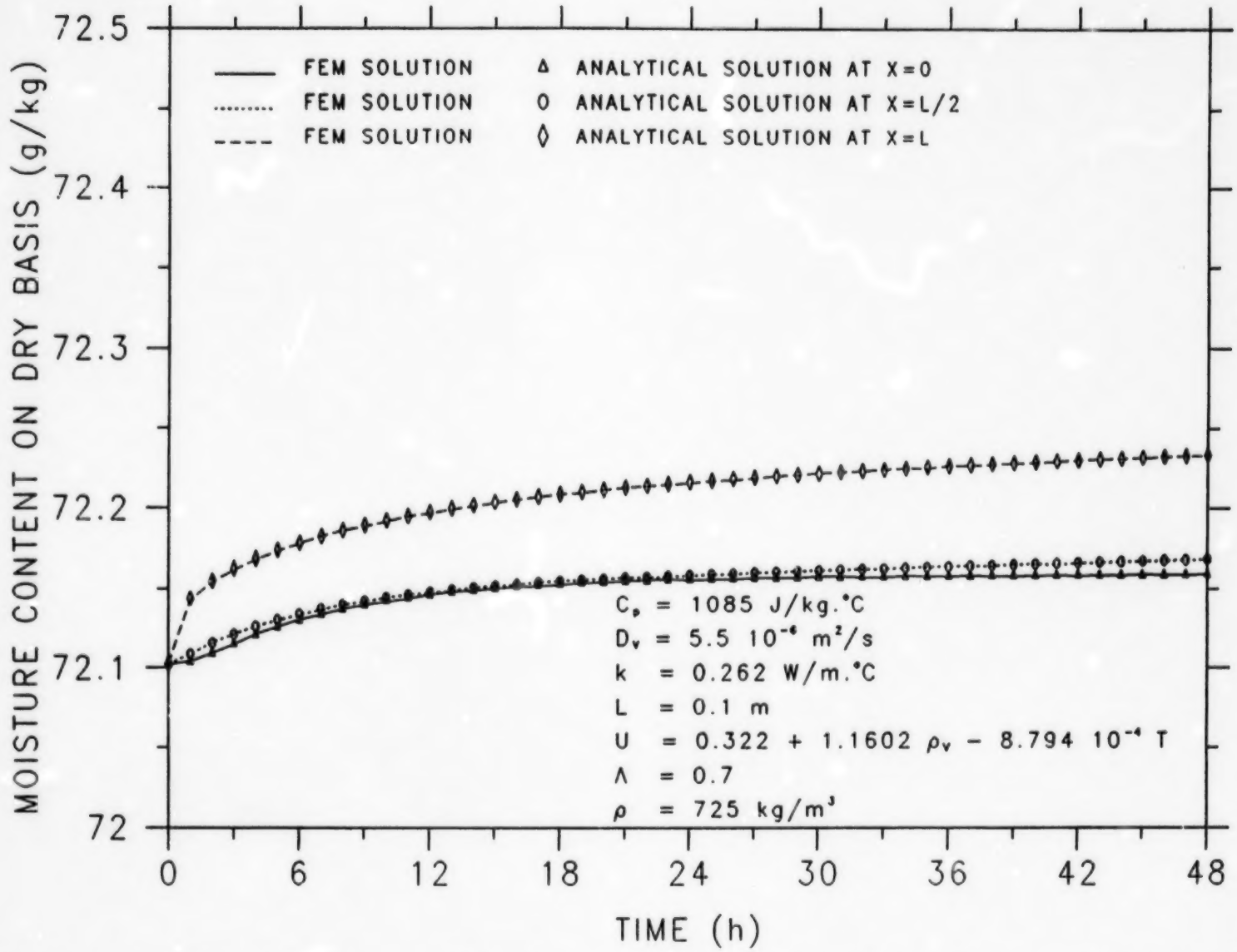

Figure 8. Comparison of analytical versus finite element moisture content distribution in a theoretical sample exposed to convective boundary conditions.

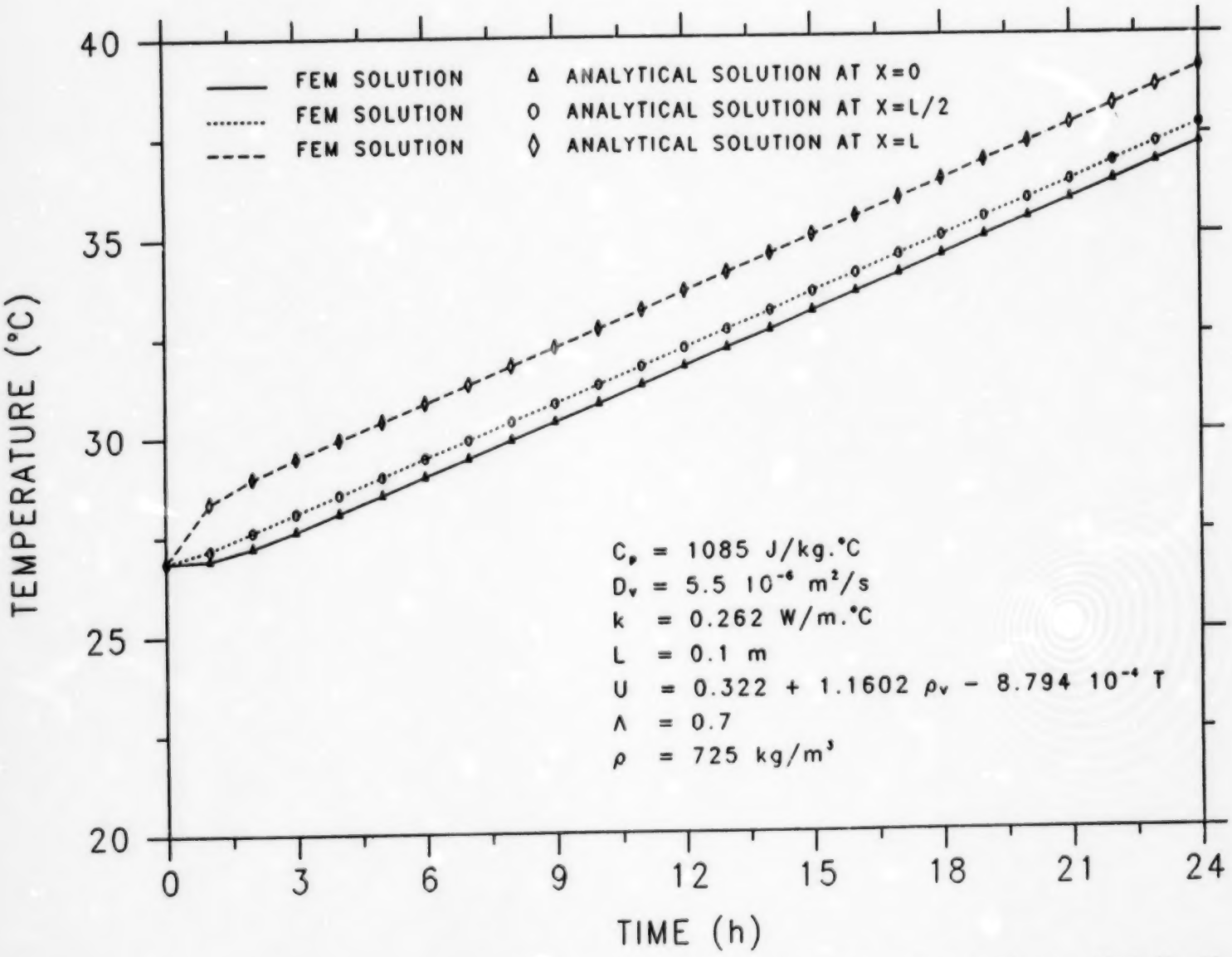

Figure 9. Comparison of analytical versus finite element temperature distribution in a theoretical sample exposed to flux boundary conditions.

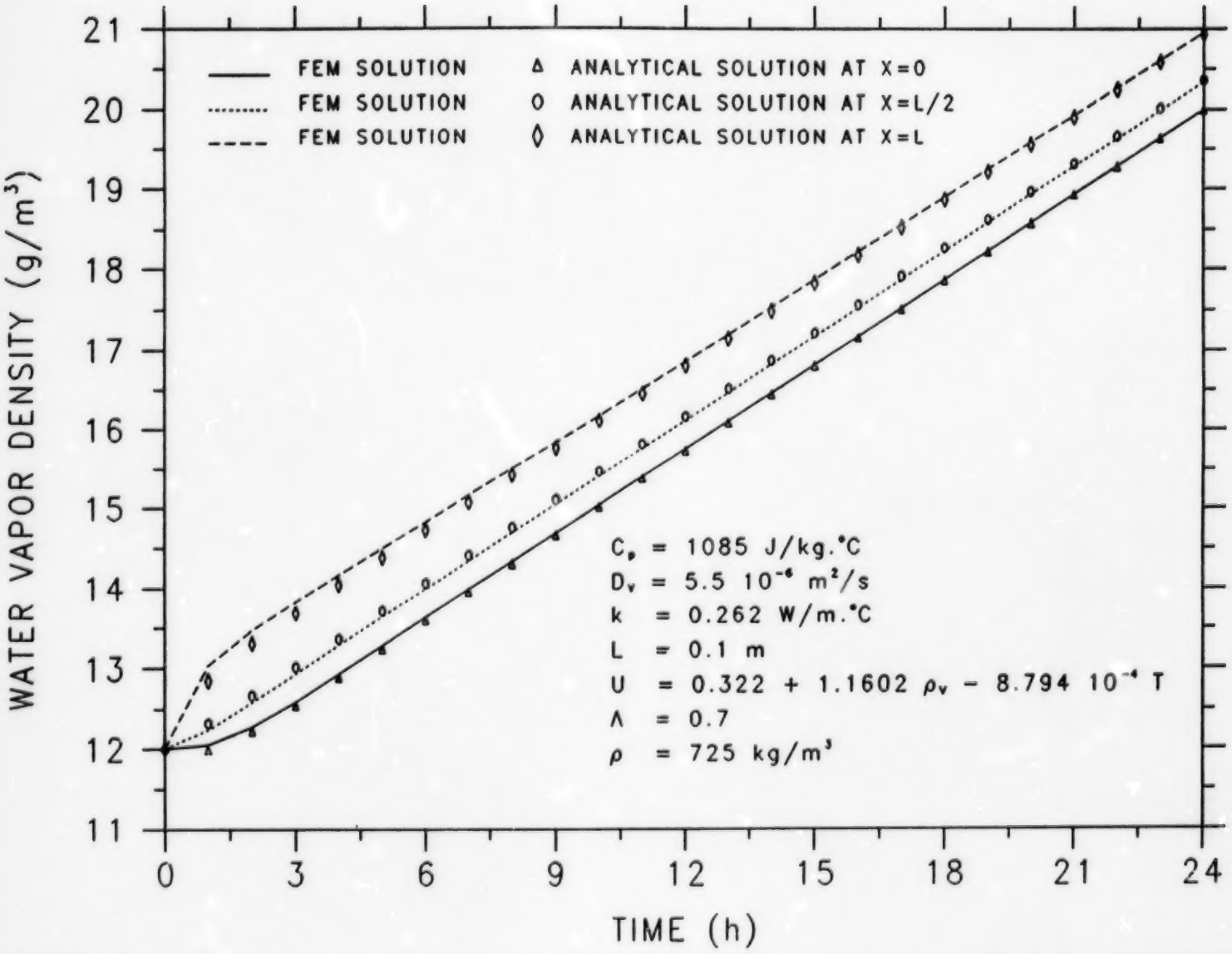

Figure 10. Comparison of analytical versus finite element vapor density distribution in a theoretical sample exposed to flux boundary conditions.

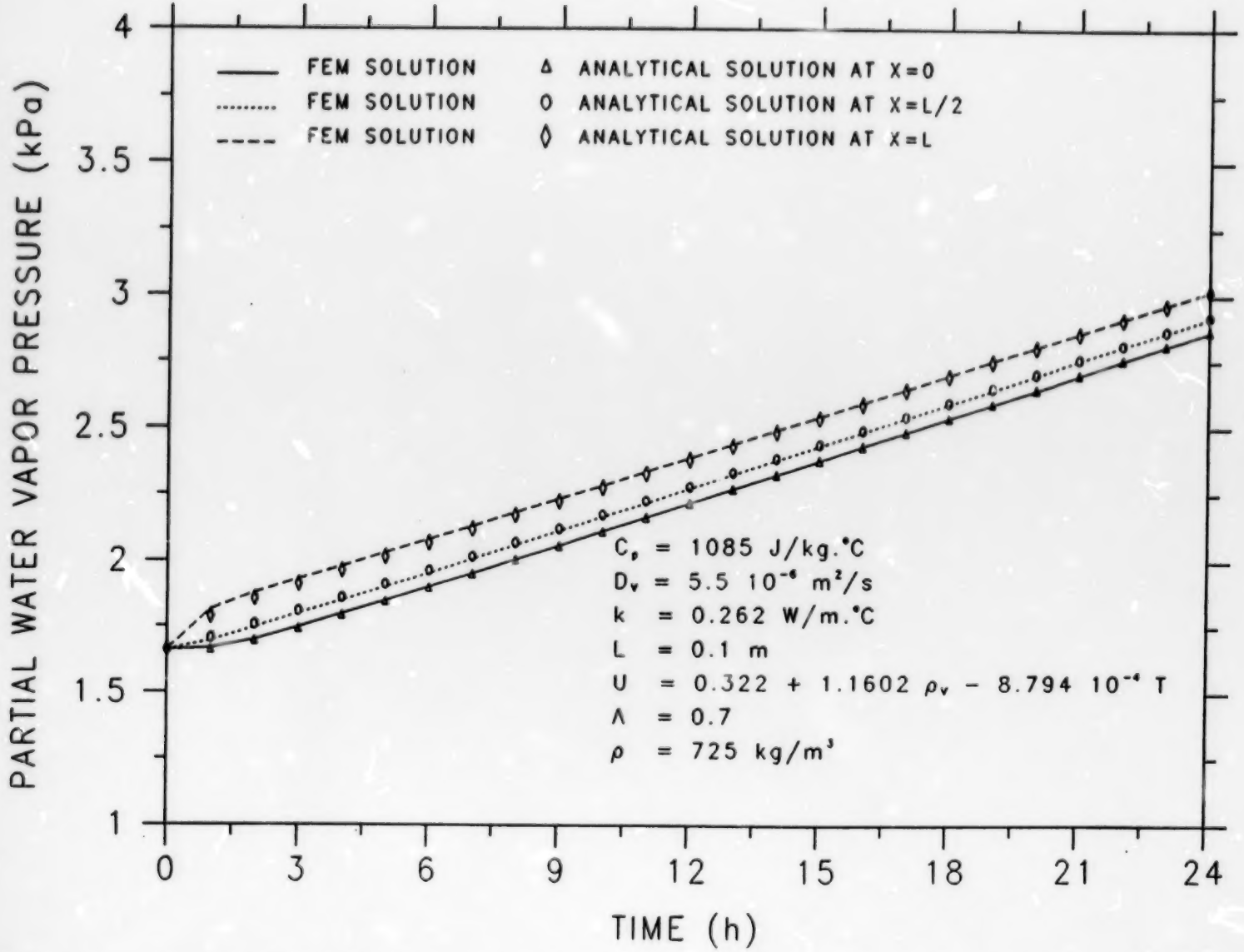

Figure 11. Comparison of analytical versus finite element vapor pressure distribution in a theoretical sample exposed to flux boundary conditions.